Syntheses of defined sulfated oligohyaluronans reveal structural effects, diversity and thermodynamics of GAG-protein binding

Sebastian Köhling,[†a] Joanna Blaszkiewicz,[†a] Gloria Ruiz-Gómez,[b] María Isabel Fernández-Bachiller,[a] Katharina Lemmnitzer,[c] Nydia Panitz,[d] Annette G. Beck-Sickinger,[d] Jürgen Schiller,[c] M. Teresa Pisabarro,[b]* Jörg Rademann[a]*

[a] *Institute of Pharmacy – Medicinal Chemistry, Freie Universität Berlin, Königin-Luise-Str. 2+4, 14195 Berlin, Germany.*
[b] *Structural Bioinformatics, BIOTEC TU Dresden, Tatzberg 47-51, Dresden 01307, Germany*
[c] *Institute of Medical Physics and Biophysics, University of Leipzig, Härtelstr. 16/18, 04107 Leipzig, Germany*
[d] *Institute of Biochemistry, University of Leipzig, Brüderstr. 34, 04103 Leipzig, Germany*

Corresponding authors´ e-mail: joerg.rademann@fu-berlin.de and maria_teresa.pisabarro@tu-dresden.de

Supporting Information

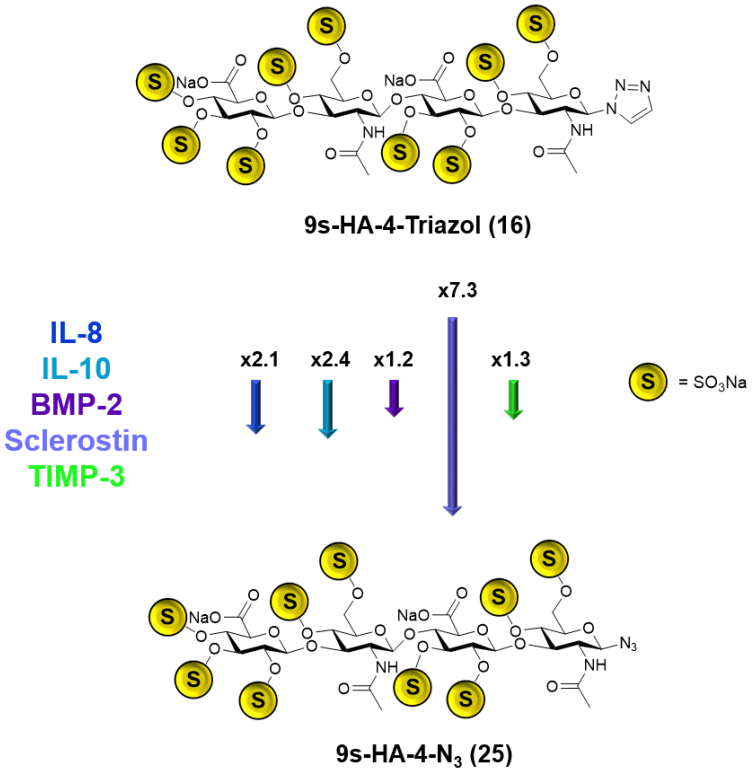

SScheme 1. Ratio of determined dissociation constants for triazol- and azide-functionalized tetrahyaluronans toward five regulatory proteins. Ratio of determined K_D values are symbolized by arrows with protein-specific color code. The arrow direction indicates increasing strength on binding. The length of the arrows corresponds to the observed binding ratio. The fold increase in binding is also numerically shown**.**

1. General Information

HRMS analyses were performed with Agilent 6210 (ESI–TOF, 10 µL/min, 1.0 bar, 4 kV). NMR experiments were conducted on JEOL ECP 500, 500 MHz and Bruker AVANCE 700, 700 MHz instrument, using MeOH-d_4 (D, 99.8%), DMSO-d_6 (D, 99.9%), D_2O (D, 99.9%) as solvents. Chemical shifts are relative to the deuterated solvent peaks and are in parts per million. The following abbreviations were used alone or in combinations: s = singlet, d =doublet, t = triplet, q = quartet. All reagents are commercial grade (purchased from Sigma-Aldrich, Merck and Alfa Aesar) and were used as received. All reactions were performed, if necessary, under inert gas atmosphere using anhydrous solvents. Anhydrous solvents were obtained from the solvent system MB SPS-800 from M. Braun. In case of reactions with anomeric glycosyl thiols, the solvents were degassed with inert gas bubbling and ultrasonic. Thin-layer chromatography (TLC) and flash chromatography separations were respectively performed on coated aluminium sheets from Merck (silica gel 60, GF254 and silica gel 60 W, F254s in case of ΔHA-8, **35**) and on Merck silica gel 60 (230–400 mesh). Visualization of the plates was achieved using a UV lamp (λ_{max} = 254 nm), and/or vanillin staining solution (0.56 g vanillin, 10 mL glacial acetic acid and 6 mL conc. H_2SO_4 in 100 mL MeOH). Proteins were purchased from Sigma Aldrich (TGF-β1: T7039, BMP-2: B3555, FGF-1: SRP3041, FGF-2: SRP4037, TIMP-3: T1327, AT-3: SRP6316) and R+D-Systems (Sclerostin: 1406-ST-025/CF) or in case of IL-8[1], IL-10[2] and SDF-1[3] expressed according to the stated protocol.

MS-Analysis of sulfated oligosaccharides was carried out by electro-spray ionization mass spectrometry (ESI-MS) with an Amazon SL ion trap mass spectrometer (BrukerDaltonics,Bremen,Germany). Nitrogen was used as the nebulizergas. The samples were introduced into the ESI source by using a syringe pump at a flow rate of 2 - 5mL min^{-1}. Data acquisition and analysis were carried out by using the programs Trap Control and DataAnalysis, respectively (BrukerDaltonics, Bremen, Germany). The sodium salt of the analyte was dissolved in deionized water (Millipore) to a concentration of 5 mg mL^{-1} and deluted 1:5 with MeOH (50%) for a final concentration of 0,5 mg mL^{-1}. The unusal high analyte concentration in combination with an optimization for every single analyte made an anion exchange step redundant and enabled the acquisition of mass spectra in positive ion mode for all analytes shown in this work. The spectral quality for the positive ion mass spectra strongly depends on the saltconcentration and on the analyte itself. In the case of azide complexes a mass loss of $\Delta m/z$ = 43.02 was found. This corresponds to a loss of HN_3 as in source fragmentation during the electrospray ionisation process as discribed in the literature before.[4]

2. Synthetic Protocols

Hyaluronan disaccharide azide, (HA-2-N_3, β-D-glucopyranuronyl-(1→3)-β-D-2-acetamido-2-deoxy-glucopyranosyl-azide (4)

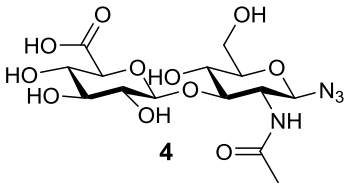

4

HA-2[5] **1** (96 mg, 0.24 mmol), *N*-methylmorpholine (398 µl, 3.62 mmol) and sodium azide (471 mg, 7.24 mmol) were dissolved in water (4 mL). The solution was cooled to 0 °C and 2-chloro-1,3-dimethylimidazolinium chloride (184 mg, 1.08 mmol) was added in one portion. The ice bath was removed after 5 min and the reaction mixture stirred for 24 h at room temperature. For purification, silica gel (3g) was added and the suspension was evaporated and dried under reduced pressure and in high vacuum. The product was first purified by flash chromatography using EtOAc/MeOH/H_2O 5:2.5:2 followed by HPLC (C-18, isocratic 95:5 H_2O (+0.1%TFA) / MeCN (+0,1%TFA), flow rate; 40 ml/min, detection UV (214 nm)). The product-containing fractions were combined and freeze dried to yield HA-2-N_3 **4** as a colorless powder (60 mg, 59%). **^{1}H-NMR** (500 MHz, D_2O) δ = 4.79 (d, *J* = 7.2 Hz, 1H), 4.54 (d, *J* = 7.9 Hz, 1H), 4.01 (d, *J* = 9.7 Hz, 1H), 3.92 (dd, *J* = 12.5, 2.1 Hz, 1H), 3.85 (dd, *J* = 10.4, 9.2 Hz, 1H), 3.80 – 3.74 (m, 2H), 3.64 – 3.47 (m, 4H), 3.35 (dd, *J* = 9.3, 7.9 Hz, 1H), 2.03 (s, 3H) ppm. **^{13}C NMR** (126 MHz, D_2O) δ = 174.99, 172.20, 102.87, 88.69, 82.85, 77.66, 75.24, 72.62, 71.29, 68.32, 60.73, 53.98, 22.38 ppm. **HRMS** (ESI) calcd for $C_{14}H_{21}N_4O_{11}$ $[M\text{-}H^+]^-$: 421.1212 Da; found: 421.132 m/z.

Hyaluronan hexasaccharide azide, (HA-6-N_3, β-D-glucopyranuronyl-(1→3)-β-D-2-acetamido-2-deoxy-glucopyranosyl-(1→4)-β-D-glucopyranuronyl-(1→3)-β-D-2-acetamido-2-deoxy-glucopyranosyl-(1→4)-β-D-glucopyranuronyl-(1→3)-β-D-2-acetamido-2-deoxy-glucopyranosyl-azide (6)

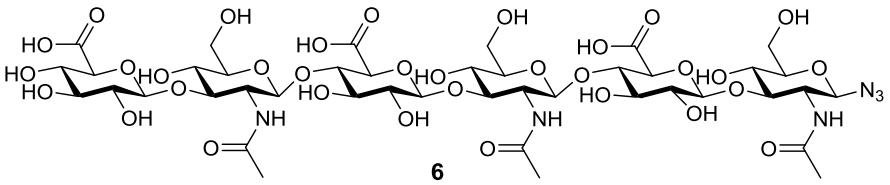

6

HA-6[5] **3** (133 mg, 0.11 mmol), *N*-methylmorpholine (359 µl, 3.26 mmol) and sodium azide (425 mg, 6.53 mmol) were dissolved in water (5 mL). The solution was cooled to 0 °C and 2-chloro-1,3-dimethylimidazolinium chloride (184 mg, 1.08 mmol) was added in one portion. The ice bath was removed after 5 min and the reaction mixture stirred for 30 h at room temperature. Subsequently, the solvent was evaporated and the crude product desalted on a Sephadex G-10 column (3x20 cm, deionized water) and purified by HPLC (C-18, isocratic 95:5 H_2O (+0.1%TFA) / MeCN (+0,1%TFA), flow rate; 40 ml/min, detection UV (214 nm)). The product-containing fractions were combined and freeze dried to yield HA-6-azide **6** as a colorless solid (65 mg, 48%). **^{1}H NMR** (700 MHz, D_2O) δ = 4.69 (d, *J* = 9.4 Hz, 1H), 4.51 – 4.46 (m, 4H), 4.45 (d, *J* = 7.9 Hz, 1H), 3.95 – 3.92 (m, 3H), 3.85 – 3.81 (m, 3H), 3.79 – 3.75 (m, 3H), 3.75 – 3.71 (m, 2H), 3.71 – 3.63 (m, 6H), 3.59 – 3.55 (m, 2H), 3.53 – 3.42 (m, 2H), 3.43 – 3.38 (m, 2H), 3.31 – 3.24 (m, 3H), 1.94 (d, *J* = 0.9 Hz, 3H), 1.91 (s, 3H), 1.91 (s, 3H) ppm. **^{13}C NMR** (176 MHz, D_2O) δ = 174.77, 174.69, 174.68, 171.95, 170.96, 102.89, 102.82, 102.59, 101.15, 101.15, 88.48, 82.62, 82.34, 80.08, 77.46, 75.31, 75.01, 74.23, 73.64, 73.64, 73.32, 73.31, 72.40, 72.04, 71.08, 68.22,

68.15, 68.04, 60.50, 60.47, 60.47, 54.29, 54.17, 53.89, 22.35, 22.17 ppm. **HRMS** (ESI) calcd for $C_{42}H_{63}N_6O_{33}$ $[M\text{-}H^+]^-$: 1179.344 Da; found: 1179.355 m/z.

5(6)-carboxytetramethyl rhodamine-2-propynylamide (7)

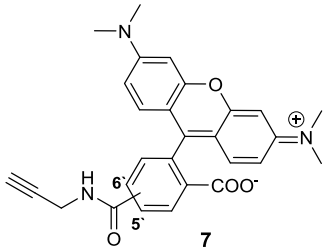

7

5(6)-Carboxytetramethylrhodamine (131 mg, 0.304 mmol), DIPEA (159 µL, 0.912 mmol) and Propargylamine (23 µL, 4.47 mmol) was dissolved in dry DMF (2 mL) followed by the addition of *O*-(7-Azabenzotriazol-1-yl)-*N*,*N*,*N*′,*N*′-tetramethyluronium-hexafluorphosphat, HATU (116 mg, 0.304 mmol). The reaction mixture was stirred at room temperature for 30 min. The solvent was evaporated under reduced pressure and the crude product was purified by HPLC (C-18, 90:10 H_2O (+0,1%TFA) / MeCN (+0,1%TFA) to 65:35 in 15 min), flow rate; 40 ml/min, detection UV(214 nm)). The product containing fractions of both regioisomers were freeze dried to yield **7 (A+B)** as dark violett powder (158 mg, 85%). **^{1}H NMR** (500 MHz, Methanol-d_4) δ = 8.78 (d, *J* = 1.8 Hz, 1H), 8.39 (d, *J* = 8.3 Hz, 1H), 8.26 (dd, *J* = 7.9, 1.7 Hz, 1H), 8.20 (dd, *J* = 8.2, 1.8 Hz, 1H), 7.84 (d, *J* = 1.8 Hz, 1H), 7.52 (d, *J* = 7.9 Hz, 1H), 7.12 (dd, *J* = 9.5, 1.7 Hz, 4H), 7.02 (ddd, *J* = 9.4, 6.8, 2.5 Hz, 4H), 6.91 (dd, *J* = 4.4, 2.4 Hz, 4H), 4.24 (d, *J* = 2.6 Hz, 2H), 4.15 (d, *J* = 2.5 Hz, 2H), 3.27 (s, 12H), 3.27 (s, 12H), 2.68 (t, *J* = 2.5 Hz, 1H), 2.62 (t, *J* = 2.5 Hz, 1H) ppm. **^{13}C NMR** (126 MHz, Methanol-d_4) δ = 166.40, 166.10, 159.20, 159.08, 157.68, 157.59, 137.47, 137.06, 136.71, 135.84, 134.28, 131.62, 131.06, 130.73, 130.63, 130.20, 129.21, 128.73, 114.24, 113.52, 113.38, 96.16, 79.22, 79.05, 71.08, 39.64, 28.84 ppm. **HRMS** (ESI) calcd for $C_{28}H_{25}N_3O_4$ $[M\text{-}H^+]^-$: 466.177; found: 466.176 m/z.

Hyaluronan tetrasaccharide-5(6)TAMRA, HA-6-5(6)TAMRA, β-D-glucopyranuronyl-(1→3)-β-D-2-acetamido-2-deoxy-glucopyranosyl-(1→4)-β-D-glucopyranuronyl-(1→3)-β-D-2-acetamido-2-deoxy-glucopyranosyl-1,2,3-triazol-4-yl-methyl-2-carbamoyl-5(6)-carboxytetramethylrhodamine (8)

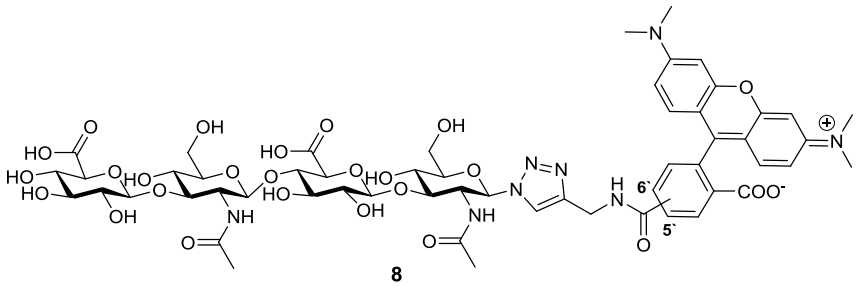

8

The tetrahyaluronan azide **5** [6] (82 mg, 0.102 mmol), 5(6)-TAMRA-Propargylamide **7** (75 mg, 0.123 mmol) and Tris[(1-benzyl-1*H*-1,2,3-triazol-4-yl)methyl]amine TBTA (3.4 mg, 6.1 µmol) was dissolved in degassed MeOH (5 mL). An degassed aqueous solution (2 mL) of copper sulfate pentahydrate (2.55 mg, 10.2 µmol) was added followed by sodium ascorbate (8 mg, 41 µmol). The reaction mixture was stirred at room temperature under argon for 2h. The solvent was evaporated under reduced pressure and the crude product was purified by HPLC (C-18, isocratic 95:5 H_2O (+0,1%TFA) / MeCN (+0,1%TFA) for 5 min to 70:30 in 20 min), flow rate; 40

ml/min, detection UV(214 nm)). The product containing fractions of both regioisomers were separately freeze dried to yield **8 (A+B)** as dark violett powder (121 mg, 93%, 49 mg of **A**). **^{1}H NMR** (700 MHz, DMSO-d_6/D_2O 6:1), 5′-Isomer of **8** (**A**): δ = 8.59 (d, *J* = 1.8 Hz, 1H), 8.22 – 8.18 (m, 1H), 8.11 (s, 1H), 7.49 (d, *J* = 7.9 Hz, 1H), 6.95 (d, *J* = 9.3 Hz, 2H), 6.90 – 6.84 (m, 2H), 6.66 (d, *J* = 2.1 Hz, 2H), 5.76 (d, *J* = 9.6 Hz, 1H), 4.59 (t, *J* = 10.1 Hz, 2H), 4.32 (d, *J* = 7.8 Hz, 1H), 4.27 (t, *J* = 9.8 Hz, 1H), 3.86 (d, *J* = 9.5 Hz, 1H), 3.82 (d, *J* = 9.5 Hz, 1H), 3.77 (d, *J* = 9.7 Hz, 1H), 3.74 – 3.66 (m, 2H), 3.64 – 3.52 (m, 5H), 3.52 – 3.44 (m, 1H), 3.42 (t, *J* = 8.8 Hz, 1H), 3.33 (t, *J* = 9.4 Hz, 1H), 3.30 – 3.25 (m, 2H), 3.22 (t, *J* = 8.9 Hz, 1H), 3.15 (t, *J* = 8.3 Hz, 1H), 3.13 – 3.03 (m, 13H), 1.80 (s, 3H), 1.62 (s, 3H) ppm. **^{13}C NMR** (176 MHz, DMSO), 5′-Isomer of **8** (A): δ = 172.85, 172.39, 170.88, 169.76, 166.42, 166.34, 160.29, 160.10, 157.81, 157.01, 145.02, 136.63, 135.50, 131.65, 131.26, 131.04, 130.65, 130.11, 122.59, 114.63, 112.88, 103.29, 103.21, 101.28, 96.42, 86.08, 83.08, 82.81, 80.71, 78.94, 75.94, 75.41, 74.72, 73.97, 73.48, 72.74, 72.23, 71.36, 68.81, 68.20, 60.80, 60.44, 54.12, 53.58, 40.53, 34.99, 22.89, 22.44 ppm. **HRMS** (ESI) calcd for $C_{56}H_{68}N_8O_{26}$ [M-H^+]$^-$: 1267.417; found: 1267.422 m/z.

^{1}H NMR (700 MHz, DMSO-d_6/D_2O 6:1), 6′-Isomer of **8** (**B**): δ = 8.26 (d, *J* = 8.3 Hz, 1H), 8.13 (dd, *J* = 8.1, 1.7 Hz, 1H), 8.04 (s, 1H), 7.72 (d, *J* = 1.7 Hz, 1H), 6.96 (d, *J* = 9.4 Hz, 2H), 6.90 (dd, *J* = 9.5, 2.3 Hz, 2H), 6.79 (d, *J* = 2.2 Hz, 2H), 5.72 (d, *J* = 9.7 Hz, 1H), 4.53 – 4.45 (m, 2H), 4.43 (d, *J* = 7.8 Hz, 1H), 4.40 (d, *J* = 8.0 Hz, 1H), 4.28 – 4.26 (m, 1H), 4.22 (t, *J* = 10.0 Hz, 1H), 3.84 (d, *J* = 9.5 Hz, 1H), 3.79 (t, *J* = 9.4 Hz, 1H), 3.75 (d, *J* = 9.7 Hz, 1H), 3.71 (d, *J* = 10.9 Hz, 1H), 3.66 (d, *J* = 10.6 Hz, 1H), 3.62 – 3.50 (m, 5H), 3.44 (dt, *J* = 12.2, 7.4 Hz, 2H), 3.40 (t, *J* = 8.8 Hz, 1H), 3.32 (t, *J* = 9.4 Hz, 1H), 3.29 – 3.19 (m, 3H), 3.17 – 3.09 (m, 14H), 3.06 (t, *J* = 8.5 Hz, 1H), 1.79 (s, 3H), 1.55 (s, 3H) ppm. **^{13}C NMR** (176 MHz, DMSO), 6′-Isomer of **8** (**B**): δ = 172.45, 171.97, 170.74, 169.60, 166.30, 165.81, 159.78, 159.59, 157.90, 157.08, 144.87, 137.26, 133.77, 133.41, 131.78, 130.83, 129.29, 129.15, 122.44, 114.71, 113.05, 103.31, 101.31, 96.46, 86.04, 83.11, 82.85, 80.85, 79.04, 76.09, 75.52, 74.89, 74.07, 73.55, 72.82, 72.29, 71.43, 68.91, 68.23, 60.88, 60.44, 54.15, 53.47, 40.65, 34.98, 22.98, 22.50 ppm. **HRMS** (ESI) calcd for $C_{56}H_{68}N_8O_{26}$ [M-H^+]$^-$: 1267.417; found: 1267.421 m/z.

Hyaluronan hexasaccharide 5(6)TAMRA, HA-6-5(6)TAMRA, β-D-glucopyranuronyl-(1→3)-β-D-2-acetamido-2-deoxy-glucopyranosyl-(1→4)-β-D-glucopyranuronyl-(1→3)-β-D-2-acetamido-2-deoxy-gluco-pyranosyl-(1→4)-β-D-glucopyranuronyl-(1→3)-β-D-2-acetamido-2-deoxy-glucopyranosyl-1,2,3-triazol-4-yl-methyl-2-carbamoyl-5(6)-carboxytetramethylrhodamine (9)

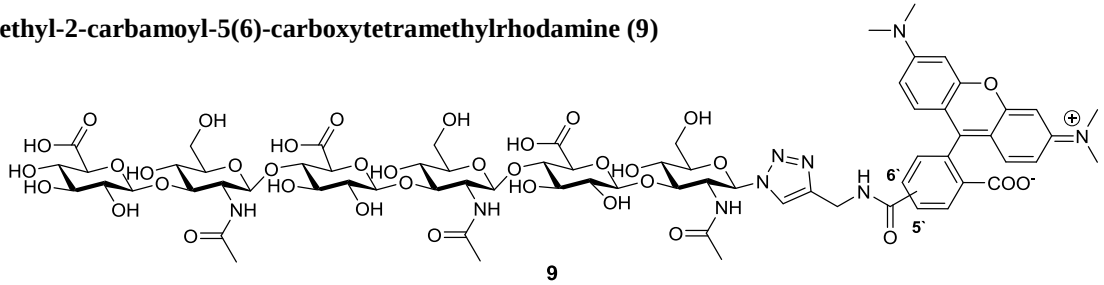

9

The hexahyaluronan azide **6** (88 mg, 0.074 mmol), 5(6)-TAMRA-Propargylamide **7** (52 mg, 0.085 mmol) and TBTA (2.4 mg, 4.47 μmol) was dissolved in degassed MeOH (4 mL). A degassed aqueous solution (1 mL) of copper sulfate pentahydrate (1.9 mg, 7.4 μmol) was added followed by sodium ascorbate (9 mg, 44 μmol). The reaction mixture was stirred at room temperature under argon for 4h. Solvent was evaporated under reduced pressure and the crude product was purified by HPLC (C-18, isocratic 95:5 H_2O (+0,1%TFA) / MeCN (+0,1%TFA) for 5 min to 40:60 in 20 min), flow rate; 40 ml/min, detection UV(214 nm)). The product containing fractions of both regioisomers were separately freeze dried to yield **9 (A+B)** as dark violett powder (97 mg, 79%, 37 mg of **A**). **^{1}H NMR** (700 MHz, DMSO-d_6) 5′-Isomer of **9** (A): δ = 8.62 (d, *J* = 1.8 Hz, 1H),

8.23 (dd, *J* = 7.9, 1.9 Hz, 1H), 8.09 (s, 1H), 7.51 (d, *J* = 7.9 Hz, 1H), 7.03 – 6.90 (m, 4H), 6.84 (d, *J* = 2.0 Hz, 2H), 5.77 (d, *J* = 9.6 Hz, 1H), 4.61 – 4.53 (m, 2H), 4.45 (d, *J* = 7.7 Hz, 1H), 4.43 – 4.36 (m, 3H), 4.31 (d, *J* = 7.8 Hz, 1H), 4.26 (t, *J* = 10.5 Hz, 2H), 3.87 – 3.79 (m, 3H), 3.73 (d, *J* = 9.7 Hz, 1H), 3.70 (d, *J* = 10.6 Hz, 3H), 3.60 – 3.52 (m, 8H), 3.48 – 3.42 (m, 3H), 3.42 – 3.36 (m, 2H), 3.31 (t, *J* = 9.4 Hz, 1H), 3.28 – 3.18 (m, 5H), 3.16 (s, 12H), 3.12 (t, *J* = 8.4 Hz, 1H), 3.08 (t, *J* = 8.4 Hz, 1H), 3.04 (t, *J* = 8.5 Hz, 1H), 1.78 (s, 6H), 1.62 (s, 6H) ppm; **^{13}C NMR** (176 MHz, DMSO), 5′-Isomer of **9** (B): δ = 172.15, 171.82, 170.65, 169.49, 166.18, 166.01, 159.77, 159.58, 158.10, 157.19, 157.12, 145.02, 136.63, 135.66, 131.68, 131.34, 131.07, 130.77, 130.14, 122.38, 114.87, 112.98, 103.36, 101.34, 96.53, 83.15, 83.01, 82.94, 76.17, 75.59, 74.99, 74.13, 74.08, 73.60, 73.56, 72.87, 72.35, 71.46, 68.94, 68.31, 60.91, 60.50, 54.17, 53.44, 40.71, 35.05, 23.05, 22.63 ppm; **HRMS** (ESI) calcd for $C_{70}H_{89}N_9O_{37}$ [M-H$^+$]$^-$: 1646.528; found: 1646.530 m/z.

^{1}H NMR (700 MHz, DMSO-d_6), 6′-Isomer of **9** (B): δ = 8.24 (d, *J* = 8.3 Hz, 1H), 8.11 – 8.08 (m, 1H), 8.04 (s, 1H), 7.68 (s, 1H), 6.95 (d, *J* = 9.4 Hz, 2H), 6.86 (dd, *J* = 9.5, 2.0 Hz, 2H), 6.76 (s, 2H), 5.70 (d, *J* = 9.6 Hz, 1H), 4.54 – 4.40 (m, 5H), 4.31 (d, *J* = 7.6 Hz, 1H), 4.21 (t, *J* = 9.9 Hz, 1H), 3.86 – 3.75 (m, 4H), 3.73 – 3.64 (m, 3H), 3.64 – 3.51 (m, 9H), 3.50 – 3.43 (m, 3H), 3.43 – 3.37 (m, 2H), 3.33 (t, *J* = 9.4 Hz, 1H), 3.30 – 3.20 (m, 5H), 3.17 – 3.05 (m, 16H), 1.79 (s, 3H), 1.79 (s, 3H), 1.54 (s, 3H) ppm. **^{13}C NMR** (176 MHz, DMSO), 6′-Isomer of **9** (A): δ = 172.87, 172.32, 170.88, 169.77, 166.44, 166.08, 160.46, 160.27, 157.72, 157.05, 144.78, 137.15, 133.76, 133.42, 131.79, 130.77, 129.28, 129.04, 122.50, 114.60, 112.98, 103.26, 103.18, 101.27, 96.44, 86.07, 83.05, 82.93, 82.70, 80.66, 78.87, 75.89, 75.40, 74.75, 73.91, 73.46, 72.72, 72.21, 71.35, 68.76, 68.14, 60.77, 60.38, 54.12, 53.57, 40.57, 34.94, 22.88, 22.37 ppm. **HRMS** (ESI) calcd for $C_{70}H_{89}N_9O_{37}$ [M-H$^+$]$^-$: 1646.528; found: 1646.535 m/z.

Hyaluronan tetrasaccharide Triazol (HA-4-Triazol, β-D-glucopyranuronyl-(1→3)-β-D-2-acetamido-2-deoxy-glucopyranosyl-(1→4)-β-D-glucopyranuronyl-(1→3)-β-D-2-acetamido-2-deoxy-glucopyranosyl-1,2,3-triazol (10)

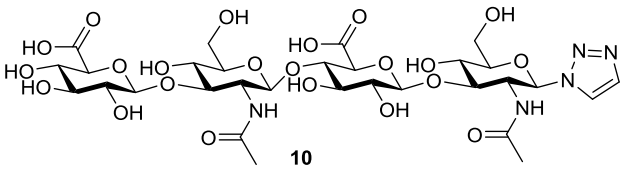

10

The tetrahyaluronan azide **5** [6] (77 mg, 0.096 mmol), Ethynyltrimethylsilane (27 µl, 0.192 mmol) and Tris[(1-benzyl-1*H*-1,2,3-triazol-4-yl)methyl]amine TBTA (3 mg, 5.7 µmol) was dissolved in degassed MeOH (3 mL). A degassed aqueous solution (1 mL) of copper sulfate pentahydrate (3.6 mg, 14.4 µmol) was added followed by sodium ascorbate (7.6 mg, 38 µmol). The reaction mixture was stirred at room temperature under argon for 2h. The solvent was evaporated under reduced pressure and the crude product dried in high vacuum. After dissolving the residue in THF:H_2O:AcOH 10:4:1 (6 mL), TBAF (96 µL, 1M TBAF in THF, 0.096 mmol) was added and the reaction mixture stirred for 16 h. The solvent was evaporated under reduced pressure and the crude product purified by HPLC (C-18, isocratic 95:5 H_2O (+0,1%TFA) / MeCN (+0,1%TFA) for 5 min to 70:30 in 20 min), flow rate; 40 ml/min, detection UV(214 nm)). The product containing fractions were freeze dried to yield **10** as white powder (60 mg, 76%). **^{1}H NMR** (500 MHz, D_2O) δ = 8.13 (s, 1H), 7.75 (s, 1H), 5.84 (d, *J* = 9.7 Hz, 1H), 4.52 (d, *J* = 7.9 Hz, 1H), 4.49 (d, *J* = 8.4 Hz, 1H), 4.45 (d, *J* = 7.9 Hz, 1H), 4.34 (t, *J* = 10.1 Hz, 1H), 3.95 (d, *J* = 9.8 Hz, 1H), 3.94 – 3.89 (m, 2H), 3.86 – 3.80 (m, 2H), 3.79 – 3.62 (m, 8H), 3.57 (dd, *J* = 9.5, 8.7 Hz, 1H), 3.53 – 3.38 (m, 5H), 3.30 (dd, *J* = 9.5, 7.9 Hz, 1H), 3.26 (dd, *J* = 9.3, 7.9 Hz, 1H), 1.91 (s, 3H), 1.69 (s, 3H) ppm.

^{13}C NMR (126 MHz, D_2O) δ = 175.29, 174.09, 171.98, 170.98, 163.03, 162.74, 134.91, 134.06, 124.84, 124.54, 102.91, 102.79, 102.57, 101.19, 101.11, 86.06, 86.01, 82.66, 82.57, 82.54, 82.20, 81.80, 80.22, 79.94, 78.62, 78.41, 75.38, 75.23, 75.04, 74.94, 74.31, 73.90, 73.62, 73.53, 73.11, 72.49, 72.29, 72.14, 71.94, 71.06, 68.21, 67.97, 67.74, 60.71, 60.53, 60.41, 60.18, 54.31, 54.25, 54.12, 54.02, 22.47, 22.21, 21.80, 21.47 ppm. **HRMS** (ESI) calcd for $C_{30}H_{45}KN_5O_{22}$ $[M+K^+]^+$: 866.218; found: 866.220 m/z.

3-β-D-Glucopyranuronyl-(1→3)-β-D-2-acetamido-2-deoxy-gluco-pyranosyl-(1→4)-β-D-glucopyranuronyl-(1→3)-β-D-2-acetamido-2-deoxy-glucopyranosyl-1-thio-methyl (12)

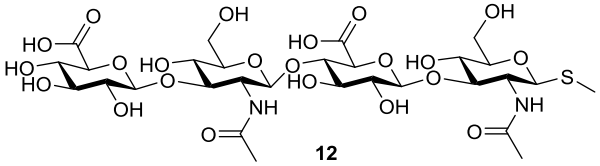

12

To a solution of β-D-glucopyranuronyl-(1→3)-β-D-2-acetamido-2-deoxy-gluco-pyranosyl-(1→4)-β-D-glucopyranuronyl-(1→3)-β-D-2-acetamido-2-deoxy-glucopyranosyl-1-thiobenzoate, HA-4-SBz [5] (72 mg, 0.08 mmol) in dry and degassed MeOH (10mL), Methyliodide (25 µL, 0.4 mmol) and sodium methoxide (43 mg, 0.8 mmol, 173 µL 25% wt. % in MeOH) was added. The solution was stirred for 16 h and evaporated under reduced pressure. The crude product was purified by HPLC (C-18, isocratic 95:5 H_2O (+0,1%TFA) / MeCN (+0,1%TFA) for 15 min), flow rate; 40 ml/min, detection UV(210 nm)). The product containing fractions were combined and freeze dried to yield **12** (41 mg, 63%) as white powder. **^{1}H NMR** (500 MHz, D_2O) δ = 4.58 – 4.55 (m, 2H), 4.54 – 4.51 (m, 2H), 4.03 – 3.99 (m, 2H), 3.96 – 3.70 (m, 10H), 3.65 (dd, *J* = 9.5, 8.7 Hz, 1H), 3.60 – 3.49 (m, 5H), 3.49 – 3.45 (m, 1H), 3.39 – 3.31 (m, 2H), 2.18 (s, 3H), 2.00 (s, 3H), 1.99 (s, 3H) ppm. **^{13}C NMR** (126 MHz, D_2O) δ = 174.89, 174.68, 172.19, 171.18, 103.15, 102.76, 101.36, 84.57, 84.06, 82.80, 80.29, 79.69, 75.50, 75.19, 74.33, 73.87, 73.46, 72.59, 72.25, 71.28, 68.56, 68.40, 60.99, 60.66, 54.37, 53.22, 22.53, 22.40, 11.99 ppm. **HRMS** (ESI) calcd for $C_{29}H_{46}N_2NaO_{22}S$ $[M+Na^+]^-$: 829.215; found: 829.217 m/z.

3-β-D-Glucopyranuronyl-(1→3)-β-D-2-acetamido-2-deoxy-gluco-pyranosyl-(1→4)-β-D-glucopyranuronyl-(1→3)-β-D-2-acetamido-1,5-anhydro-2-deoxy-sorbitol (13)

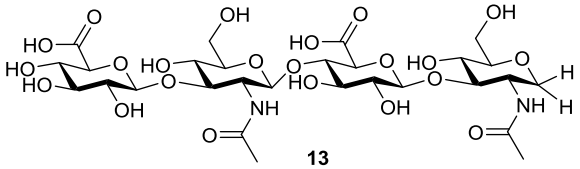

13

β-D-glucopyranuronyl-(1→3)-β-D-2-acetamido-2-deoxy-gluco-pyranosyl-(1→4)-β-D-glucopyranuronyl-(1→3)-β-D-2-acetamido-2-deoxy-glucopyranosyl-thiol, HA-4-SH[5] (66 mg, 0.083 mmol) and tris(2-carboxyethyl)phosphine, TCEP (26 mg, 0.091 mmol) were placed in UV-cuvette and dissolved in MeOH/H_2O 4:1 (2 mL). The photosensitizer 2-hydroxy-1-[4-(2-hydroxyethoxy)phenyl]-2-methyl-1-propanone, Irgacure 2959 (5 mg, 0.024 mmol) was added and the mixture stirred for 2h under irradiation with UV light from an Exo Terra Repti Glo 5.0 Compact lamp (UVB100, 25W, No. PT2187). The solvents were evaporated under reduced pressure and the crude product pre-cleaned on Sephadex G-10 column (22x3.5 cm, eluent: dest. water, product detected by TLC, EtOAc/MeOH/H_2O 4.5:2.5:2, vanilin-staining). The product was finally purified by HPLC (C-

18, isocratic 95:5 H_2O (+0,1%TFA) / MeCN (+0,1%TFA) for 8 min), flow rate; 40 ml/min, detection UV(210 nm)). The product containing fractions are combined and freeze dried to yield **13** (45 mg, 71%) as white powder. **^{1}H NMR** (700 MHz, D_2O) δ = 4.53 (dd, *J* = 7.9, 0.7 Hz, 1H), 4.50 (d, *J* = 8.5 Hz, 1H), 4.46 (d, *J* = 7.9 Hz, 1H), 3.97 – 3.91 (m, 3H), 3.85 – 3.75 (m, 4H), 3.74 (ddd, *J* = 9.6, 8.7, 0.8 Hz, 1H), 3.70 – 3.60 (m, 4H), 3.58 (ddd, *J* = 9.5, 8.7, 0.8 Hz, 1H), 3.53 – 3.48 (m, 2H), 3.46 – 3.40 (m, 3H), 3.32 – 3.25 (m, 3H), 3.19 (t, *J* = 11.3 Hz, 1H), 1.91 (s, 3H), 1.89 (s, 3H). ppm. **^{13}C NMR** (176 MHz, D_2O) δ = 176.03, 175.95, 174.67, 174.46, 171.85, 170.88, 102.56, 101.15, 83.78, 82.60, 80.08, 75.30, 75.00, 74.27, 73.66, 73.31, 72.39, 72.10, 71.06, 68.44, 68.20, 67.06, 60.83, 60.46, 54.16, 49.93, 22.33, 22.03 ppm. **HRMS** (ESI) calcd for $C_{28}H_{43}N_2O_{22}$ $[M\text{-}H^+]^-$: 759.2313 Da; found: 759.231 m/z.

(HA-4-S-PEG-S-)$_2$, 1-(β-D-Glucopyranuronyl-(1→3)-β-D-2-acetamido-2-deoxy-gluco-pyranosyl-(1→4)-β-D-glucopyranuronyl-(1→3)-β-D-2-acetamido-2-deoxy-β-D-glucopyranosyl)-thio-2-ethyloxy-2-ethylox-2-ethyl-disulfide (14)

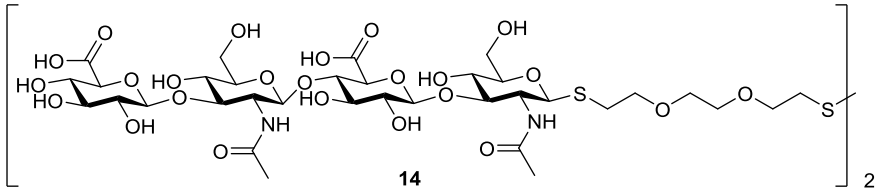

14

To a suspension of 1-(β-D-Glucopyranuronyl-(1→3)-β-D-2-acetamido-2-deoxy-gluco-pyranosyl-(1→4)-β-D-glucopyranuronyl-(1→3)-β-D-2-acetamido-2-deoxy-β-D-glucopyranosyl)-thio-2-ethyloxy-2-ethylox-2-ethyl-triphenylmethylthiol, HA-4-S-PEG-STrt [5] (58 mg, 0.05 mmol) in DCM/Triethylsilane 10:1 (1.1 mL), TFA/H_2O 10:1 (1.1 mL) was added. The solution was stirred for 5 min, evaporated under reduced pressure and dried in high vacuum. The residue was dissolved in 0.1M NaOH (5 mL) saturated with oxygen (by constant air bubbling) and stirred at 35°C until TLC (EtOAc/MeOH/H_2O 4.5:2.5:2, vanilin-staining) shows that the reaction is complete. The reaction mixture was dilluted with water (20 mL), extracted once with hexane (10 mL) to remove triphenylmethane and evaporated under reduced pressure. The crude product was purified by HPLC (C-18, isocratic 95:5 H_2O (+0,1%TFA) / MeCN (+0,1%TFA) for 12 min to 50:50 in 20 min), flow rate; 40 ml/min, detection UV(214 nm)). The product containing fractions were freeze dried to yield **14** as white powder (42 mg, 91%). **^{1}H NMR** (700 MHz, D_2O) δ = 5.18 (d, *J* = 3.9 Hz, 2H), 5.06 (t, *J* = 5.8 Hz, 4H), 4.92 (d, *J* = 6.4 Hz, 2H), 4.84 (dt, *J* = 5.1, 2.6 Hz, 4H), 4.79 (d, *J* = 10.3 Hz, 2H), 4.59 – 4.56 (m, 2H), 4.55 – 4.51 (m, 4H), 4.46 (s, 2H), 4.45 (d, *J* = 7.0 Hz, 2H), 4.42 – 4.39 (m, 2H), 4.31 (dt, *J* = 18.4, 9.1 Hz, 4H), 4.24 – 4.16 (m, 6H), 4.12 – 4.07 (m, 2H), 4.03 (t, *J* = 9.2 Hz, 2H), 3.89 (t, *J* = 8.8 Hz, 6H), 3.84 (t, *J* = 6.0 Hz, 2H), 3.82 – 3.78 (m, 5H), 3.74 (qdd, *J* = 10.7, 5.5, 1.3 Hz, 5H), 3.70 – 3.67 (m, 9H), 2.92 (td, *J* = 6.2, 1.6 Hz, 6H), 2.86 (dt, *J* = 13.5, 6.4 Hz, 2H), 2.12 (s, 6H), 2.08 (s, 6H) ppm. **^{13}C NMR** (176 MHz, D_2O) δ = 174.65, 174.46, 174.27, 174.18, 173.90, 100.89, 100.84, 99.87, 99.45, 99.39, 84.72, 79.67, 77.97, 77.13, 76.80, 76.77, 76.50, 76.44, 76.38, 75.65, 75.61, 75.52, 75.46, 75.32, 74.86, 74.80, 72.83, 72.77, 70.06, 69.38, 69.31, 68.39, 67.83, 67.77, 67.50, 67.46, 55.60, 54.42, 37.22, 30.23, 22.89, 22.68 ppm. **HRMS** (ESI) calcd for $C_{68}H_{108}N_4O_{48}S_4$ $[M\text{-}2H^+]^{2-}$: 938.251; found: 938.251 m/z.

General Sulfation Procedure:

To a solution of the starting material in dry DMF (c = 0.02 mol/l) sulfur trioxide pyridine complex (4 eq. per hydroxyl-group) was added and the solution was stirred for 4h at room temperature. Thereafter additional sulfur trioxide pyridine complex (2eq. per hydroxyl group) was added and the reaction mixture stirred for one hour. The reaction was stopped by the addition of 2 mL water, stirred for 2 minutes and the product precipitated by addition of sodium acetate (2.5-fold excess of used SO_3•Py-complex equivalents) solution in ethanol at 0 °C for 30 min. The crude product was filtered off, washed three times with cold ethanol and desalted by dialysis against destilled water (MWCO=1000Da)

Nona-sulfo hyaluronan tetrasaccharide triazol, 9s-HA-4-Triazol, 2,3,4,6-tetra-O-sulfo-β-D-glucopyranuronyl-(1→3)-4,6-di-O-sulfo-β-D-2-acetamido-2-deoxy-glucopyranosyl-(1→4)-2,3-di-O-sulfo-β-D-glucopyranuronyl-(1→3)-4,6-di-O-sulfo-β-D-2-acetamido-2-deoxy-glucopyranosyl-1,2,3-triazol (16)

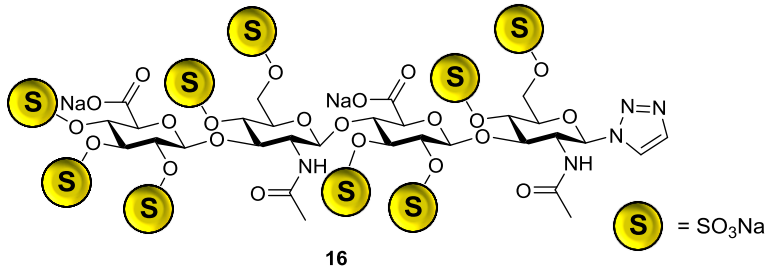

16

β-D-glucopyranuronyl-(1→3)-β-D-2-acetamido-2-deoxy-glucopyranosyl-(1→4)-β-D-glucopyranuronyl-(1→3)-β-D-2-acetamido-2-deoxy-glucopyranosyl-1,2,3-triazol **10** (60 mg, 0.072 mmol) was sulfated according to the general sulfation procedure to give **16** as colourless gum (97 mg, 61%). **^{1}H NMR** (700 MHz, D_2O) δ = 8.22 (s, 1H), 7.81 (s, 1H), 6.06 (d, *J* = 9.5 Hz, 1H), 5.21 (d, *J* = 3.1 Hz, 1H), 5.09 – 5.05 (m, 2H), 5.04 – 5.01 (m, 1H), 4.89 (dd, *J* = 4.4, 2.0 Hz, 2H), 4.79 (s, 1H), 4.63 – 4.58 (m, 2H), 4.58 – 4.51 (m, 2H), 4.51 – 4.47 (m, 1H), 4.45 – 4.39 (m, 3H), 4.34 – 4.29 (m, 1H), 4.28 – 4.15 (m, 5H), 3.93 – 3.88 (m, 1H), 3.87 – 3.81 (m, 1H), 2.14 (s, 3H), 1.85 (s, 3H) ppm. **^{13}C NMR** (176 MHz, D_2O) δ = 174.40, 174.36, 172.43, 172.19, 134.33, 125.09, 100.37 (d, *J* = 11.2 Hz), 99.98, 99.35 (d, *J* = 10.9 Hz), 85.51, 78.94, 77.81, 77.74, 77.20, 77.12, 76.33 (d, *J* = 8.1 Hz), 75.63, 75.31 (d, *J* = 10.4 Hz), 75.17, 75.06, 73.95, 73.90, 72.90 (d, *J* = 10.2 Hz), 67.36, 55.52, 54.98, 22.81, δ 22.09 (d, *J* = 6.2 Hz) ppm. For MS-analysis see below.

Nona-sulfo hyaluronan tetrasaccharide 5(6)TAMRA, 9s-HA-4-5(6)TAMRA, 2,3,4,6-tetra-O-sulfo-β-D-glucopyranuronyl-(1→3)-4,6-di-O-sulfo-β-D-2-acetamido-2-deoxy-glucopyranosyl-(1→4)-2,3-di-O-sulfo-β-D-glucopyranuronyl-(1→3)-4,6-di-O-sulfo-β-D-2-acetamido-2-deoxy-glucopyranosyl-1,2,3-triazol-4-yl-methyl-2-carbamoyl-5(6)-carboxytetramethylrhodamine (15A+15B)

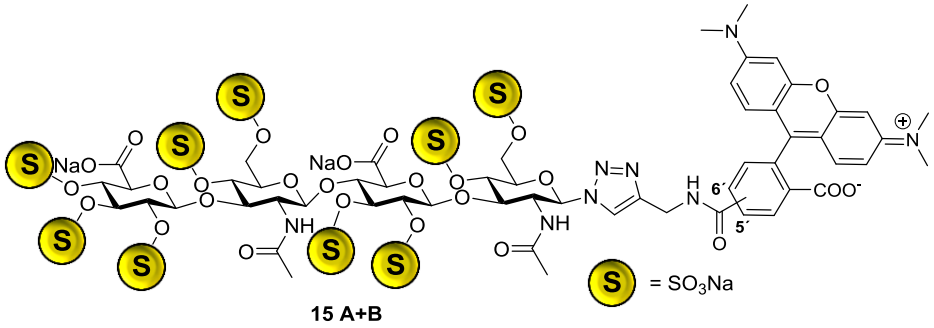

15 A+B

Hyaluronan tetrasaccharide (5′)TAMRA, HA-4-(5′)TAMRA, β-D-glucopyranuronyl-(1→3)-β-D-2-acetamido-2-deoxy-glucopyranosyl-(1→4)-β-D-glucopyranuronyl-(1→3)-β-D-2-acetamido-2-deoxy-glucopyranosyl-1,2,3-triazol-4-yl-methyl-2-carbamoyl-5-carboxytetra-methylrhodamine **8A** (65 mg, 0.052 mmol) and Hyaluronan tetrasaccharide (6′)TAMRA, HA-4-(6′)TAMRA, β-D-glucopyranuronyl-(1→3)-β-D-2-acetamido-2-deoxy-glucopyranosyl-(1→4)-β-D-glucopyranuronyl-(1→3)-β-D-2-acetamido-2-deoxy-glucopyranosyl-1,2,3-triazol-4-yl-methyl-2-carbamoyl-6′-carboxytetramethylrhodamine **8B** (51 mg, 0.040 mmol) were separately sulfated according to the general sulfation procedure to give **15A+15B** as dark violett powder (95 mg, 82% for 15A the 5′-Isomer) and (55 mg, 61% for **15B** the 6′-Isomer **^{1}H NMR** (700 MHz, D_2O) of **15A** the 5′-isomer: δ = 8.46 (s, 1H), 8.27 (s, 1H), 8.14 (d, *J* = 7.8 Hz, 1H), 7.58 (d, *J* = 7.8 Hz, 1H), 7.07 (d, *J* = 9.4 Hz, 2H), 6.81 – 6.69 (m, 2H), 6.12 – 6.04 (m, 2H), 6.03 (d, *J* = 9.6 Hz, 1H), 5.20 (d, *J* = 4.1 Hz, 1H), 5.08 – 5.04 (m, 2H), 5.01 (d, *J* = 4.1 Hz, 1H), 4.93 – 4.85 (m, 2H), 4.79 (s, 1H), 4.78 – 4.72 (m, 2H), 4.64 – 4.57 (m, 2H), 4.55 – 4.47 (m, 3H), 4.45 – 4.38 (m, 3H), 4.32 – 4.11 (m, 5H), 4.11 – 4.04 (m, 1H), 3.90 – 3.84 (m, 1H), 3.84 – 3.73 (m, 1H), 2.97 (s, 12H), 2.13 (s, 3H), 1.82 (s, 3H) ppm; **^{13}C NMR** (176 MHz, D_2O) of **15A** the 5′-isomer: δ = 174.35, 174.21, 172.26, 171.94, 170.22, 168.66, 157.18, 156.67, 156.63, 145.25, 135.78, 135.03, 130.91, 130.65, 130.32, 128.88, 123.38, 113.99, 112.77, 100.35, 99.90, 99.43, 95.93, 85.70, 78.88, 77.75, 77.22, 77.09, 76.35, 75.75, 75.51, 75.23, 75.06, 73.78, 72.89, 67.37, 67.34, 55.49, 55.03, 40.04, 35.10, 22.82, 22.11ppm. For MS-analysis see below.

^{1}H NMR (700 MHz, D_2O) of **15B** the 6′-isomer: δ = 8.13 – 8.02 (m, 2H), 7.98 (d, *J* = 8.4 Hz, 1H), 7.67 (s, 1H), 6.90 (s, 2H), 6.65 – 6.58 (m, 1H), 6.55 (d, *J* = 9.4 Hz, 1H), 6.33 – 6.12 (m, 2H), 5.91 (d, *J* = 8.8 Hz, 1H), 5.19 (d, *J* = 3.7 Hz, 1H), 5.05 (d, *J* = 6.9 Hz, 1H), 5.02 (d, *J* = 6.0 Hz, 1H), 5.00 (d, *J* = 3.9 Hz, 1H), 4.87 (s, 1H), 4.82 (s, 1H), 4.79 (s, 1H), 4.60 – 4.49 (m, 5H), 4.47 – 4.35 (m, 4H), 4.30 (t, *J* = 9.3 Hz, 1H), 4.27 – 4.20 (m, 2H), 4.20 – 4.01 (m, 4H), 3.87 (t, *J* = 8.6 Hz, 1H), 3.82 (s, 1H), 2.93 (s, 12H), 2.10 (s, 3H), 1.79 (s, 3H) ppm. **^{13}C NMR** (176 MHz, D_2O) of **15B** the 6′-isomer: δ = 174.51, 174.23, 172.29, 171.94, 170.11, 167.38, 156.94, 156.67, 156.44, 144.84, 137.08, 135.25, 132.55, 130.78, 130.53, 129.52, 128.38, 122.68, 113.72, 112.59, 112.51, 100.45, 99.68, 99.39, 95.99, 85.67, 78.59, 77.75, 77.37, 77.06, 76.39, 75.69, 75.34, 75.24, 75.19, 75.12, 73.81, 72.89, 67.34, 55.39, 55.22, 39.98, 35.31, 22.74, 22.04 ppm.

Nona-sulfo hyaluronan hexasaccharide 5(6)TAMRA, 9s-HA-6-5(6)TAMRA, 2,3,4,6-tetra-O-sulfo-β-D-glucopyranuronyl-(1→3)-4,6-di-O-sulfo-β-D-2-acetamido-2-deoxy-glucopyranosyl-(1→4)-2,3,4,6-tetra-O-sulfo-β-D-glucopyranuronyl-(1→3)-4,6-di-O-sulfo-β-D-2-acetamido-2-deoxy-glucopyranosyl-(1→4)-2,3-di-O-sulfo-β-D-glucopyranuronyl-(1→3)-4,6-di-O-sulfo-β-D-2-acetamido-2-deoxy-glucopyranosyl-1,2,3-triazol-4-yl-methyl-2-carbamoyl-5(6)-carboxytetramethylrhodamine (19A+19B)

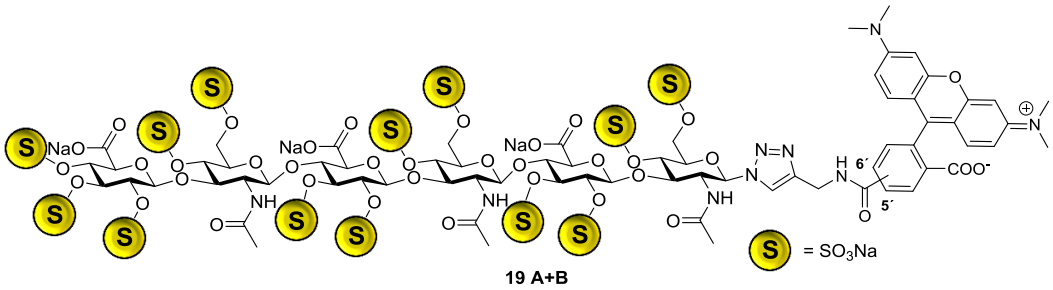

19 A+B

Hyaluronan hexasaccharide (5′)TAMRA, HA-6-(5′)TAMRA, β-D-glucopyranuronyl-(1→3)-β-D-2-acetamido-2-deoxy-glucopyranosyl-(1→4)-β-D-glucopyranuronyl-(1→3)-β-D-2-acetamido-2-deoxy-glucopyranosyl-1,2,3-triazol-4-yl-methyl-2-carbamoyl-5`-carboxytetra-methylrhodamine **9A** (58 mg, 0.035 mmol) and Hyaluronan hexasaccharide (6′)TAMRA, HA-6-(6′)TAMRA, β-D-glucopyranuronyl-(1→3)-β-D-2-acetamido-2-deoxy-glucopyranosyl-(1→4)-β-D-glucopyranuronyl-(1→3)-β-D-2-acetamido-2-deoxy-glucopyranosyl-1,2,3-triazol-4-yl-methyl-2-carbamoyl-6′-carboxytetramethylrhodamine **9B** (39 mg, 0.023 mmol) were separately sulfated according to the general sulfation procedure to give **19A+19B** as dark violett powder (65 mg, 61% for **19A** the 5′-Isomer) and (55 mg, 76% for **19B** the 6′-Isomer). **^{1}H NMR** (700 MHz, D_2O) of **19A** the 5′-isomer: δ = 8.26 (s, 2H), 8.12 – 8.08 (m, 1H), 7.67 (d, *J* = 7.8 Hz, 1H), 7.14 (dd, *J* = 14.5, 9.5 Hz, 2H), 6.80 (d, *J* = 9.5 Hz, 2H), 6.32 (s, 2H), 6.02 (d, *J* = 9.6 Hz, 1H), 5.17 (s, 1H), 5.05 (d, *J* = 7.8 Hz, 1H), 5.04 (d, *J* = 3.8 Hz, 1H), 4.97 (d, *J* = 6.4 Hz, 1H), 4.91 (s, 1H), 4.88 – 4.79 (m, 4H), 4.76 – 4.73 (m, 2H), 4.63 – 4.47 (m, 6H), 4.47 – 4.38 (m, 5H), 4.35 – 4.08 (m, 11H), 3.90 – 3.78 (m, 4H), 3.05 (s, 12H), 2.15 (s, 3H), 2.09 (s, 3H), 1.84 (s, 3H) ppm. **^{13}C NMR** (176 MHz, D_2O) δ = 174.70, 174.59, 174.25, 173.51, 173.18, 172.99, 169.33, 157.78, 156.82, 144.91, 139.86, 134.94, 134.65, 130.79, 130.41, 128.64, 127.60, 123.29, 113.91, 112.82, 101.40, 100.95, 100.05, 99.70, 99.45, 96.12, 85.71, 79.03, 78.60, 77.97, 77.80, 77.36, 76.78, 76.56, 76.11, 75.93, 75.77, 75.60, 75.36, 75.04, 74.53, 72.78, 67.52, 67.40, 67.34, 55.36, 55.09, 40.01, 35.01, 23.11, 22.79, 22.10 ppm. For MS-analysis see below.

^{1}H NMR (700 MHz, D_2O) of **19A** the 6′-isomer: δ = 8.14 (d, *J* = 8.3 Hz, 1H), 8.05 (s, 1H), 7.99 (d, *J* = 7.9 Hz, 1H), 7.66 (s, 1H), 6.89 (s, 2H), 6.70 – 6.53 (m, 2H), 6.44 – 6.25 (m, 2H), 5.90 (d, *J* = 9.4 Hz, 1H), 5.19 (d, *J* = 4.2 Hz, 1H), 5.05 (d, *J* = 6.8 Hz, 1H), 5.03 (d, *J* = 6.1 Hz, 1H), 5.02 – 4.98 (m, 2H), 4.90 – 4.81 (m, 5H), 4.62 – 4.52 (m, 7H), 4.50 (s, 1H), 4.46 (s, 1H), 4.44 – 4.38 (m, 3H), 4.36 (d, *J* = 5.1 Hz, 1H), 4.34 – 4.29 (m, 2H), 4.29 – 4.23 (m, 1H), 4.23 – 4.11 (m, 5H), 4.10 – 4.06 (m, 1H), 4.03 (s, 1H), 3.92 – 3.80 (m, 4H), 2.99 (d, *J* = 28.9 Hz, 12H), 2.12 (s, 3H), 2.08 (s, 3H), 1.80 (s, 3H) ppm. **^{13}C NMR** (176 MHz, D_2O) δ = 174.55, 174.17, 172.05, 171.69, 169.24, 167.43, 156.82, 156.54, 156.48, 144.74, 135.71, 133.03, 130.95, 130.74, 130.61, 129.47, 128.51, 122.70, 113.81, 112.60, 112.51, 100.64, 100.30, 100.21, 99.79, 99.35, 96.08, 85.73, 79.02, 78.53, 77.90, 77.80, 77.71, 77.60, 76.71, 76.61, 76.49, 76.34, 76.24, 75.82, 75.67, 75.44, 75.18, 75.08, 74.99, 73.66, 72.95, 67.46, 67.33, 55.24, 54.91, 40.11, 40.01, 35.37, 22.99, 22.68, 22.02 ppm.

Nona-sulfo hyaluronan tetrasaccharide thiomethyl, 9s-HA-4-SMe, 2,3,4,6-tetra-O-sulfo-β-D-glucopyranuronyl-(1→3)-4,6-di-O-sulfo-β-D-2-acetamido-2-deoxy-glucopyranosyl-(1→4)-2,3-di-O-sulfo-β-D-glucopyranuronyl-(1→3)-4,6-di-O-sulfo-β-D-2-acetamido-2-deoxy-glucopyranosyl-1-thio-methyl (17)

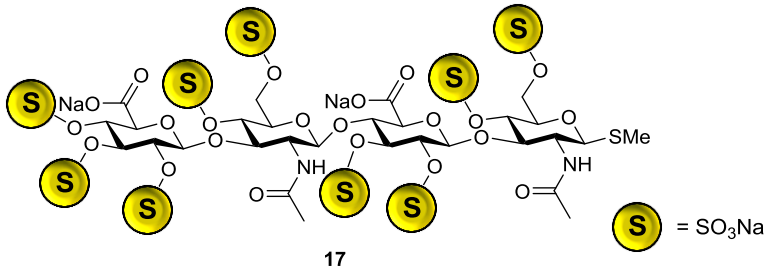

17

3-β-D-Glucopyranuronyl-(1→3)-β-D-2-acetamido-2-deoxy-gluco-pyranosyl-(1→4)-β-D-glucopyranuronyl-(1→3)-β-D-2-acetamido-2-deoxy-glucopyranosyl-1-thio-methyl **12** (35 mg, 0.043 mmol) was sulfated according to the general sulfation procedure to give **17** as colourless gum (36 mg, 47%). **^{1}H NMR** (700 MHz, D_2O) δ = 5.21 – 5.17 (m, 1H), 5.06 (dd, *J* = 10.2 Hz, 6.6 Hz, 2H), 4.98 (d, *J* = 4.2 Hz, 1H), 4.90 – 4.86 (m, 3H), 4.65 – 4.61 (m, 1H), 4.59 (t, *J* = 3.5 Hz, 1H), 4.55 – 4.49 (m, 3H), 4.42 – 4.36 (m, 2H), 4.31 – 4.24 (m, 2H), 4.16 (dd, *J* = 11.4 Hz, 6.3 Hz, 2H), 4.09 (dd, *J* = 11.4, 7.5 Hz, 1H), 3.97 – 3.81 (m, 5H), 2.16 (s, 3H), 2.08 (s, 3H), 2.06 (s, 3H) ppm. **^{13}C NMR** (176 MHz, D_2O) δ = 174.74, 174.39, 171.98, 171.54, 99.98, 99.90, 99.34, 99.25, 84.40, 80.04, 79.97, 77.99, 77.91, 77.83, 77.79, 77.65, 76.55, 76.47, 76.09, 76.05, 75.96, 75.89, 75.64, 75.58, 75.39, 75.20, 75.12, 73.55, 73.47, 72.99, 72.91, 67.77, 67.68, 67.39, 67.31, 55.35, 53.76, 22.59, 22.55, 12.06 ppm. For MS-analysis see below.

Nona-sulfo hyaluronan tetrasaccharide triazol, 9s-HA-4-H,H; 2,3,4,6-tetra-O-sulfo-β-D-glucopyranuronyl-(1→3)-4,6-di-O-sulfo-β-D-2-acetamido-2-deoxy-glucopyranosyl-(1→4)-2,3-di-O-sulfo-β-D-glucopyranuronyl-(1→3)-4,6-di-O-sulfo-β-D-2-acetamido-1,5-anhydro-2-deoxy-sorbitol (18)

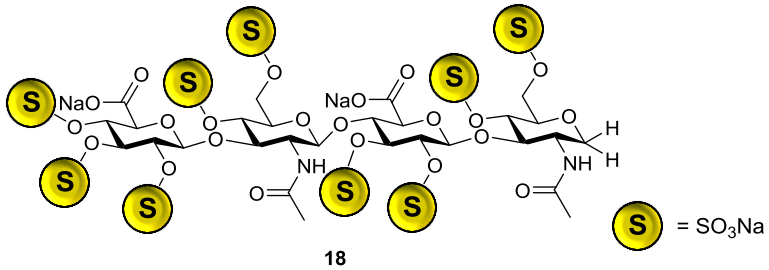

18

3-β-D-Glucopyranuronyl-(1→3)-β-D-2-acetamido-2-deoxy-gluco-pyranosyl-(1→4)-β-D-glucopyranuronyl-(1→3)-β-D-2-acetamido-1,5-anhydro-2-deoxy-sorbitol **13** (43 mg, 0.056 mmol) was sulfated according to the general sulfation procedure to give **18** as colourless powder (70 mg, 72%). **^{1}H NMR** (700 MHz, D_2O) δ = 5.19 (d, *J* = 4.0 Hz, 1H), 5.09 – 5.03 (m, 2H), 4.93 (d, *J* = 6.8 Hz, 1H), 4.82 (d, *J* = 7.2 Hz, 1H), 4.77 (dd, *J* = 5.2, 3.2 Hz, 1H), 4.59 – 4.54 (m, 2H), 4.46 (t, *J* = 4.5 Hz, 1H), 4.43 (d, *J* = 7.0 Hz, 1H), 4.42 – 4.39 (m, 2H), 4.36 – 4.27 (m, 3H), 4.18 (dt, *J* = 11.1, 5.1 Hz, 3H), 4.04 – 3.95 (m, 4H), 3.91 – 3.80 (m, 2H), 3.41 (td, *J* = 8.6, 7.5, 4.2 Hz, 1H), 2.10 (s, 3H), 2.05 (s, 3H) ppm. **^{13}C NMR** (176 MHz, D_2O) δ = 174.43, 173.85, 173.57, 100.55, 99.68, 99.34, 79.54, 78.92, 77.93, 77.72, 77.35, 77.13, 77.03, 76.22, 75.49, 75.44, 75.26, 74.70, 72.76 (d, *J* = 7.3 Hz), 67.46, 66.63, 64.00, 55.52, 49.12, 22.83, 22.35 ppm. For MS-analysis see below.

(9s-HA-4-S-PEG-S)$_2$, 2,3,4,6-tetra-O-sulfo-β-D-glucopyranuronyl-(1→3)-4,6-di-O-sulfo-β-D-2-acetamido-2-deoxy-glucopyranosyl-(1→4)-2,3-di-O-sulfo-β-D-glucopyranuronyl-(1→3)-4,6-di-O-sulfo-β-D-2-acetamido-2-deoxy-glucopyranosyl-1-thio-2-ethyloxy-2-ethylox-2-ethyl-disulfide (20)

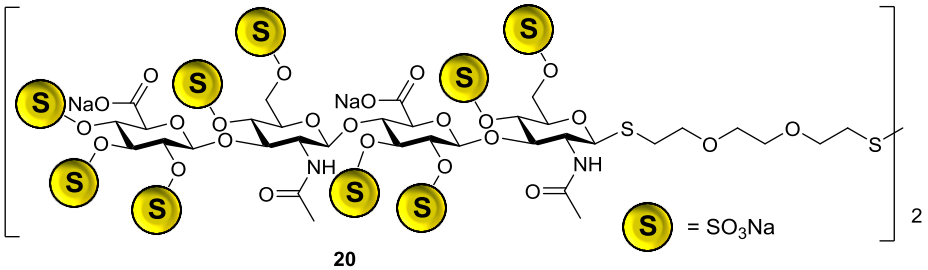

20

1-(β-D-Glucopyranuronyl-(1→3)-β-D-2-acetamido-2-deoxy-gluco-pyranosyl-(1→4)-β-D-glucopyranuronyl-(1→3)-β-D-2-acetamido-2-deoxy-β-D-glucopyranosyl)-thio-2-ethyloxy-2-ethylox-2-ethyl-disulfide **14** (40 mg, 0.021 mmol) was sulfated according to the general sulfation procedure to give **20** as colourless gum (60 mg, 74%). **^{1}H NMR** (700 MHz, D_2O) δ = 5.18 (d, *J* = 3.9 Hz, 1H), 5.08 – 5.04 (m, 2H), 4.92 (d, *J* = 6.4 Hz, 1H), 4.87 – 4.82 (m, 2H), 4.79 (d, *J* = 10.3 Hz, 1H), 4.59 – 4.56 (m, 1H), 4.55 – 4.51 (m, 2H), 4.46 (s, 1H), 4.45 (d, *J* = 7.0 Hz, 1H), 4.42 – 4.39 (m, 1H), 4.34 – 4.27 (m, 2H), 4.24 – 4.16 (m, 3H), 4.12 – 4.07 (m, 1H), 4.03 (t, *J* = 9.2 Hz, 1H), 3.92 – 3.87 (m, 3H), 3.87 – 3.82 (m, 1H), 3.82 – 3.78 (m, 2H), 3.77 – 3.70 (m, 2H), 3.70 – 3.67 (m, 4H), 2.96 – 2.91 (m, 3H), 2.86 (dt, *J* = 13.5, 6.4 Hz, 1H), 2.12 (s, 3H), 2.08 (s, 3H) ppm. **^{13}C NMR** (176 MHz, D_2O) δ = 174.65, 174.46, 174.27, 173.90, 100.86 (d, *J* = 8.5 Hz), 99.87, 99.42 (d, *J* = 11.1 Hz), 84.72, 79.67, 79.37, 79.25, 77.97, 77.13, 76.78 (d, *J* = 6.2 Hz), 76.50, 76.44, 76.38, 75.63 (d, *J* = 5.4 Hz), 75.49 (d, *J* = 11.0 Hz), 75.32, 74.83 (d, *J* = 9.9 Hz), 72.80 (d, *J* = 10.9 Hz), 70.06, 69.38, 69.31, 68.39, 67.80 (d, *J* = 9.7 Hz), 67.48 (d, *J* = 7.6 Hz), 55.60, 54.42, 37.22, 30.23, 22.89, 22.68 ppm. For MS-analysis see below.

Di-sulfo hyaluronan tetrasaccharide (2s-HA-4-N_3; β-D-glucopyranuronyl-(1→3)- β-D-2-acetamido-2-deoxy-6-sodium sulfo-glucopyranosyl-(1→4)- β-D-glucopyranuronyl-(1→3)- β-D-2-acetamido-2-deoxy-6-sodium sulfo-glucopyranosyl-1-azide (21)

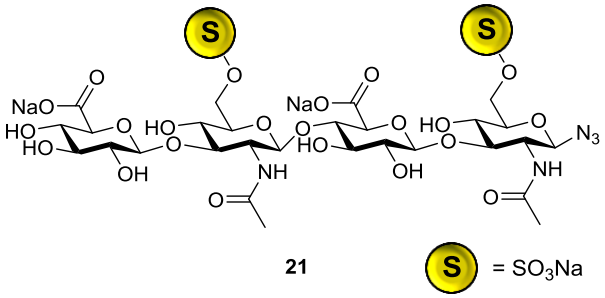

21

Respective amount of HA-4-azide **5** (55 mg, 0.069 mmol) was dissolved in dry DMF (~10 wt%) and kept under an inert argon atmosphere. Sulfur trioxide pyridine complex (66 mg; 0.412 mmol, 6.0 eq.) was added at 0 °C. After 1 h of stirring, the ice bath was removed and the solution was stirred over night at room temperature. The reaction was quenched with sodium acetate (68 mg, 0.829 mmol, 2.0 eq./$PySO_3$) in methanol. The solvent was evaporated under reduced pressure, the residue was dissolved in water and chromatographed on Macro-Prep® DEAE resin (20 mm x 180 mm, gradient: 0 – 1 M NaCl-solution, flow rate: 6 mL·min^{-1}). The product was replaced from Macro-Prep® DEAE resin by approximately 0,4 M NaCl-solution. Product fractions were combined, evaporated under reduced pressure and desalted two times by Sephadex G-10 (25 mm x 220 mm, eluent: deionized water). Freeze drying of the product-containing fractions gave a white, fluffy powder (26 mg,

35 %).**^{1}H-NMR (700 MHz, D_2O):** δ [ppm] = 4.86 (d, $J_{1,2}$ = 8.5 Hz, 1H, H-1/I); 4.63 (d, $J_{1,2}$ = 9.0 Hz, 1H, H-1/III); 4.56 (d, $J_{1,2}$ = 8.5 Hz, 1H, H-1/II); 4.54 (d, $J_{1,2}$ = 8.2 Hz, 1H, H-1/IV); 4.41 -4.39 (dd, *J* = 10.0, 5.5 Hz, 2H, H-6´/I, H-6´/III); 4.28 - 4.26 (dd, *J* = 10.0, 5.5 Hz, 2H, H-6´´/I, H-6´´/III); 3.95 – 3.91 (m, 2H, H-5/IV; H-5/II); 3.90 – 3.86 (m, 2H, H-2/I; H-2/III); 3.85 – 3.78 (m, 4H, H-4/II; H-3/I, H-3/III, H-5/I); 3.75 (m, 1H, H-5/III); 3.68 – 3.61 (m, 3H, H-3/II; H-4/I, H-4/III), 3.59 (m, 1H, H-4/IV); 3.54 (m, 1H, H-3/IV); 3.40 (m, 1H, H-2/II); 3.37 (m, 1H, H-2/IV); 2.06 (s, 3H, CH_3/III); 2.04 (s, 3H, CH_3/I). **^{13}C-NMR (176 MHz, D_2O):** δ [ppm] = 174.80 (N*C*=O/III), 174.78 (N*C*=O/I), 173.37 (*C*OOH/IV), 172.08 (*C*OOH/II), 103.00 (C-1/IV), 102.73 (C-1/II), 101.22 (C-1/III), 88.60 (C-1/I), 82.20 (C-3/III), 81.76 (*C*-3/I), 80.86 (*C*-4/II), 75.40 (*C*-5/I), 75.14 (*C*-3/IV), 74.98 (*C*-5/II), 74.62 (*C*-5/IV), 73.72 (*C*-3/II), 73.26 (*C*-5/III), 72.55 (*C*-2/IV), 72.17 (*C*-2/II), 71.37 (*C*-4/IV), 68.17 (*C*-4/III), 67.92 (*C*-4/I), 67.05 (*C*-6/III), 66.95 (*C*-6/I), 54.17 (*C*-2/III), 53.91 (*C*-2/I), 22.44 (NHCO*C*H$_3$/III), 22.19 (NHCO*C*H$_3$/I). For MS-analysis see below**.**

Penta-sulfo hyaluronan tetrasaccharide (5s-HA-4-N_3; β-D-2,3,4-sodium sulfo-glucopyranuronyl-(1→3)- β-D-2-acetamido-2-deoxy-glucopyranosyl-(1→4)- β-D-2,3-sodium-sulfo-glucopyranuronyl-(1→3)- β-D-2-acetamido-2-deoxy-glucopyranosyl-1-azide sodium salt (22)

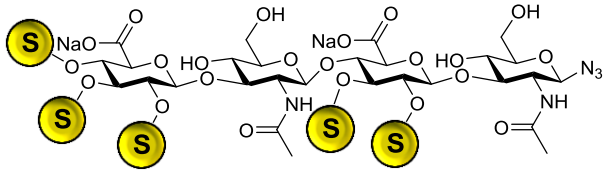

22

HA-4-azide **5** (50 mg, 0.062 mmol) was dissolved in 1 mL dry DMF, freshly dried molsieve powder (4 Å) and phenyl boronic acid (114 mg, 0.936 mmol) was added. The mixture was stirred at 80 °C under inert atmosphere overnight. Sulfur trioxide pyridine complex (199 mg, 1.248 mmol, 4.0 eq./OH) was added and stirred for 1 h at 40 °C. The reaction was quenched by stirring the solution with sodium acetate (205 mg, 2.501 mmol, 2.0 eq./$PySO_3$) dissolved in 5 mL methanol for 10 min at room temperature. Solvent was evaporated under reduced pressure, the residue was suspended in water and filtered over a filter paper. The residue was extensively washed with water (5 x 5 mL) and the filtrate was evaporated under reduced pressure. Intense Dialysis against water (cellulose acetate membrane; MWCO = 100 – 500 Da) for 3 days and freeze drying of the clear liquid gave a white, fluffy powder (38 mg, 45 %) **^{1}H NMR** (700 MHz, D_2O) δ [ppm] = 5.18 (s, 1H, H-3/IV), 5.08 -5.05 (m, 2H, H-1/III, H-1/I), 5.06-5.02 (m, 2H, H-1/II, H-1/IV), 4.92 (s, 1H, H-4/IV), 4.48 (s, 2H, H-3/II, H-5/I), 4.46 – 4.45 (dd, *J* = 4.4, 2.0 Hz, 2H, H-5/IV; H-5/II), 4.42 – 4.30 (m, 2H, H-5/III, H-2/I;), 4.32 (s, 2H, H-3/I, H-3/III), 4.03 – 4.01 (m, 2H, H-2/IV, H-2/II), 3.90 – 3.84 (m, 3H, H-6´´/III; H-4/I, H-4/III), 3.65-3.55 (m, 2H, H-6´/I, H-6´/III), 2.14 (s, 6H, CH_3/III, CH_3/I).**^{13}C NMR** (176 MHz, D_2O) δ [ppm] = 181.09 (N*C*=O/III), 174.98 (N*C*=O/I), 174.74 (*C*OOH/IV), 174.73 (*C*OOH/II), 100.58 (C-1/IV), 100.16 (C-1/II), 99.30 (C-1/III), 88.31 (C-1/I), 79.54 (*C*-4/II), 78.70 (C-3/III), 77.95 (*C*-2/IV, *C*-2/II), 76.87 (*C*-5/I), 75.47 (*C*-3/IV, *C*-3/II)), 75.13 (*C*-5/II), 74.64 (*C*-3/I, *C*-3/III), 69.07 (*C*-5/IV), 68.68 (*C*-4/III, *C*-4/I), 60.59 (*C*-6/III, *C*-6/I), 55.61 (*C*-2/III), 54.47 (*C*-2/I), 22.81(NHCO*C*H$_3$/III), 22.57 (NHCO*C*H$_3$/I). ESI-MS could not be detected due to unsufficient ionization.

Hepta-sulfo hyaluronan tetrasaccharide (7s-HA-4-N_3; β-D-2,3,4-sodium sulfo-glucopyranuronyl-(1→3)- β-D-2-acetamido-2-deoxy-4-sodium sulfo-glucopyranosyl-(1→4)- β-D-glucopyranuronyl-(1→3)- β-D-2-acetamido-2-deoxy-4-sodium sulfo -glucopyranosyl-1-azide sodium salt (23)

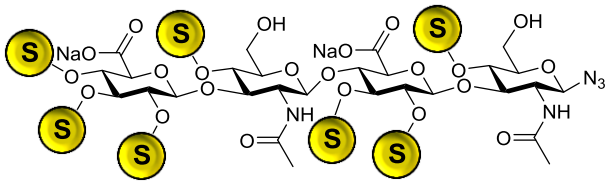

23

HA-4-azide **5** (50 mg, 0.062 mmol) was dissolved in 1 mL dry pyridine, 4,4′-Dimethoxytrityl chloride (211 mg; 0.623 mmol, 10.0 eq.) was added and the solution was stirred at 85 °C under inert atmosphere overnight. Sulfur trioxide pyridine complex (278 mg, 1.747 mmol, 4.0 eq./OH) was added and stirred for 6 h at 40 °C. The reaction was quenched by stirring the solution with sodium acetate (287 mg, 3.495 mmol, 2.0 eq./PySO_3) and a solid precipitated in methanol. The solid was filtered over a filter paper, re-dissolved in water and treated with 2 mL of 1,1,1,3,3,3-Hexafluoro-2-propanol for 40 min. The solvent was evaporated under reduced pressure. Intense Dialysis against water (cellulose acetate membrane; MWCO = 100 – 500 Da) for 3 days and freeze drying of the clear liquid gave a white, fluffy powder (37 mg, 38 %). **^{1}H NMR** (700 MHz, D_2O) δ [ppm] = 5.20 (s, 1H, H-3/IV), 5.09 -5.02 (m, 3H, H-1/III, H-1/I, H-1/II), 4.89 (dd, *J* = 4.4, 2.0 Hz, 2H, H-1/IV, H-4/IV), 4.79 (s, 1H, H-3/II), 4.56 – 4.54 (m, 3H, H-3/II, H-4/I, H-4/III), 4.42 – 4.39 (m, 3H, H-5/II, H-5/III, H-2/I), 4.32 (s, 2H, H-3/I, H-3/III), 3.99 – 3.97 (m, 1H, H-2/IV), 3.90 – 3.84 (m, 3H, H-2/II, H-6´´/I, H-6´´/III), 3.65-3.55 (m, 2H, H-6´/I, H-6´/III), 2.14 (s, 6H, C*H*$_3$/III; C*H*$_3$/I) ppm. **^{13}C NMR** (176 MHz, D_2O) δ [ppm] = 175.02 (N*C*=O/III), 174.34 (N*C*=O/I), 171.79 (*C*OOH/IV), 171.51 (*C*OOH/II), 100.36 (C-1/IV), 100.04 (C-1/II), 99.35 (C-1/III), 88.29 (C-1/I), 78.94 (*C*-4/II, *C*-4/IV), 77.76 (C-3/III), 76.41 (*C*-2/IV, *C*-2/II), 75.80 (*C*-5/I), 75.17 (*C*-3/IV, *C*-3/II), 74.60 (*C*-5/II, *C*-5/IV), 74.09 (*C*-3/I, *C*-3/III), 72.93 (*C*-4/III, *C*-4/I), 60.99 (*C*-6/III, *C*-6/I), 55.42 (*C*-2/III), 54.47, 22.81 (NHCO*C*H$_3$/III), 22.57 (NHCO*C*H$_3$/I). ESI-MS could not be detected due to unsufficient ionization.

Penta-sulfo hyaluronan disaccharide azide, 5s-HA-2-N_3, 2,3,4,6-tetra-O-sulfo-β-D-glucopyranuronyl-(1→3)-4,6-di-O-sulfo-β-D-2-acetamido-2-deoxy-glucopyranosyl-1-azide (24)

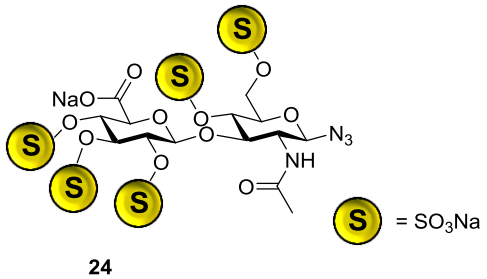

24

β-D-glucopyranuronyl-(1→3)-β-D-2-acetamido-2-deoxy-glucopyranosyl-azide **4** (40 mg, 0.010 mmol) was sulfated according to the general sulfation procedure to give **24** as colourless powder (65 mg, 72%). **^{1}H NMR** (700 MHz, D_2O) δ = 5.28 (s, 1H), 5.13 (d, *J* = 6.5 Hz, 1H), 5.01 (d, *J* = 9.2 Hz, 1H), 4.89 (s, 1H), 4.62 (d, *J* = 11.3 Hz, 1H), 4.48 (d, *J* = 6.6 Hz, 1H), 4.36 (t, *J* = 9.1 Hz, 1H), 4.22 (dt, *J* = 18.7, 9.9 Hz, 2H), 4.03 (t, *J* = 8.6 Hz, 1H), 3.85 (t, *J* = 9.1 Hz, 1H), 2.13 (s, 3H) ppm. **^{13}C NMR** (176 MHz, D_2O) δ = 174.84, 99.35, 87.93, 77.65, 75.20, 74.85, 74.50, 73.65, 67.35, 55.02, 22.31 ppm. For MS-analysis see below.

Nona-sulfo hyaluronan hexasaccharide azide, 13s-HA-6-N_3, 2,3,4,6-tetra-O-sulfo-β-D-glucopyranuronyl-(1→3)-4,6-di-O-sulfo-β-D-2-acetamido-2-deoxy-glucopyranosyl-(1→4)-2,3,4,6-tetra-O-sulfo-β-D-glucopyranuronyl-(1→3)-4,6-di-O-sulfo-β-D-2-acetamido-2-deoxy-glucopyranosyl-(1→4)-2,3-di-O-sulfo-β-D-glucopyranuronyl-(1→3)-4,6-di-O-sulfo-β-D-2-acetamido-2-deoxy-glucopyranosyl-1-azide (26)

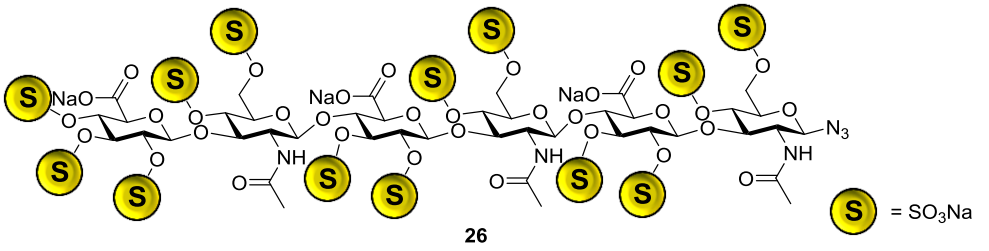

26

β-D-glucopyranuronyl-(1→3)-β-D-2-acetamido-2-deoxy-glucopyranosyl-(1→4)-β-D-glucopyranuronyl-(1→3)-β-D-2-acetamido-2-deoxy-glucopyranosyl-(1→4)-β-D-glucopyranuronyl-(1→3)-β-D-2-acetamido-2-deoxy-glucopyranosyl-azide **6** (72 mg, 0.061 mmol) was sulfated according to the general sulfation procedure to give **26** as colourless powder (130 mg, 83%). **^{1}H NMR** (700 MHz, D_2O) δ = 5.18 (d, *J* = 4.0 Hz, 1H), 5.07 – 5.03 (m, 2H), 4.98 (d, *J* = 6.6 Hz, 1H), 4.94 (d, *J* = 5.8 Hz, 1H), 4.91 (d, *J* = 9.3 Hz, 1H), 4.89 (dd, *J* = 4.5, 2.0 Hz, 1H), 4.87 – 4.82 (m, 3H), 4.63 (s, 1H), 4.60 – 4.53 (m, 4H), 4.49 (t, *J* = 3.4 Hz, 1H), 4.43 (d, *J* = 7.0 Hz, 1H), 4.41 (dd, *J* = 6.1, 2.5 Hz, 1H), 4.39 – 4.37 (m, 1H), 4.36 – 4.27 (m, 5H), 4.23 – 4.15 (m, 4H), 4.09 (t, *J* = 9.2 Hz, 1H), 4.01 – 3.95 (m, 2H), 3.94 – 3.82 (m, 5H), 2.14 (s, 3H), 2.11 (d, *J* = 1.8 Hz, 6H) ppm. **^{13}C NMR** (176 MHz, D_2O) δ = 174.98, 174.53, 173.47, 173.40, 173.22, 100.95 (d, *J* = 12.7 Hz), 100.47, 100.40, 100.32, 99.81, 99.77, 99.37 (d, *J* = 13.9 Hz), 88.37 (d, *J* = 12.7 Hz), 78.94, 78.89, 78.68, 78.62, 77.88, 77.80, 77.78, 77.38, 76.60, 76.54, 76.28, 75.78, 75.75, 75.42, 75.34, 75.23, 75.07, 75.04, 74.55, 74.49, 74.43, 72.87, 72.81, 67.53 (d, *J* = 9.2 Hz), 67.40 (d, *J* = 8.2 Hz), 55.36, 55.01, 54.51, 23.13, 23.11, 22.80, 22.77, 22.60, 22.57 ppm. For MS-analysis see below.

3. NMR and MS-Spectra

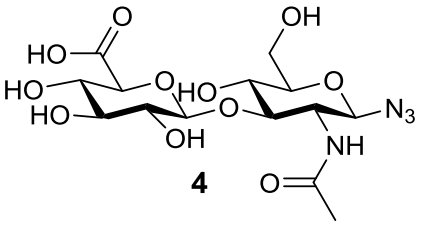

4

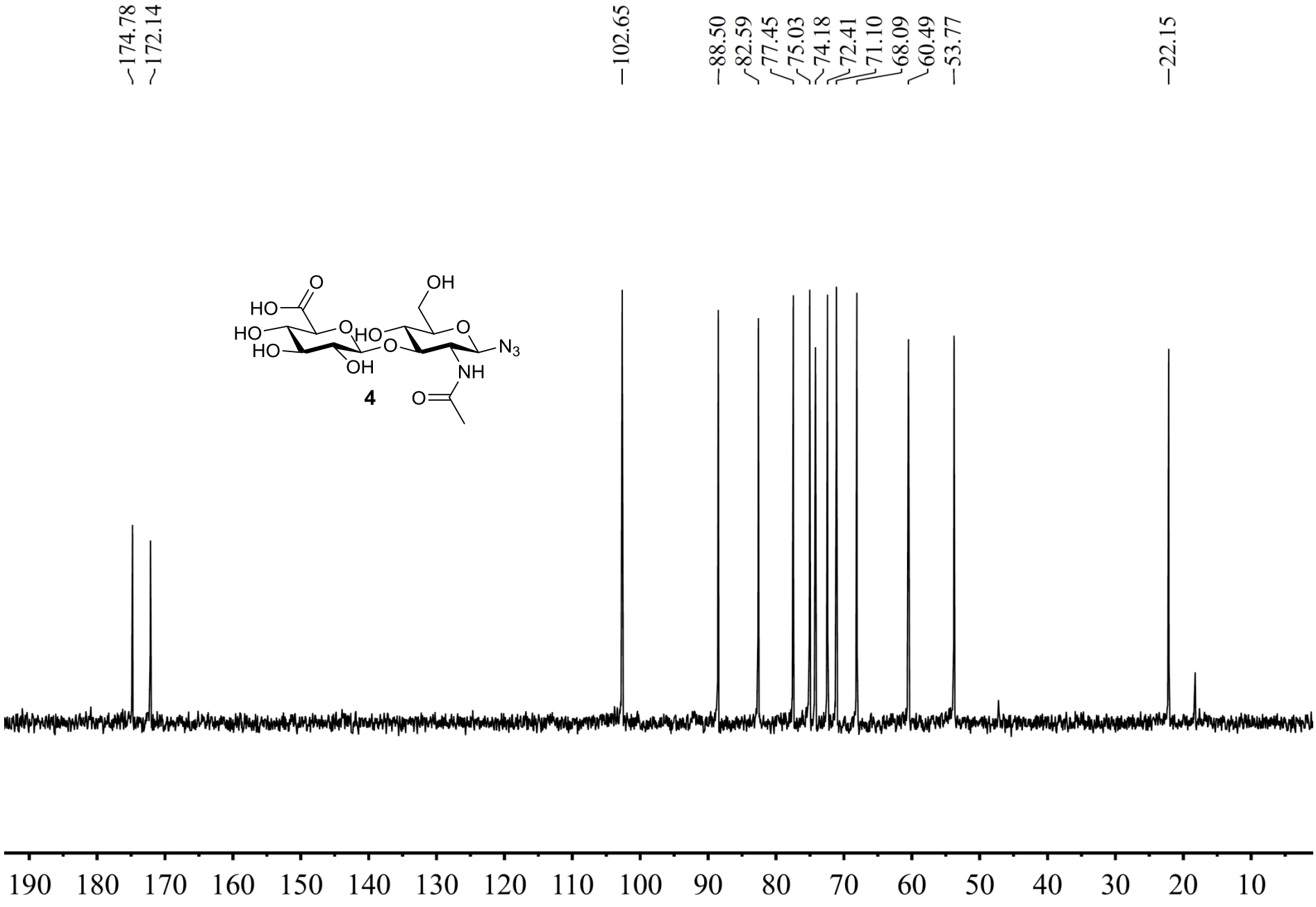
174.78
172.14
102.65
88.50
82.59
77.45
75.03
74.18
72.41
71.10
68.09
60.49
53.77
22.15
HO
O
OH
HO
HO
O
HO
O
N3
OH
NH
O
4
190
180
170
160
150
140
130
120
110
100
90
80
70
60
50
40
30
20
10

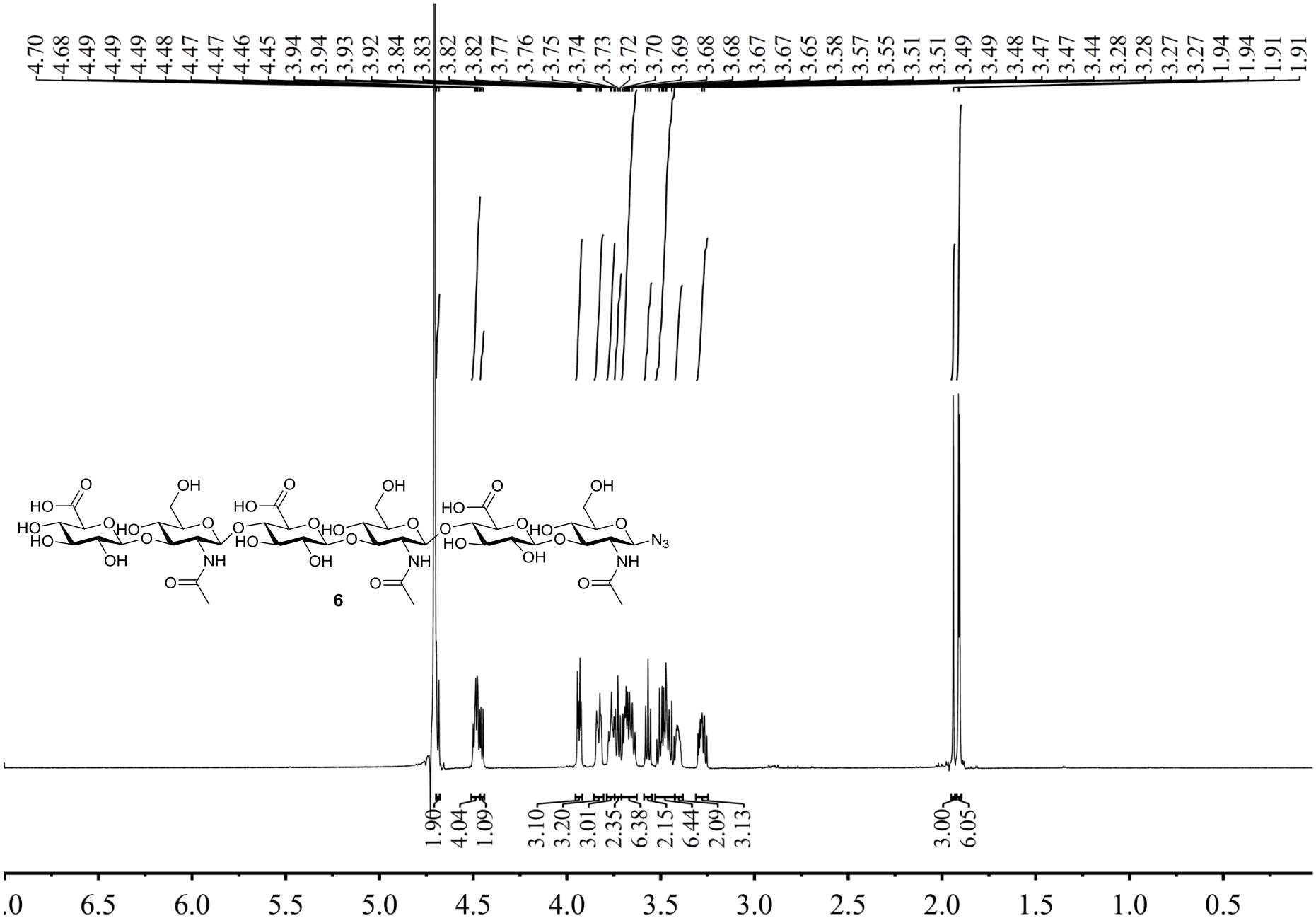
4.70
4.68
4.49
4.49
4.49
4.48
4.47
4.47
4.46
4.45
3.94
3.94
3.93
3.92
3.84
3.83
3.82
3.82
3.77
3.76
3.75
3.74
3.73
3.72
3.70
3.69
3.68
3.68
3.67
3.67
3.65
3.58
3.57
3.55
3.51
3.51
3.49
3.49
3.48
3.47
3.47
3.44
3.28
3.28
3.27
3.27
1.94
1.94
1.91
1.91
6
1.90
4.04
1.09
3.10
3.20
3.01
2.35
6.38
2.15
6.44
2.09
3.13
3.00
6.05
.0
6.5
6.0
5.5
5.0
4.5
4.0
3.5
3.0
2.5
2.0
1.5
1.0
0.5

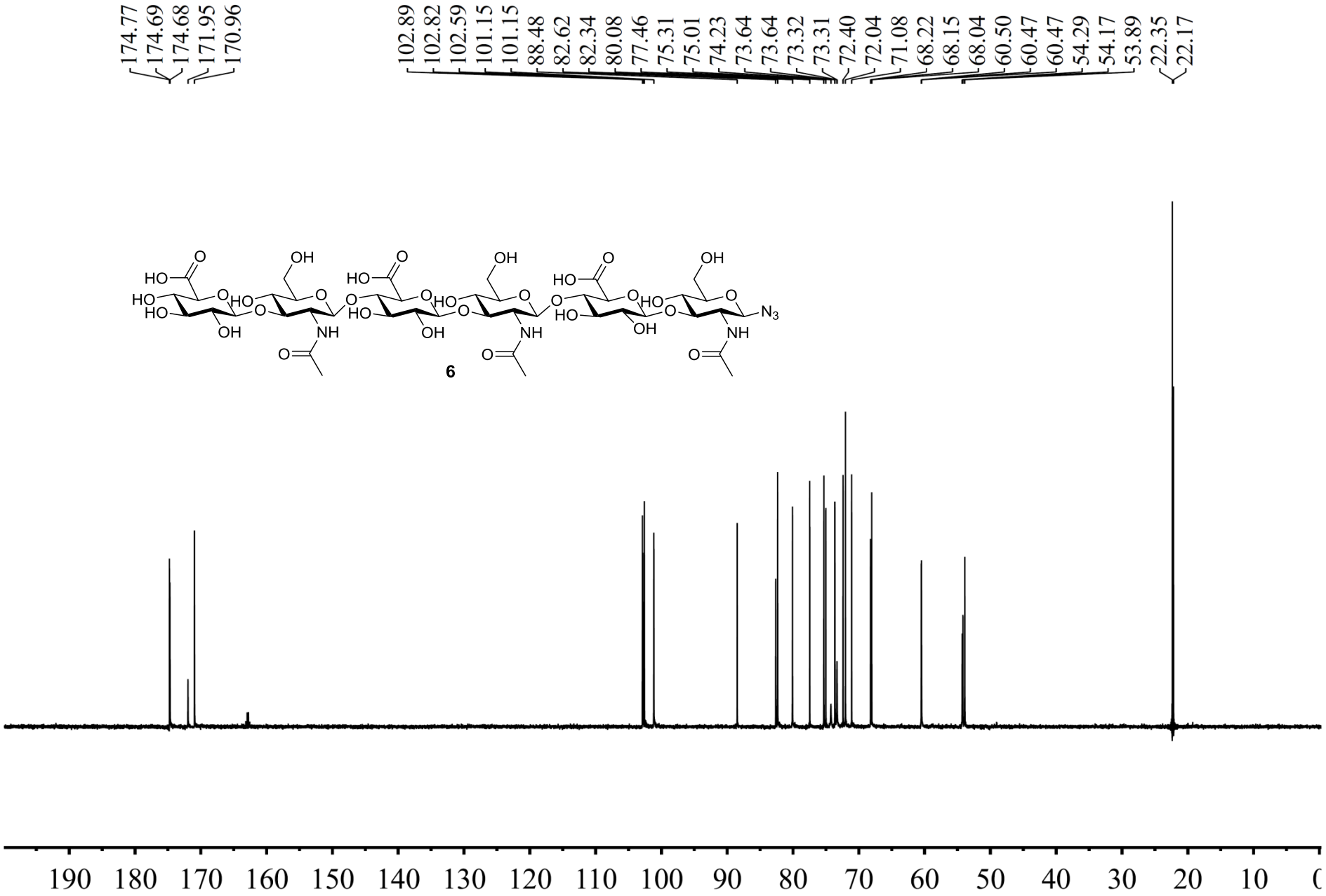
174.77
174.69
174.68
171.95
170.96
102.89
102.82
102.59
101.15
101.15
88.48
82.62
82.34
80.08
77.46
75.31
75.01
74.23
73.64
73.64
73.32
73.31
72.40
72.04
71.08
68.22
68.15
68.04
60.50
60.47
60.47
54.29
54.17
53.89
22.35
22.17
6
190
180
170
160
150
140
130
120
110
100
90
80
70
60
50
40
30
20
10

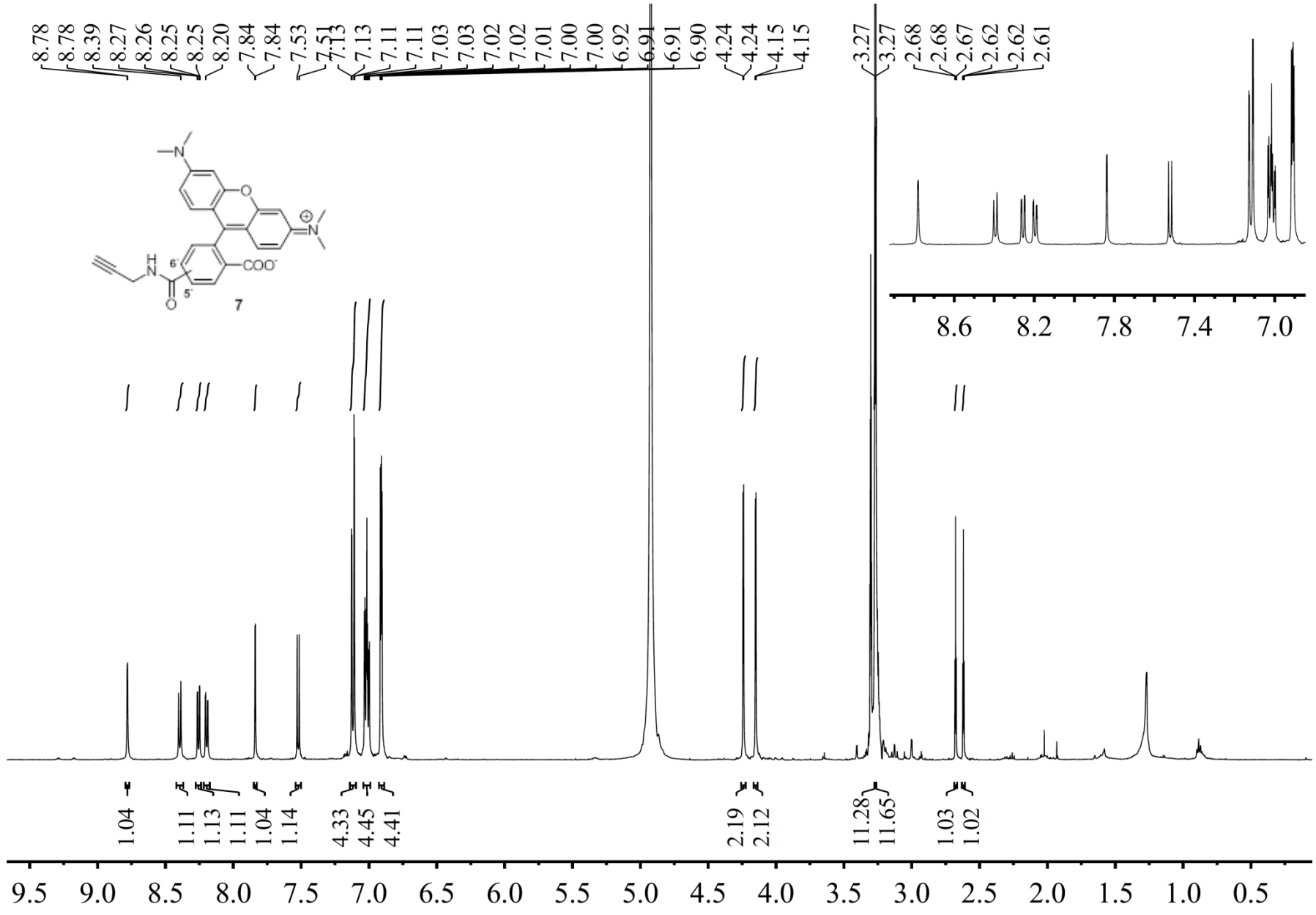
8.78
8.78
8.39
8.27
8.26
8.25
8.25
8.20
7.84
7.84
7.53
7.51
7.13
7.13
7.11
7.11
7.03
7.03
7.02
7.02
7.01
7.00
7.00
6.92
6.91
6.91
6.90
4.24
4.24
4.15
4.15
3.27
3.27
2.68
2.68
2.67
2.62
2.62
2.61
7
8.6
8.2
7.8
7.4
7.0
1.04
1.11
1.13
1.11
1.04
1.14
4.33
4.45
4.41
2.19
2.12
11.28
11.65
1.03
1.02
9.5
9.0
8.5
8.0
7.5
7.0
6.5
6.0
5.5
5.0
4.5
4.0
3.5
3.0
2.5
2.0
1.5
1.0
0.5

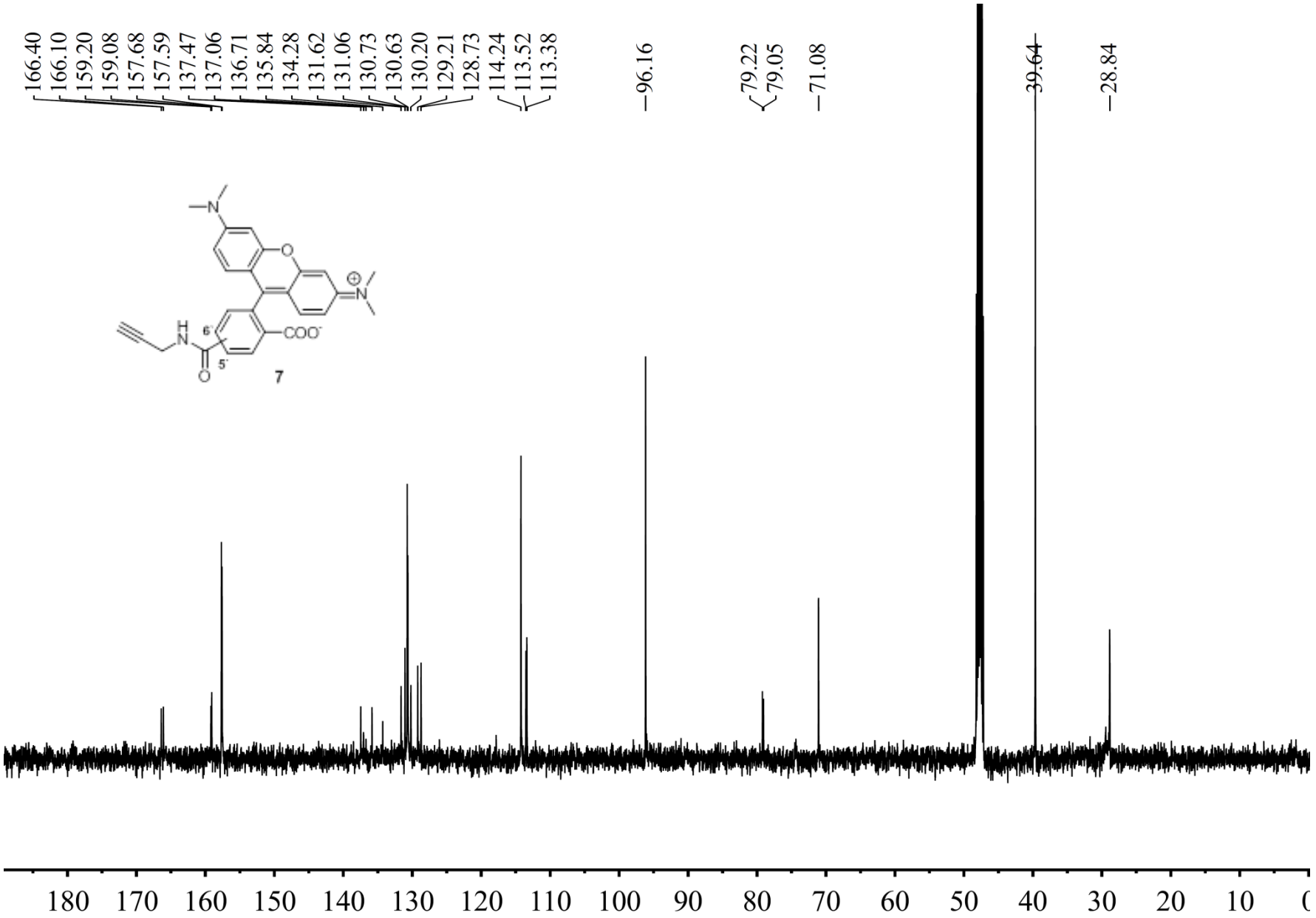
166.40
166.10
159.20
159.08
157.68
157.59
137.47
137.06
136.71
135.84
134.28
131.62
131.06
130.73
130.63
130.20
129.21
128.73
114.24
113.52
113.38
96.16
79.22
79.05
71.08
39.64
28.84
7
180
170
160
150
140
130
120
110
100
90
80
70
60
50
40
30
20
10

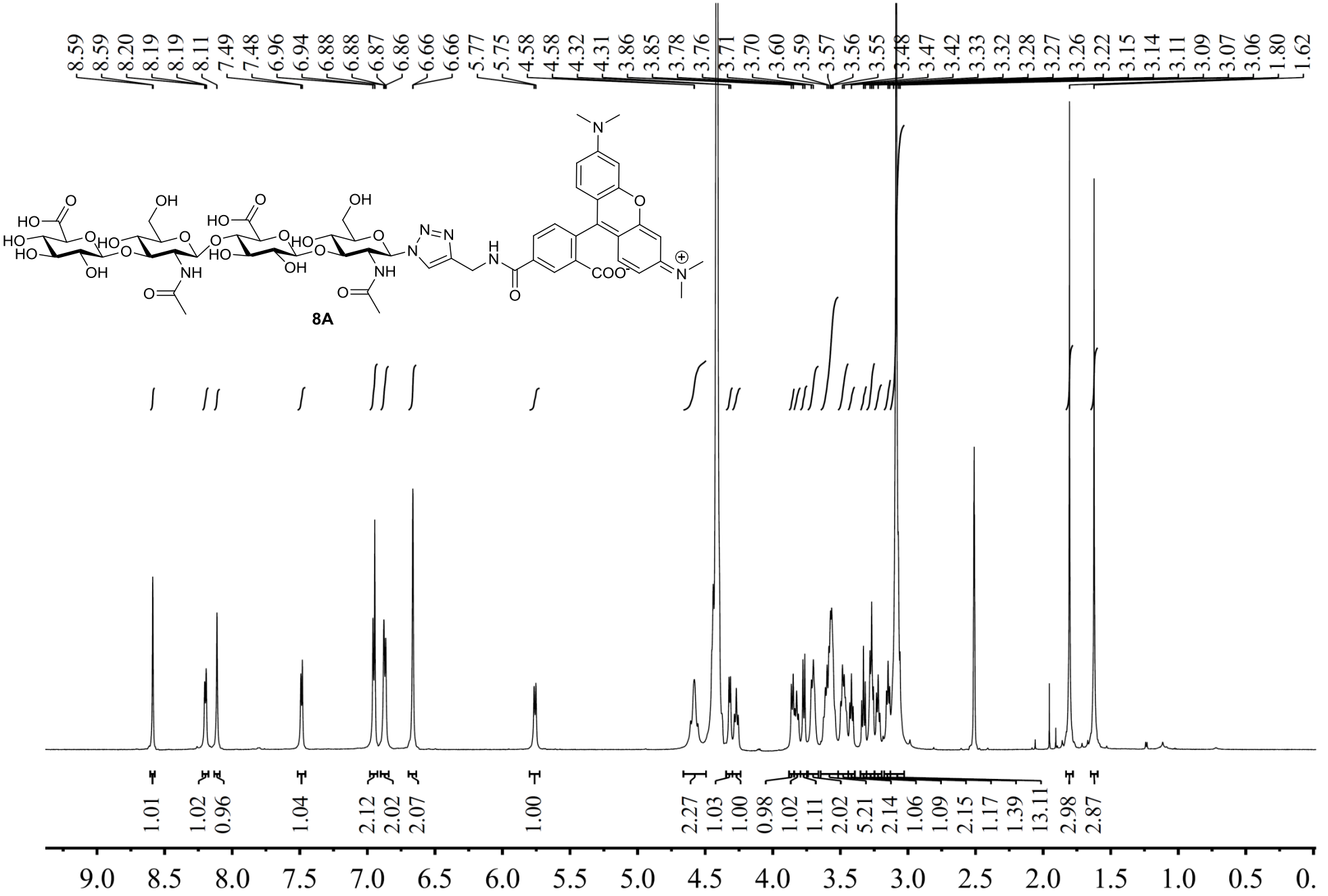
8.59
8.59
8.20
8.19
8.19
8.11
7.49
7.48
6.96
6.94
6.88
6.88
6.87
6.86
6.66
6.66
5.77
5.75
4.58
4.58
4.32
4.31
3.86
3.85
3.78
3.76
3.71
3.70
3.60
3.59
3.57
3.56
3.55
3.48
3.47
3.42
3.33
3.32
3.28
3.27
3.26
3.22
3.15
3.14
3.11
3.09
3.07
3.06
1.80
1.62
8A
1.01
1.02
0.96
1.04
2.12
2.02
2.07
1.00
2.27
1.03
1.00
0.98
1.02
1.11
2.02
5.21
2.14
1.06
1.09
2.15
1.17
1.39
13.11
2.98
2.87
9.0
8.5
8.0
7.5
7.0
6.5
6.0
5.5
5.0
4.5
4.0
3.5
3.0
2.5
2.0
1.5
1.0
0.5
0.

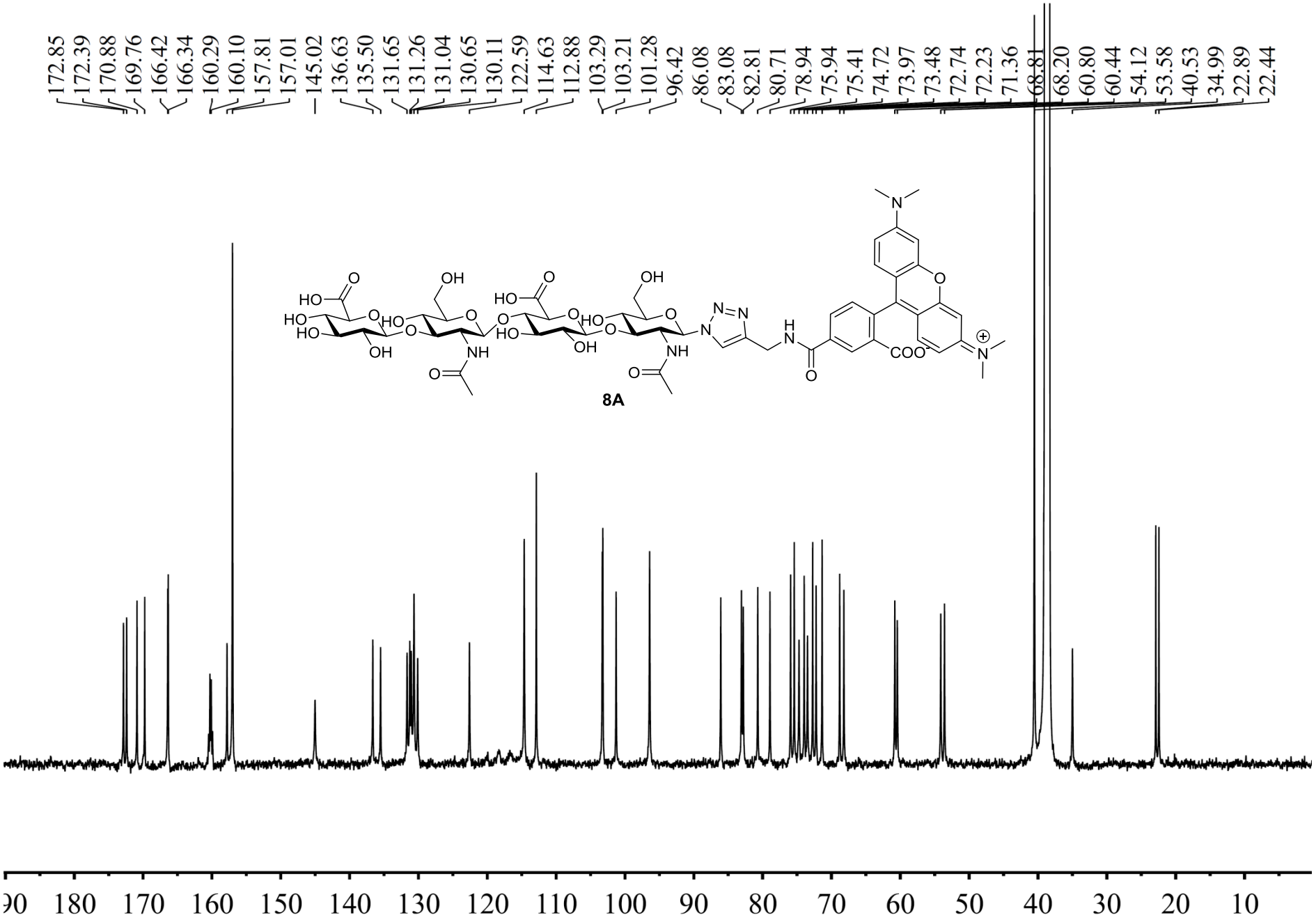
172.85
172.39
170.88
169.76
166.42
166.34
160.29
160.10
157.81
157.01
145.02
136.63
135.50
131.65
131.26
131.04
130.65
130.11
122.59
114.63
112.88
103.29
103.21
101.28
96.42
86.08
83.08
82.81
80.71
78.94
75.94
75.41
74.72
73.97
73.48
72.74
72.23
71.36
68.81
68.20
60.80
60.44
54.12
53.58
40.53
34.99
22.89
22.44
8A
90 180 170 160 150 140 130 120 110 100 90 80 70 60 50 40 30 20 10

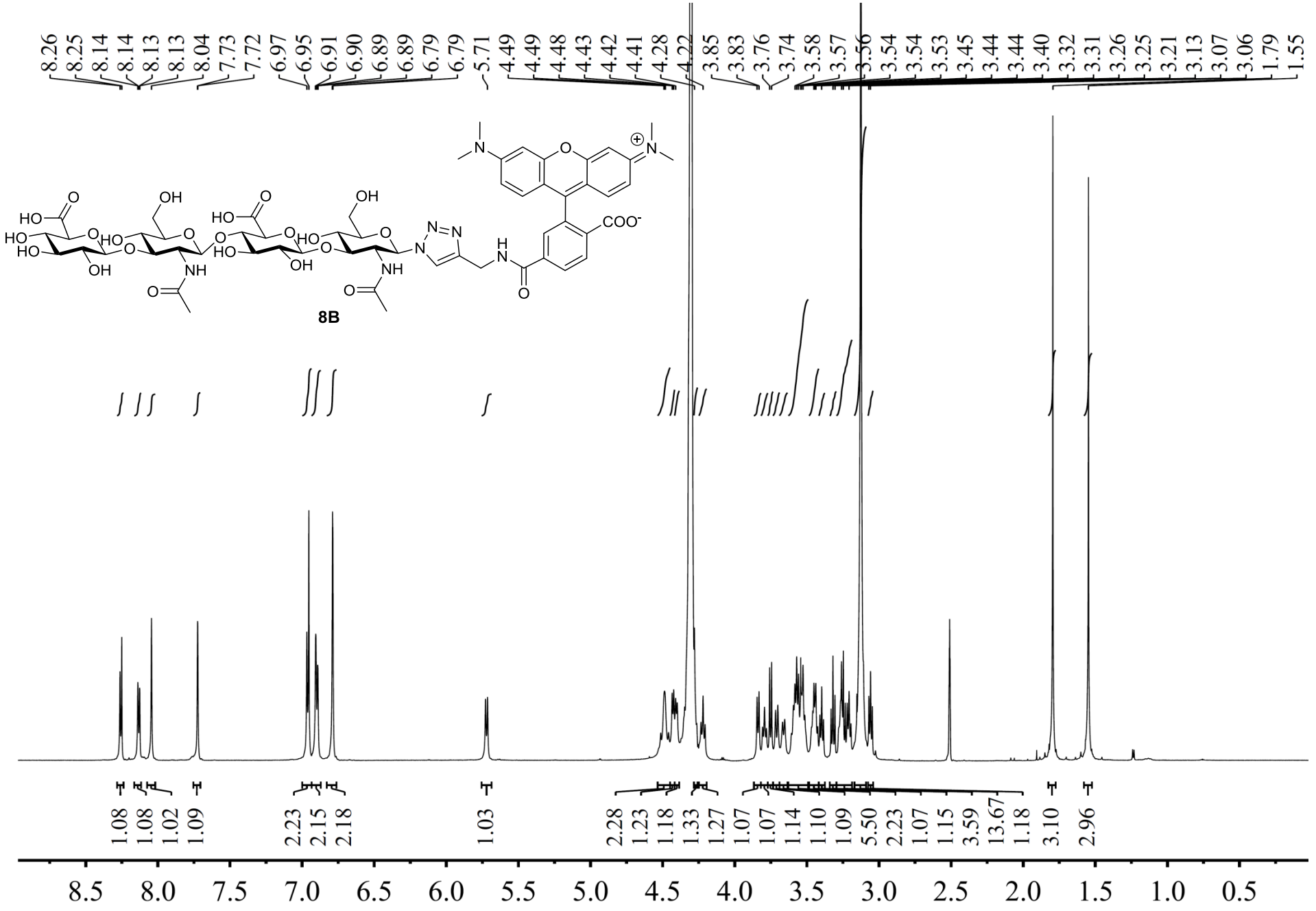
8.26
8.25
8.14
8.14
8.13
8.13
8.04
7.73
7.72
6.97
6.95
6.91
6.90
6.89
6.89
6.79
6.79
5.71
4.49
4.49
4.48
4.43
4.42
4.41
4.28
4.22
3.85
3.83
3.76
3.74
3.58
3.57
3.56
3.54
3.54
3.53
3.45
3.44
3.44
3.40
3.32
3.31
3.26
3.25
3.21
3.13
3.07
3.06
1.79
1.55
8B
1.08
1.08
1.02
1.09
2.23
2.15
2.18
1.03
2.28
1.23
1.18
1.33
1.27
1.07
1.07
1.14
1.10
1.09
5.50
2.23
1.07
1.15
3.59
13.67
1.18
3.10
2.96
8.5
8.0
7.5
7.0
6.5
6.0
5.5
5.0
4.5
4.0
3.5
3.0
2.5
2.0
1.5
1.0
0.5

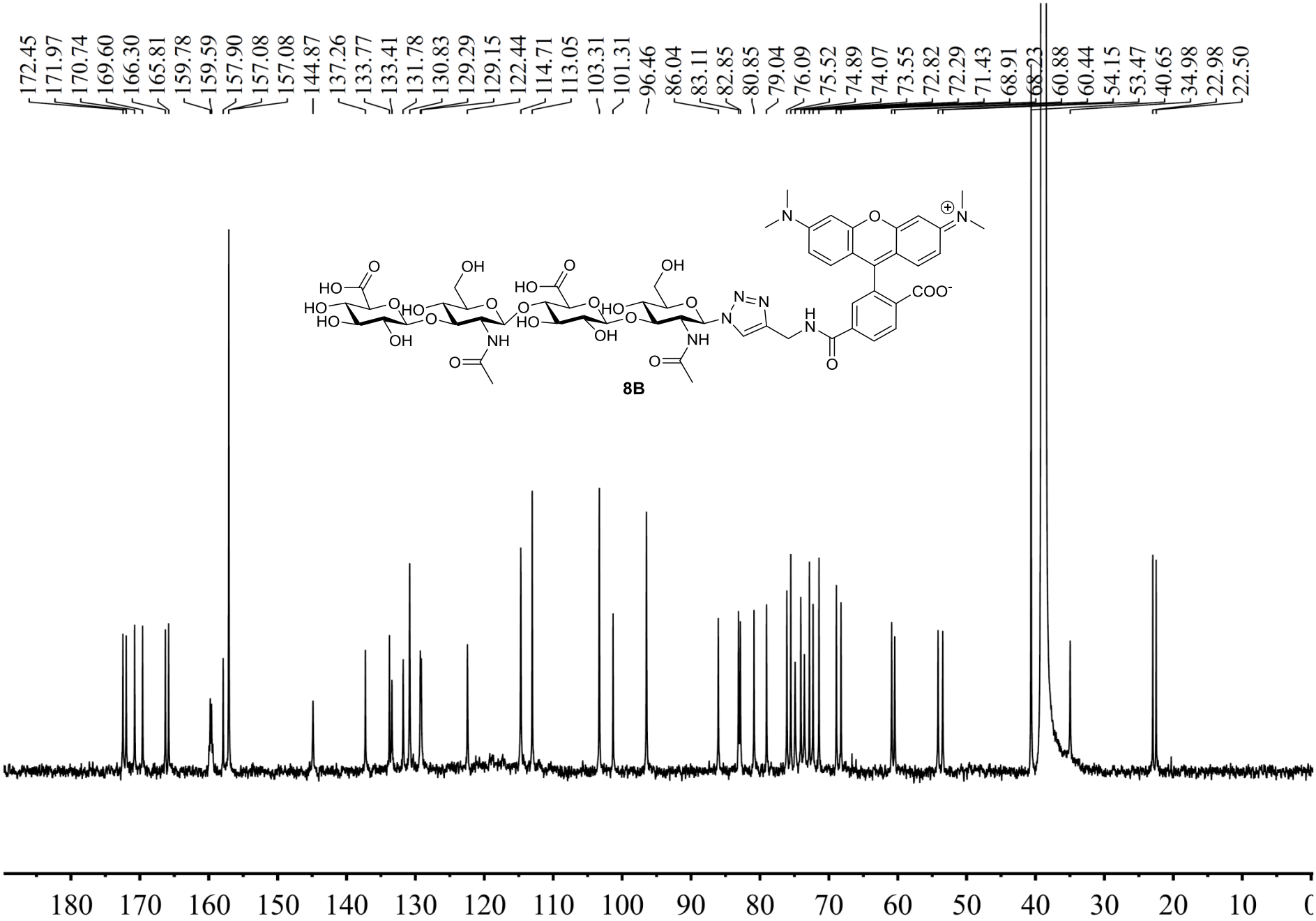
172.45
171.97
170.74
169.60
166.30
165.81
159.78
159.59
157.90
157.08
157.08
144.87
137.26
133.77
133.41
131.78
130.83
129.29
129.15
122.44
114.71
113.05
103.31
101.31
96.46
86.04
83.11
82.85
80.85
79.04
76.09
75.52
74.89
74.07
73.55
72.82
72.29
71.43
68.91
68.23
60.88
60.44
54.15
53.47
40.65
34.98
22.98
22.50
8B
180
170
160
150
140
130
120
110
100
90
80
70
60
50
40
30
20
10

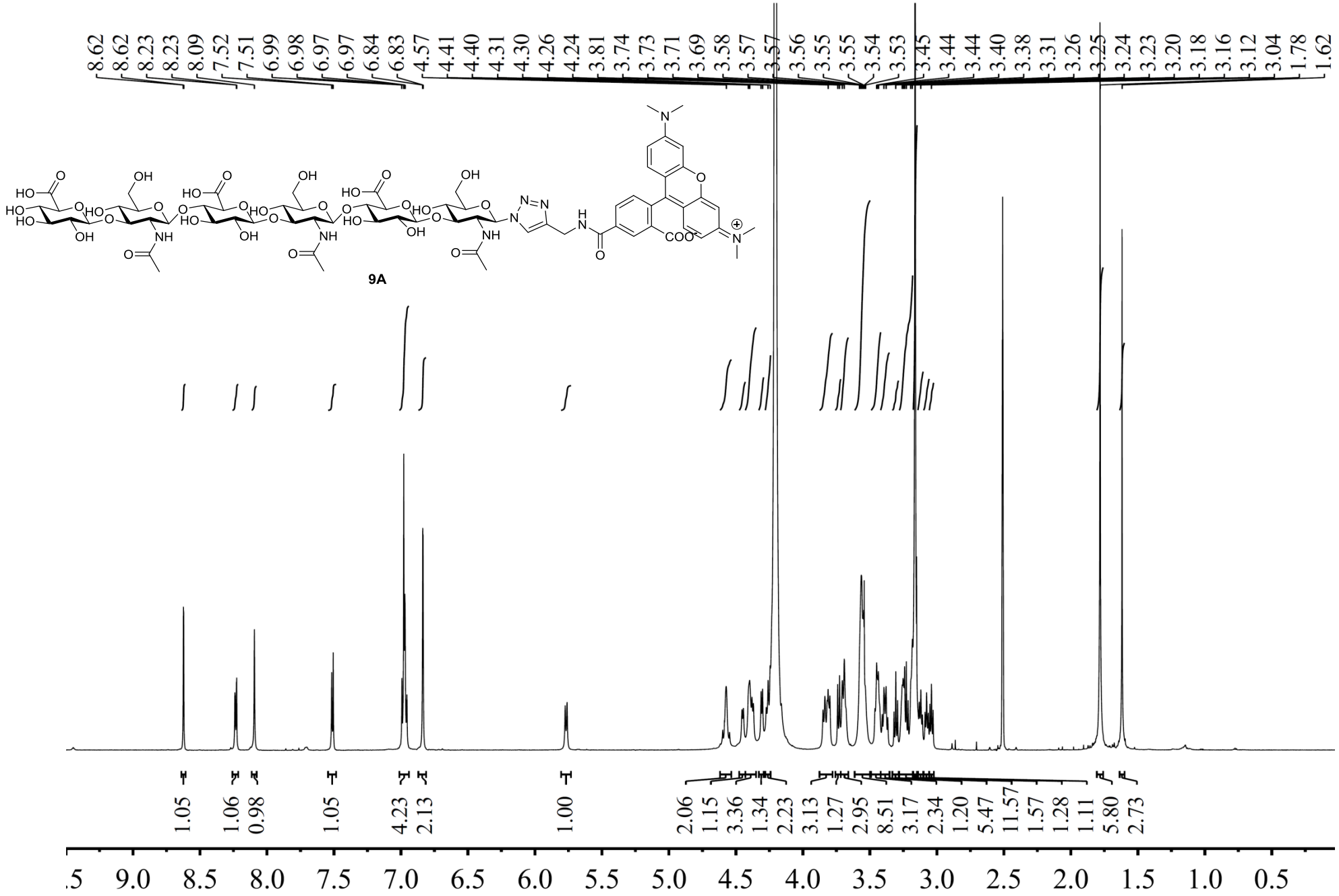
8.62
8.62
8.23
8.23
8.09
7.52
7.51
6.99
6.98
6.97
6.97
6.84
6.83
4.57
4.41
4.40
4.31
4.30
4.26
4.24
3.81
3.74
3.73
3.71
3.69
3.58
3.57
3.57
3.56
3.55
3.55
3.54
3.53
3.45
3.44
3.44
3.40
3.38
3.31
3.26
3.25
3.24
3.23
3.20
3.18
3.16
3.12
3.04
1.78
1.62
9A
1.05
1.06
0.98
1.05
4.23
2.13
1.00
2.06
1.15
3.36
1.34
2.23
3.13
1.27
2.95
8.51
3.17
2.34
1.20
5.47
11.57
1.57
1.28
1.11
5.80
2.73
.5
9.0
8.5
8.0
7.5
7.0
6.5
6.0
5.5
5.0
4.5
4.0
3.5
3.0
2.5
2.0
1.5
1.0
0.5

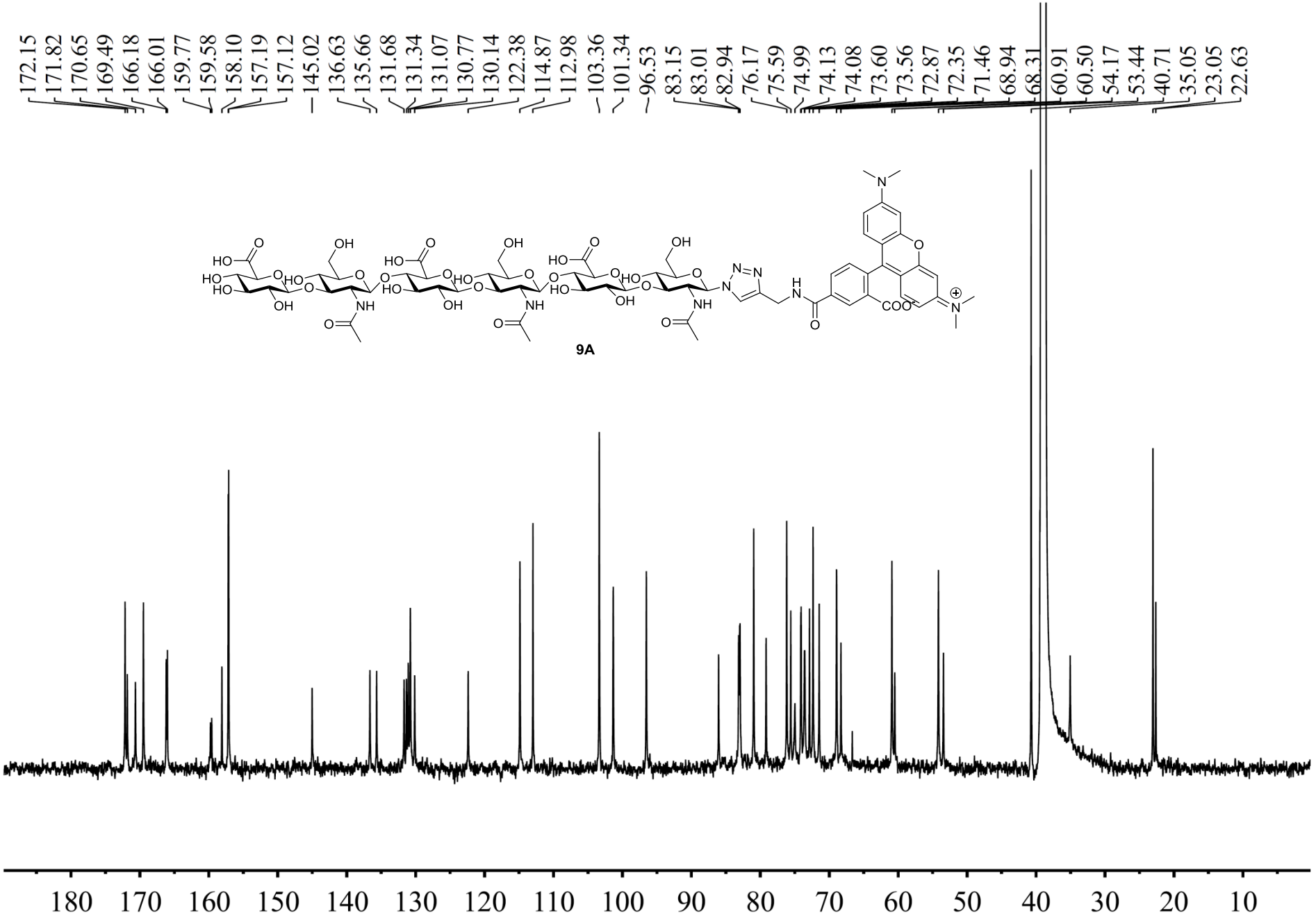
172.15
171.82
170.65
169.49
166.18
166.01
159.77
159.58
158.10
157.19
157.12
145.02
136.63
135.66
131.68
131.34
131.07
130.77
130.14
122.38
114.87
112.98
103.36
101.34
96.53
83.15
83.01
82.94
76.17
75.59
74.99
74.13
74.08
73.60
73.56
72.87
72.35
71.46
68.94
68.31
60.91
60.50
54.17
53.44
40.71
35.05
23.05
22.63
9A
180
170
160
150
140
130
120
110
100
90
80
70
60
50
40
30
20
10

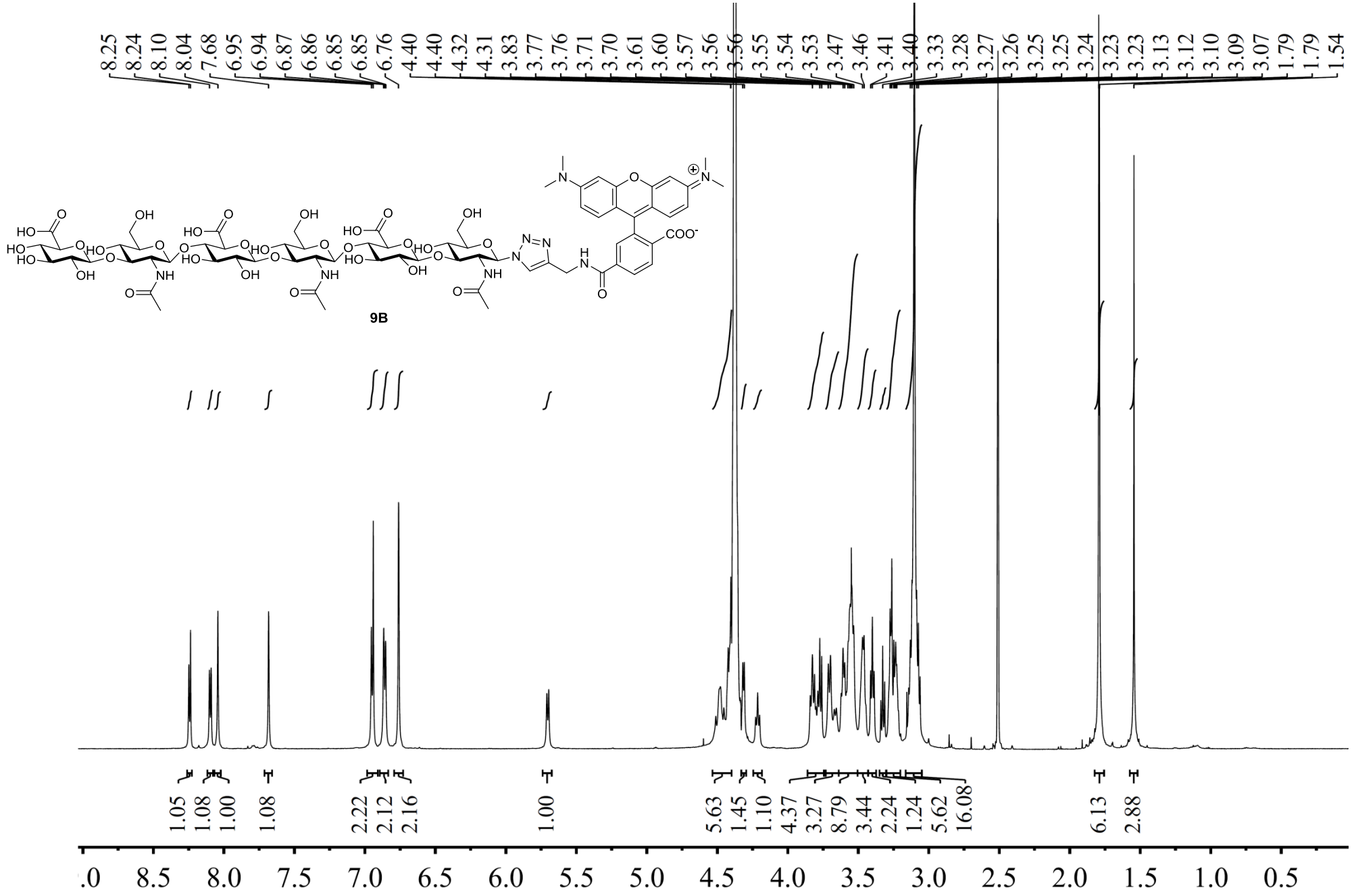
8.25 8.24 8.10 8.04 7.68 6.95 6.94 6.87 6.86 6.85 6.85 6.76 4.40 4.40 4.32 4.31 3.83 3.77 3.76 3.71 3.70 3.61 3.60 3.57 3.56 3.56 3.55 3.54 3.53 3.47 3.46 3.41 3.40 3.33 3.28 3.27 3.26 3.25 3.25 3.24 3.23 3.23 3.13 3.12 3.10 3.09 3.07 1.79 1.79 1.54
9B
1.05 1.08 1.00 1.08 2.22 2.12 2.16 1.00 5.63 1.45 1.10 4.37 3.27 8.79 3.44 2.24 1.24 5.62 16.08 6.13 2.88
.0 8.5 8.0 7.5 7.0 6.5 6.0 5.5 5.0 4.5 4.0 3.5 3.0 2.5 2.0 1.5 1.0 0.5

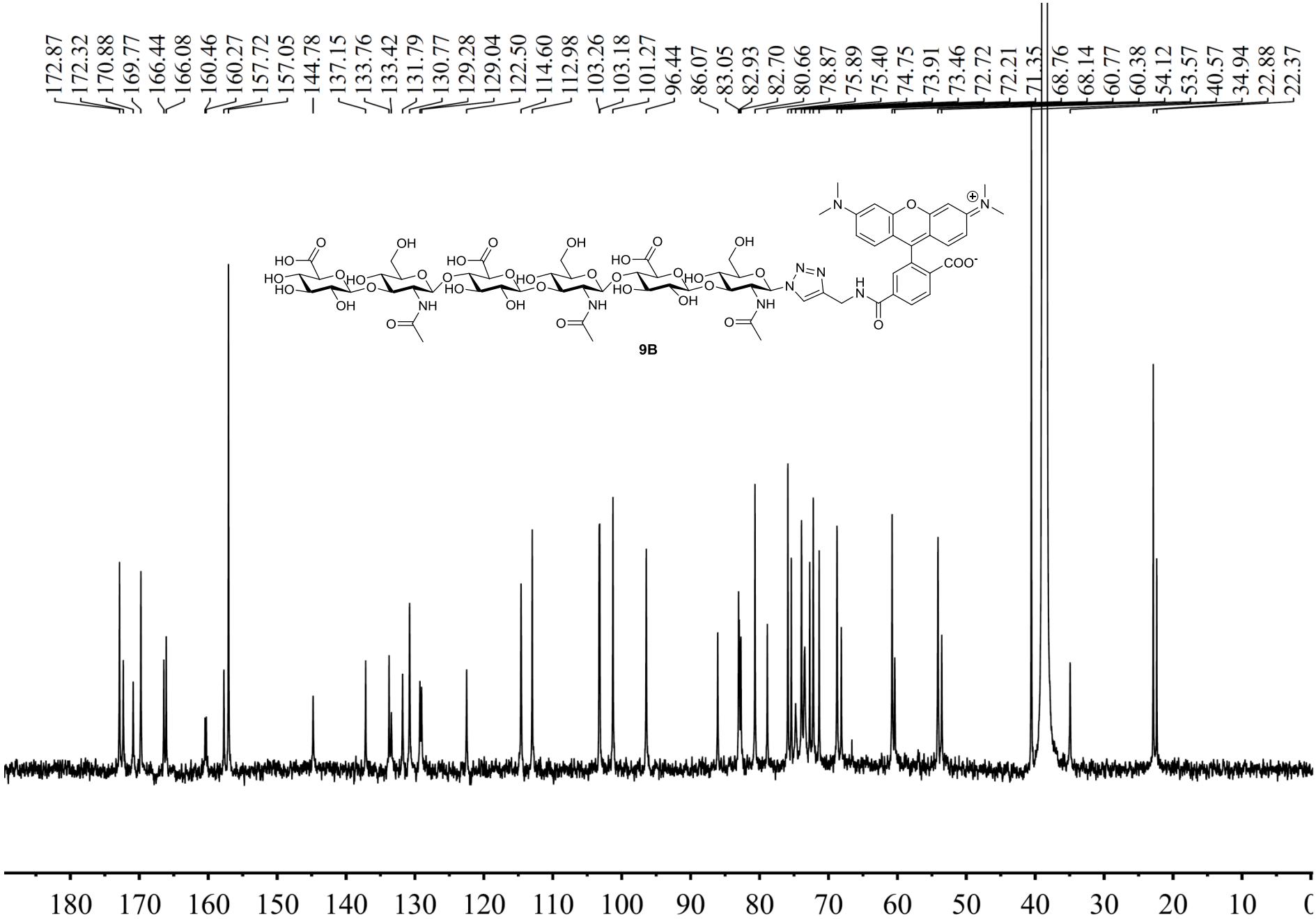
172.87
172.32
170.88
169.77
166.44
166.08
160.46
160.27
157.72
157.05
144.78
137.15
133.76
133.42
131.79
130.77
129.28
129.04
122.50
114.60
112.98
103.26
103.18
101.27
96.44
86.07
83.05
82.93
82.70
80.66
78.87
75.89
75.40
74.75
73.91
73.46
72.72
72.21
71.35
68.76
68.14
60.77
60.38
54.12
53.57
40.57
34.94
22.88
22.37
9B
180
170
160
150
140
130
120
110
100
90
80
70
60
50
40
30
20
10

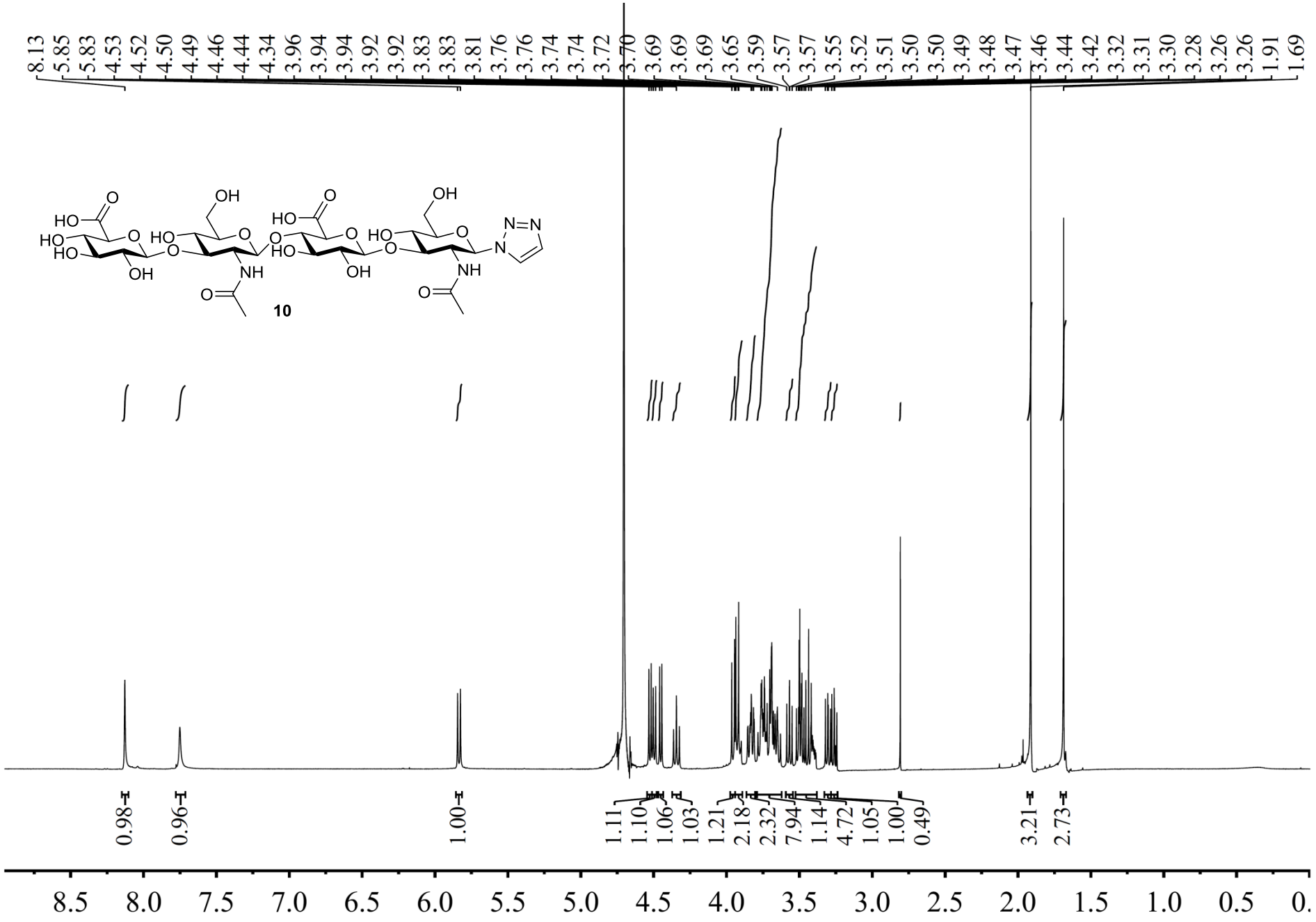
8.13
5.85
5.83
4.53
4.52
4.50
4.49
4.46
4.44
4.34
3.96
3.94
3.94
3.92
3.92
3.83
3.83
3.81
3.76
3.76
3.74
3.74
3.72
3.70
3.69
3.69
3.69
3.65
3.59
3.57
3.57
3.55
3.52
3.51
3.50
3.50
3.49
3.48
3.47
3.46
3.44
3.42
3.32
3.31
3.30
3.28
3.26
3.26
1.91
1.69
10
0.98
0.96
1.00
1.11
1.10
1.06
1.03
1.21
2.18
2.32
7.94
1.14
4.72
1.05
1.00
0.49
3.21
2.73
8.5
8.0
7.5
7.0
6.5
6.0
5.5
5.0
4.5
4.0
3.5
3.0
2.5
2.0
1.5
1.0
0.5
0.

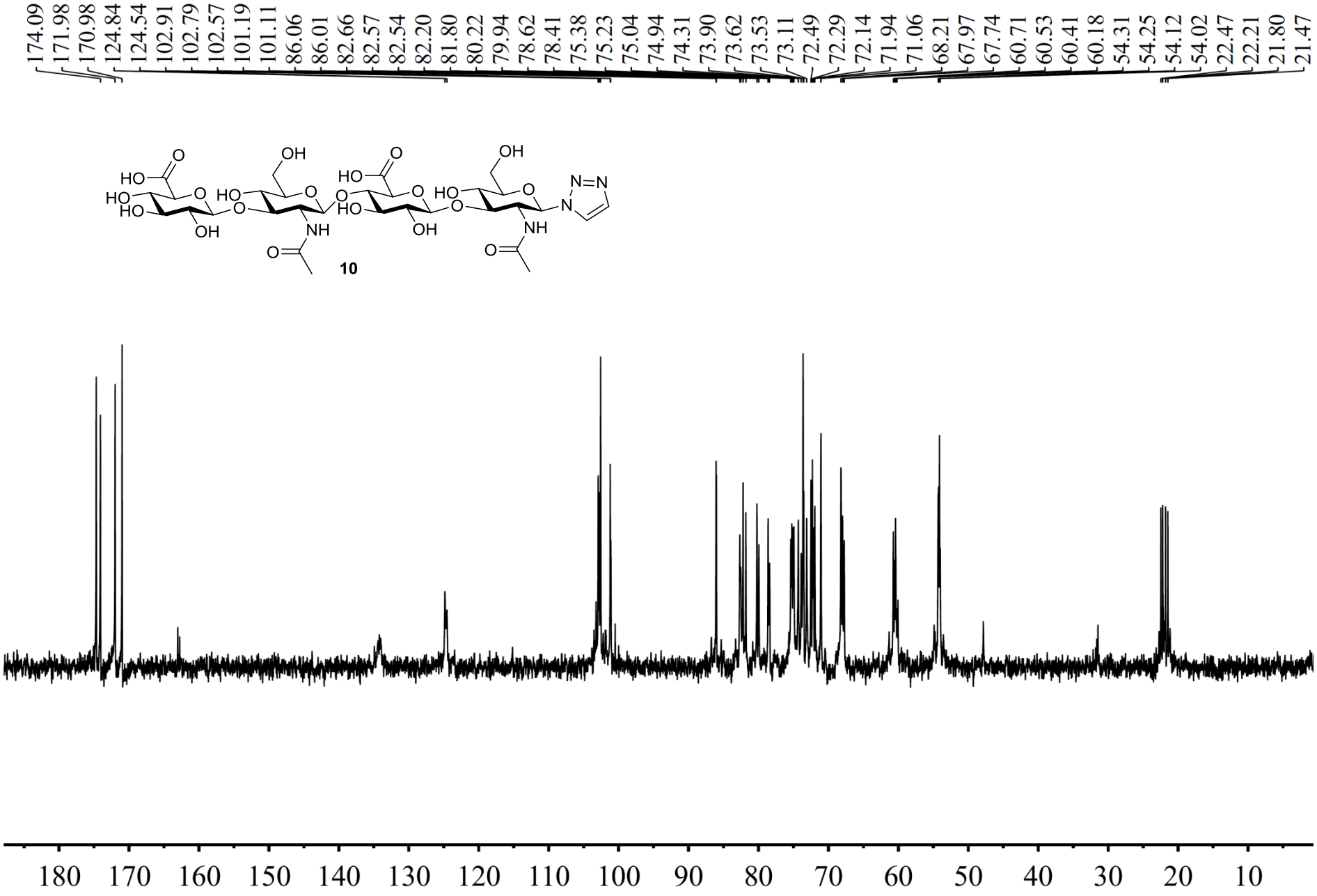
174.09
171.98
170.98
124.84
124.54
102.91
102.79
102.57
101.19
101.11
86.06
86.01
82.66
82.57
82.54
82.20
81.80
80.22
79.94
78.62
78.41
75.38
75.23
75.04
74.94
74.31
73.90
73.62
73.53
73.11
72.49
72.29
72.14
71.94
71.06
68.21
67.97
67.74
60.71
60.53
60.41
60.18
54.31
54.25
54.12
54.02
22.47
22.21
21.80
21.47
10
180
170
160
150
140
130
120
110
100
90
80
70
60
50
40
30
20
10

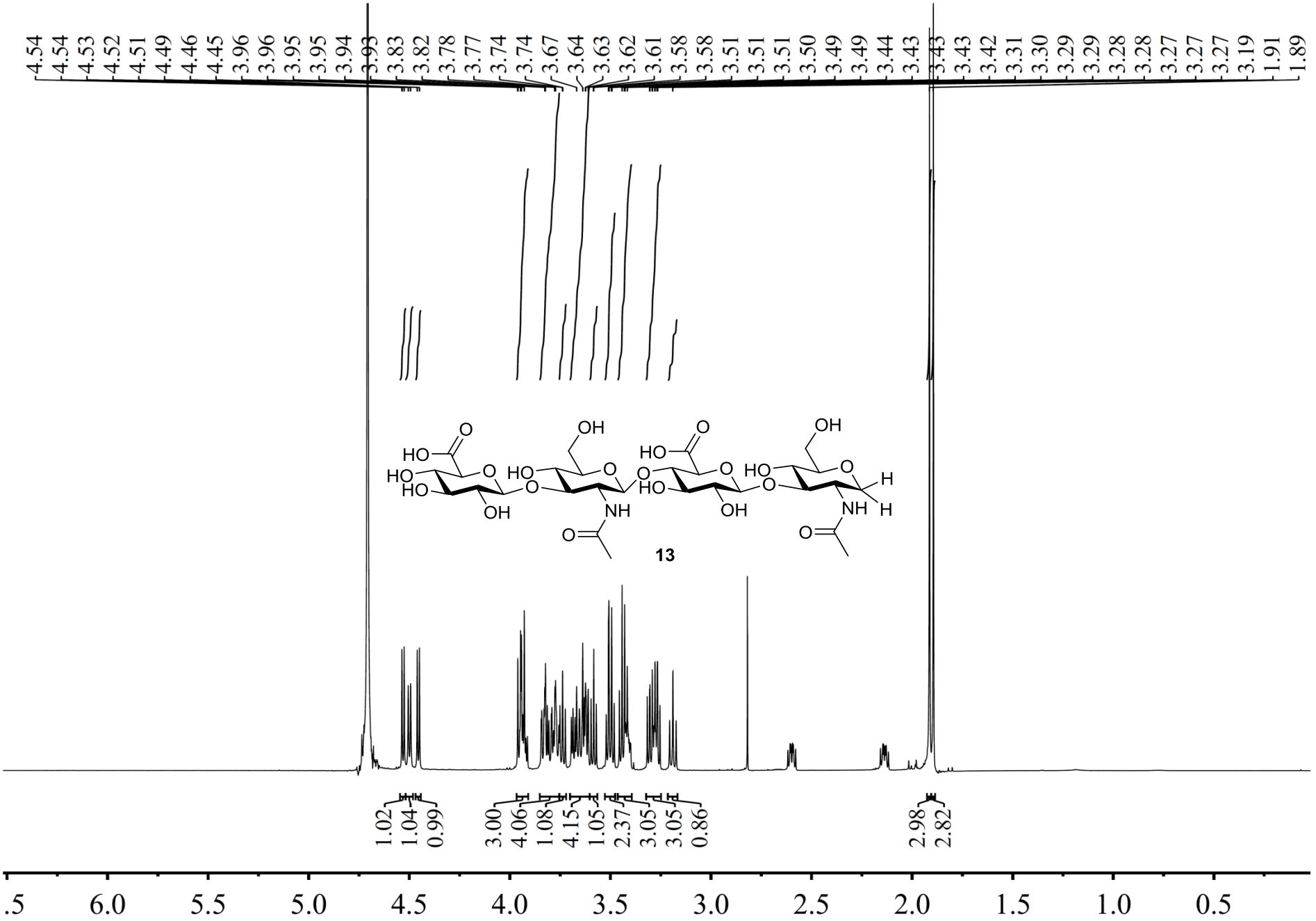
4.54 4.54 4.53 4.52 4.51 4.49 4.46 4.45 3.96 3.96 3.95 3.95 3.94 3.93 3.83 3.82 3.78 3.77 3.74 3.74 3.67 3.64 3.63 3.62 3.61 3.58 3.58 3.51 3.51 3.51 3.50 3.49 3.49 3.44 3.43 3.43 3.43 3.42 3.31 3.30 3.29 3.29 3.28 3.28 3.27 3.27 3.27 3.19 1.91 1.89
13
1.02 1.04 0.99 3.00 4.06 1.08 4.15 1.05 2.37 3.05 3.05 0.86 2.98 2.82
.5 6.0 5.5 5.0 4.5 4.0 3.5 3.0 2.5 2.0 1.5 1.0 0.5

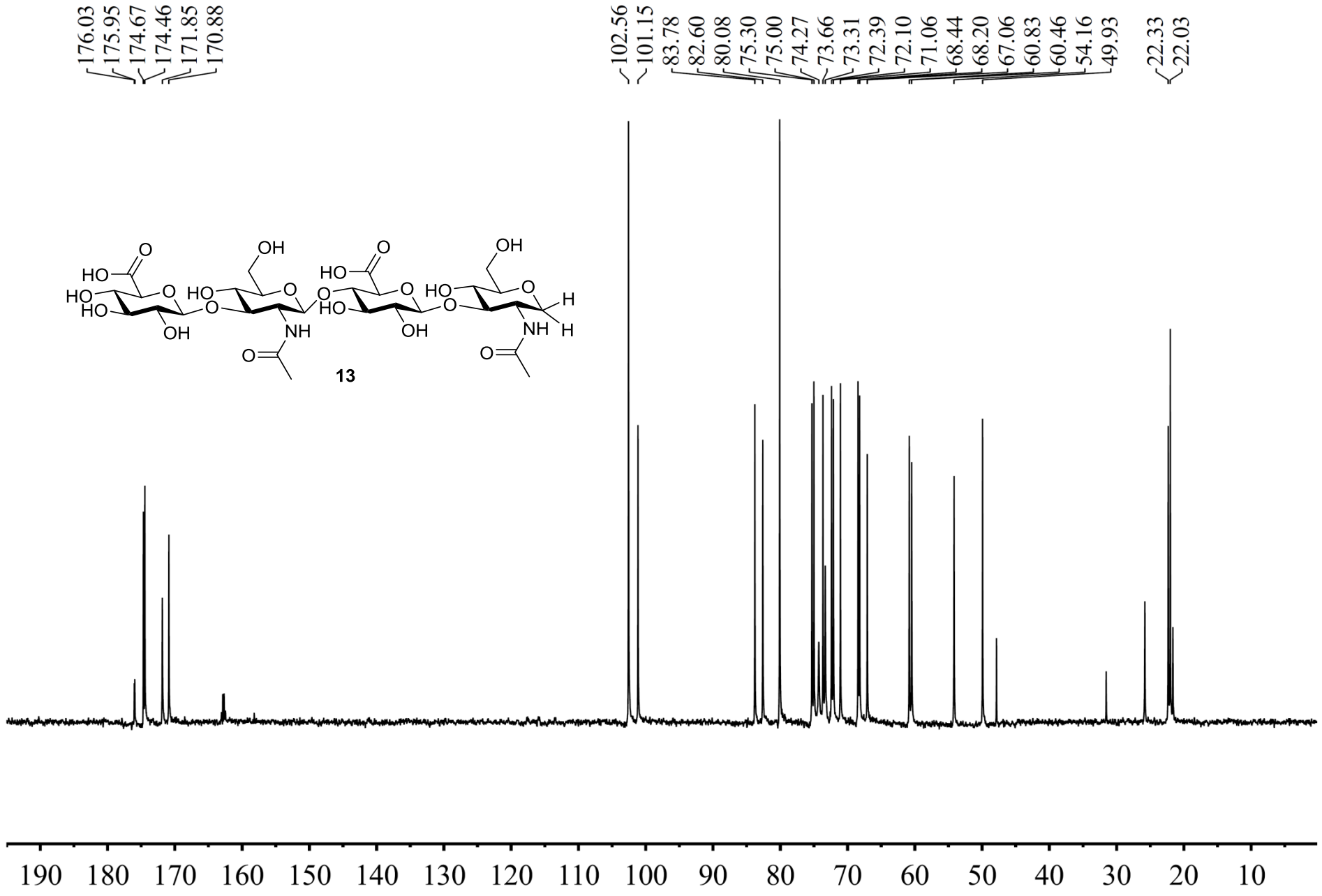
176.03
175.95
174.67
174.46
171.85
170.88
102.56
101.15
83.78
82.60
80.08
75.30
75.00
74.27
73.66
73.31
72.39
72.10
71.06
68.44
68.20
67.06
60.83
60.46
54.16
49.93
22.33
22.03
13
190
180
170
160
150
140
130
120
110
100
90
80
70
60
50
40
30
20
10

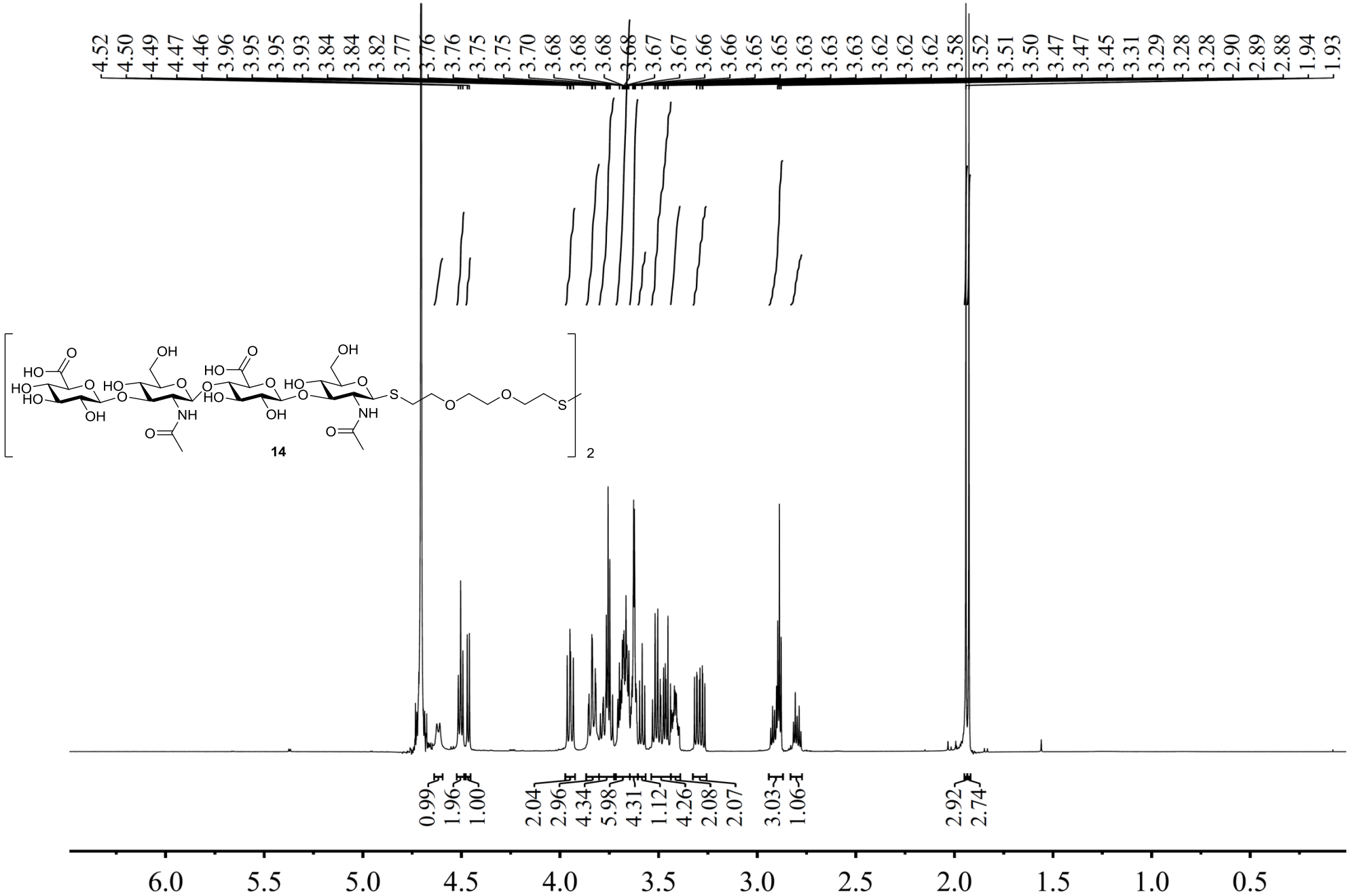
4.52 4.50 4.49 4.47 4.46 3.96 3.95 3.95 3.93 3.84 3.84 3.82 3.77 3.76 3.76 3.75 3.75 3.70 3.68 3.68 3.68 3.68 3.67 3.67 3.66 3.66 3.65 3.65 3.63 3.63 3.63 3.62 3.62 3.62 3.58 3.52 3.51 3.50 3.47 3.47 3.45 3.31 3.29 3.28 3.28 2.90 2.89 2.88 1.94 1.93
14
2
0.99 1.96 1.00 2.04 2.96 4.34 5.98 4.31 1.12 4.26 2.08 2.07 3.03 1.06 2.92 2.74
6.0 5.5 5.0 4.5 4.0 3.5 3.0 2.5 2.0 1.5 1.0 0.5

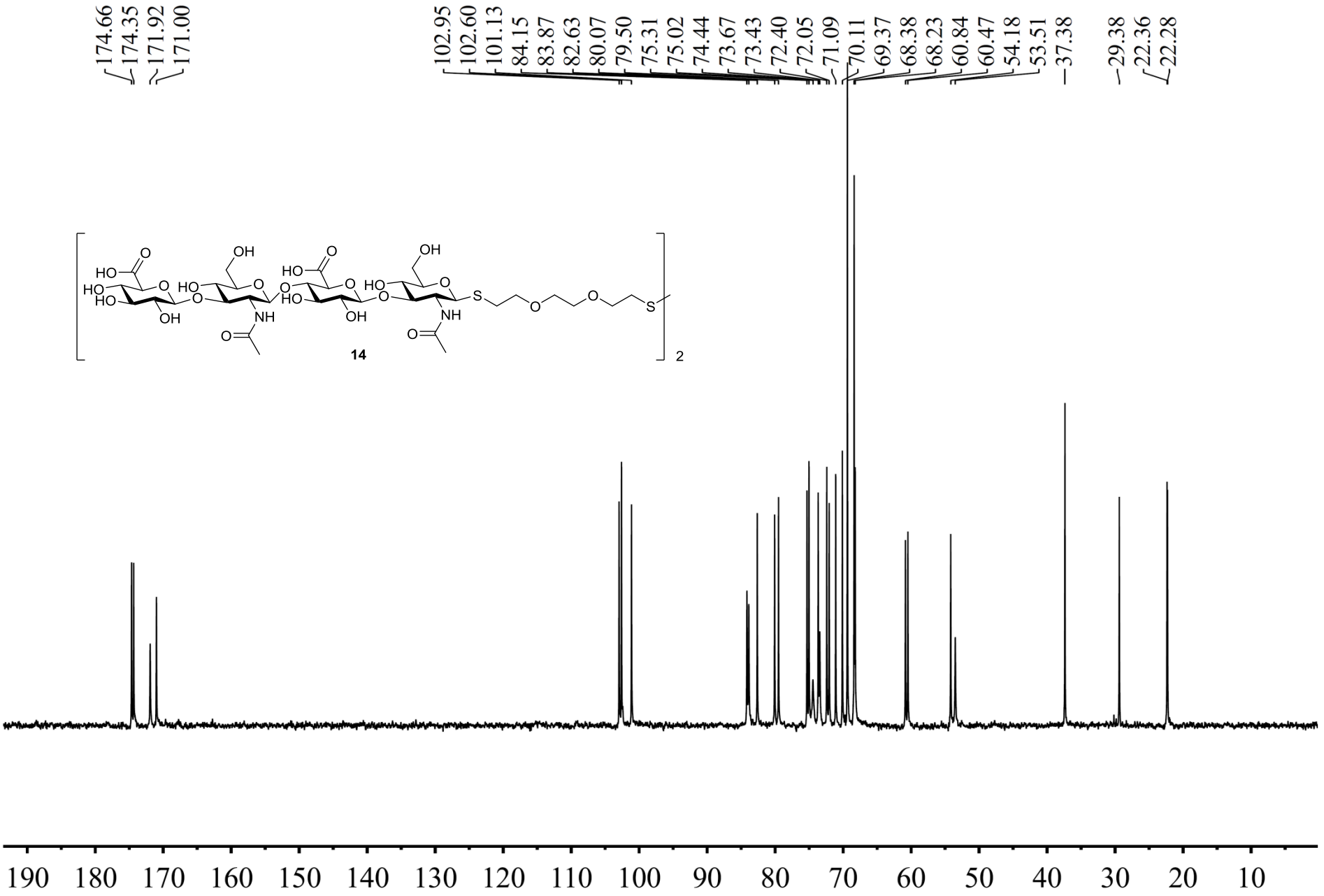
174.66
174.35
171.92
171.00
102.95
102.60
101.13
84.15
83.87
82.63
80.07
79.50
75.31
75.02
74.44
73.67
73.43
72.40
72.05
71.09
70.11
69.37
68.38
68.23
60.84
60.47
54.18
53.51
37.38
29.38
22.36
22.28
14
2
190
180
170
160
150
140
130
120
110
100
90
80
70
60
50
40
30
20
10

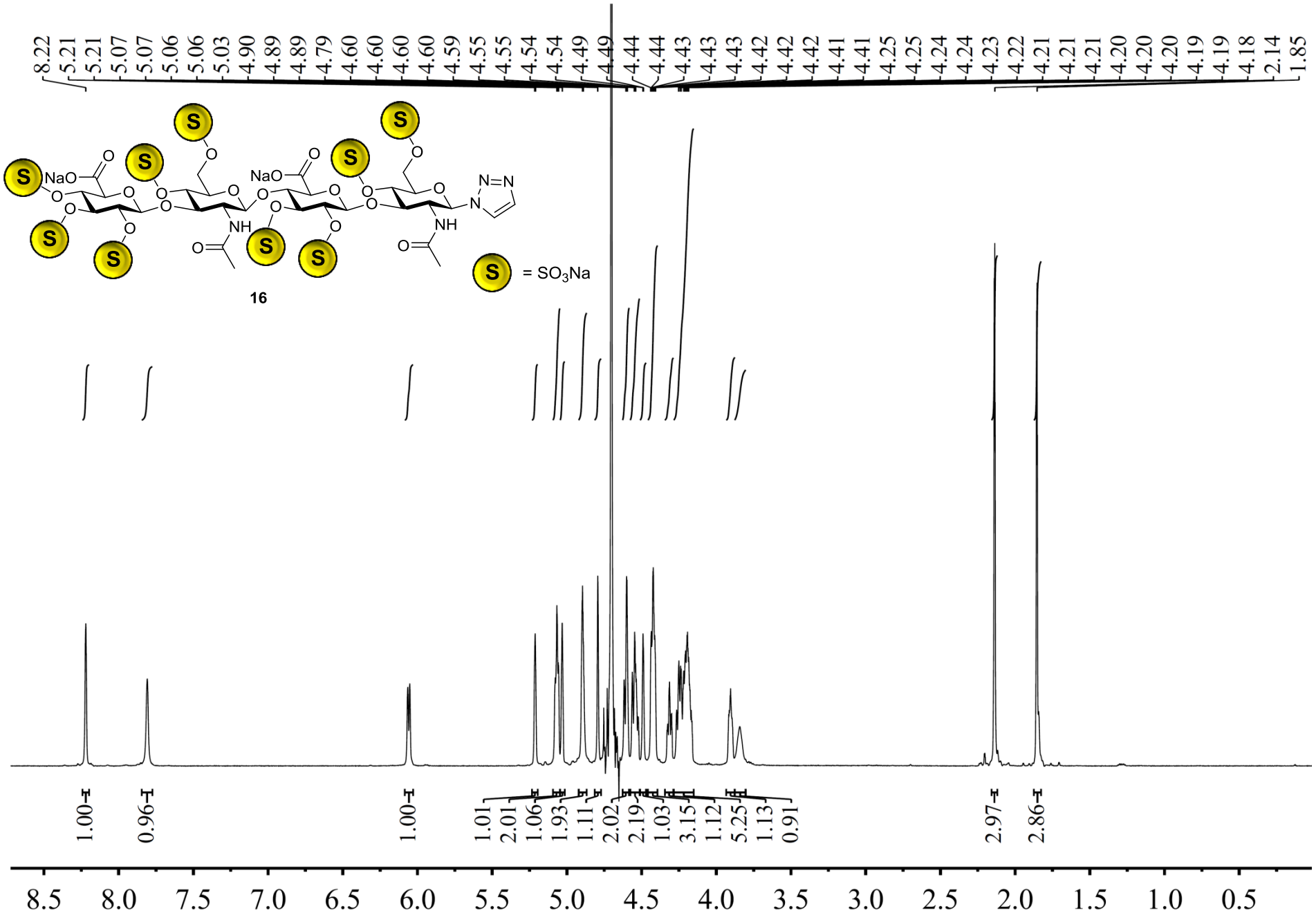
8.22
5.21
5.21
5.07
5.07
5.06
5.06
5.03
4.90
4.89
4.89
4.79
4.60
4.60
4.60
4.60
4.59
4.55
4.55
4.54
4.54
4.49
4.49
4.44
4.44
4.43
4.43
4.43
4.42
4.42
4.42
4.41
4.41
4.25
4.25
4.24
4.24
4.23
4.22
4.21
4.21
4.21
4.20
4.20
4.20
4.19
4.19
4.18
2.14
1.85
NaO
NaO
NH
NH
N=N
N
S
= SO3Na
16
1.00
0.96
1.00
1.01
2.01
1.06
1.93
1.11
2.02
2.19
1.03
3.15
1.12
5.25
1.13
0.91
2.97
2.86
8.5
8.0
7.5
7.0
6.5
6.0
5.5
5.0
4.5
4.0
3.5
3.0
2.5
2.0
1.5
1.0
0.5

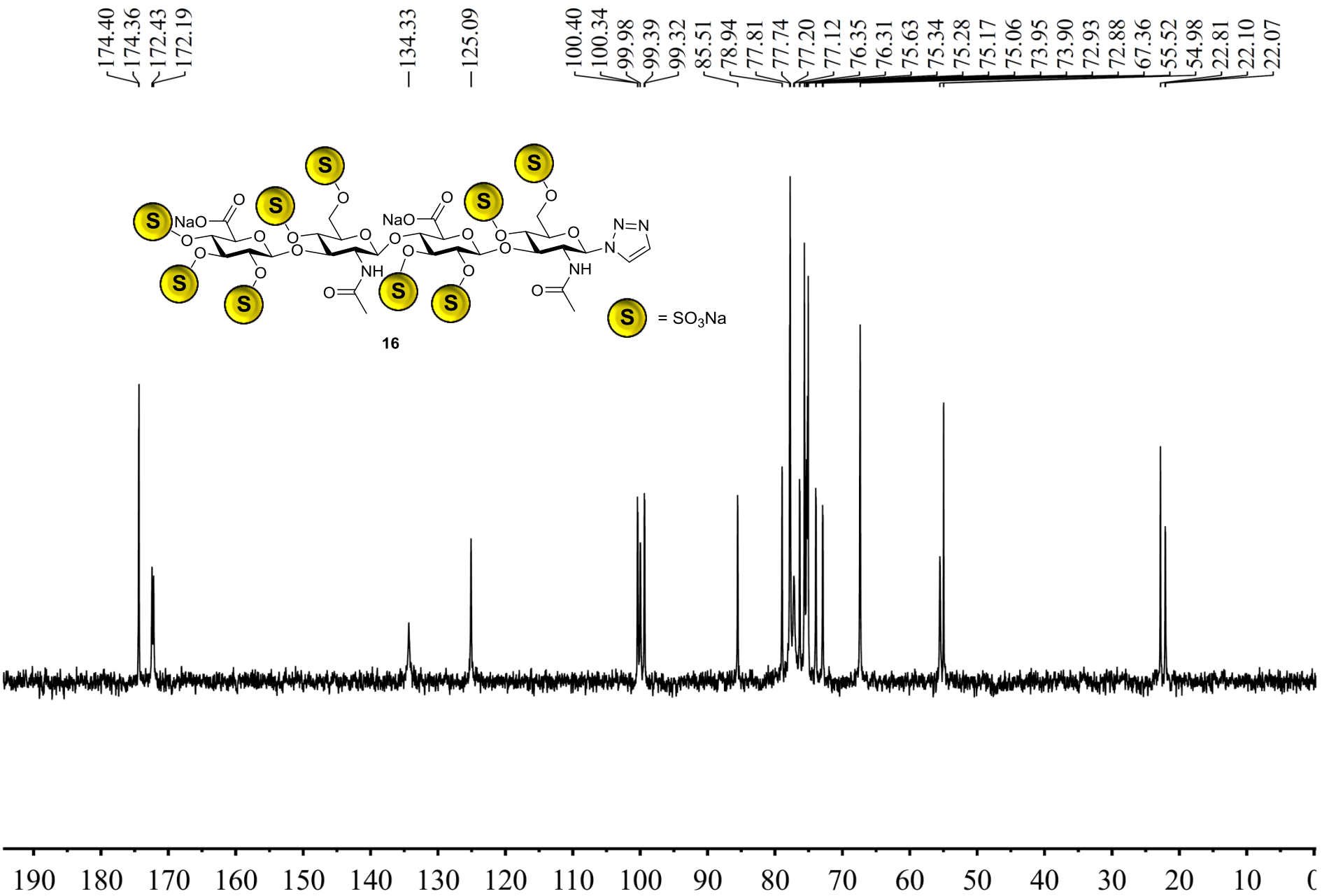
174.40
174.36
172.43
172.19
134.33
125.09
100.40
100.34
99.98
99.39
99.32
85.51
78.94
77.81
77.74
77.20
77.12
76.35
76.31
75.63
75.34
75.28
75.17
75.06
73.95
73.90
72.93
72.88
67.36
55.52
54.98
22.81
22.10
22.07
NaO
NaO
NH
NH
N=N
N
S
= SO3Na
16
190
180
170
160
150
140
130
120
110
100
90
80
70
60
50
40
30
20
10

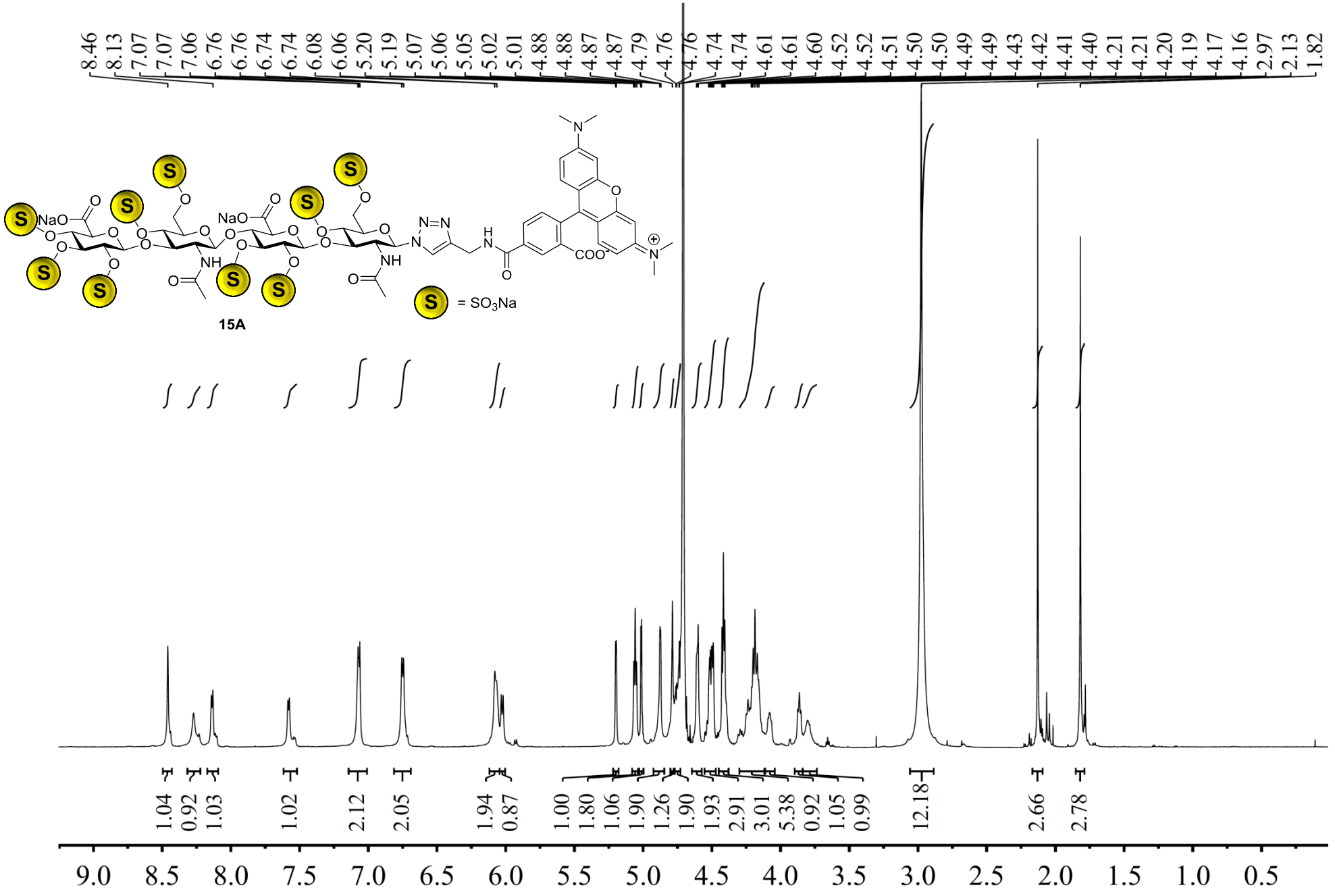
8.46 8.13 7.07 7.07 7.06 6.76 6.76 6.74 6.74 6.08 6.06 5.20 5.19 5.07 5.06 5.05 5.02 5.01 4.88 4.88 4.87 4.87 4.79 4.76 4.76 4.74 4.74 4.61 4.61 4.60 4.52 4.52 4.51 4.50 4.50 4.49 4.49 4.43 4.42 4.41 4.40 4.21 4.21 4.20 4.19 4.17 4.16 2.97 2.13 1.82
15A
S = SO3Na
1.04 0.92 1.03 1.02 2.12 2.05 1.94 0.87 1.00 1.80 1.06 1.90 1.26 1.90 1.93 2.91 3.01 5.38 0.92 1.05 0.99 12.18 2.66 2.78
9.0 8.5 8.0 7.5 7.0 6.5 6.0 5.5 5.0 4.5 4.0 3.5 3.0 2.5 2.0 1.5 1.0 0.5

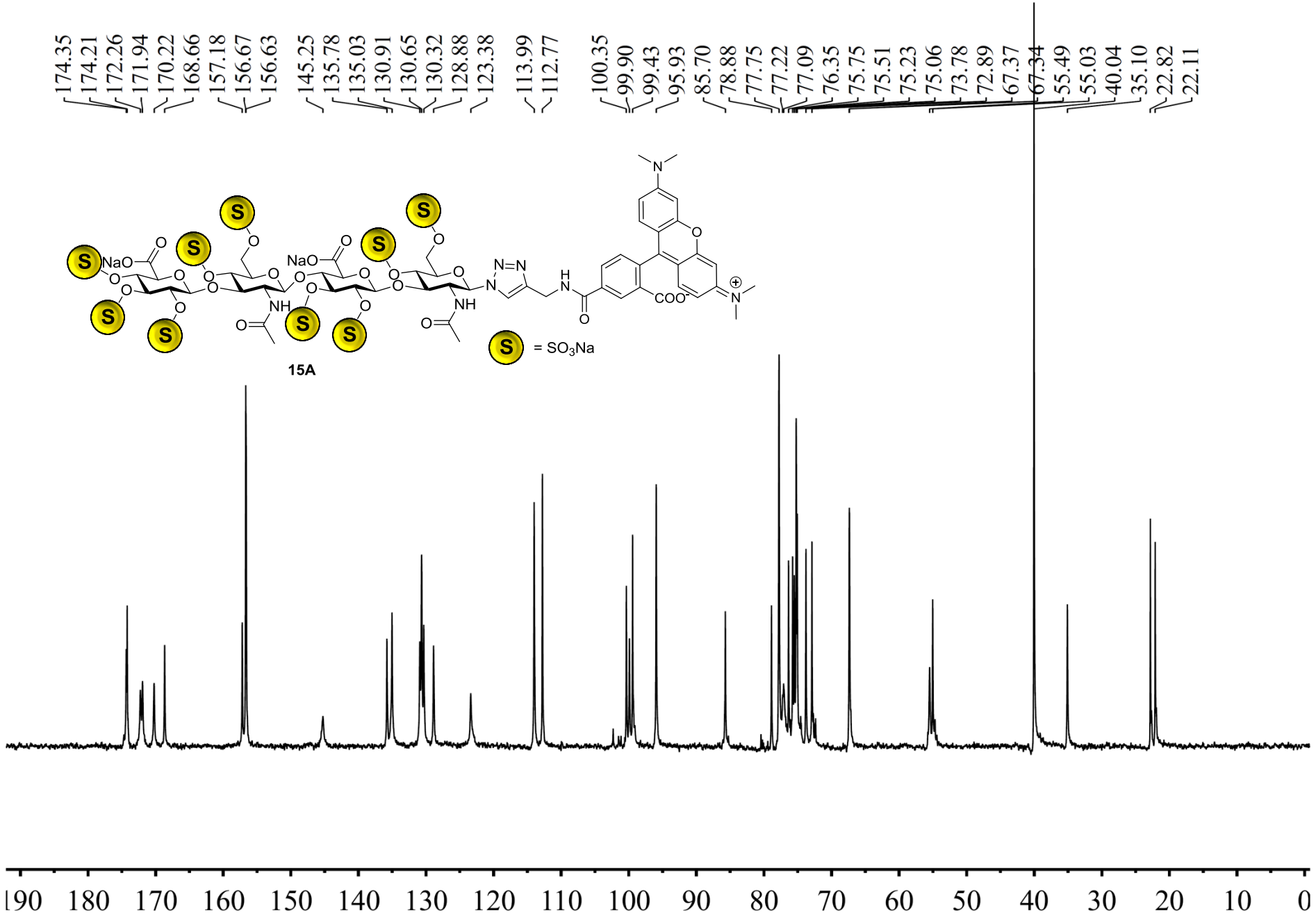
174.35
174.21
172.26
171.94
170.22
168.66
157.18
156.67
156.63
145.25
135.78
135.03
130.91
130.65
130.32
128.88
123.38
113.99
112.77
100.35
99.90
99.43
95.93
85.70
78.88
77.75
77.22
77.09
76.35
75.75
75.51
75.23
75.06
73.78
72.89
67.37
67.34
55.49
55.03
40.04
35.10
22.82
22.11
S = SO3Na
15A
190
180
170
160
150
140
130
120
110
100
90
80
70
60
50
40
30
20
10
0

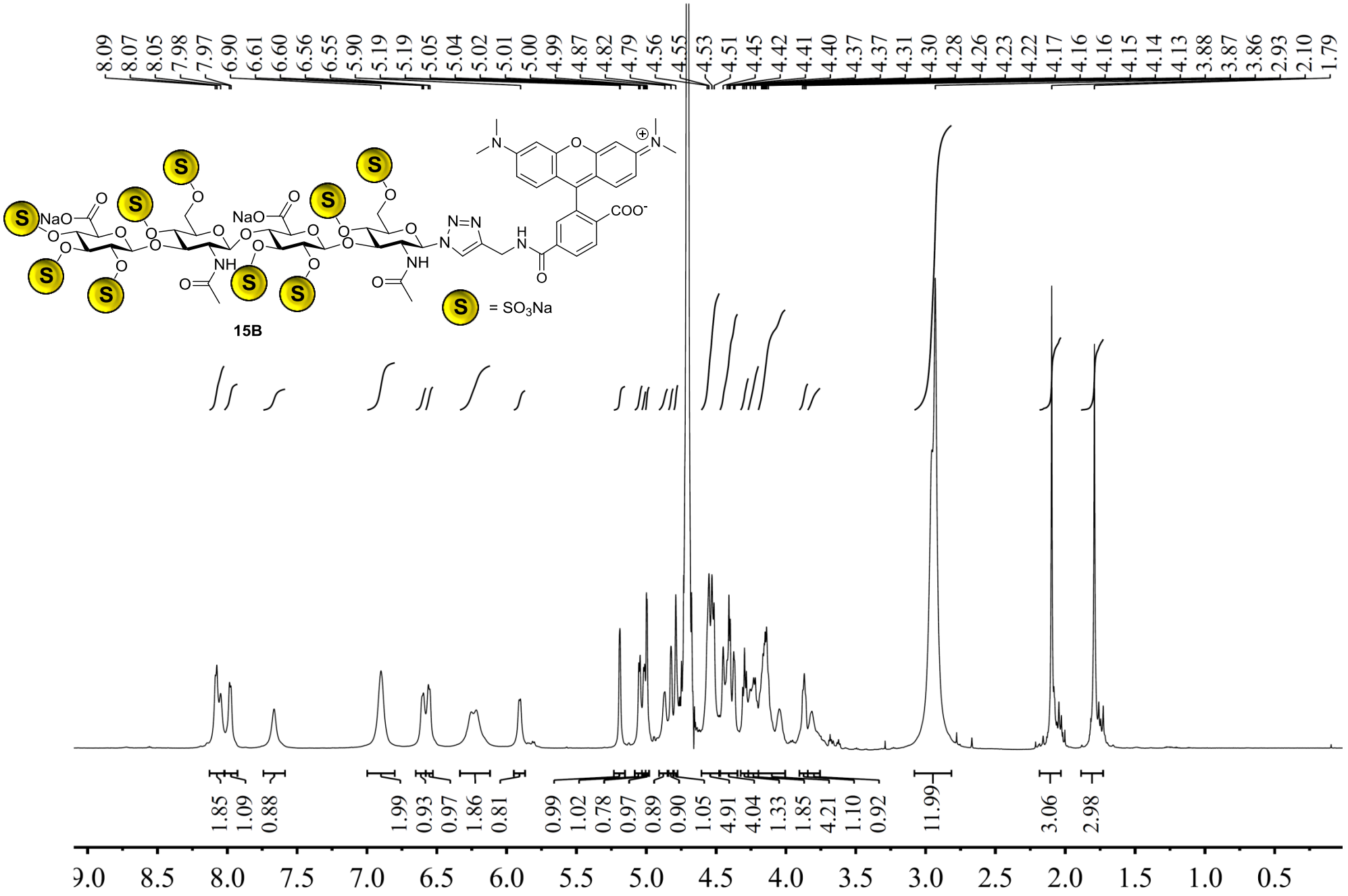
8.09 8.07 8.05 7.98 7.97 6.90 6.61 6.60 6.56 6.55 5.90 5.19 5.19 5.05 5.04 5.02 5.01 5.00 4.99 4.87 4.82 4.79 4.56 4.55 4.53 4.51 4.45 4.42 4.41 4.40 4.37 4.37 4.31 4.30 4.28 4.26 4.23 4.22 4.17 4.16 4.16 4.15 4.14 4.13 3.88 3.87 3.86 2.93 2.10 1.79
NaO
NH
N=N
COO-
S = SO3Na
15B
1.85 1.09 0.88 1.99 0.93 0.97 1.86 0.81 0.99 1.02 0.78 0.97 0.89 0.90 1.05 4.91 4.04 1.33 1.85 4.21 1.10 0.92 11.99 3.06 2.98
9.0 8.5 8.0 7.5 7.0 6.5 6.0 5.5 5.0 4.5 4.0 3.5 3.0 2.5 2.0 1.5 1.0 0.5

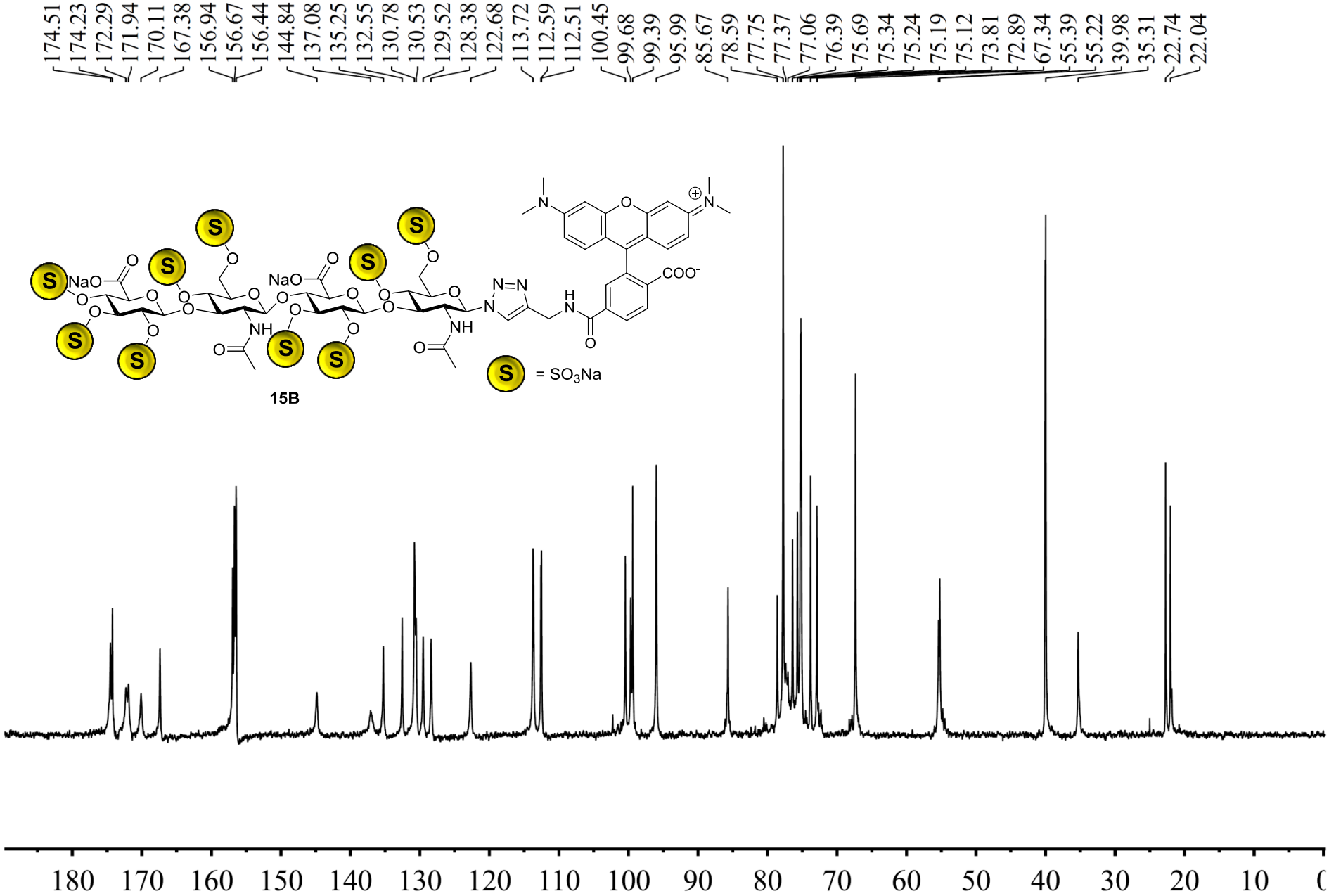
174.51
174.23
172.29
171.94
170.11
167.38
156.94
156.67
156.44
144.84
137.08
135.25
132.55
130.78
130.53
129.52
128.38
122.68
113.72
112.59
112.51
100.45
99.68
99.39
95.99
85.67
78.59
77.75
77.37
77.06
76.39
75.69
75.34
75.24
75.19
75.12
73.81
72.89
67.34
55.39
55.22
39.98
35.31
22.74
22.04
NaO
NH
N=N
COO-
= SO3Na
15B
180
170
160
150
140
130
120
110
100
90
80
70
60
50
40
30
20
10

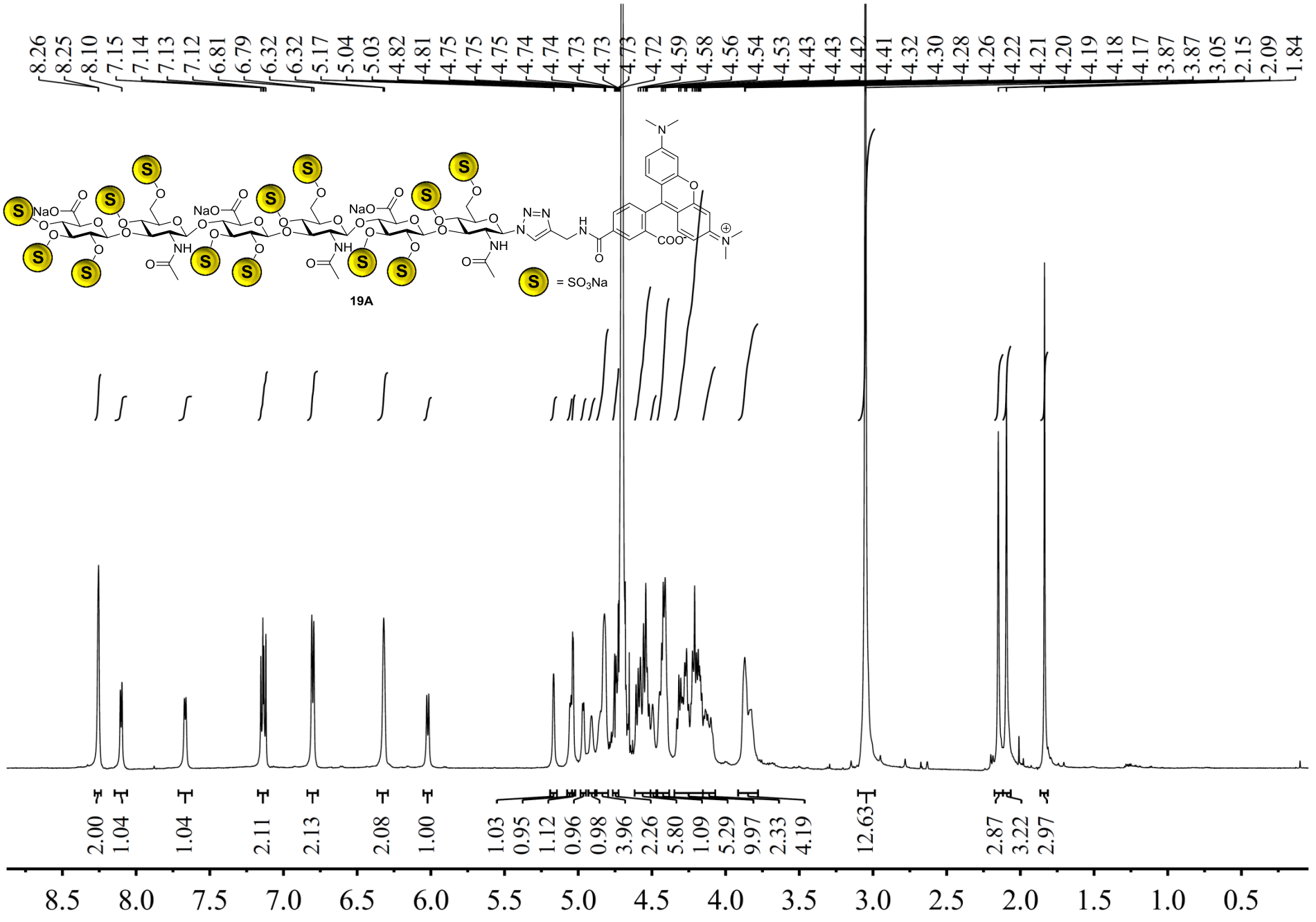
8.26 8.25 8.10 7.15 7.14 7.13 7.12 6.81 6.79 6.32 6.32 5.17 5.04 5.03 4.82 4.81 4.75 4.75 4.75 4.74 4.74 4.73 4.73 4.73 4.72 4.59 4.58 4.56 4.54 4.53 4.43 4.43 4.42 4.41 4.32 4.30 4.28 4.26 4.22 4.21 4.20 4.19 4.18 4.17 3.87 3.87 3.05 2.15 2.09 1.84
S = SO3Na
19A
2.00 1.04 1.04 2.11 2.13 2.08 1.00 1.03 0.95 1.12 0.96 0.98 3.96 2.26 5.80 1.09 5.29 9.97 2.33 4.19 12.63 2.87 3.22 2.97
8.5 8.0 7.5 7.0 6.5 6.0 5.5 5.0 4.5 4.0 3.5 3.0 2.5 2.0 1.5 1.0 0.5

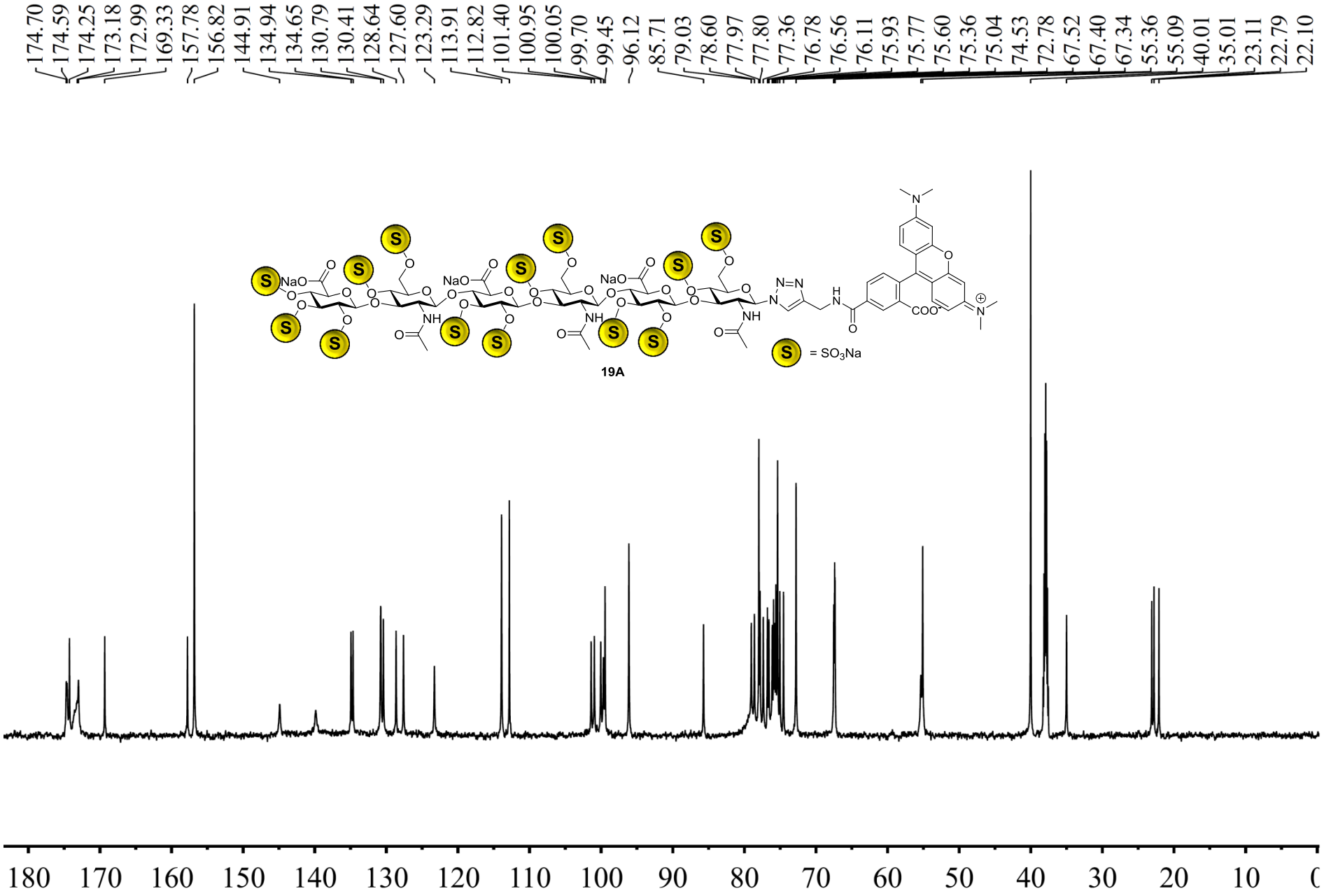
174.70
174.59
174.25
173.18
172.99
169.33
157.78
156.82
144.91
134.94
134.65
130.79
130.41
128.64
127.60
123.29
113.91
112.82
101.40
100.95
100.05
99.70
99.45
96.12
85.71
79.03
78.60
77.97
77.80
77.36
76.78
76.56
76.11
75.93
75.77
75.60
75.36
75.04
74.53
72.78
67.52
67.40
67.34
55.36
55.09
40.01
35.01
23.11
22.79
22.10
S = SO3Na
19A
180
170
160
150
140
130
120
110
100
90
80
70
60
50
40
30
20
10

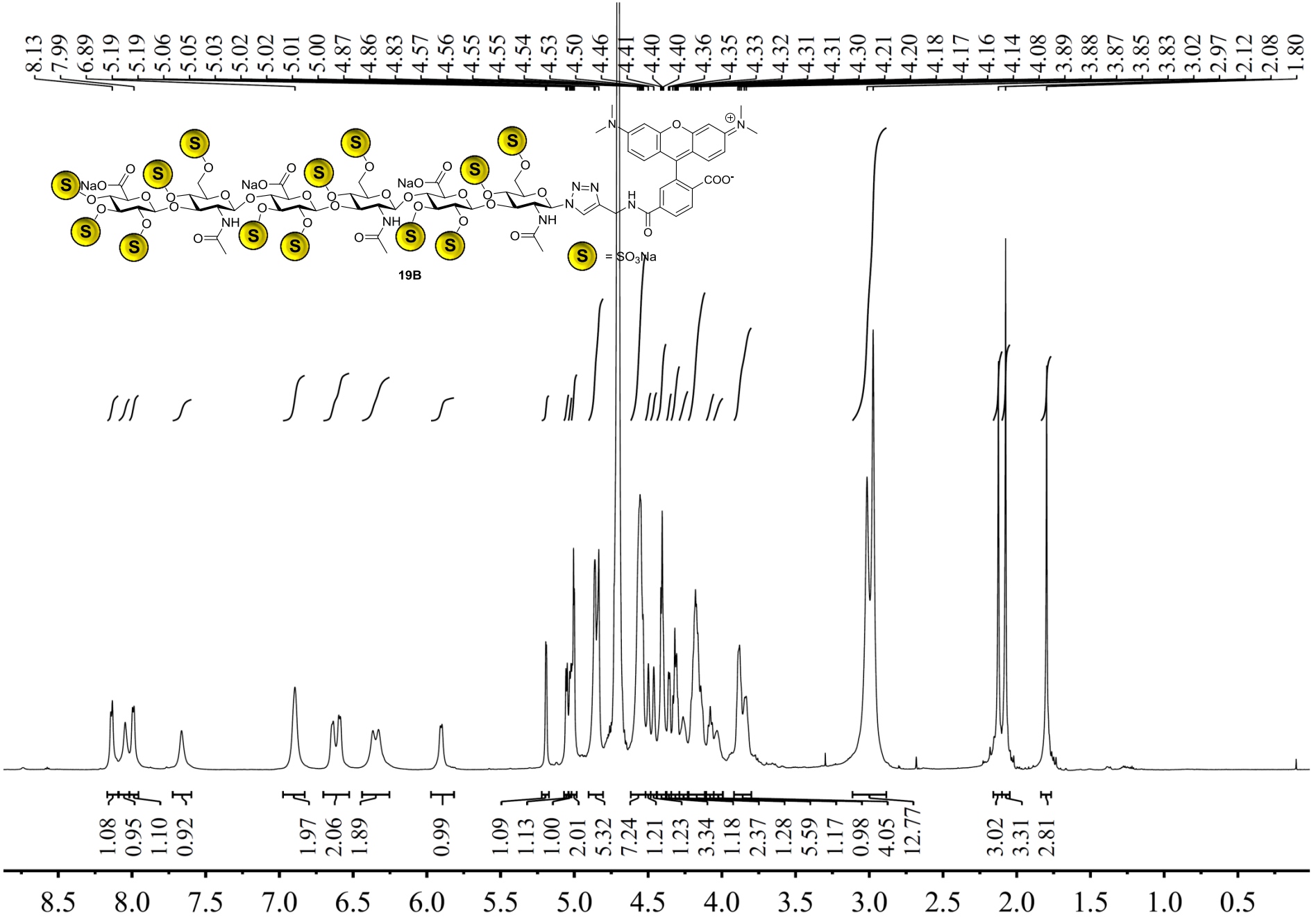
8.13 7.99 6.89 5.19 5.19 5.06 5.05 5.03 5.02 5.02 5.01 5.00 4.87 4.86 4.83 4.57 4.56 4.55 4.55 4.54 4.53 4.50 4.46 4.41 4.40 4.40 4.36 4.35 4.33 4.32 4.31 4.31 4.30 4.21 4.20 4.18 4.17 4.16 4.14 4.08 3.89 3.88 3.87 3.85 3.83 3.02 2.97 2.12 2.08 1.80
19B
S = SO3Na
1.08 0.95 1.10 0.92 1.97 2.06 1.89 0.99 1.09 1.13 1.00 2.01 5.32 7.24 1.21 1.23 3.34 1.18 2.37 1.28 5.59 1.17 0.98 4.05 12.77 3.02 3.31 2.81
8.5 8.0 7.5 7.0 6.5 6.0 5.5 5.0 4.5 4.0 3.5 3.0 2.5 2.0 1.5 1.0 0.5

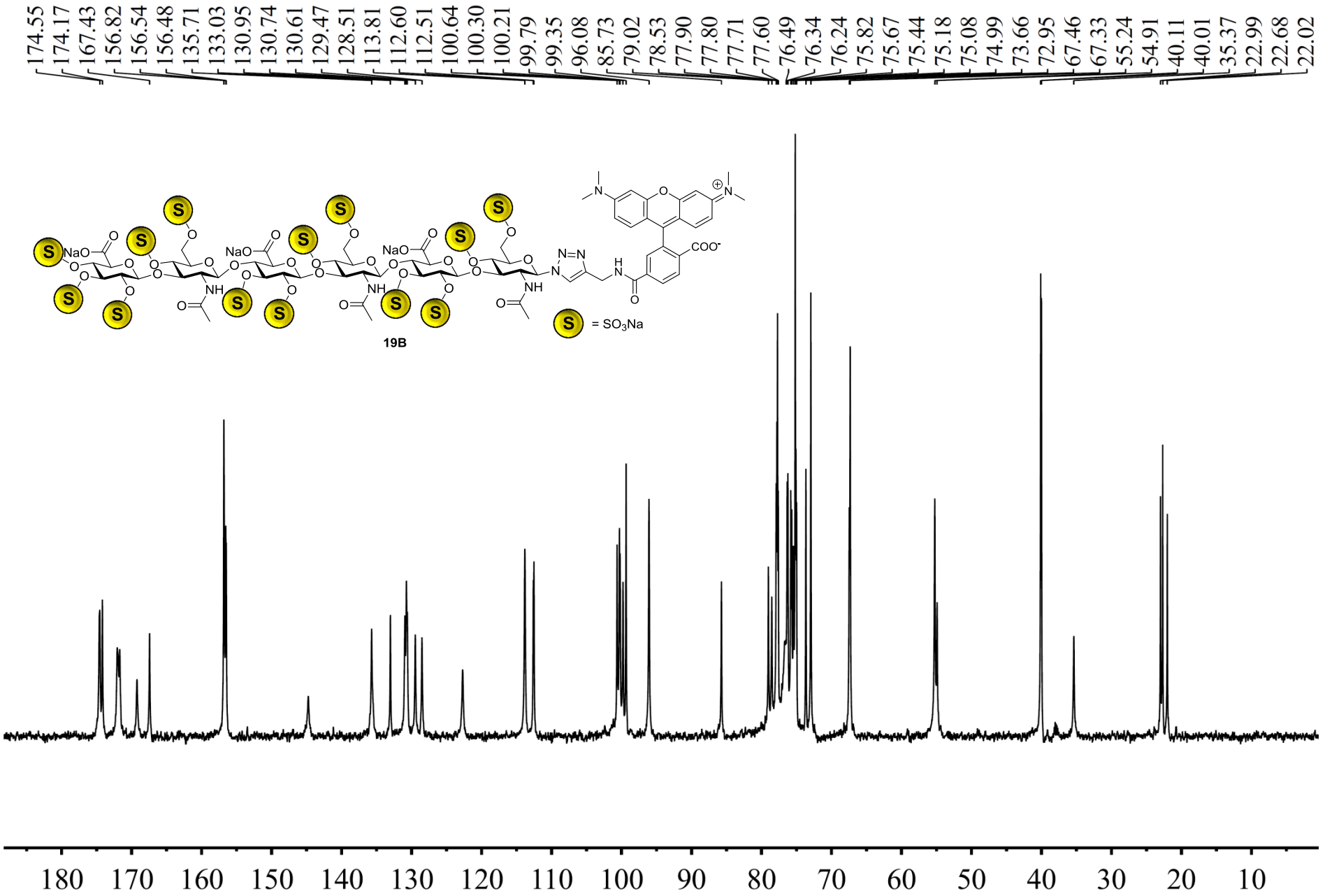
174.55
174.17
167.43
156.82
156.54
156.48
135.71
133.03
130.95
130.74
130.61
129.47
128.51
113.81
112.60
112.51
100.64
100.30
100.21
99.79
99.35
96.08
85.73
79.02
78.53
77.90
77.80
77.71
77.60
76.49
76.34
76.24
75.82
75.67
75.44
75.18
75.08
74.99
73.66
72.95
67.46
67.33
55.24
54.91
40.11
40.01
35.37
22.99
22.68
22.02
S = SO3Na
19B
180
170
160
150
140
130
120
110
100
90
80
70
60
50
40
30
20
10

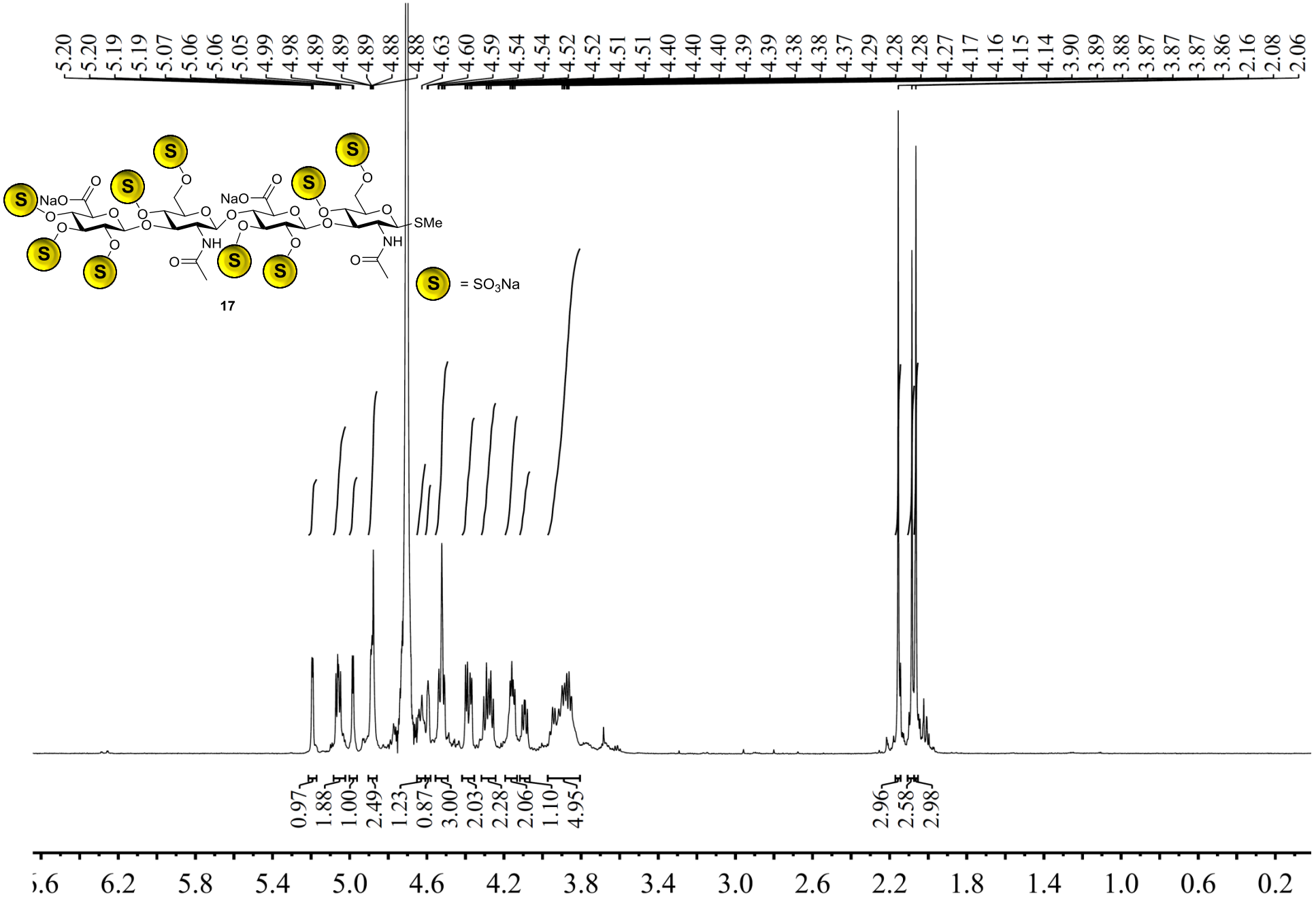
5.20 5.20 5.19 5.19 5.07 5.06 5.06 5.05 4.99 4.98 4.89 4.89 4.89 4.88 4.88 4.63 4.60 4.59 4.54 4.54 4.52 4.52 4.51 4.51 4.40 4.40 4.40 4.39 4.39 4.38 4.38 4.37 4.29 4.28 4.28 4.27 4.17 4.16 4.15 4.14 3.90 3.89 3.88 3.87 3.87 3.87 3.86 2.16 2.08 2.06
NaO
NaO
SMe
NH
NH
= SO3Na
17
0.97 1.88 1.00 2.49 1.23 0.87 3.00 2.03 2.28 2.06 1.10 4.95
2.96 2.58 2.98
6.6 6.2 5.8 5.4 5.0 4.6 4.2 3.8 3.4 3.0 2.6 2.2 1.8 1.4 1.0 0.6 0.2

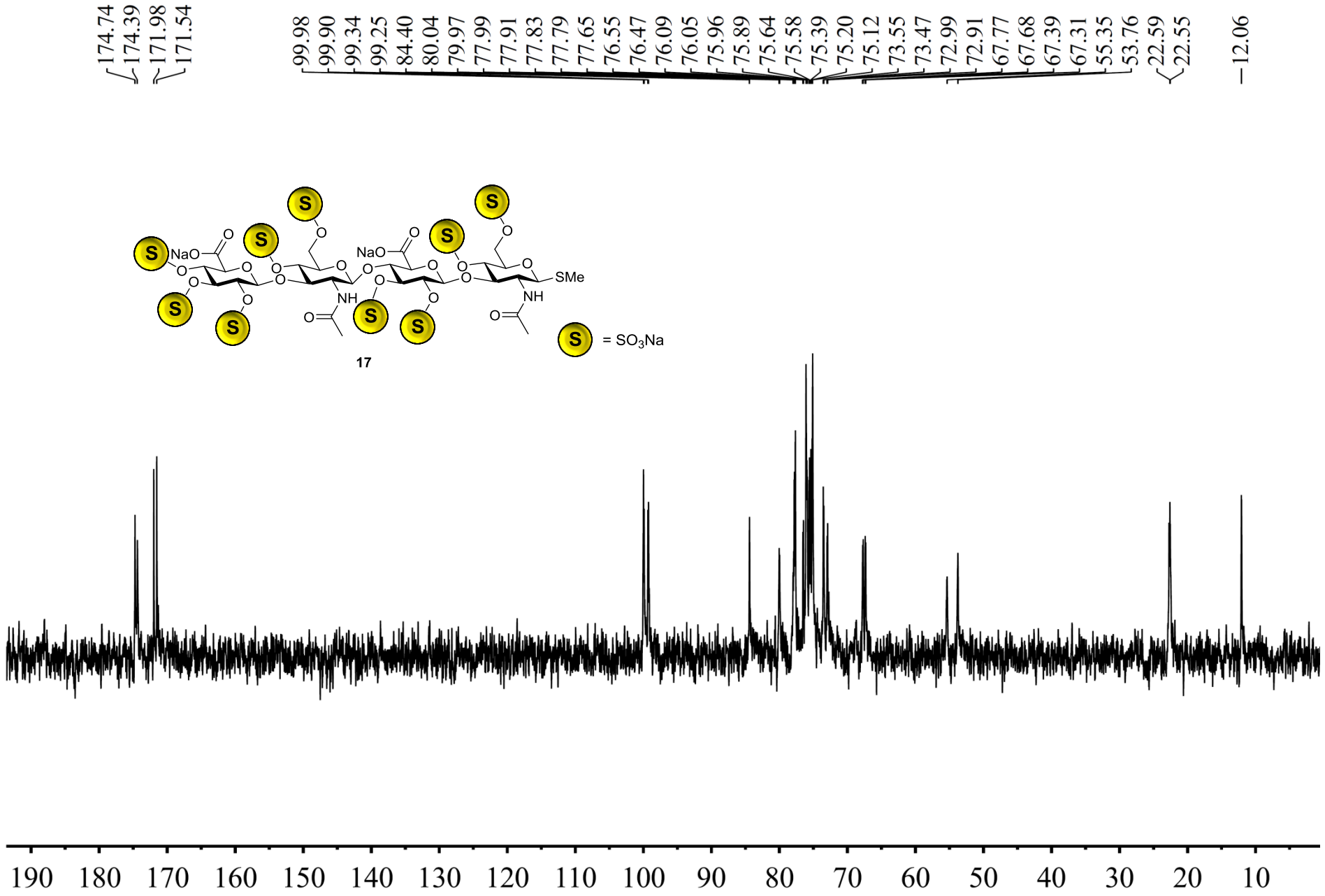
174.74
174.39
171.98
171.54
99.98
99.90
99.34
99.25
84.40
80.04
79.97
77.99
77.91
77.83
77.79
77.65
76.55
76.47
76.09
76.05
75.96
75.89
75.64
75.58
75.39
75.20
75.12
73.55
73.47
72.99
72.91
67.77
67.68
67.39
67.31
55.35
53.76
22.59
22.55
12.06
NaO
NaO
NH
NH
SMe
S
= SO3Na
17
190
180
170
160
150
140
130
120
110
100
90
80
70
60
50
40
30
20
10

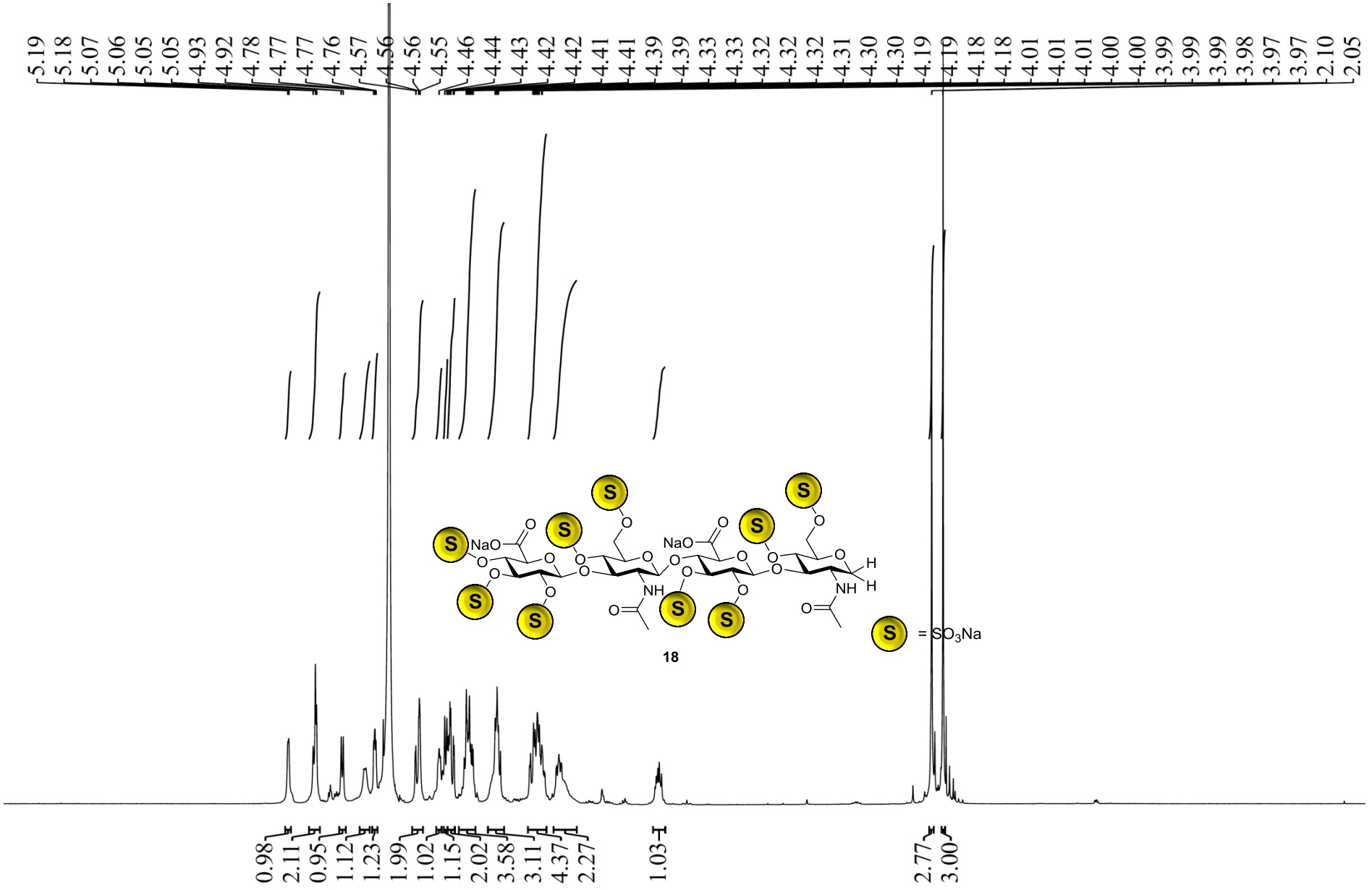
5.19 5.18 5.07 5.06 5.05 5.05 4.93 4.92 4.78 4.77 4.77 4.76 4.57 4.56 4.56 4.55 4.46 4.44 4.43 4.42 4.42 4.41 4.41 4.39 4.39 4.33 4.33 4.32 4.32 4.32 4.31 4.30 4.30 4.19 4.19 4.18 4.18 4.01 4.01 4.01 4.00 4.00 3.99 3.99 3.99 3.98 3.97 3.97 2.10 2.05
NaO
NH
H
S = SO3Na
18
0.98 2.11 0.95 1.12 1.23 1.99 1.02 1.15 2.02 3.58 3.11 4.37 2.27 1.03 2.77 3.00
6.5 6.0 5.5 5.0 4.5 4.0 3.5 3.0 2.5 2.0 1.5 1.0 0.5

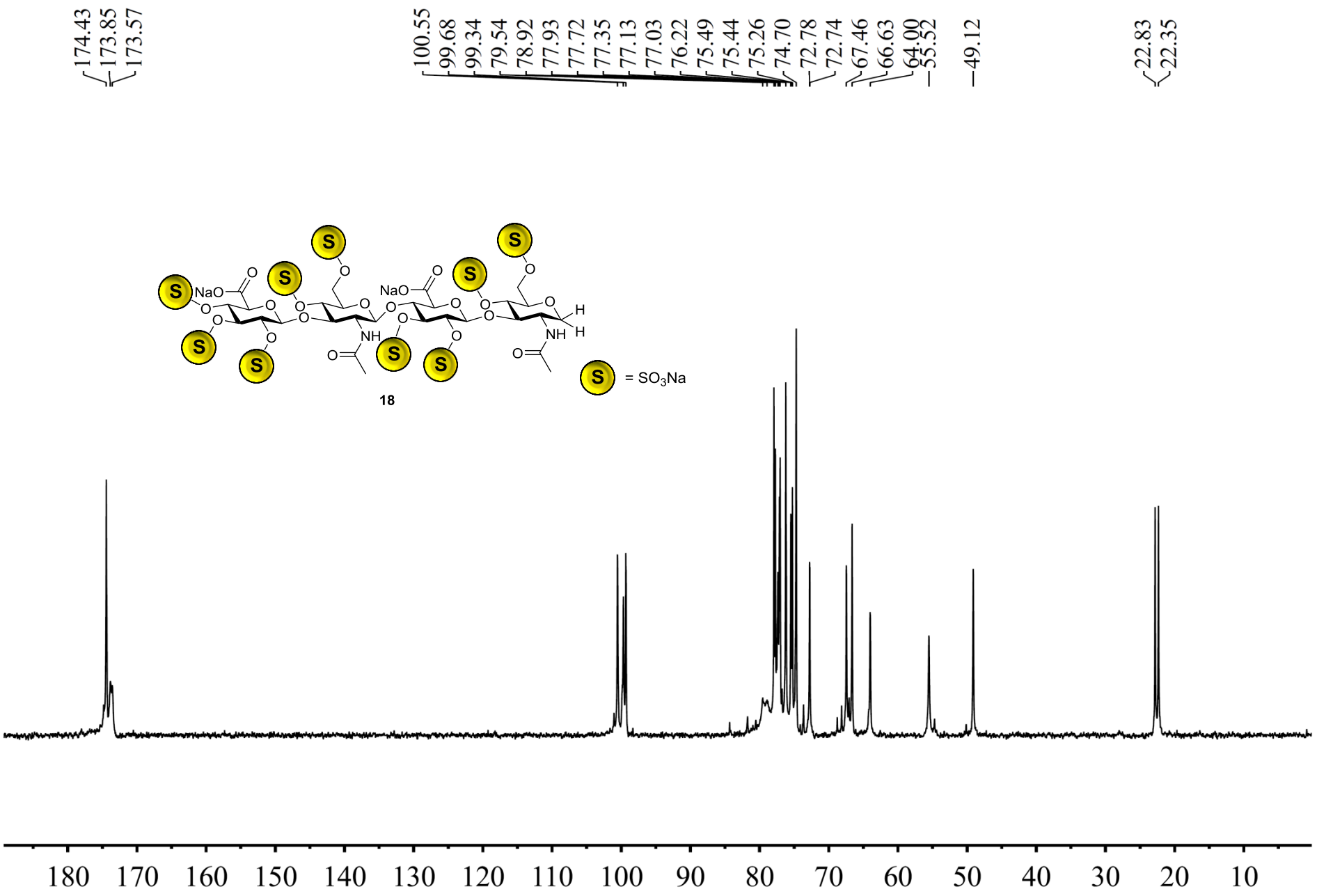
174.43
173.85
173.57
100.55
99.68
99.34
79.54
78.92
77.93
77.72
77.35
77.13
77.03
76.22
75.49
75.44
75.26
74.70
72.78
72.74
67.46
66.63
64.00
55.52
49.12
22.83
22.35
NaO
NH
H
S = SO3Na
18
180
170
160
150
140
130
120
110
100
90
80
70
60
50
40
30
20
10

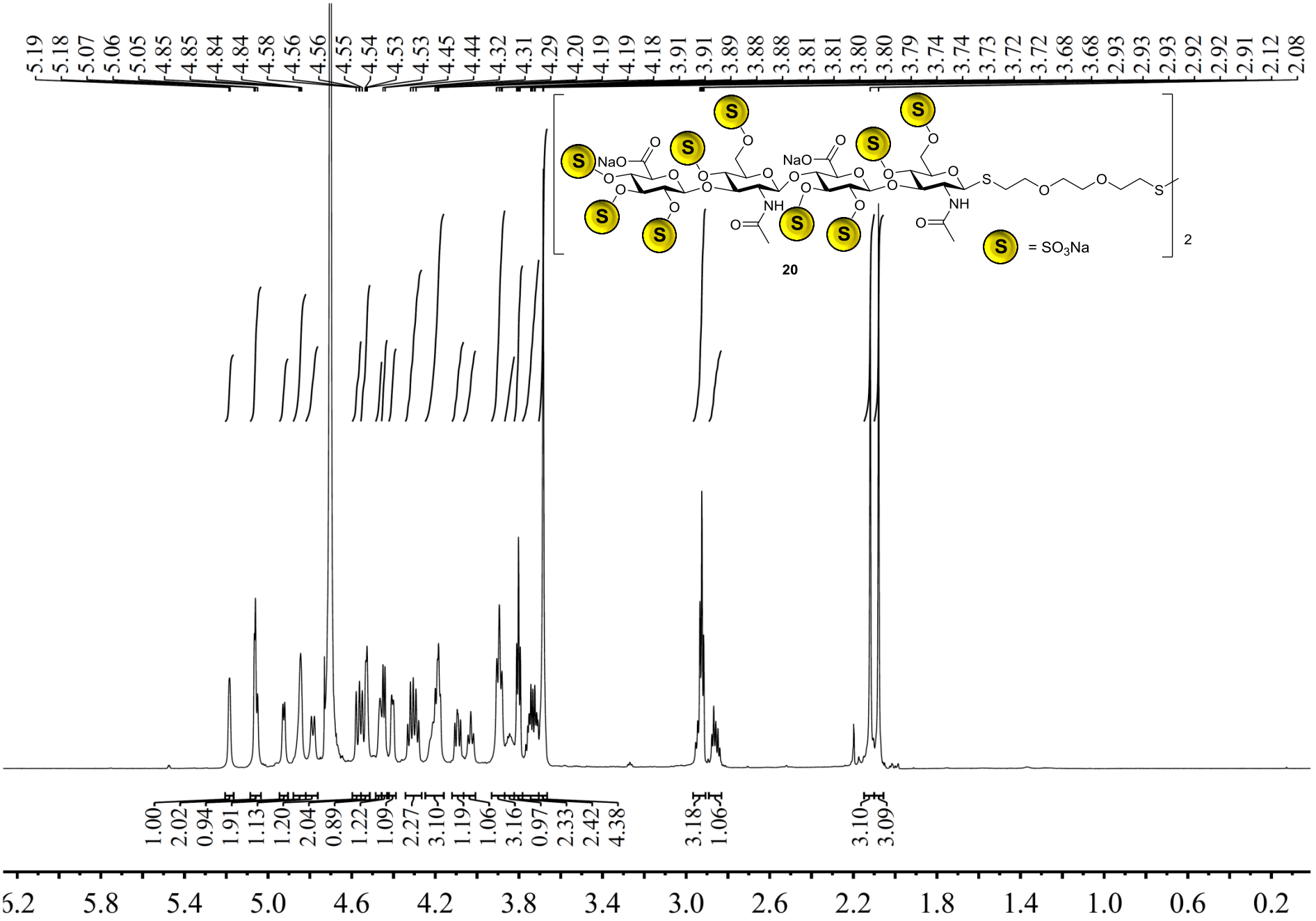
5.19 5.18 5.07 5.06 5.05 4.85 4.85 4.84 4.84 4.58 4.56 4.56 4.55 4.54 4.53 4.53 4.45 4.44 4.32 4.31 4.29 4.20 4.19 4.19 4.18 3.91 3.91 3.89 3.88 3.88 3.81 3.81 3.80 3.80 3.79 3.74 3.74 3.73 3.72 3.72 3.68 3.68 2.93 2.93 2.93 2.92 2.92 2.91 2.12 2.08
NaO
NH
S = SO3Na
2
20
1.00 2.02 0.94 1.91 1.13 1.20 2.04 0.89 1.22 1.09 2.27 3.10 1.19 1.06 3.16 0.97 2.33 2.42 4.38 3.18 1.06 3.10 3.09
6.2 5.8 5.4 5.0 4.6 4.2 3.8 3.4 3.0 2.6 2.2 1.8 1.4 1.0 0.6 0.2

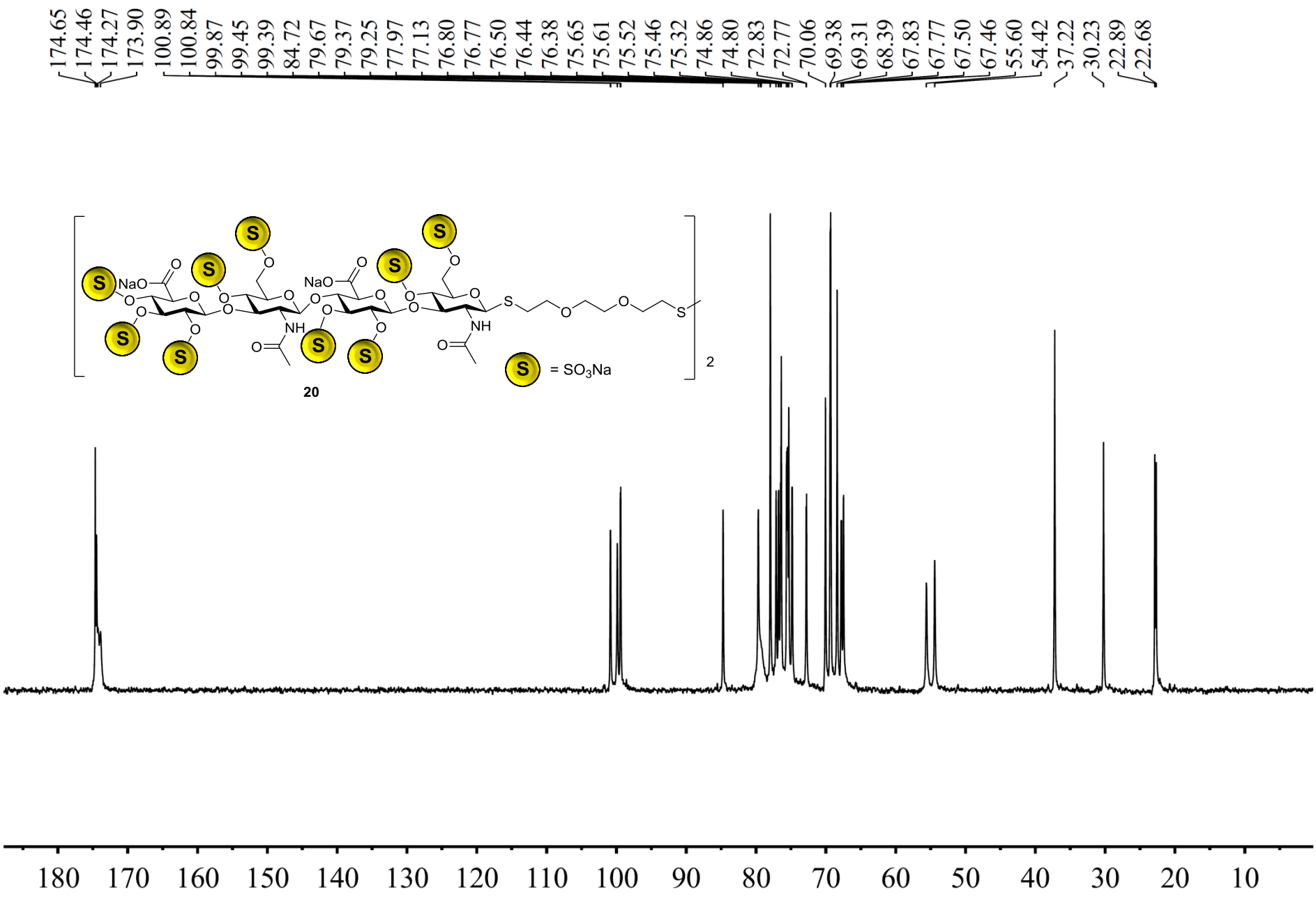
174.65
174.46
174.27
173.90
100.89
100.84
99.87
99.45
99.39
84.72
79.67
79.37
79.25
77.97
77.13
76.80
76.77
76.50
76.44
76.38
75.65
75.61
75.52
75.46
75.32
74.86
74.80
72.83
72.77
70.06
69.38
69.31
68.39
67.83
67.77
67.50
67.46
55.60
54.42
37.22
30.23
22.89
22.68
NaO
NH
S
O
= SO3Na
2
20
180
170
160
150
140
130
120
110
100
90
80
70
60
50
40
30
20
10

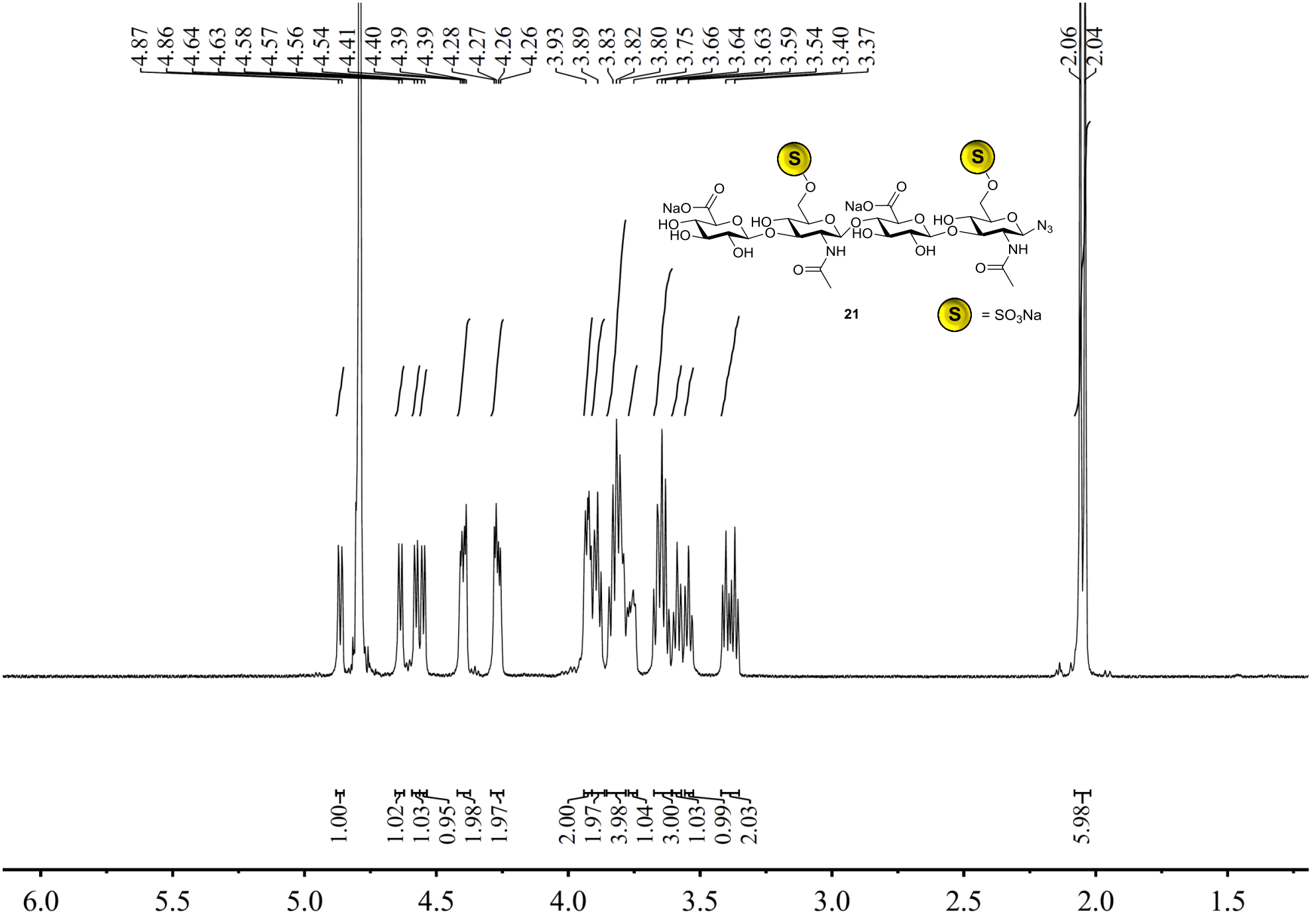
4.87
4.86
4.64
4.63
4.58
4.57
4.56
4.54
4.41
4.40
4.39
4.39
4.28
4.27
4.26
4.26
3.93
3.89
3.83
3.82
3.80
3.75
3.66
3.64
3.63
3.59
3.54
3.40
3.37
2.06
2.04
NaO
HO
HO
OH
NH
O
N3
21
S
= SO3Na
1.00
1.02
1.03
0.95
1.98
1.97
2.00
1.97
3.98
1.04
3.00
1.03
0.99
2.03
5.98
6.0
5.5
5.0
4.5
4.0
3.5
3.0
2.5
2.0
1.5

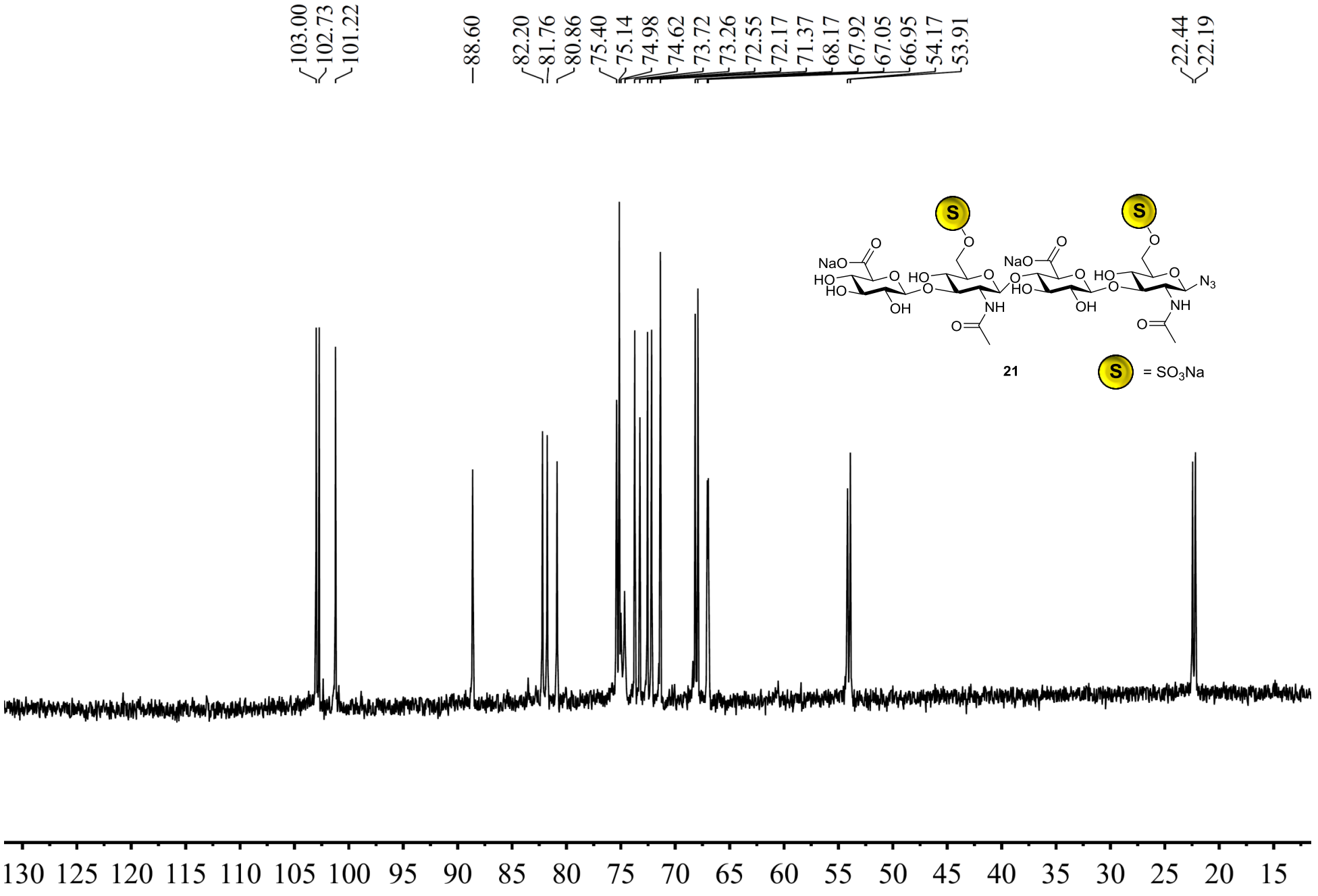
103.00
102.73
101.22
88.60
82.20
81.76
80.86
75.40
75.14
74.98
74.62
73.72
73.26
72.55
72.17
71.37
68.17
67.92
67.05
66.95
54.17
53.91
22.44
22.19
S
NaO
HO
OH
NH
N3
21
= SO3Na
130 125 120 115 110 105 100 95 90 85 80 75 70 65 60 55 50 45 40 35 30 25 20 15

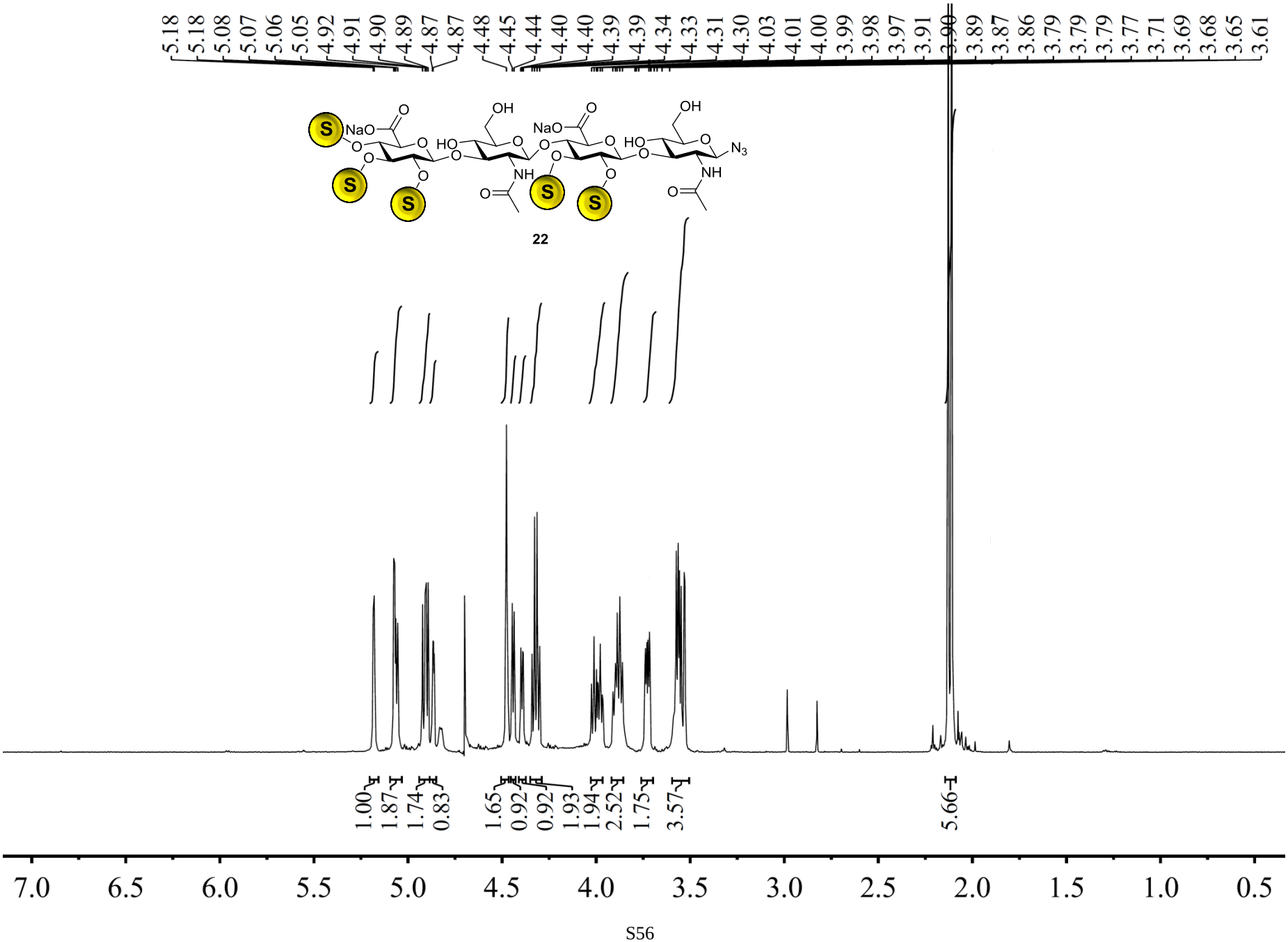
5.18 5.18 5.08 5.07 5.06 5.05 4.92 4.91 4.90 4.89 4.87 4.87 4.48 4.45 4.44 4.40 4.40 4.39 4.39 4.34 4.33 4.31 4.30 4.03 4.01 4.00 3.99 3.98 3.97 3.91 3.90 3.89 3.87 3.86 3.79 3.79 3.79 3.77 3.71 3.69 3.68 3.65 3.61
NaO
HO
OH
NH
N3
S
22
1.00 1.87 1.74 0.83 1.65 0.92 0.92 1.93 1.94 2.52 1.75 3.57 5.66
7.0 6.5 6.0 5.5 5.0 4.5 4.0 3.5 3.0 2.5 2.0 1.5 1.0 0.5

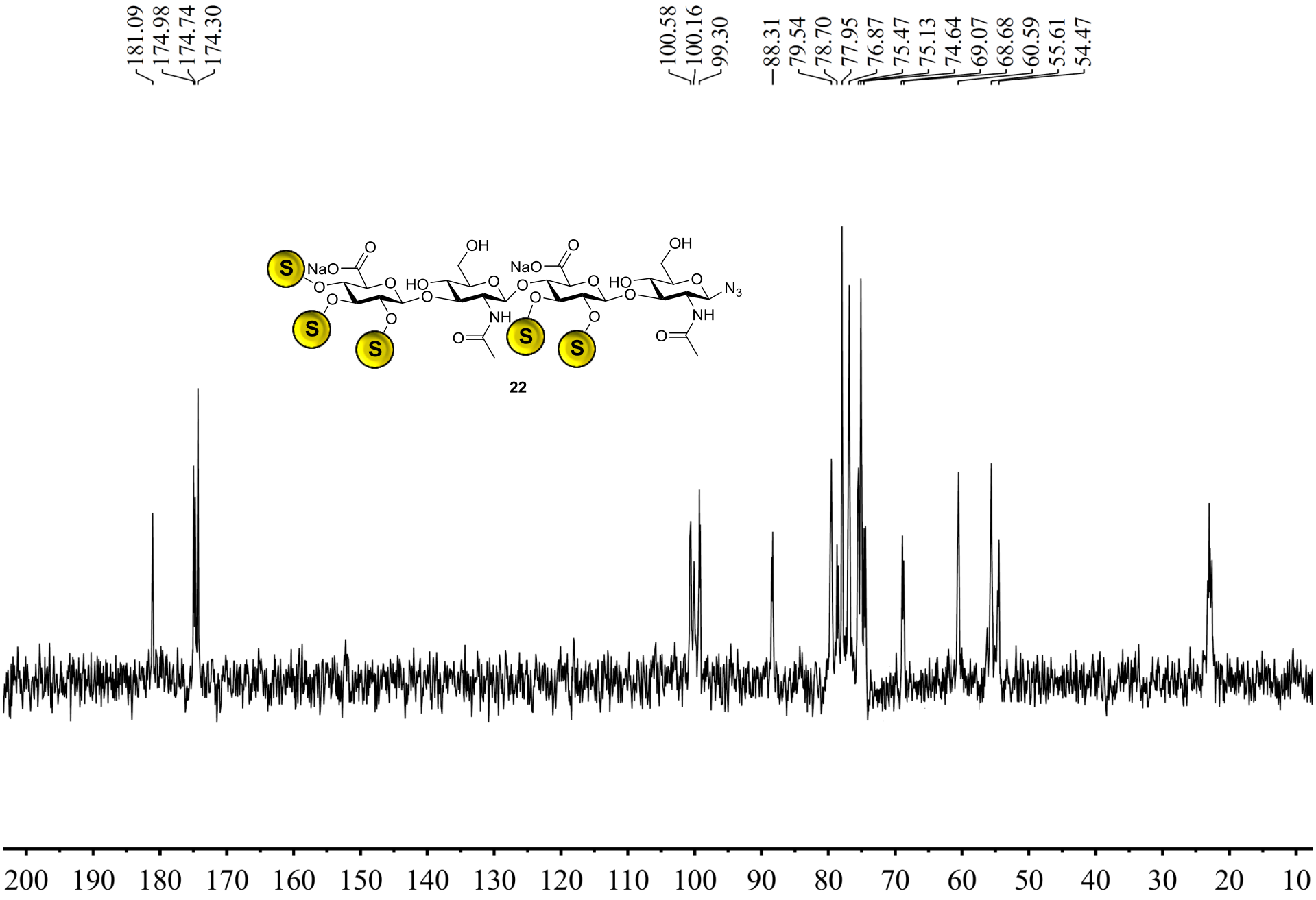
181.09
174.98
174.74
174.30
100.58
100.16
99.30
88.31
79.54
78.70
77.95
76.87
75.47
75.13
74.64
69.07
68.68
60.59
55.61
54.47
NaO
HO
OH
NH
N3
S
22
200
190
180
170
160
150
140
130
120
110
100
90
80
70
60
50
40
30
20
10

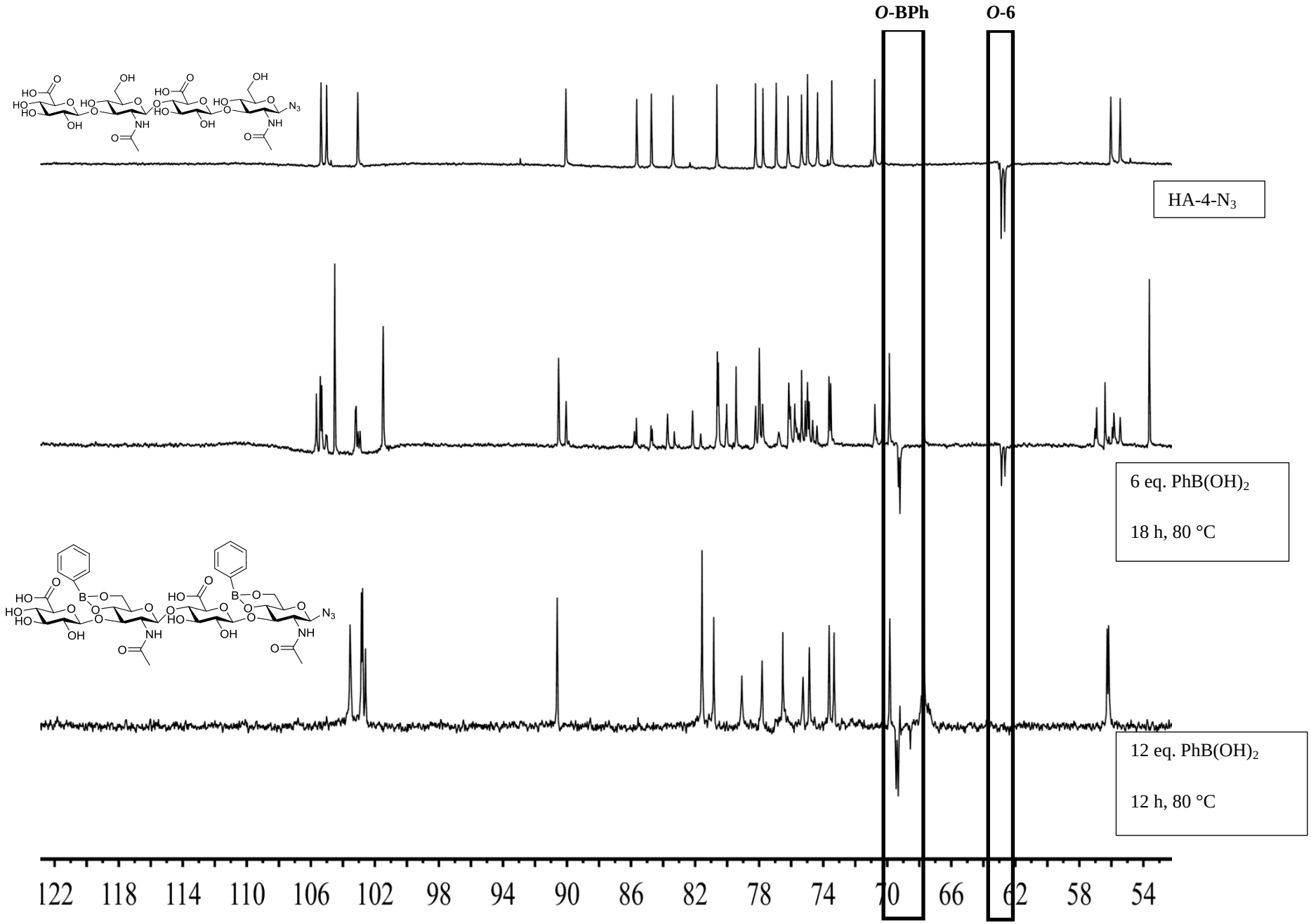

Figure S1: Monitored progress of O-4,6 protection of tetrahyaluronan azide 5 with successively added phenyl boronic acid.

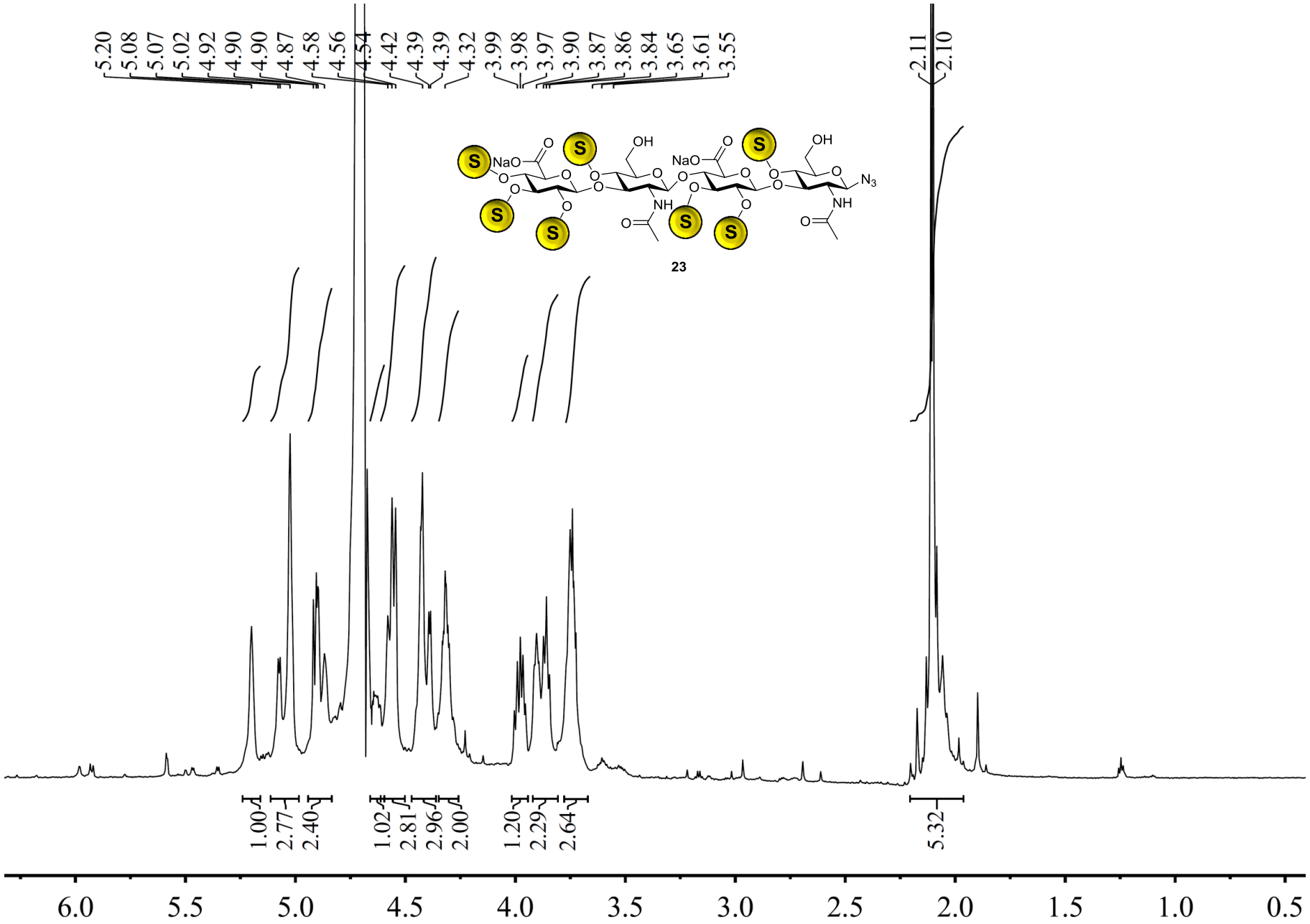
5.20
5.08
5.07
5.02
4.92
4.90
4.90
4.87
4.58
4.56
4.54
4.42
4.39
4.39
4.32
3.99
3.98
3.97
3.90
3.87
3.86
3.84
3.65
3.61
3.55
2.11
2.10
NaO
OH
NH
N3
23
1.00
2.77
2.40
1.02
2.81
2.96
2.00
1.20
2.29
2.64
5.32
6.0
5.5
5.0
4.5
4.0
3.5
3.0
2.5
2.0
1.5
1.0
0.5

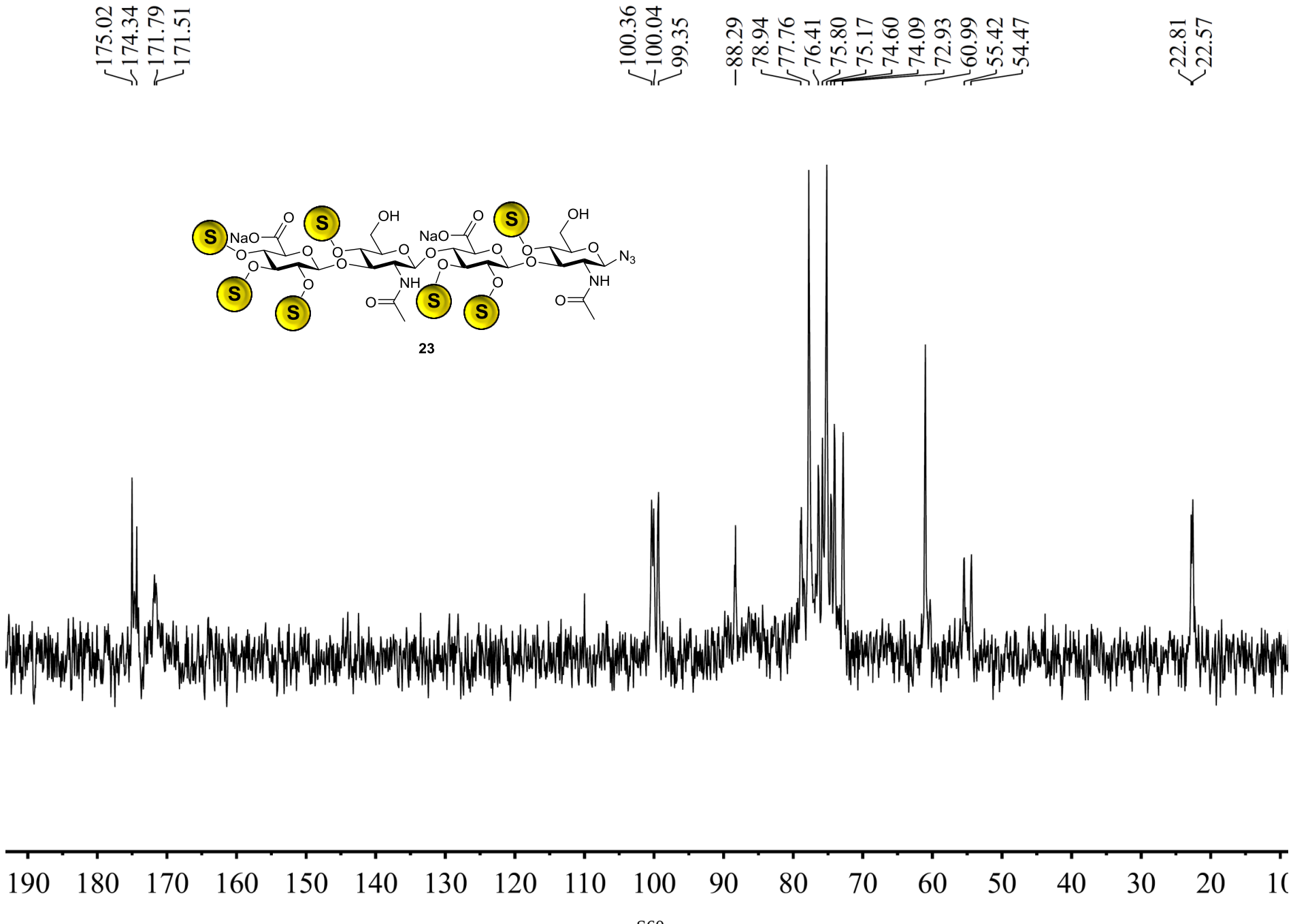
175.02
174.34
171.79
171.51
100.36
100.04
99.35
88.29
78.94
77.76
76.41
75.80
75.17
74.60
74.09
72.93
60.99
55.42
54.47
22.81
22.57
NaO
OH
NH
N3
S
23
190
180
170
160
150
140
130
120
110
100
90
80
70
60
50
40
30
20
10

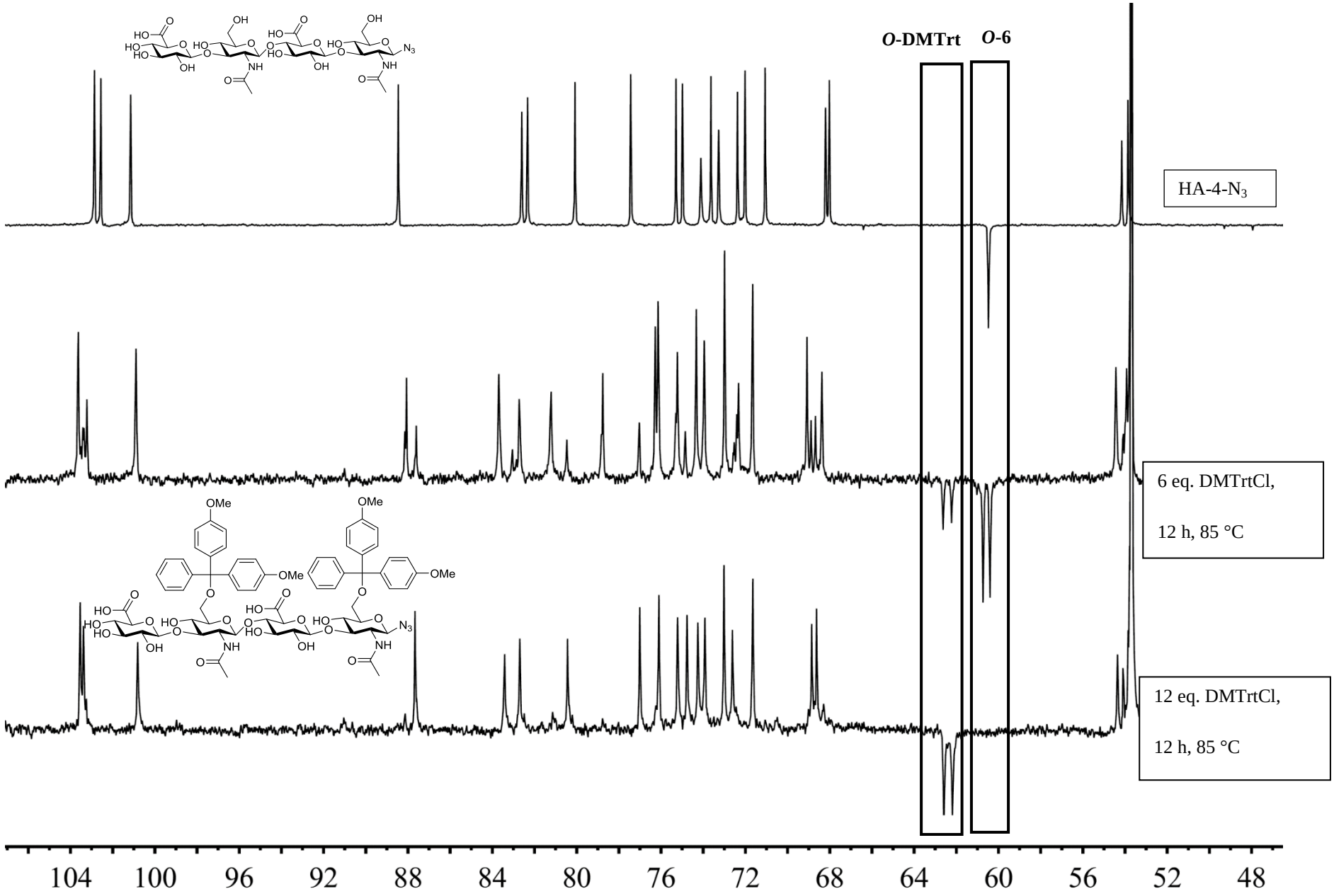

Figure S2: Monitored progress of O-6 protection of tetrahyaluronan azide 5 with with successively added dimethoxytrityl chloride.

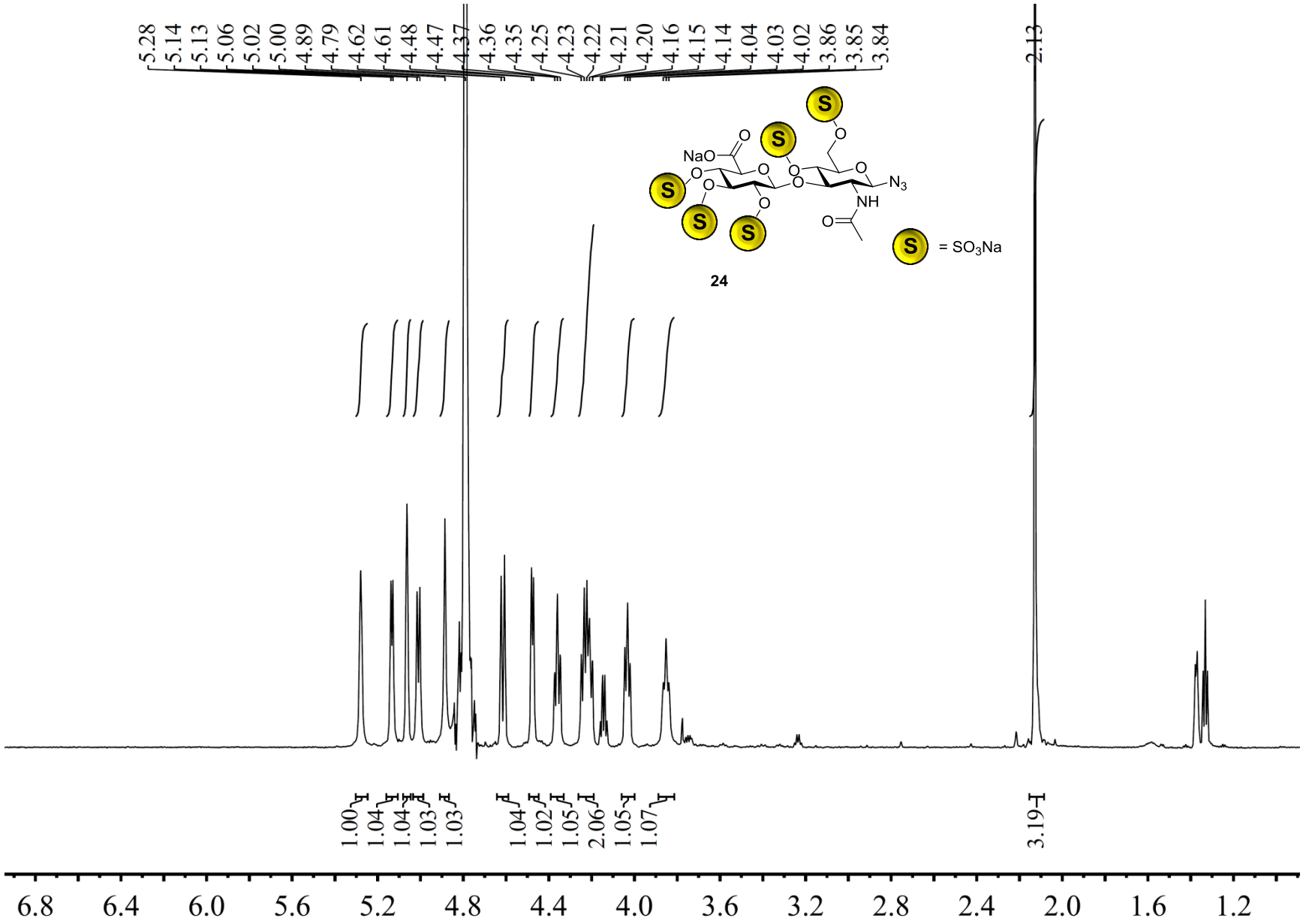
5.28
5.14
5.13
5.06
5.02
5.00
4.89
4.79
4.62
4.61
4.48
4.47
4.37
4.36
4.35
4.25
4.23
4.22
4.21
4.20
4.16
4.15
4.14
4.04
4.03
4.02
3.86
3.85
3.84
2.13
NaO
O
S
O
N3
NH
= SO3Na
24
1.00
1.04
1.04
1.03
1.03
1.04
1.02
1.05
2.06
1.05
1.07
3.19
6.8
6.4
6.0
5.6
5.2
4.8
4.4
4.0
3.6
3.2
2.8
2.4
2.0
1.6
1.2

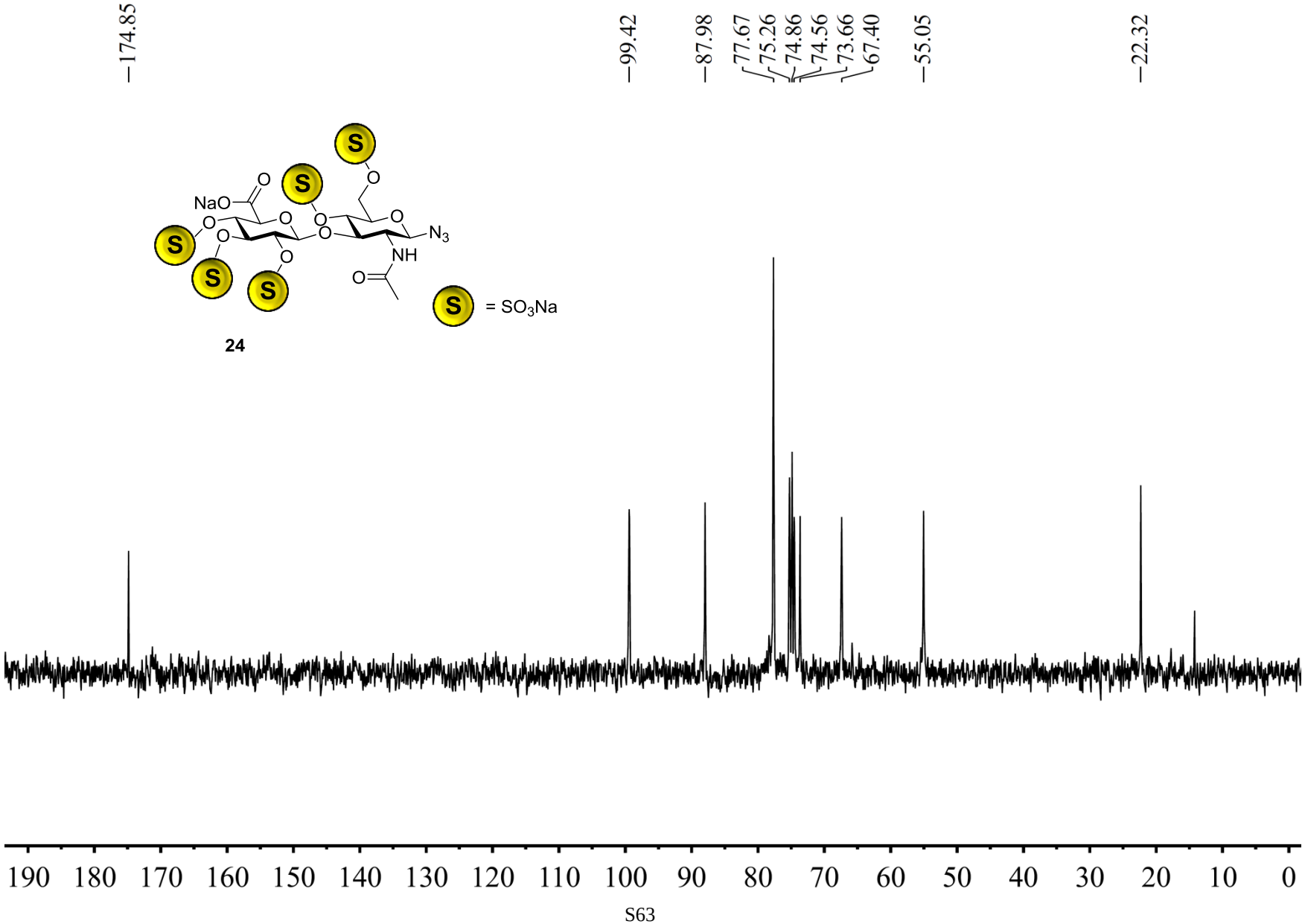
174.85
99.42
87.98
77.67
75.26
74.86
74.56
73.66
67.40
55.05
22.32
NaO
N3
NH
= SO3Na
24
190 180 170 160 150 140 130 120 110 100 90 80 70 60 50 40 30 20 10 0

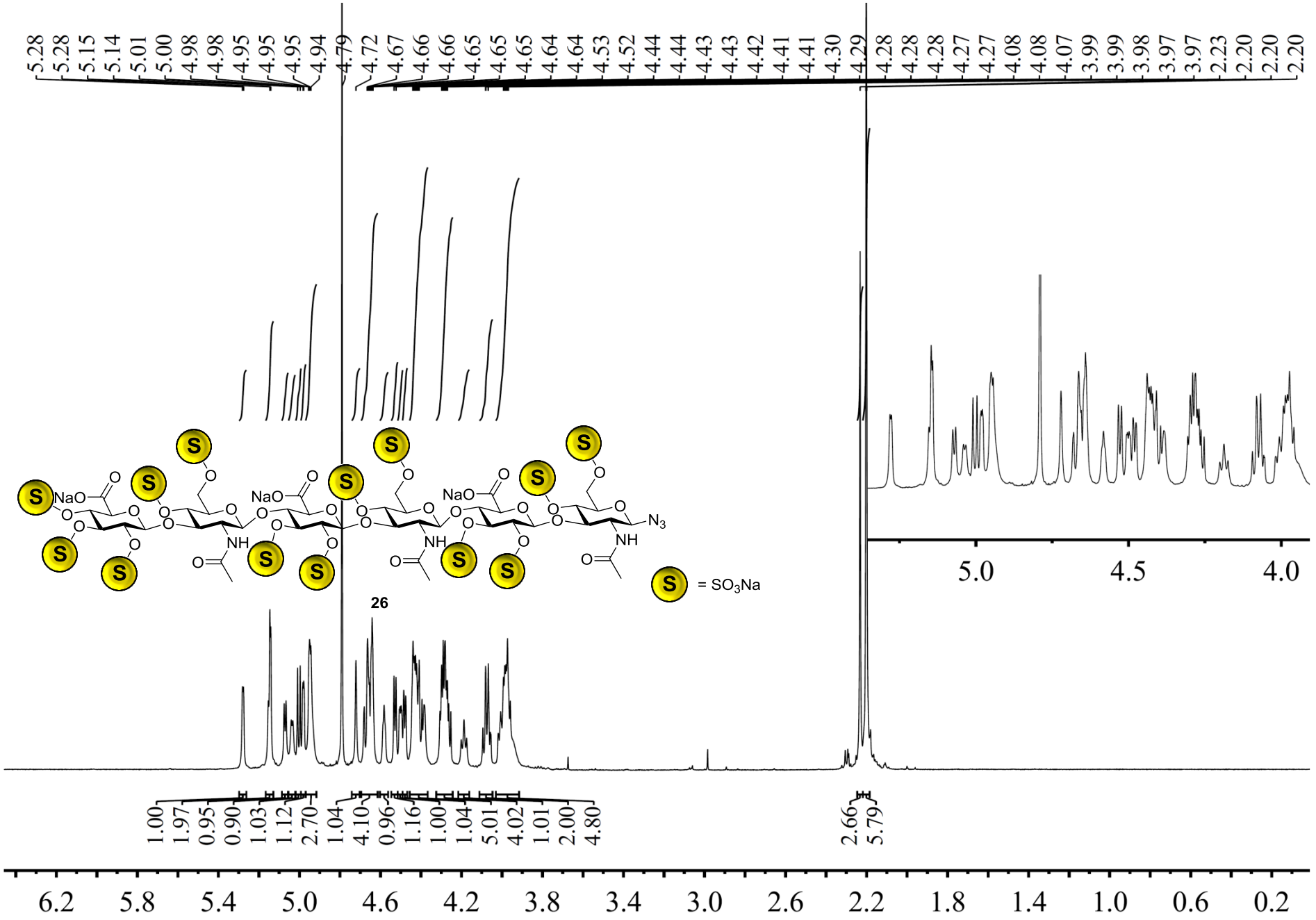
5.28 5.28 5.15 5.14 5.01 5.00 4.98 4.98 4.95 4.95 4.95 4.94 4.79 4.72 4.67 4.66 4.66 4.65 4.65 4.65 4.64 4.64 4.53 4.52 4.44 4.44 4.43 4.43 4.42 4.41 4.41 4.30 4.29 4.28 4.28 4.28 4.27 4.27 4.08 4.08 4.07 3.99 3.99 3.98 3.97 3.97 2.23 2.20 2.20 2.20
NaO
NH
N3
S = SO3Na
26
1.00 1.97 0.95 0.90 1.03 1.12 2.70 1.04 4.10 0.96 1.16 1.00 1.04 5.01 4.02 1.01 2.00 4.80
2.66 5.79
6.2 5.8 5.4 5.0 4.6 4.2 3.8 3.4 3.0 2.6 2.2 1.8 1.4 1.0 0.6 0.2
5.0 4.5 4.0

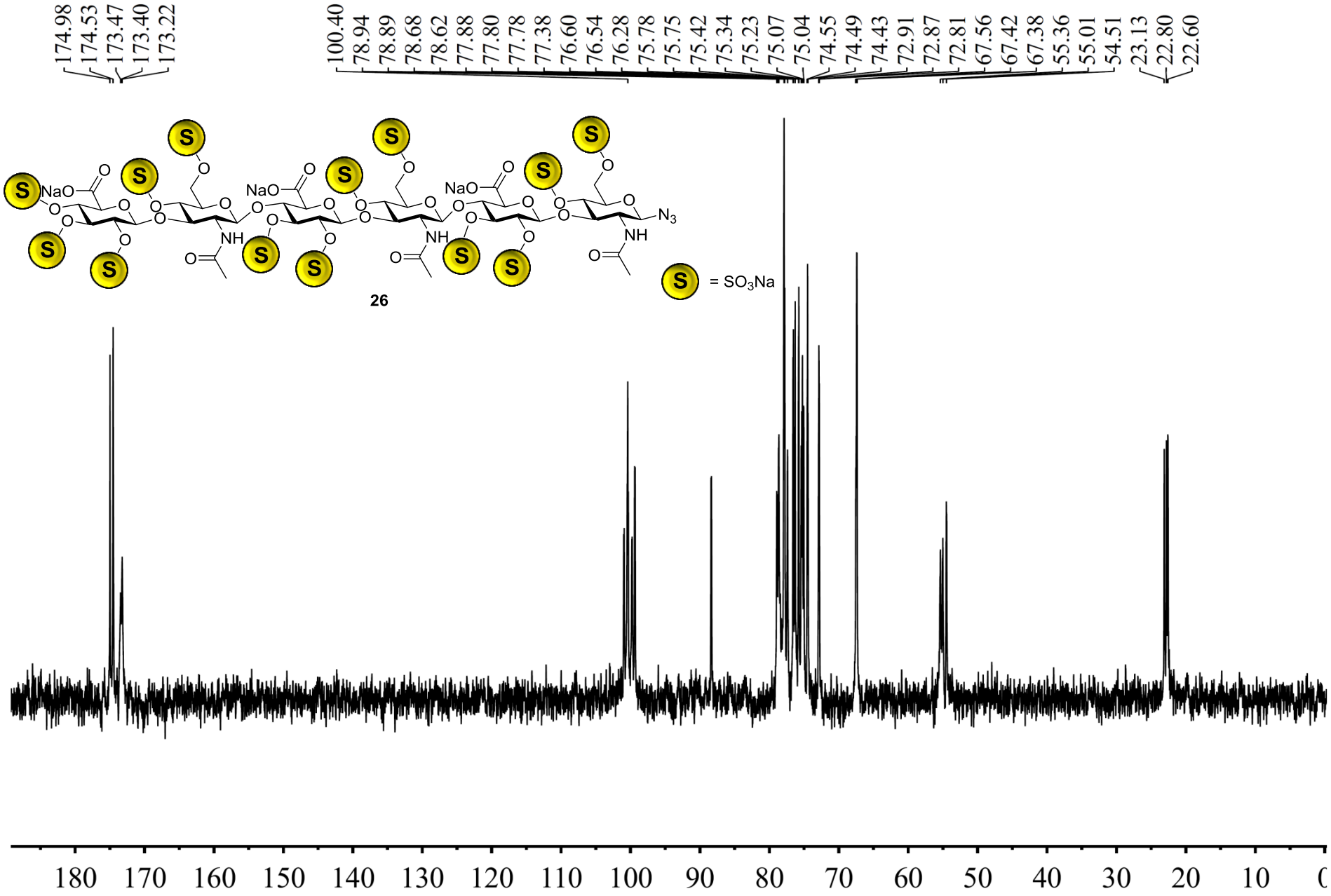
174.98
174.53
173.47
173.40
173.22
100.40
78.94
78.89
78.68
78.62
77.88
77.80
77.78
77.38
76.60
76.54
76.28
75.78
75.75
75.42
75.34
75.23
75.07
75.04
74.55
74.49
74.43
72.91
72.87
72.81
67.56
67.42
67.38
55.36
55.01
54.51
23.13
22.80
22.60
NaO
NH
N3
S = SO3Na
26
180
170
160
150
140
130
120
110
100
90
80
70
60
50
40
30
20
10

MS-Analysis of defined sulfated compounds

All signals with relative intensities about 10% were considered for the assignment. The most significant signal for the intakt product is marked in the mass spectra and the corresponding allignment table with a black border. Asterix (*) marks unsigned signals.

9s-HA-4-TAMRA (15)

Assignment positive ion mode M ($C_{56}H_{68}N_8O_{53}S_9$) = 1988.04

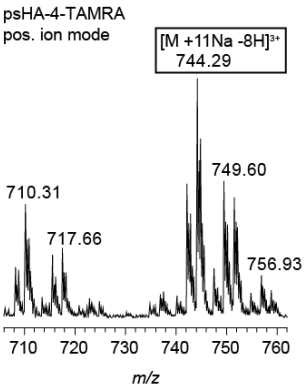

m/z	z	I	M neutral	assignment	Hill Notation	calc. mass
744.29	3	18539120	2229.87	$[M+11Na-8H]^{3+}$	$C_{56}H_{57}N_8Na_{11}O_{53}S_9$	2229.84
749.60	3	10376376	2245.80	$[M+10Na+K-8H]^{3+}$	$C_{56}H_{57}KN_8Na_{10}O_{53}S_9$	2245.81
742.29	3	10202585	2223.87	$[M+9Na+K-7H]^{3+}$	$C_{56}H_{58}KN_8Na_9O_{53}S_9$	2223.83
751.61	3	8965715	2251.83	$[M+12Na-9H]^{3+}$	$C_{56}H_{56}N_8Na_{12}O_{53}S_9$	2251.82
710.31	3	8791755	2127.93	$[M-SO_3+10Na-7H]^{3+}$	$C_{56}H_{58}N_8Na_{10}O_{50}S_8$	2127.90
717.65	3	5211279	2149.95	$[M-SO_3+11Na-8H]^{3+}$	$C_{56}H_{57}N_8Na_{11}O_{50}S_8$	3149.88
715.64	3	4742634	2143.92	$[M-SO_3+9Na+K-7H]^{3+}$	$C_{56}H_{58}KN_8Na_9O_{50}S_8$	2143.87
708.32	3	3857570	2121.96	$[M-SO_3+8Na+K-6H]^{3+}$	$C_{56}H_{59}KN_8Na_8O_{50}S_8$	2121.89
747.61	3	3506916	2239.83	$[M+8Na+2K-7H]^{3+}$	$C_{56}H_{58}K_2N_8Na_8O_{53}S_9$	2239.80
756.92	3	3242149	2267.76	$[M+11Na+K-9H]^{3+}$	$C_{56}H_{56}KN_8Na_{11}O_{53}S_9$	2267.79
758.93	3	2182586	2273.79	$[M+13Na-10H]^{3+}$	$C_{56}H_{55}N_8Na_{13}O_{53}S_9$	2273.80
754.92	3	1896999	2261.76	$[M+9Na+2K-8H]^{3+}$	$C_{56}H_{57}K_2N_8Na_9O_{53}S_9$	2261.79
736.95	3	1824411	2207.85	$[M+10Na-7H]^{3+}$	$C_{56}H_{58}N_8Na_{10}O_{53}S_9$	2207.86

9s-HA-4-Triazol (16)

Assignment positive ion mode M ($C_{30}H_{45}N_5O_{49}S_9$) = 1546.87

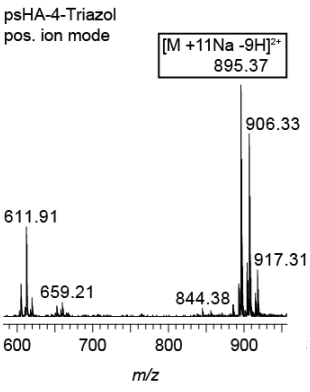

m/z	z	I	M neutral	assignment	Hill Notation	calc. Mass
895.37	2	310938	1788.74	$[M+11Na-9H]^{2+}$	$C_{30}H_{34}N_5Na_{11}O_{49}S_9$	1788.67
906.33	2	245677	1810.66	$[M+12Na-10H]^{2+}$	$C_{30}H_{33}N_5Na_{12}O_{49}S_9$	1810.65
611.91	3	120812	1832.73	$[M+13Na-10H]^{3+}$	$C_{30}H_{32}N_5Na_{13}O_{49}S_9$	1832.63
903.32	2	71294	1804.64	$[M+10Na+K-9H]^{2+}$	$C_{30}H_{34}KN_5Na_{10}O_{49}S_9$	1804.64
917.31	2	61245	1832.62	$[M+13Na-11H]^{2+}$	$C_{30}H_{32}N_5Na_{13}O_{49}S_9$	1832.63
307.30	1	57615	306.30	*		
892.34	2	44134	1782.68	$[M+9Na+K-8H]^{2+}$	$C_{30}H_{35}KN_5Na_9O_{49}S_9$	1782.66
604.58	3	43494	1810.74	$[M+12Na-9H]^{3+}$	$C_{30}H_{33}N_5Na_{12}O_{49}S_9$	1810.65
914.32	2	31673	1826.64	$[M+11Na+K-10H]^{2+}$	$C_{30}H_{33}KN_5Na_{11}O_{49}S_9$	1826.62

9s-HA-4-SMe (17)

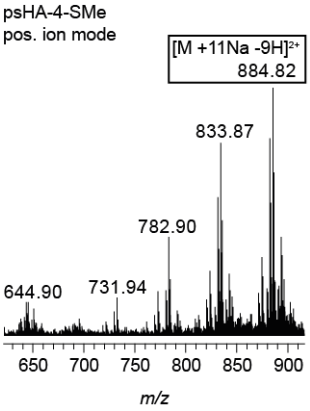

Assignment positive ion mode M ($C_{29}H_{46}N_2O_{49}S_{10}$) = 1525.84

m/z	z	I	M neutral	assignment	Hillnotation	calc mass
884.81	2	1357741	1767.62	$[M+11Na-9H]^{2+}$	$C_{29}H_{35}N_2Na_{11}O_{49}S_{10}$	1767.64
833.87	2	1186271	1665.74	$[M-SO_3+10Na-8H]^{2+}$	$C_{29}H_{36}N_2Na_{10}O_{46}S_9$	1665.70
881.81	2	1077695	1761.62	$[M+9Na+K-8H]^{2+}$	$C_{29}H_{36}KN_2Na_9O_{49}S_{10}$	1761.63
830.86	2	687050	1659.72	$[M-SO_3+8Na+K-7H]^{2+}$	$C_{29}H_{37}KN_2Na_8O_{46}S_9$	1659.69
782.89	2	546818	1563.78	$[M-2SO_3+9Na-7H]^{2+}$	$C_{29}H_{37}N_2Na_9O_{43}S_8$	1563.76
892.79	2	539397	1783.58	$[M+10Na+K-9H]^{2+}$	$C_{29}H_{35}KN_2Na_{10}O_{49}S_{10}$	1783.61
873.82	2	410516	1745.64	$[M+10Na-8H]^{2+}$	$C_{29}H_{36}N_2Na_{10}O_{49}S_{10}$	1745.66
878.82	2	344834	1755.64	$[M+7Na+2K-7H]^{2+}$	$C_{29}H_{37}K_2N_2Na_7O_{49}S_{10}$	1755.62
895.83	2	343000	1789.66	$[M+12Na-10H]^{2+}$	$C_{29}H_{34}N_2Na_{12}O_{49}S_{10}$	1789.62
822.88	2	313784	1643.76	$[M-SO_3+9Na-7H]^{2+}$	$C_{29}H_{37}N_2Na_9O_{46}S_9$	1643.72
841.83	2	293989	1681.66	$[M-SO_3+9Na+K-8H]^{2+}$	$C_{29}H_{36}KN_2Na_9O_{46}S_9$	1681.67
779.90	2	292403	1557.80	$[M-2SO_3+7Na+K-6H]^{2+}$	$C_{29}H_{38}KN_2Na_7O_{43}S_8$	1557.75
844.85	2	265025	1687.70	$[M-SO_3+11Na-9H]^{2+}$	$C_{29}H_{35}N_2Na_{11}O_{46}S_9$	1687.68
819.89	2	261780	1637.78	$[M-SO_3+7Na+K-6H]^{2+}$	$C_{29}H_{38}KN_2Na_7O_{46}S_9$	1637.71
771.90	2	252117	1541.80	$[M-2SO_3+8Na-6H]^{2+}$	$C_{29}H_{38}N_2Na_8O_{43}S_8$	1541.78
332.42	1	250697	331.42	*		
595.54	3	246709	1783.62	$[M+10Na+K-8H]^{3+}$	$C_{29}H_{35}KN_2Na_{10}O_{49}S_{10}$	1783.61
889.80	2	241443	1777.60	$[M+8Na+2K-7H]^{2+}$	$C_{29}H_{36}K_2N_2Na_8O_{49}S_{10}$	1777.61
870.84	2	234000	1739.68	$[M+8Na+K-7H]^{2+}$	$C_{29}H_{37}KN_2Na_8O_{49}S_{10}$	1739.65
838.85	2	214583	1675.70	$[M-SO_3+8Na+K-7H]^{2+}$	$C_{29}H_{37}KN_2Na_8O_{46}S_9$	1675.67
642.90	3	197990	1925.70	*		
597.57	3	197355	1789.71	$[M+12Na-9H]^{3+}$	$C_{29}H_{34}N_2Na_{12}O_{49}S_{10}$	1789.62
644.87	3	195085	1931.61	*		
952.77	2	191228	1903.54	*		
900.79	2	159456	1799.58	$[M+9Na+2K-9H]^{2+}$	$C_{29}H_{35}K_2N_2Na_9O_{49}S_{10}$	1799.59
731.93	2	142165	1461.86	$[M-3SO_3+8Na-6H]^{2+}$	$C_{29}H_{38}N_2Na_8O_{40}S_7$	1461.82
604.89	3	140446	1811.67	$[M+13Na-10H]^{3+}$	$C_{29}H_{33}N_2Na_{13}O_{49}S_{10}$	1811.60
955.76	2	134694	1909.52	*		
861.84	2	131311	1721.68	$[M+8Na+K-H_2O-7H]^{2+}$	$C_{29}H_{35}KN_2Na_8O_{48}S_{10}$	1721.64

9s-HA-4-H,H (18)

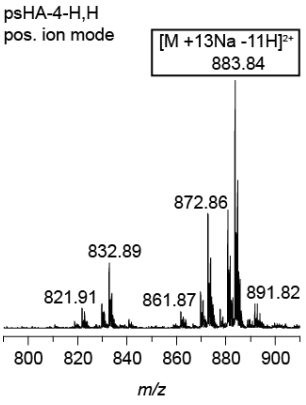

Assignment positive ion mode M ($C_{28}H_{44}N_2O_{49}S_9$) = 1479.85

m/z	z	I	M neutral	assignment	Hill Notation	calc mass
883.84	2	10481601	1765.68	$[M+13Na-11H]^{2+}$	$C_{28}H_{31}N_2Na_{13}O_{49}S_9$	1765,62
880.85	2	5005344	1759.70	$[M+11Na+K-11H]^{2+}$	$C_{28}H_{32}KN_2Na_{11}O_{49}S_9$	1759,61
872.86	2	4830793	1743.72	$[M+12Na-10H]^{2+}$	$C_{28}H_{32}N_2Na_{12}O_{49}S_9$	1743,63
832.89	2	2764340	1663.78	$[M-SO_3+12Na-10H]^{2+}$	$C_{28}H_{32}N_2Na_{12}O_{46}S_8$	1663,68
869.84	2	1560448	1737.68	$[M+10Na+K-11H]^{2+}$	$C_{28}H_{33}KN_2Na_{10}O_{49}S_9$	1737,63
330.14	1	1155132	329.14	*		
891.82	2	1046645	1781.64	$[M+12Na+K]-11H^{2+}$	$C_{28}H_{31}KN_2Na_{12}O_{49}S_9$	1781,59
829.86	2	1014891	1657.72	$[M-SO_3+10Na+K-9H]^{2+}$	$C_{28}H_{33}KN_2Na_{10}O_{46}S_8$	1657,67
821.91	2	854239	1641.82	$[M-SO_3+11Na-9H]^{2+}$	$C_{28}H_{33}N_2Na_{11}O_{46}S_8$	1641,69
877.82	2	818670	1753.64	$[M+9Na+2K-9H]^{2+}$	$C_{28}H_{33}K_2N_2Na_9O_{49}S_9$	1753,60
921.82	2	709113	1841.64	$[M+13Na+2K-13H]^{2+}$	$C_{28}H_{29}K_2N_2Na_{13}O_{49}S_9$	1841,53
861.87	2	705510	1721.74	$[M+11Na-9H]^{2+}$	$C_{28}H_{33}N_2Na_{11}O_{49}S_9$	1721,65
924.85	2	681380	1847.70	$[M+15Na+K-14H]^{2+}$	$C_{28}H_{28}KN_2Na_{15}O_{49}S_9$	1847,54
781.89	2	434072	1561.78	$[M-2SO_3+11Na-9H]^{2+}$	$C_{28}H_{33}N_2Na_{11}O_{43}S_7$	1561,74
763.22	2	393859	1524.44	*		
393.12	1	391086	392.12	*		
910.85	2	376980	1819.70	$[M+12Na+2K-12H]^{2+}$	$C_{28}H_{30}K_2N_2Na_{12}O_{49}S_9$	1819,55
840.87	2	356325	1679.74	$[M-SO_3+11Na+K-10H]^{2+}$	$C_{28}H_{32}KN_2Na_{11}O_{46}S_8$	1679,65
888.85	2	342841	1775.70	$[M+10Na+2K-10H]^{2+}$	$C_{28}H_{32}K_2N_2Na_{10}O_{49}S_9$	1775,58
818.87	2	301330	1635.74	$[M-SO_3+9Na+K-8H]^{2+}$	$C_{28}H_{34}KN_2Na_9O_{46}S_8$	1635,69
913.85	2	298926	1825.70	$[M+14Na+K-13H]^{2+}$	$C_{28}H_{29}KN_2Na_{14}O_{49}S_9$	1825,55

13s-HA-6-TAMRA (19)

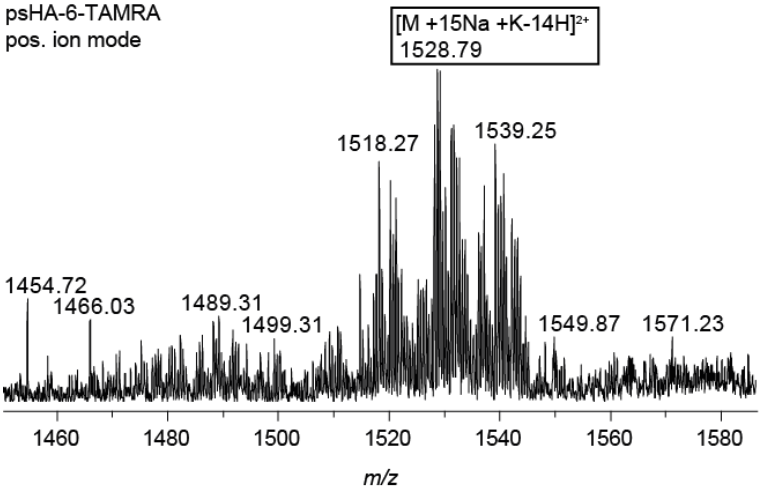

m/z	z	I	M neutral	assignment	Hill Notation	calc. Mass
1528.28	2	63569	3054.56	$[M+15Na+K-14H]^{2+}$	$C_{70}H_{73}KN_9Na_{15}O_{76}S_{13}$	3054.66
1531.30	2	62665	3060.60	$[M+17Na-15H]^{2+}$	$C_{70}H_{72}N_9Na_{17}O_{76}S_{13}$	3060.67
1539.25	2	59070	3076.50	$[M+16Na+K-15H]^{2+}$	$C_{70}H_{72}KN_9Na_{16}O_{76}S_{13}$	3076.64
1518.27	2	54876	3034.54	$[M+15Na+H_2O-13H]^{2+}$	$C_{70}H_{76}N_9Na_{15}O_{77}S_{13}$	3034.71
1520.27	2	50701	3038.54	$[M+16Na-14H]^{2+}$	$C_{70}H_{73}N_9Na_{16}O_{76}S_{13}$	3038.69
1542.26	2	41913	3082.52	$[M+18Na-16H]^{2+}$	$C_{70}H_{71}N_9Na_{18}O_{76}S_{13}$	3082.65
1536.26	2	38708	3070.52	$[M+14Na+2K-13H]^{2+}$	$C_{70}H_{73}K_2N_9Na_{14}O_{76}S_{13}$	3070.63
1514.79	2	28946	3027.58	*		
1525.28	2	27805	3048.56	$[M+13Na+2K-13H]^{2+}$	$C_{70}H_{74}K_2N_9Na_{13}O_{76}S_{13}$	3048.65
1534.77	2	18773	3067.54	*		
1509.29	2	16103	3016.58	$[M+15Na-13H]^{2+}$	$C_{70}H_{74}N_9Na_{15}O_{76}S_{13}$	3016.70
1498.25	2	11318	2994.50	$[M+14Na-12H]^{2+}$	$C_{70}H_{75}N_9Na_{14}O_{76}S_{13}$	2994.72
1584.96	2	10753	3167.92	*		
1567.25	2	10719	3132.50	*		
1547.27	2	10346	3092.54	$[M+17Na+K-16H]^{2+}$	$C_{70}H_{72}K_2N_9Na_{15}O_{76}S_{13}$	3092.62
1563.35	2	10184	3124.70	*		
1573.30	2	10176	3144.60	$[M+20Na+H_2O-18H]^{2+}$	$C_{70}H_{71}N_9Na_{20}O_{77}S_{13}$	3144.62
1581.32	2	9961	3160.64	$[M+19Na+K+H_2O-17H]^{2+}$	$C_{70}H_{71}KN_9Na_{19}O_{77}S_{13}$	3160.60
1576.75	2	9612	3151.50	*		
1559.80	2	9366	3117.60	*		
1506.29	2	8992	3010.58	$[M+13Na+K-12H]^{2+}$	$C_{70}H_{75}KN_9Na_{13}O_{76}S_{13}$	3010.70
1570.26	2	8427	3138.52	$[M+18Na+K+H_2O-17H]^{2+}$	$C_{70}H_{72}KN_9Na_{18}O_{77}S_{13}$	3138.62
1575.26	2	8344	3148.52	$[M+21Na-19H]^{2+}$	$C_{70}H_{68}N_9Na_{21}O_{76}S_{13}$	3148.60
1554.76	2	8306	3107.52	$[M+19Na-17H]^{2+}$	$C_{70}H_{70}N_9Na_{19}O_{76}S_{13}$	3104.63

(9s-HA-4-S-PEG-S)$_2$ (20)

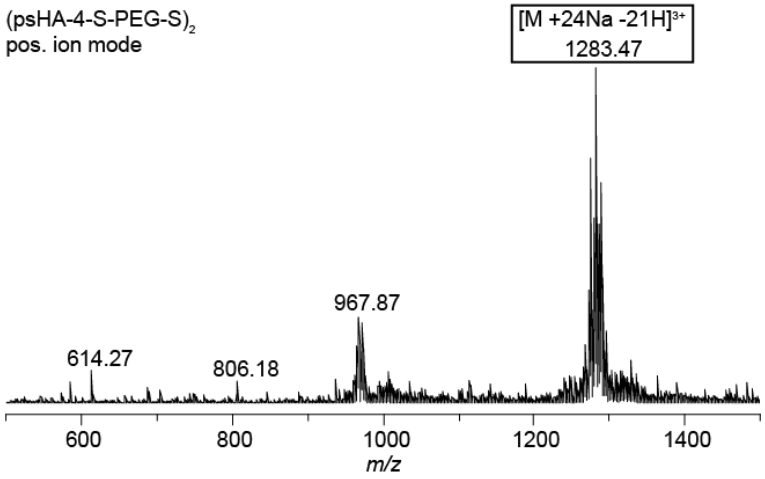

Assignment positive ion mode M ($C_{68}H_{110}N_4O_{102}S_{22}$) = 3317.74

m/z	z	I	M neutral	assignment	Hill Notation	calc mass monoisotopic	most abundant isotop
1283.47	3	1388402	3847.41	$[M+24Na-21H]^{3+}$	$C_{68}H_{86}N_4Na_{24}O_{102}S_{22}$	3845.31	3847.31
1276.14	3	1014043	3825.42	$[M+23Na-20H]^{3+}$	$C_{68}H_{87}N_4Na_{23}O_{102}S_{22}$	3823.33	3525.33
1282.80	3	980028	3845.40	$[M+24Na-21H]^{3+}$	$C_{68}H_{86}N_4Na_{24}O_{102}S_{22}$	3845.31	3847.31
1290.78	3	912035	3869.34	$[M+25Na-22H]^{3+}$	$C_{68}H_{85}N_4Na_{25}O_{102}S_{22}$	3867.29	3869.29
1290.11	3	772408	3867.33	$[M+25Na-22H]^{3+}$	$C_{68}H_{85}N_4Na_{25}O_{102}S_{22}$	3867.29	3869.29
1281.45	3	765825	3841.35	$[M+23Na+H_2O-20H]^{3+}$	$C_{68}H_{89}N_4Na_{23}O_{103}S_{22}$	3841.34	3843.34
1288.78	3	740172	3863.34	$[M+23Na+K-21H]^{3+}$	$C_{68}H_{86}KN_4Na_{23}O_{102}S_{22}$	3861.28	3863.28
1275.47	3	636490	3823.41	$[M+23Na-20H]^{3+}$	$C_{68}H_{87}N_4Na_{23}O_{102}S_{22}$	3823.33	3525.33
1282.13	3	607055	3843.39	$[M+23Na+H_2O-20H]^{3+}$	$C_{68}H_{89}N_4Na_{23}O_{103}S_{22}$	3841.34	3843.34
1280.81	3	596561	3839.43	$[M+22Na+K-20H]^{3+}$	$C_{68}H_{87}KN_4Na_{22}O_{102}S_{22}$	3839.30	3941.30
1288.13	3	513533	3861.39	$[M+23Na+K-21H]^{3+}$	$C_{68}H_{86}KN_4Na_{23}O_{102}S_{22}$	3861.28	3863.28
1274.80	3	383093	3821.40	$[M+22Na+H_2O-19H]^{3+}$	$C_{68}H_{90}N_4Na_{22}O_{103}S_{22}$	3819.35	3821.35
1286.77	3	373453	3857.31	$[M+21Na+2K-20H]^{3+}$	$C_{68}H_{87}K_2N_4Na_{21}O_{102}S_{22}$	3855.27	3857.27
1274.16	3	360207	3819.48	$[M+22Na+H2O-19H]^{3+}$	$C_{68}H_{90}N_4Na_{22}O_{103}S_{22}$	3819.35	3821.35
967.87	4	353815	3867.48	$[M+25Na-21H]^{4+}$	$C_{68}H_{85}N_4Na_{25}O_{102}S_{22}$	3867.29	3869.29
972.37	4	331947	3885.48	$[M+25Na+H_2O-21H]^{4+}$	$C_{68}H_{87}N_4Na_{25}O_{103}S_{22}$	3885.30	3887.30
968.37	4	330970	3869.48	$[M+25Na-21H]^{4+}$	$C_{68}H_{85}N_4Na_{25}O_{102}S_{22}$	3867.29	3869.29
1286.11	3	318118	3855.33	$[M+21Na+2K-20H]^{3+}$	$C_{68}H_{87}K_2N_4Na_{21}O_{102}S_{22}$	3855.27	3857.27
1279.46	3	316548	3835.38	$[M+20Na+2K-19H]^{3+}$	$C_{68}H_{88}K_2N_4Na_{20}O_{102}S_{22}$	3833.29	3835.29
973.87	4	303180	3891.48	$[M+26Na-22H]^{4+}$	$C_{68}H_{84}N_4Na_{26}O_{102}S_{22}$	3889.27	3891.27
1273.48	3	291942	3817.44	$[M+21Na+K-19H]^{3+}$	$C_{68}H_{88}KN_4Na_{21}O_{102}S_{22}$	3817.32	3819.32
393.09	1	290372	392.09	*			
972.89	4	267415	3887.56	$[M+25Na+H_2O-21H]^{4+}$	$C_{68}H_{87}N_4Na_{25}O_{103}S_{22}$	3885.30	3887.30
973.36	4	263254	3889.44	$[M+26Na-22H]^{4+}$	$C_{68}H_{84}N_4Na_{26}O_{102}S_{22}$	3889.27	3891.27
969.37	4	246322	3873.48	*			
1278.82	3	244923	3833.46	$[M+20Na+2K-19H]^{3+}$	$C_{68}H_{88}K_2N_4Na_{20}O_{102}S_{22}$	3833.29	3835.29
1268.81	3	241202	3803.43	$[M+22Na-19H]^{3+}$	$C_{68}H_{88}N_4Na_{22}O_{102}S_{22}$	3801.34	3803.34
971.88	4	240273	3883.52	$[M+24Na+K-21H]^{4+}$	$C_{68}H_{85}KN_4Na_{24}O_{102}S_{22}$	3883.26	3885.26
1296.77	3	239535	3887.31	$[M+25Na+H_2O-22H]^{3+}$	$C_{68}H_{87}N_4Na_{25}O_{103}S_{22}$	3885.30	3887.30
966.89	4	237603	3863.56	$[M+24Na+H_2O-20H]^{4+}$	$C_{68}H_{88}N_4Na_{24}O_{103}S_{22}$	3863.32	3865.32
1296.09	3	218351	3885.27	$[M+24Na+K-22H]^{3+}$	$C_{68}H_{85}KN_4Na_{24}O_{102}S_{22}$	3883.26	3885.26
1295.46	3	218224	3883.38	$[M+24Na+K-22H]^{3+}$	$C_{68}H_{85}KN_4Na_{24}O_{102}S_{22}$	3883.26	3885.26
1294.09	3	202931	3879.27	$[M+22Na+2K-21H]^{3+}$	$C_{68}H_{86}K_2N_4Na_{22}O_{102}S_{22}$	3877.25	3879.25
1297.40	3	184008	3889.20	$[M+26Na-23H]^{3+}$	$C_{68}H_{84}N_4Na_{26}O_{102}S_{22}$	3889.27	3891.27
301.12	1	179939	300.12	*			
1268.14	3	172128	3801.42	$[M+22Na-19H]^{3+}$	$C_{68}H_{88}N_4Na_{22}O_{102}S_{22}$	3801.34	3803.34
966.39	4	142775	3861.56	$[M+23Na+K-20H]^{4+}$	$C_{68}H_{86}KN_4Na_{23}O_{102}S_{22}$	3861.28	3863.28
1272.14	3	137977	3813.42	$[M+19Na+2K-18H]^{3+}$	$C_{68}H_{89}K_2N_4Na_{19}O_{102}S_{22}$	3811.31	3813.31
1304.09	3	136605	3909.27	$[M+26Na+H_2O-23H]^{3+}$	$C_{68}H_{86}N_4Na_{26}O_{103}S_{22}$	3907.28	3909.28
614.27	1	135399	613.27	*			
357.17	1	132407	356.17	*			

2s-HA4-N_3 (21)

MS-spectrum and Assignment positive ion mode, M = 961.15

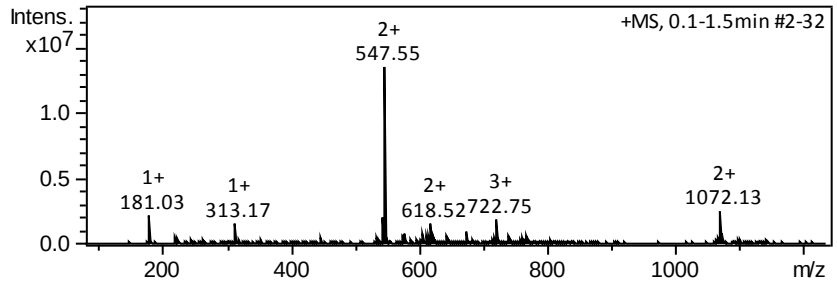

m/z	z	I	M neutral	assignment	Hillnotation	calc mass
547.55	2	13352009	1093.10	$[M+6Na-4H]^{2+}$	$C_{28}H_{37}N_5Na_6O_{28}S_2$	1093.05
1072.13	2	2404363	2142.26	$[2M+10Na-8H]^{2+}$	$C_{56}H_{76}N_{10}Na_{10}O_{56}S_4$	2142.13
181.03	1	2061940	180.03			
544.53	2	2027764	1087.06			
722.43	3	1655720	2164.29	$[2M+11Na-8H]^{3+}$	$C_{56}H_{75}N_{10}Na_{11}O_{56}S_4$	2164.11
618.52	2	1534465	1235.04			
313.17	1	1507271	312.17			

MS-spectrum and Assignment negative ion mode, M = 961.15

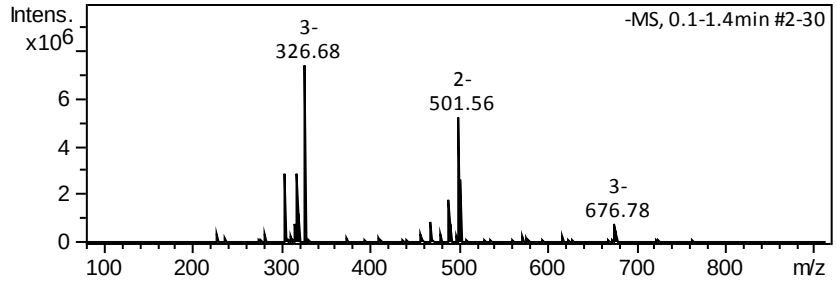

m/z	z	I	M neutral	assignment	Hillnotation	calc mass
326.68	3	7323908	983.04	$[M+Na-4H]^{3-}$	$C_{28}H_{42}N_5NaO_{28}S_2$	983.14
501.56	2	5149314	1005.12	$[M+2Na-4H]^{2-}$	$C_{28}H_{41}N_5Na_2O_{28}S_2$	1005.12
305.00	3	2855341	918.00	$[M-HN_3-3H]^{3-}$	$C_{28}H_{42}N_2O_{28}S_2$	918.76
319.36	3	2820579	961.08	$[M-3H]^{3-}$	$C_{28}H_{43}N_5O_{28}S_2$	961.15
490.56	2	1706058	983.12	$[M+Na-3H]^{2-}$	$C_{28}H_{42}N_5NaO_{28}S_2$	983.14
469.05	2	794477	940.10	$[M+Na-HN_3-3H]^{2-}$	$C_{28}H_{41}N_2NaO_{28}S_2$	940.12
316.51	2	753950	635.02			
676.44	3	735860	2032.32	$[2M+5Na-8H]^{3-}$	$C_{56}H_{81}N_{10}Na_5O_{56}S_4$	2032.22

5s-HA-2-N_3 (24)

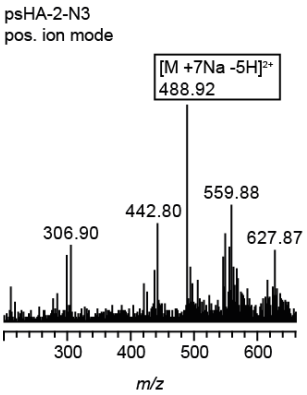

Assignment positive ion mode M ($C_{14}H_{22}N_4O_{26}S_5$) = 821.91

m/z	z	I	M neutral	assignment	Hill Notation	calc mass
488.92	2	6570339	975.84	$[M+7Na-5H]^{2+}$	$C_{14}H_{15}N_4Na_7O_{26}S_5$	975.79
559.88	2	3549266	1117.76	$[M+10Na+2K-10H]^{2+}$	$C_{14}H_{10}K_2N_4Na_{10}O_{26}S_5$	1117.64
442.80	2	2977644	883.60	$[M+2Na+H_2O]^{2+}$	$C_{14}H_{22}N_4Na_2O_{27}S_5$	883.89
548.89	2	2686230	1095.78	$[M+9Na+2K-9H]^{2+}$	$C_{14}H_{11}K_2N_4Na_9O_{26}S_5$	1095.66
306.90	3	2332502	917.70	$[M-SO_3+8Na-5H]^{3+}$	$C_{14}H_{14}N_4Na_8O_{23}S_4$	917.81
556.89	2	2271198	1111.78	$[M+8Na+3K-9H]^{2+}$	$C_{14}H_{11}K_3N_4Na_8O_{26}S_5$	1111.64
627.87	2	2167676	1253.74	$[M+SO_3+10Na+3K+H_2O-11H]^{2+}$	$C_{14}H_{11}K_3N_4Na_{10}O_{30}S_6$	1253.57
300.86	3	2008585	899.58	$[M+Na+K+H_2O+H]^{3+}$	$C_{14}H_{22}KN_4NaO_{27}S_5$	899.86
545.86	2	1949072	1089.72	$[M+7Na+3K-7H]^{2+}$	$C_{14}H_{12}K_3N_4Na_7O_{26}S_5$	1089.65
562.79	2	1647483	1123.58	$[M+6Na+4K+H_2O-8H]^{2+}$	$C_{14}H_{14}K_4N_4Na_6O_{27}S_5$	1123.64
494.85	2	1642882	987.70	$[M+5Na+K+H_2O-4H]^{2+}$	$C_{14}H_{18}KN_4Na_5O_{27}S_5$	987.79
567.88	2	1624850	1133.76	$[M+9Na+3K-10H]^{2+}$	$C_{14}H_{10}K_3N_4Na_9O_{26}S_5$	1133.62
437.96	2	1562895	873.92	$[M-SO_3+6Na-4H]^{2+}$	$C_{14}H_{16}N_4Na_6O_{23}S_4$	873.85
616.82	2	1243053	1231.64	$[M+SO_3+9Na+3K+H_2O-10H]^{2+}$	$C_{14}H_{12}K_3N_4Na_9O_{30}S_6$	1231.59
505.87	2	1239225	1009.74	$[M+6Na+K+H_2O-5H]^{2+}$	$C_{14}H_{17}KN_4Na_6O_{27}S_5$	1009.77
497.91	2	1159225	993.82	$[M+7Na+H_2O-5H]^{2+}$	$C_{14}H_{17}N_4Na_7O_{27}S_5$	993.80
420.84	2	1151681	839.68	*		
564.82	2	1104708	1127.64	$[M+7Na+4K-9H]^{2+}$	$C_{14}H_{11}K_4N_4Na_7O_{26}S_5$	1127.61
547.34	2	1073578	1092.68	*		
624.83	2	1053081	1247.66	$[M+SO_3+8Na+4K+H_2O-10H]^{2+}$	$C_{14}H_{12}K_4N_4Na_8O_{30}S_6$	1247.56
584.72	1	1015186	583.72	*		
630.81	2	1004505	1259.62	$[M+SO_3+12Na+2K+H_2O-12H]^{2+}$	$C_{14}H_{10}K_2N_4Na_{12}O_{30}S_6$	1259.58
426.83	2	925518	851.66	$[M-SO_3+5Na-3H]^{2+}$	$C_{14}H_{17}N_4Na_5O_{23}S_4$	851.87
553.90	2	916653	1105.80	$[M+6Na+4K-8H]^{2+}$	$C_{14}H_{12}K_4N_4Na_6O_{26}S_5$	1105.63
574.89	2	886337	1147.78	*		
284.92	3	870242	851.76	$[M-SO_3+5Na-2H]^{3+}$	$C_{14}H_{17}N_4Na_5O_{23}S_4$	851.87
635.84	2	854511	1269.68	$[M+SO_3+9Na+4K+H_2O-11H]^{2+}$	$C_{14}H_{11}K_4N_4Na_9O_{30}S_6$	1269.54
576.88	2	833787	1151.76	$[M+9Na+3K+H_2O-10H]^{2+}$	$C_{14}H_{12}K_3N_4Na_9O_{27}S_5$	1151.63
524.80	2	800281	1047.60	$[M+6Na+2K+H_2O-5H]^{2+}$	$C_{14}H_{16}K_2N_4Na_6O_{27}S_5$	1047.73
619.83	2	763851	1237.66	$[M+SO_3+11Na+2K+H_2O-11H]^{2+}$	$C_{14}H_{11}K_2N_4Na_{11}O_{30}S_6$	1237.59
613.36	2	749933	1224.72	*		
508.96	2	731164	1015.92	$[M+8Na+H_2O-6H]^{2+}$	$C_{14}H_{16}N_4Na_8O_{27}S_5$	1015.78
279.24	3	728502	834.72	*		
608.83	2	727289	1215.66	$[M+SO_3+10Na+2K+H_2O-10H]^{2+}$	$C_{14}H_{12}K_2N_4Na_{10}O_{30}S_6$	1215.61
587.87	2	721021	1173.74	$[M+10Na+3K+H_2O-11H]^{2+}$	$C_{14}H_{11}K_3N_4Na_{10}O_{27}S_5$	1173.61
578.75	2	690956	1155.50	$[M+10Na+3K-11H]^{2+}$	$C_{14}H_9K_3N_4Na_{10}O_{26}S_5$	1155.60
516.88	2	663507	1031.76	$[M+7Na+K+H_2O-6H]^{2+}$	$C_{14}H_{16}KN_4Na_7O_{27}S_5$	1031.75
537.32	2	663487	1072.64	*		
444.79	2	642426	887.58	$[M+3Na-H]^{2+}$	$C_{14}H_{19}N_4Na_3O_{26}S_5$	887.86
639.26	2	636651	1276.52	*		
219.20	3	629011	654.60	*		

13s-HA-6-N_3 (26)

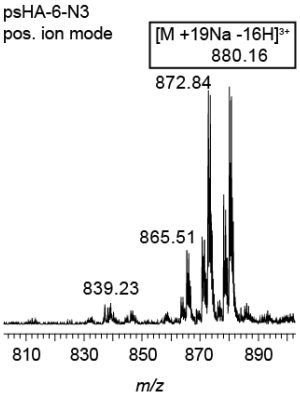

Assignment positive ion mode M ($C_{42}H_{64}N_6O_{72}S_{13}$) = 2219.79

m/z	z	I	M neutral	assignment	Hill notation	calc. mass
880.16	3	101659	2637.48	$[M+19Na-16H]^{3+}$	$C_{42}H_{45}N_6Na_{19}O_{72}S_{13}$	2637.45
872.84	3	93691	2615.52	$[M+18Na-15H]^{3+}$	$C_{42}H_{46}N_6Na_{18}O_{72}S_{13}$	2615.47
878.16	3	48902	2631.48	$[M+17Na+K-15H]^{3+}$	$C_{42}H_{46}KN_6Na_{17}O_{72}S_{13}$	2631.44
870.83	3	33144	2609.49	$[M+16Na+K-14H]^{3+}$	$C_{42}H_{47}KN_6Na_{16}O_{72}S_{13}$	2609.46
865.51	3	28655	2593.53	$[M+17Na-14H]^{3+}$	$C_{42}H_{47}N_6Na_{17}O_{72}S_{13}$	2593.48
863.51	3	10497	2587.53	$[M+15Na+K-13H]^{3+}$	$C_{42}H_{48}KN_6Na_{15}O_{72}S_{13}$	2587.48
876.15	3	9071	2625.45	$[M+15Na+2K-14H]^{3+}$	$C_{42}H_{47}K_2N_6Na_{15}O_{72}S_{13}$	2625.43
885.46	3	8013	2653.38	$[M+18Na+K-16H]^{3+}$	$C_{42}H_{45}KN_6Na_{18}O_{72}S_{13}$	2653.42
884.10	3	7447	2649.30	$[M-SO_3+18Na+3K-18H]^{3+}$	$C_{42}H_{43}K_3N_6Na_{18}O_{69}S_{12}$	2649.38
838.86	3	6217	2513.58	$[M-SO_3+17Na-14H]^{3+}$	$C_{42}H_{47}N_6Na_{17}O_{69}S_{12}$	2513.53
846.17	3	4801	2535.51	$[M-SO_3+18Na-15H]^{3+}$	$C_{42}H_{46}N_6Na_{18}O_{69}S_{12}$	2535.51
868.83	3	4335	2603.49	$[M+14Na+2K-13H]^{3+}$	$C_{42}H_{48}K_2N_6Na_{14}O_{72}S_{13}$	2603.45
858.19	3	3563	2571.57	$[M+16Na-13H]^{3+}$	$C_{42}H_{48}N_6Na_{16}O_{72}S_{13}$	2571.50
890.77	3	2355	2669.31	$[M+17Na+2K-16H]^{3+}$	$C_{42}H_{45}K_2N_6Na_{17}O_{72}S_{13}$	2669.40
903.48	3	2322	2707.44	$[M+17Na+3K-17H]^{3+}$	$C_{42}H_{44}K_3N_6Na_{17}O_{72}S_{13}$	2707.35
894.80	3	2319	2681.40	$[M+21Na-18H]^{3+}$	$C_{42}H_{43}N_6Na_{21}O_{72}S_{13}$	2681.41
910.82	3	2286	2729.46	$[M+18Na+3K-18H]^{3+}$	$C_{42}H_{43}K_3N_6Na_{18}O_{72}S_{13}$	2729.33
844.17	3	2108	2529.51	$[M-SO_3+16Na+K-14H]^{3+}$	$C_{42}H_{47}KN_6Na_{16}O_{69}S_{12}$	2529.50
896.13	3	1968	2685.39	$[M+16Na+3K-16H]^{3+}$	$C_{42}H_{45}K_3N_6Na_{16}O_{72}S_{13}$	2685.37
836.83	3	1905	2507.49	$[M-SO_3+15Na+K-13H]^{3+}$	$C_{42}H_{48}KN_6Na_{15}O_{69}S_{12}$	2507.52
831.54	3	1788	2491.62	$[M-SO_3+16Na-13H]^{3+}$	$C_{42}H_{48}N_6Na_{16}O_{69}S_{12}$	2491.54
856.86	3	1665	2567.58	$[M-SO_3+16Na+2K-15H]^{3+}$	$C_{42}H_{46}K_2N_6Na_{16}O_{69}S_{12}$	2567.46
812.19	3	1648	2433.57	$[M-2SO_3+17Na-14H]^{3+}$	$C_{42}H_{47}N_6Na_{17}O_{66}S_{11}$	2433.57
861.50	3	1578	2581.50	$[M+13Na+2K-12H]^{3+}$	$C_{42}H_{49}K_2N_6Na_{13}O_{72}S_{13}$	2581.47
898.10	3	1502	2691.30	$[M+18Na+2K-17H]^{3+}$	$C_{42}H_{44}K_2N_6Na_{18}O_{72}S_{13}$	2691.38
1308.66	2	1232	2615.32	$[M+18Na-16H]^{2+}$	$C_{42}H_{46}N_6Na_{18}O_{72}S_{13}$	2615.47
1297.67	2	1021	2593.34	$[M+17Na-15H]^{2+}$	$C_{42}H_{47}N_6Na_{17}O_{72}S_{13}$	2593.48
1286.68	2	805	2571.36	$[M+16Na-14H^{2+}$	$C_{42}H_{48}N_6Na_{16}O_{72}S_{13}$	2571.50
1294.66	2	611	2587.32	$[M+15Na+K-14H^{2+}$	$C_{42}H_{48}KN_6Na_{15}O_{72}S_{13}$	2587.48

4. Calculation of the overall binding affinity of a ligand A binding to a protein P with n different, mutually excluding binding modes

Ligand A binds to i = 1,2,...,n binding sites with the K_{Di} values K_{D1}, K_{D2}, ..., K_{Dn} forming the protein-ligand complexes PA_1, ... PA_n.

Each of these K_D values is defined by the equation $K_{Di} = [A^{free}]*[P^{free}]/[PA_i]$.

The overall binding affinity of ligand A, $K_{D\ total}$ is then defined as: $K_{D\ total} = [A^{free}]*[P^{free}]/([PA_1]+[PA_2]+...+[PA_n])$ as $[PA_{total}] = [PA_1]+[PA_2]+...+[PA_n]$.

If now - in a simplied special case - all specific affinities K_{Di} are equal: $K_{D1} = K_{D2} = ... = K_{Dn}$, the total affinity is: $K_{D\ total} = [A^{free}]*[P^{free}]/n*[PA_i] = 1/n * K_{D1}$.

5. Fluorescence Polarization Assays

Binding Assay

Determination of the binding affinities of the carboxytetramethylrhodamine labeled polysulfated tetra- and hexahyaluronan **15** *and* **19**: For all experiments the same PBS-buffer (10 mM Na_2HPO_4, 1.8 mM KH_2PO_4, 2.7 mM KCl, 0.1% Triton X-100, adjusted with 0.2 M NaOH to pH 7.5) was used. For fluorescence polarization measurements, both TAMRA-regioisomers from fluorescent probe **15 (A+B)** and **19 (A+B)** were dissolved in PBS-buffer and mixed 1:1. The assay was carried out on untreated black 384-well microtiter plates (Low volume, Non-Binding Surface, Round Botton, Non-Sterile Black Polystyrene, Corning B.V. Life Sciences, Nr. 3676) in a final volume of 10 µL PBS-buffer. The measurements were performed on microplate reader SAFIRE II (Tecan, Crailsheim, Germany), using excitation wavelength 530 nm (5 nm band pass) and emission wavelength 590 nm (20 nm band pass). The plates were read with an instrument setting of 10 flashed per well (G-factor: 0.97809).

The final assays mixtures were composed by 5 µL **15** or **19** (maintaining a final assay concentration of 10 nM), and 5 µL of increasing amounts of the protein dissolved in PBS-buffer. The negative control was composed by 5 µl of **15** or **19** (maintaining its final assay concentration of 10 nM) and 5 µl in PBS-buffer. To avoid protein aggregation Triton X-100 (0.1%, final concentration) was used in all experiments as detergent. After addition of the components, the plates were centrifuged (2000 min^{-1}, 30 sec.), shaken briefly (2000 rpm for 10 min at room temperature), and polarization of the emitted fluorophore was directly recorded. The polarization values (mP) were plotted as a function of the logarithm of the protein concentration. All the experiments were carried out in triplicates in three, or in few cases, two independent experiments and the results are expressed as the medium ± standard deviation (SD).

Competitive Binding Assay

Determination of the binding affinities of non-fluorescent competitors **16**, **17**, **18**, **20**, **21**, **22**, **23**, **24**, **25**, **26**: For fluorescence polarization competition experiments, fluorescent probe **15** or **19,** competitors and proteins were dissolved in PBS-buffer. The assay was carried out on untreated black 384-well microtiter plates (Low volume, Non-Binding Surface, Round Botton, Non-Sterile Black Polystyrene, Corning B.V. Life Sciences, Nr. 3676) in a final volume of 10 µL PBS-buffer. The measurements were performed on microplate reader SAFIRE II (Tecan, Crailsheim, Germany), using excitation wavelength 530 nm (5 nm band pass) and emission wavelength 590 nm (20 nm band pass). The plates were read with an instrument setting of 10 flashed per well (G-factor: 0.97809).

The final assays mixtures were composed by 4 µL **15** or **19** (maintaining a final assay concentration of 10 nM), 4 µL of the protein (maintaining a final assay concentration which corresponds to the EC_{50}, 2xEC_{50} or 4xEC_{50}) and 2µl of increasing concentrations of the competitor. The negative control was composed by 4 µl of **15** or **19** (maintaining its final assay concentration of 10 nM), 4 µl PBS-buffer and 2µl of increasing concentrations of the competitor.

After addition of the 4 µL **15** or **19** and 4 µL of the protein, the plates were centrifuged (2000 min^{-1}, 30 sec.) and shaken briefly (2000 rpm for 10 min at room temperature) to form the protein-fluorescent probe-complex. Thereafter, 2µl of competitor was added, the plates were centrifuged again (2000 min^{-1}, 30 sec.), shaken briefly (2000 rpm for 10 min at room temperature) and polarization of the emitted fluorophor was directly recorded. All the experiments were carried out in triplicates in three, or few cases two, independent experiments and the results are expressed as the medium ± standard deviation (SD).

FP-Assay data analysis

Binding assay

As first parameter, the final assay concentration for the tetra- and hexameric fluorescent probes **15** and **19** was set to 10 nM to have sufficient changes in the polarization signal (ΔmP) for all proteins. The determination of half maximal effective concentrations (EC_{50}) was carried out by recording the polarization signals for increasing protein concentrations until saturation was reached. The observed polarization values were plotted against the logarithmic protein concentration and fitted with Graph Pad Prism 6, using the four-parameter (bottom, top, log EC_{50}, and Hill slope) sigmoidal curve fit as non-linear regression model. The inflection point of the fitted curve corresponds to the EC_{50} value. These values not necessarily exhibit biological relevance due to possible fluorophore quenching effects caused by local pH-changes, hydrophobic interactions or different mobility upon binding.[7] The proportion of bound and unbound fraction to the observable EC_{50} value is in direct correlation to the Q-factor defined as quotient of fluorescent intensity of bound- and free ligand ($Q = I_B/I_F$). In practice, Q-factors are determined by plotting the fluorescence intensity against logarithmic protein concentration, where the bottom of the sigmodal curve represents I_B and the top I_F. In cases with Q<1 the observable anisotropy-values (A_{Obs}) need to be corrected by equation (1), where F_{SB} is the real bound fraction and A_F and A_B are the anisotropy values of free and bound ligand (bottom and top of the fitted curve).

$$\boldsymbol{F_{SB}} = \frac{\boldsymbol{A_{Obs} - A_F}}{\boldsymbol{(A_B - A_{Obs})Q + A_{Obs} - A_F}} \qquad (1)$$

The calculated F_{SB}-values were plotted against the logarithmic protein concentration and the inflection point of the fitted curve represents the EC_{50FSB} and for the FP-binding assay corresponds to the K_D value.

Competition assay

In a typical competition experiment the fluorescent probe is replaced from the previously formed protein-ligand-complex by titration with increasing amounts of a non-fluorescent competitor, which results in a decreased FP-signal. In this work, the proteins were typically used in the EC_{50}-concentrations (50% dynamic window) and, in cases with ΔmP <100, the double EC_{50} (100% dynamic window). The resulting curve was fitted with four-parameter sigmoidal curve fit and the obtained competitor EC_{50} was, if necessary, corrected through equation (1) using the Q-factor previously determined in the binding assay. The corrected EC_{50FSB} was transferred into K_D values using the BotDB IC_{50}-to-Ki online converter[8], which is based on equation (2) developed by *Nikolovska-*

Coleska and *Wang*,[9] where, $[I]_{50}$=concentration of the free inhibitor/competitor at 50% inhibition, $[L]_{50}$=concentration of the free labeled ligand at 50% inhibition and $[P]_0$=concentration of the free protein at 0% inhibition.

$$\boldsymbol{K_I} = \frac{[I]_{50}}{\left(\frac{[L]_{50}}{K_D} + \frac{[P]_0}{K_D} + 1\right)} \qquad (2)$$

Typically, the fluorescent probe with the highest affinity is selected to minimize the amount of consumed protein in the competition experiment.

6. Fluorescence Polarization Assay Curves

6.1 Binding Assays with 9s-HA-4-5(6)-TAMRA (15)

Binding assay: interleukin-8 versus 9s-HA-4-5(6)-TAMRA (**15**)

Polarization

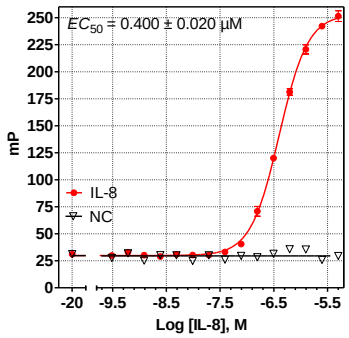

Q-factor

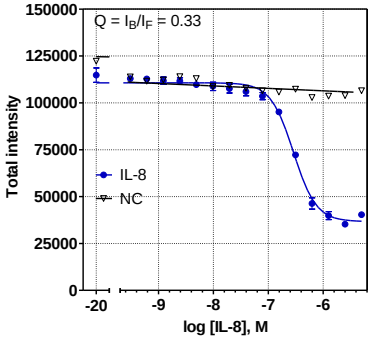

F_{SB}

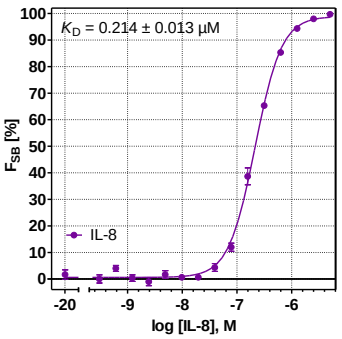

NC = negative control

Binding assay: interleukin-10 versus 9s-HA-4-5(6)-TAMRA (**15**)

Polarization

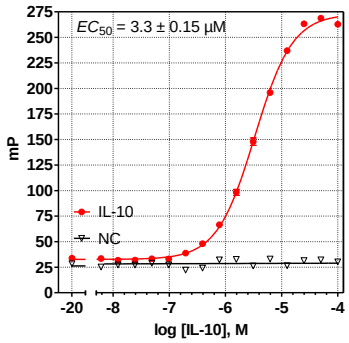

Q-factor

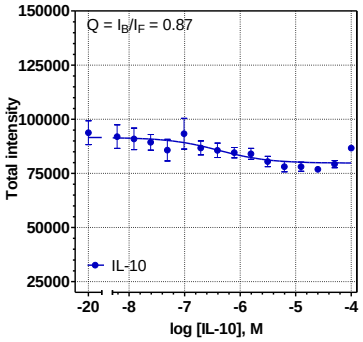

F_{SB}

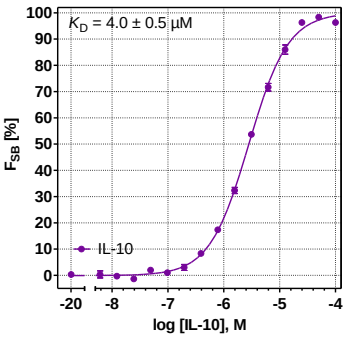

NC = negative control

Binding assay: bone morphogenetic protein 2 versus 9s-HA-4-5(6)-TAMRA (**15**)

Polarization

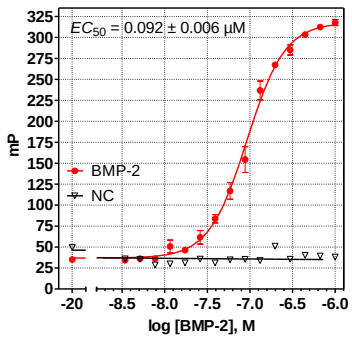

Q-factor

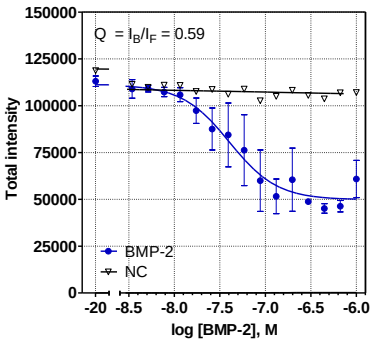

F_{SB}

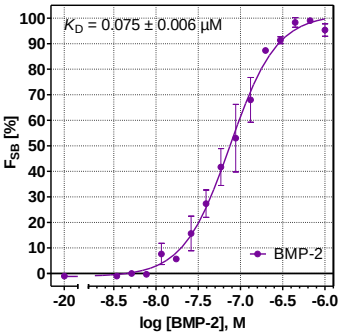

NC = negative control

Binding assay: sclerostin versus 9s-HA-4-5(6)-TAMRA (**15**)

Polarization

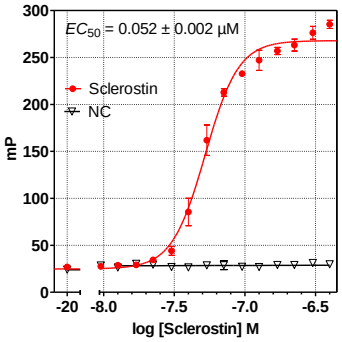

Q-factor

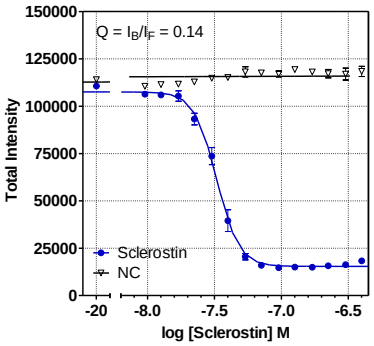

F_{SB}

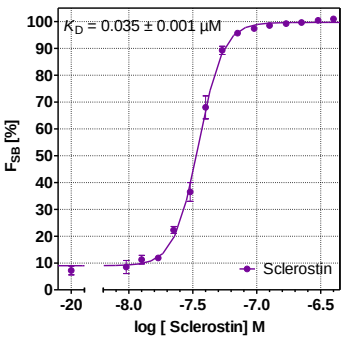

NC = negative control

Binding assay: tissue inhibitor of metalloproteinase 3 versus 9s-HA-4-5(6)-TAMRA (**15**)

Polarization

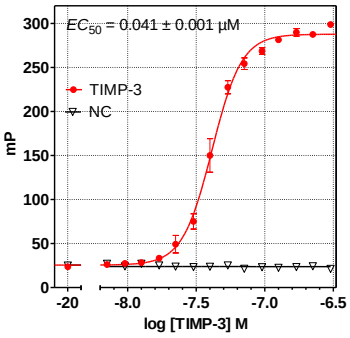

Q-factor

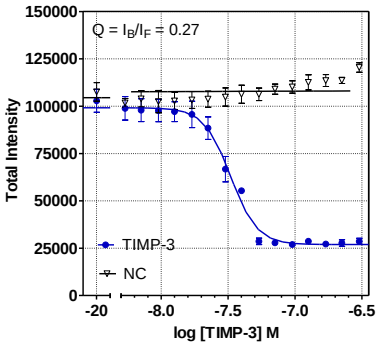

F_{SB}

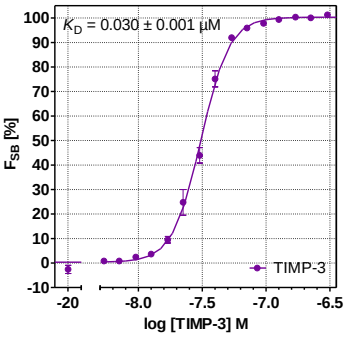

NC = negative control

Binding assay: CXCL12 (stromal derived factor, SDF-1) versus 9s-HA-4-5(6)-TAMRA (**15**)

Polarization

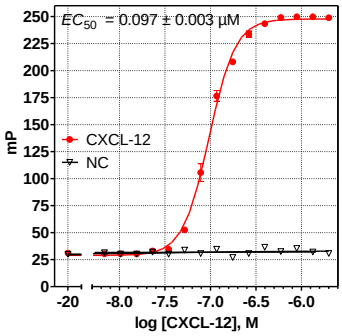

Q-factor

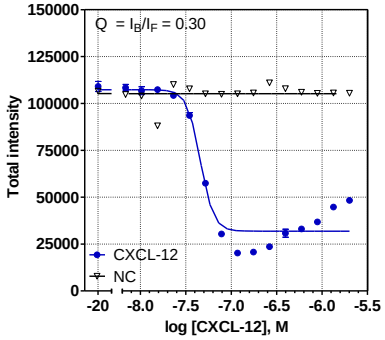

F_{SB}

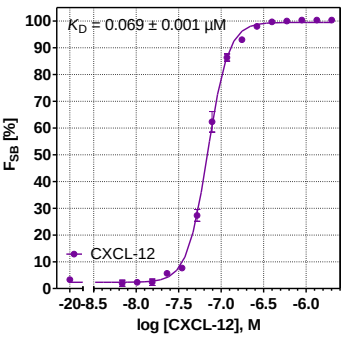

NC = negative control

Binding assay: transforming growth factor-β1 versus 9s-HA-4-5(6)-TAMRA (**15**)

Polarization

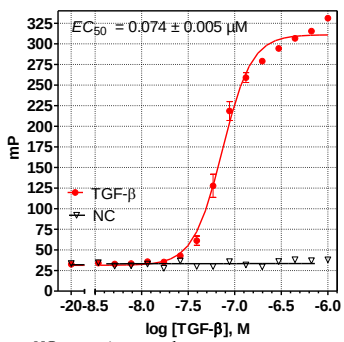

Q-factor

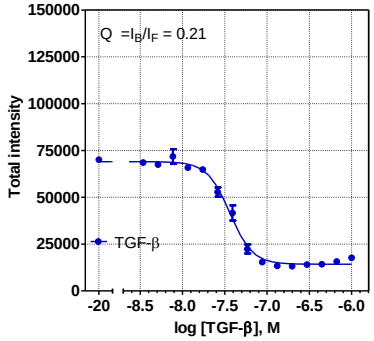

F_{SB}

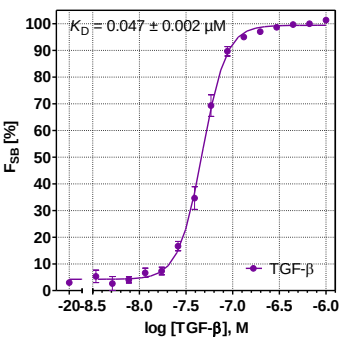

NC = negative control

Binding assay: fibroblast growth factor 1 versus 9s-HA-4-5(6)-TAMRA (**15**)

Polarization | Q-factor | F_{SB}

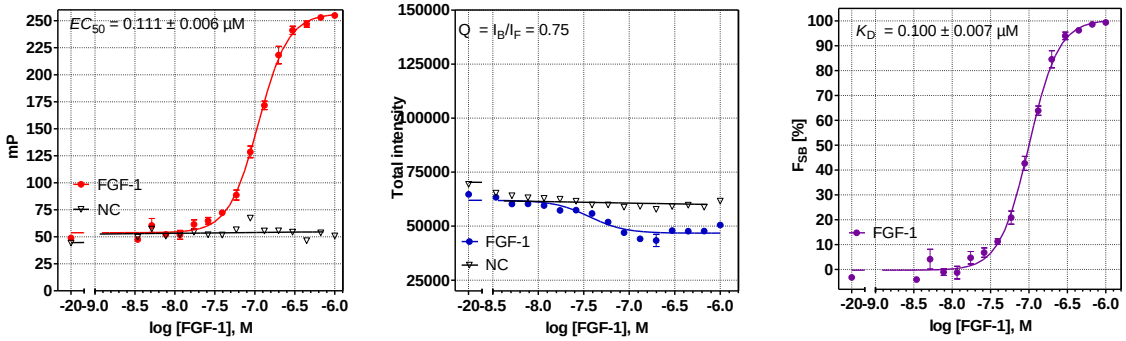

NC = negative control

Binding assay: fibroblast growth factor 2 versus 9s-HA-4-5(6)-TAMRA (**15**)

Polarization | Q-factor | F_{SB}

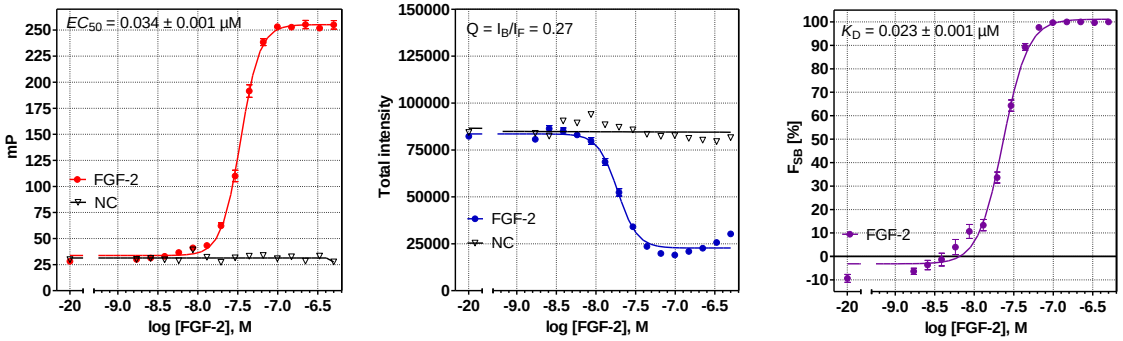

NC = negative control

Binding assay: antithrombine III versus 9s-HA-4-5(6)-TAMRA (**15**)

Polarization | Q-factor

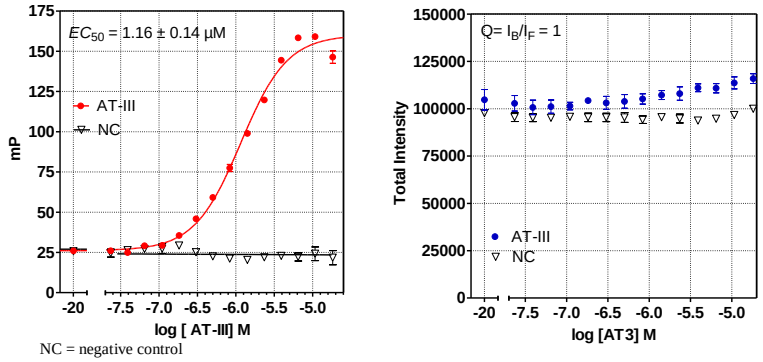

NC = negative control

6.2 Binding Assays with 13s-HA-6-5(6)-TAMRA (19)

Binding assay: interleukin 8 versus 13s-HA-6-5(6)-TAMRA (**19**)

Polarization | Q-Factor | F_{SB}

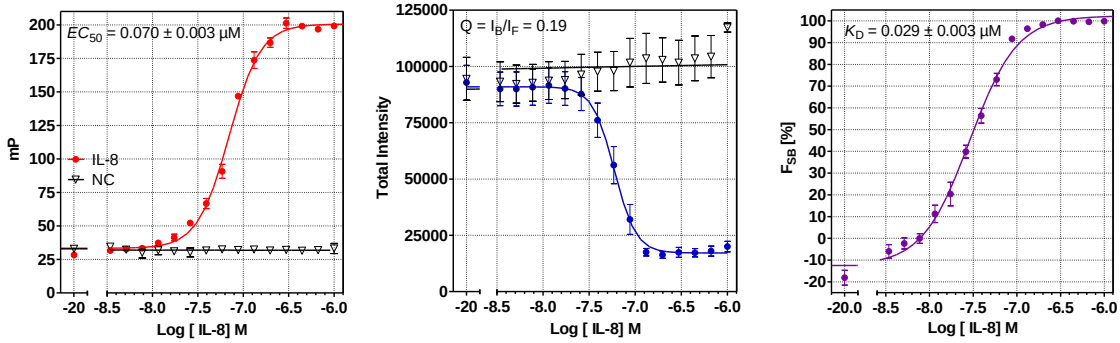

NC = negative control

Binding assay: interleukin 10 versus 13s-HA-6-5(6)-TAMRA (**19**)

Polarization

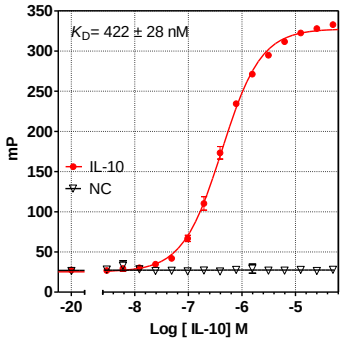

Q-Factor

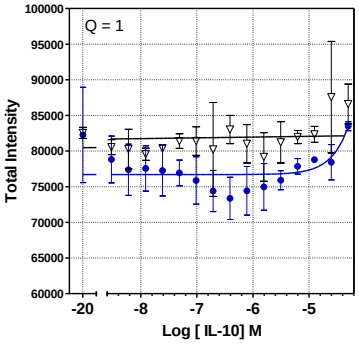

NC = negative control

Binding assay: bone morphogenetic protein 2 versus 13s-HA-6-5(6)-TAMRA (**19**)

Polarization

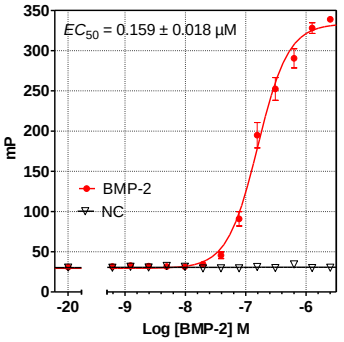

Q-factor

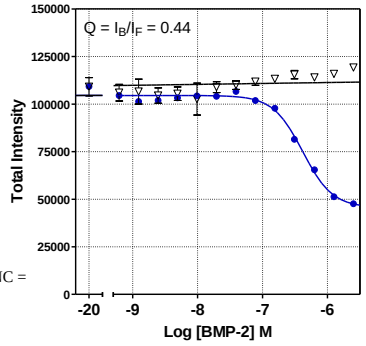

NC =

F_{SB}

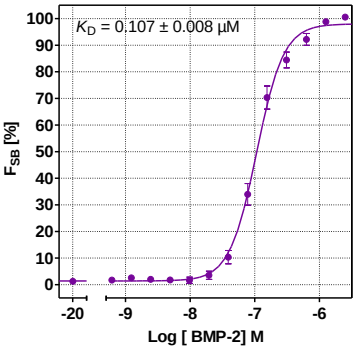

NC = negative control

Binding assay: sclerostin versus 13s-HA-6-5(6)-TAMRA (**19**)

Polarization

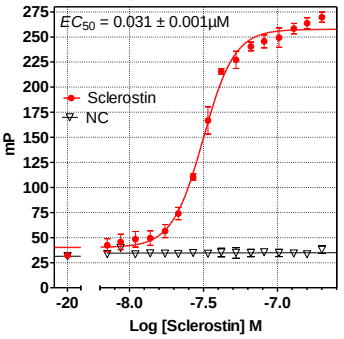

Q-factor

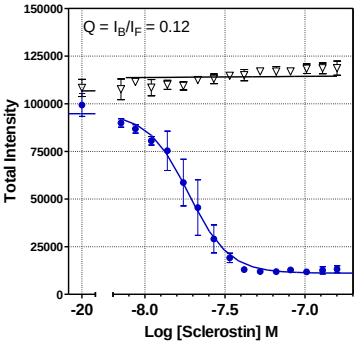

F_{SB}

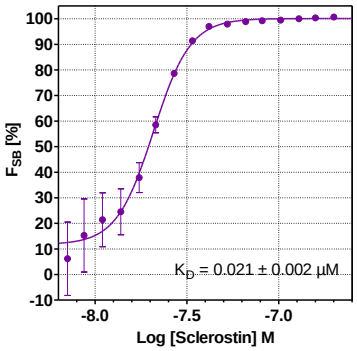

NC = negative control

Binding assay: tissue inhibitor of metalloproteinase 3 versus 13s-HA-6-5(6)-TAMRA (**19**)

Polarization

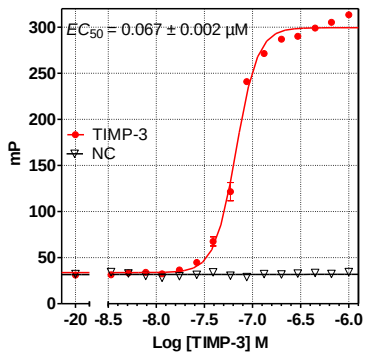

Q-factor

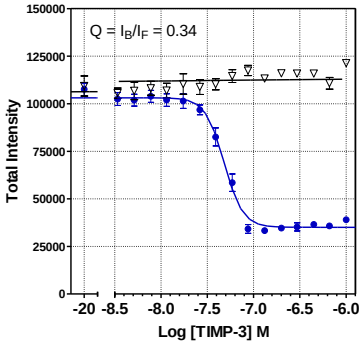

F_{SB}

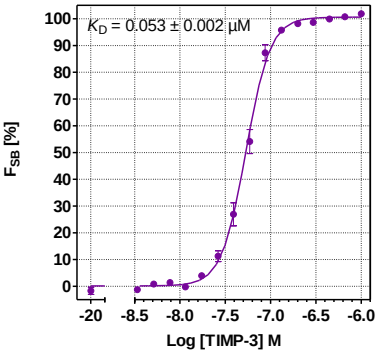

NC = negative control

Binding assay: CXCL12 (stromal derived factor, SDF-1) versus 13s-HA-6-5(6)-TAMRA (**19**)

Polarization | Q-factor | F_{SB}

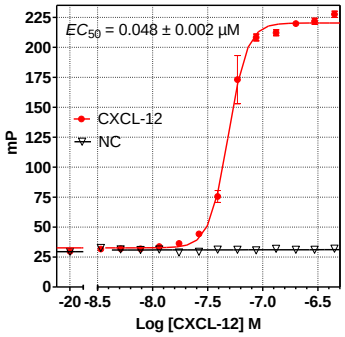

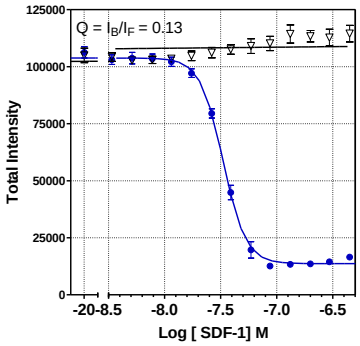

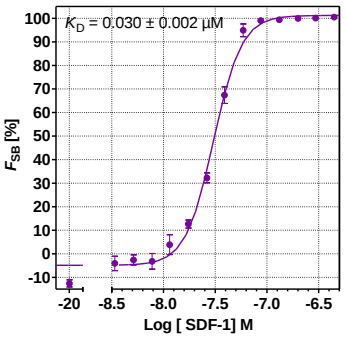

F_{SB}

NC = negative control

Binding assay: transforming growth factor-β1 versus 13s-HA-6-5(6)-TAMRA (**19**)

Polarization | Q-factor | F_{SB}

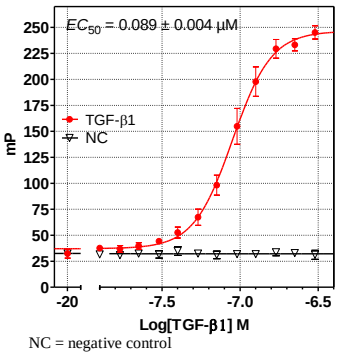

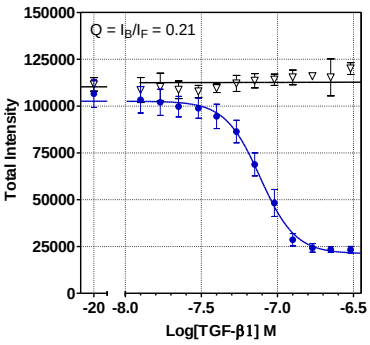

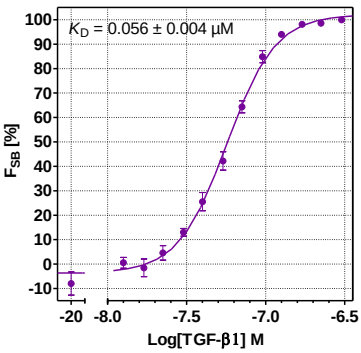

NC = negative control

Binding assay: fibroblast growth factor 1 versus 13s-HA-6-5(6)-TAMRA (**19**)

Polarization | Q-factor | F_{SB}

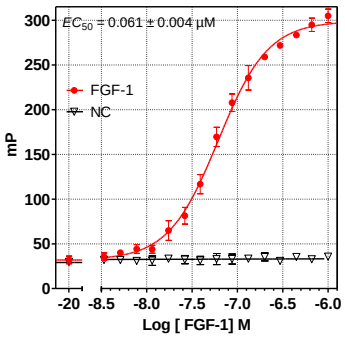

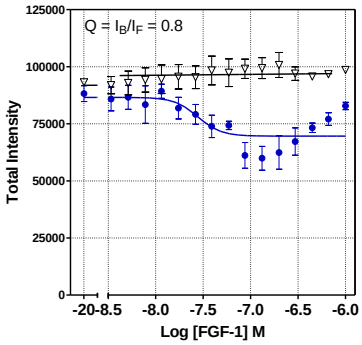

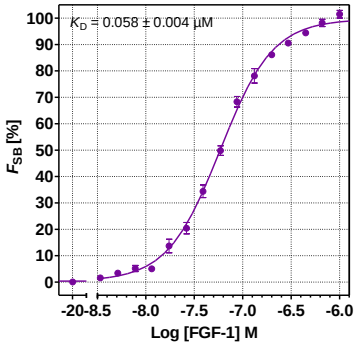

NC = negative control

Binding assay: fibroblast growth factor 2 versus 13s-HA-6-5(6)-TAMRA (**19**)

Polarization | Q-factor | F_{SB}

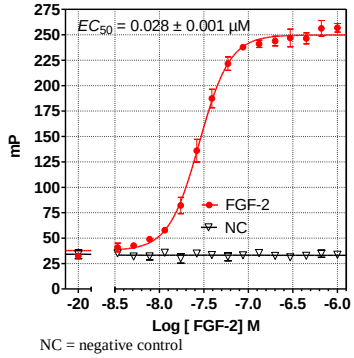

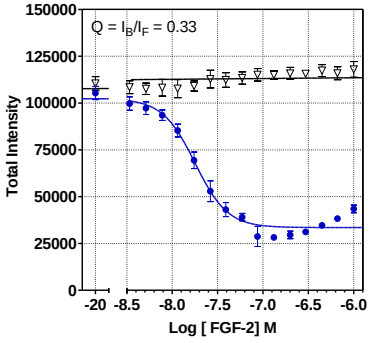

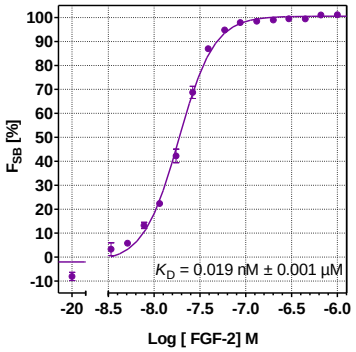

NC = negative control

Binding assay: antithrombine III versus 13s-HA-6-5(6)-TAMRA (**19**)

Polarization

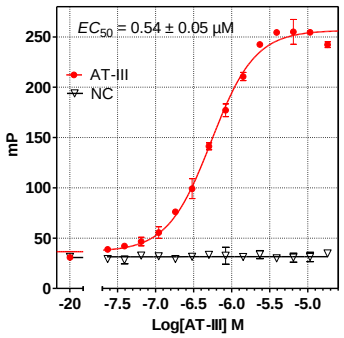

Q-factor

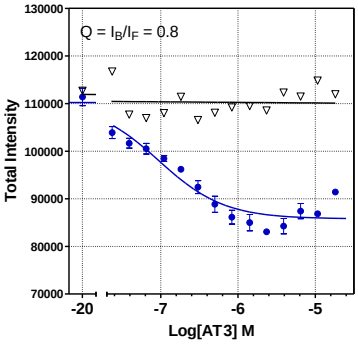

F_{SB}

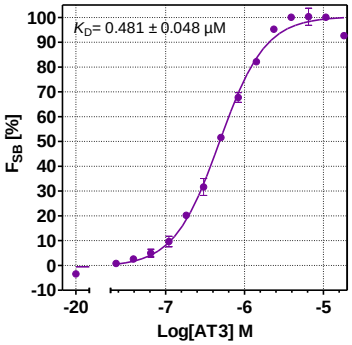

NC = negative control

6.3 Competition Assays with HA-4-N_3 (5)

Competition assay: interleukin 8 + 9s-HA-4-5(6)-TAMRA (**15**) versus HA-4-N_3 (**5**)

Polarization

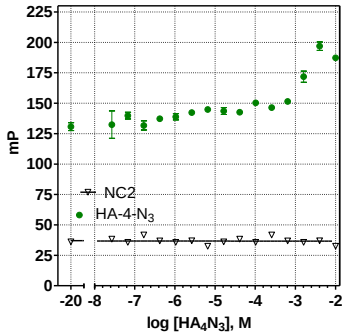

Assay conditions: interleukin-8 final assay concentration c = 800 nM (DW = 100 %), NC = negative control.

Competition assay: interleukin 10 + 9s-HA-4-5(6)-TAMRA (**15**) versus HA-4-N_3 (**5**)

Polarization

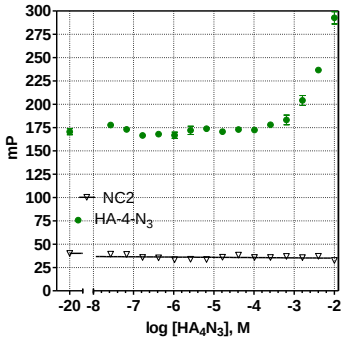

Assay conditions: interleukin-10 final assay concentration c = 3.3 µM, NC = negative control.

Competition assay: bone morphogenetic protein 2 + 9s-HA-4-5(6)-TAMRA (**15**) versus HA-4-N_3 (**5**)

Polarization

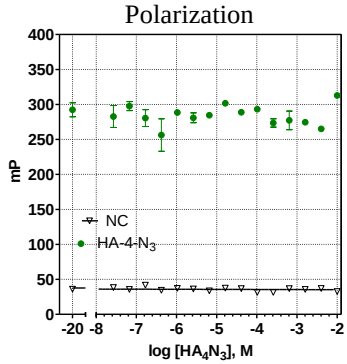

Assay conditions: BMP-2 final assay concentration c = 92 nM, NC = negative control.

Competition assay: sclerostin + 13s-HA-6-5(6)-TAMRA (**19**) versus HA-4-N_3 (**5**)

Polarization

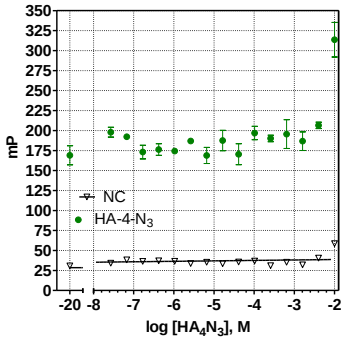

Assay conditions: sclerostin final assay concentration c = 35 nM, NC = negative control.

6.4 Competition Assays with 9s-HA-4-Triazol (16)

Competition assay: interleukin 8 + 13s-HA-6-5(6)-TAMRA (**19**) versus 9s-HA-4-Triazol (**16**)

Polarization

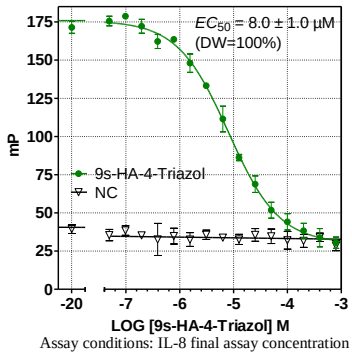

F_{SB}

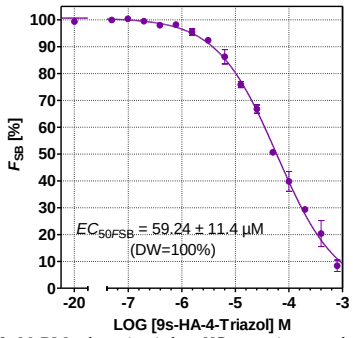

Assay conditions: IL-8 final assay concentration c = 140 nM, DW = dynamic window, NC = negative control

Competition assay: interleukin 10 + 13s-HA-6-5(6)-TAMRA (**19**) versus 9s-HA-4-Triazol (**16**)

Polarization

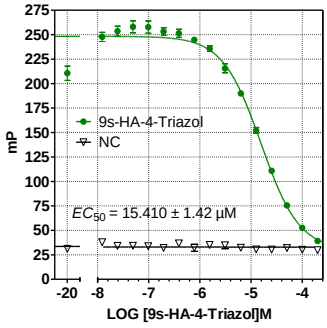

Assay conditions: IL-10 final assay concentration c = 422 nM, DW = dynamic window, NC = negative control

Competition assay: bone morphogenetic protein 2 + 9s-HA-4-5(6)-TAMRA (**15**) versus 9s-HA-4-Triazol (**16**)

Polarization

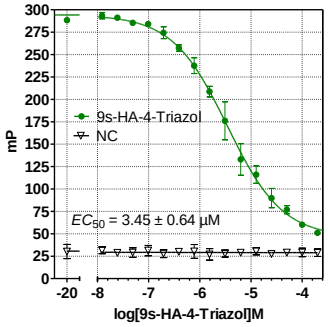

F_{SB}

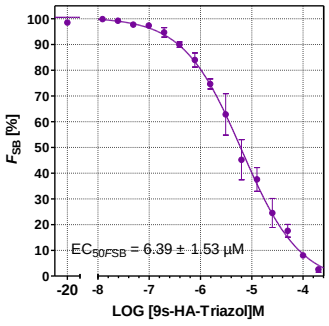

Assay conditions: BMP-2 final assay concentration c = 92 nM, DW = dynamic window, NC = negative control

Competition assay: sclerostin + 13s-HA-6-5(6)-TAMRA (**19**) versus 9s-HA-4-Triazol (**16**)

Polarization

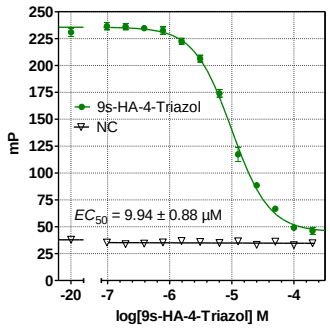

F_{SB}

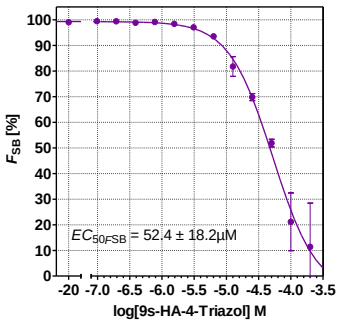

Assay conditions: sclerostin final assay concentration c = 31 nM, NC = negative control

Competition assay: TIMP-3 + 9s-HA-4-5(6)-TAMRA (**15**) versus 9s-HA-4-Triazol (**16**)

Polarization

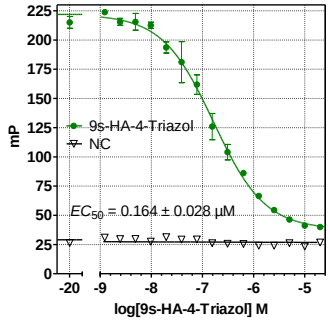

F_{SB}

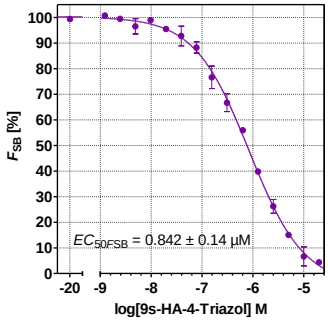

Assay conditions: TIMP-3 final assay concentration c = 41 nM, NC = negative control.

6.5 Competition Assays with 9s-HA-4-SMe (17)

Competition assay: interleukin 8 + 13s-HA-6-5(6)-TAMRA (**19**) versus 9s-HA-4-SMe (**17**)

Polarization

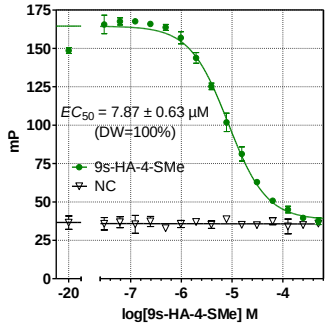

F_{SB}

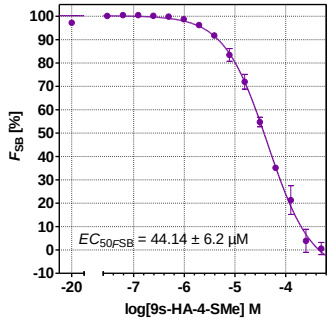

Assay conditions: IL-8 final assay concentration c = 140 nM, DW = dynamic window, NC = negative control

Competition assay: interleukin 10 + 13s-HA-6-5(6)-TAMRA (**19**) versus 9s-HA-4-SMe (**17**)

Polarization

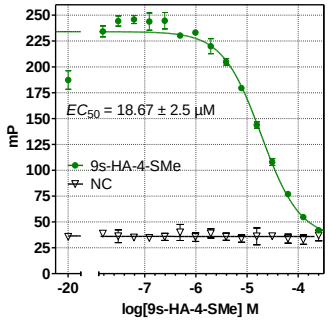

Assay conditions: IL-10 final assay concentration c = 422 nM, DW = dynamic window, NC = negative control

Competition assay: bone morphogenetic protein 2 + 9s-HA-4-5(6)-TAMRA (**15**) versus 9s-HA-4-SMe (**17**)

Polarization

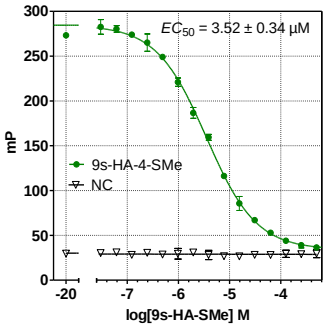

F_{SB}

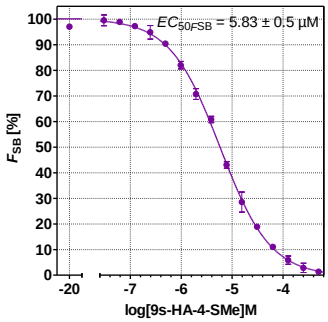

Assay conditions: BMP-2 final assay concentration c = 92 nM, DW = dynamic window, NC = negative control

Competition assay: sclerostin + 13s-HA-6-5(6)-TAMRA (**19**) versus 9s-HA-4-SMe (**17**)

Polarization

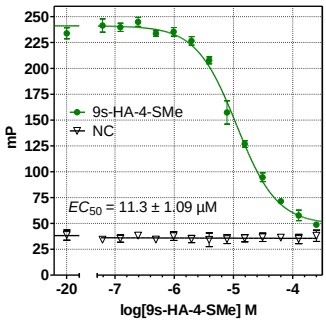

F_{SB}

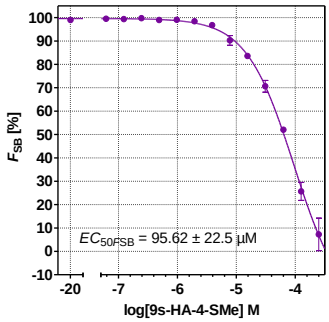

Assay conditions: sclerostin final assay concentration c = 31 nM, NC = negative control

Competition assay: TIMP 3 + 9s-HA-4-5(6)-TAMRA (**15**) versus 9s-HA-4-SMe (**17**)

Polarization

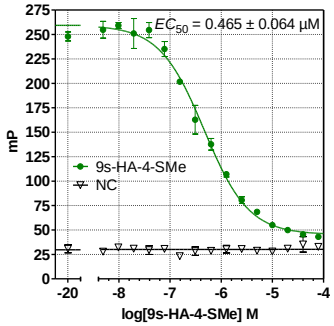

F_{SB}

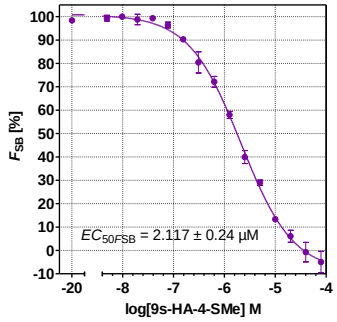

Assay conditions: TIMP-3 final assay concentration c = 41 nM, NC = negative control

6.6 Competition Assays with 9s-HA-4-H,H (18)

Competition assay: interleukin 8 + 13s-HA-6-5(6)-TAMRA (**19**) versus 9s-HA-4-H,H (**18**)

Polarization

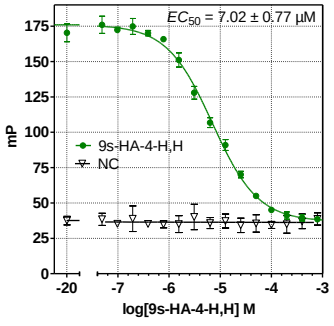

F_{SB}

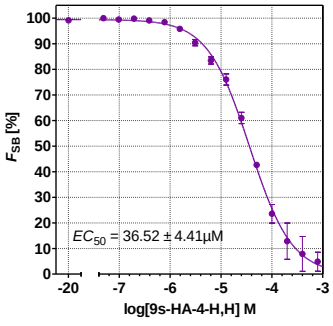

Assay conditions: IL-8 final assay concentration c = 140 nM, DW = dynamic window, NC = negative control

Competition assay: interleukin 10 + 13s-HA-6-5(6)-TAMRA (**19**) versus 9s-HA-4-H,H (**18**)

Polarization

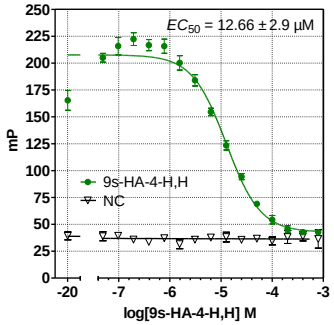

Assay conditions: IL-10 final assay concentration c = 422 nM, DW = dynamic window, NC = negative control

Competition assay: bone morphogenetic protein 2 + 9s-HA-4-5(6)-TAMRA (**15**) versus 9s-HA-4-H,H (**18**)

Polarization F_{SB}

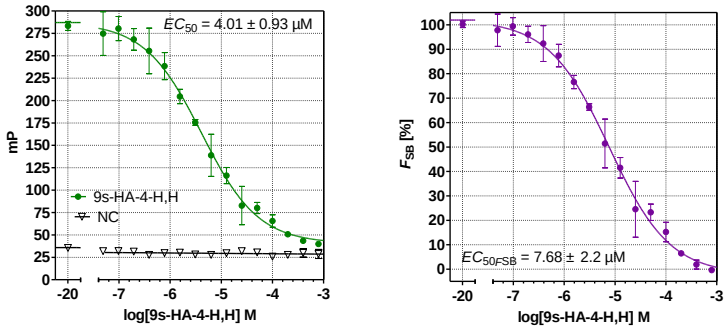

Assay conditions: BMP-2 final assay concentration c = 92 nM, DW = dynamic window, NC = negative control

Competition assay: sclerostin + 13s-HA-6-5(6)-TAMRA (**19**) versus 9s-HA-4-H,H (**18**)

Polarization F_{SB}

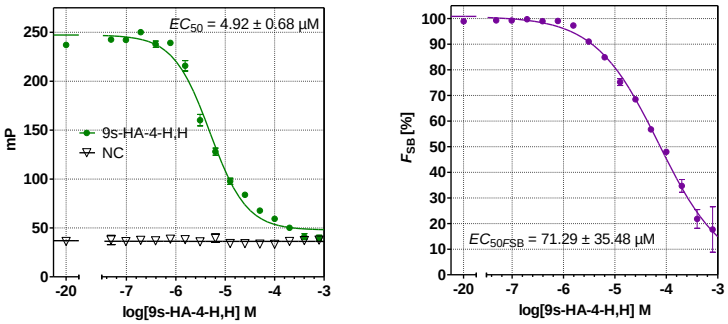

Assay conditions: sclerostin final assay concentration c = 31 nM, NC = negative control

Competition assay: TIMP 3 + 9s-HA-4-5(6)-TAMRA (**15**) versus 9s-HA-4-H,H (**18**)

Polarization F_{SB}

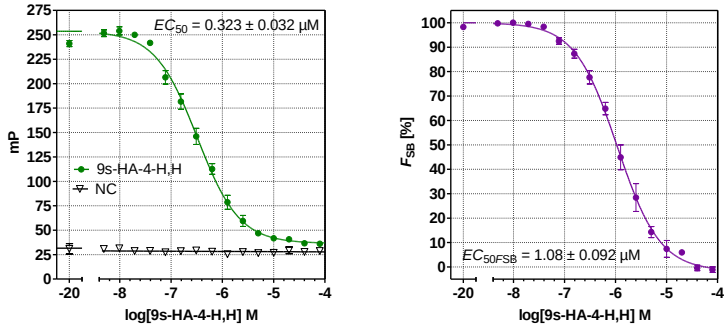

Assay conditions: TIMP-3 final assay concentration c = 41 nM, NC = negative control

6.7 Competition Assays with (9s-HA-4-S-PEG-S)$_2$ (20)

Competition assay: interleukin 8 + 13s-HA-6-5(6)-TAMRA (**19**) versus (9s-HA-4-S-PEG-S)$_2$ **(20)**

Polarization

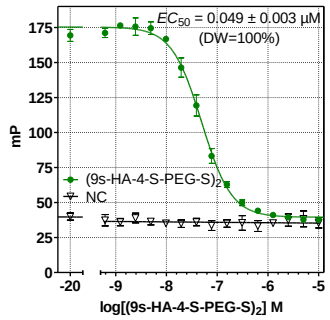

F_{SB}

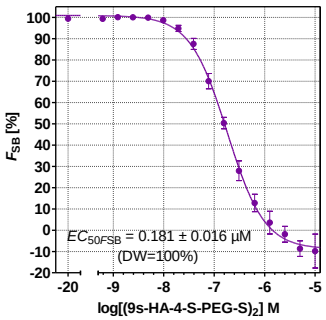

Assay conditions: IL-8 final assay concentration c = 140 nM, DW = dynamic window, NC = negative control

Competition assay: interleukin 10 + 13s-HA-6-5(6)-TAMRA (**19**) versus (9s-HA-4-S-PEG-S)$_2$ **(20)**

Polarization

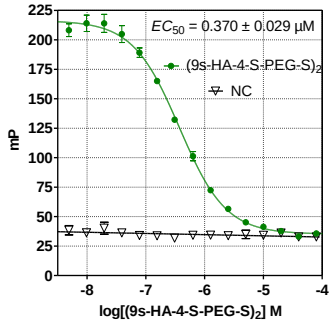

Assay conditions: IL-10 final assay concentration c = 422 nM, NC = negative control

Competition assay: BMP-2 + 9s-HA-4-5(6)-TAMRA (**15**) versus (9s-HA-4-S-PEG-S)$_2$ **(20)**

Polarization

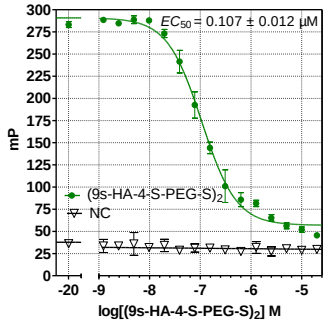

F_{SB}

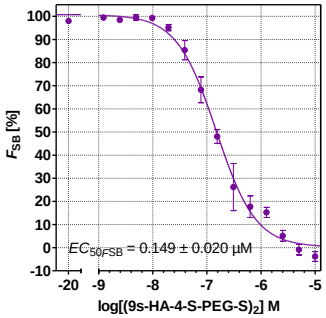

Assay conditions: BMP-2 final assay concentration c = 92 nM, DW = dynamic window, NC = negative control

Competition assay: sclerostin + 13s-HA-6-5(6)-TAMRA (**19**) versus (9s-HA-4-S-PEG-S)$_2$ **(20)**

Polarization

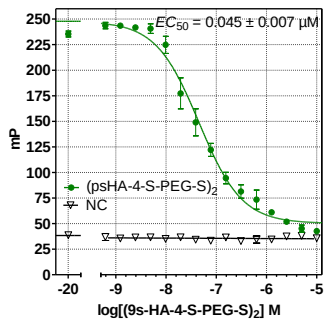

F_{SB}

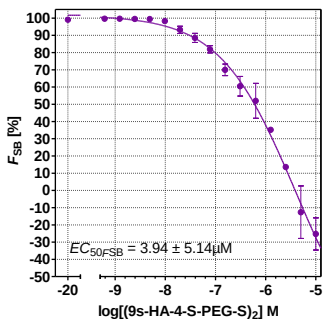

Assay conditions: sclerostin final assay concentration c = 31 nM, NC = negative control

Competition assay: TIMP 3 + 9s-HA-4-5(6)-TAMRA (**15**) versus $(9s\text{-}HA\text{-}4\text{-}S\text{-}PEG\text{-}S)_2$ **(20)**

Polarization F_{SB}

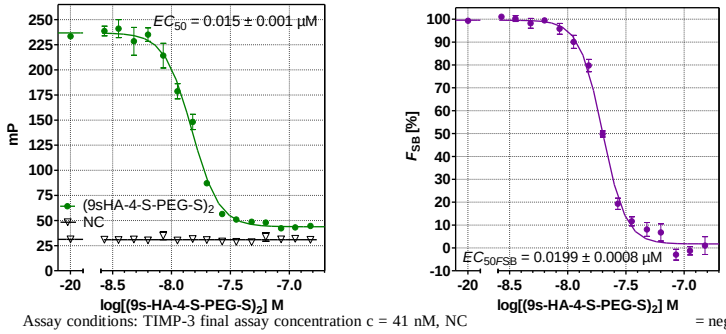

Assay conditions: TIMP-3 final assay concentration c = 41 nM, NC = negative control

6.8 Competition Assays with 2s-HA-4-N_3 (21)

Competition assay: interleukin 8 + 9s-HA-4-5(6)-TAMRA (**15**) versus 2s-HA-4-N_3 (**21**)

Polarization F_{SB}

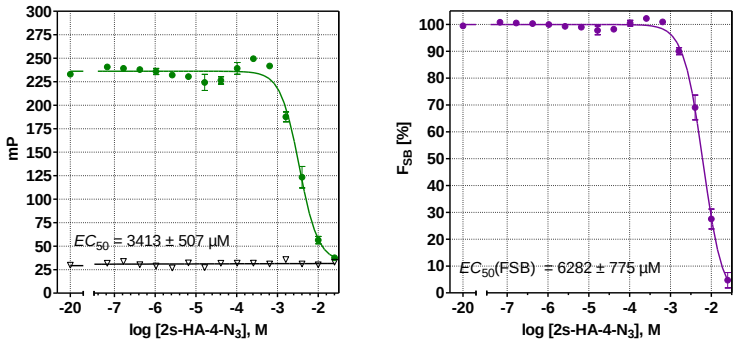

Assay conditions: interleukin-8 final assay concentration c = 800 nM (DW = 100 %), NC = negative control.

Competition assay: interleukin 10 + 9s-HA-4-5(6)-TAMRA (**15**) versus 2s-HA-4-N_3 (**21**)

Polarization F_{SB}

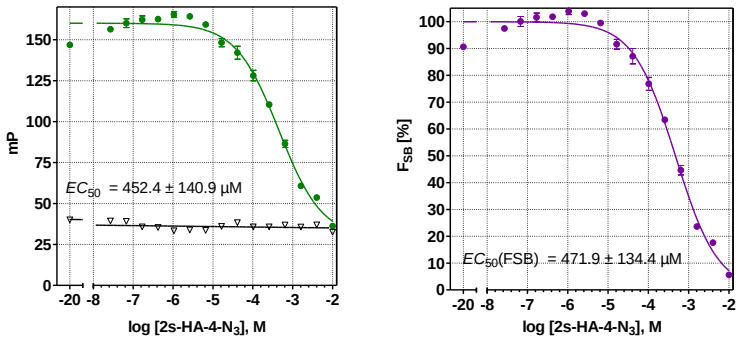

Assay conditions: interleukin-10 final assay concentration c = 3.3 µM, NC = negative control.

Competition assay: bone morphogenetic protein 2 + 9s-HA-4-5(6)-TAMRA (**15**) versus 2s-HA-4-N_3 (**21**)

Polarization F_{SB}

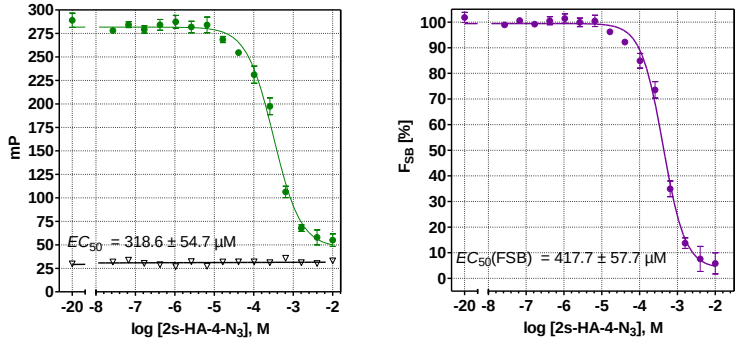

Assay conditions: BMP-2 final assay concentration c = 92 nM, NC = negative control

Competition assay: sclerostin + 13s-HA-6-5(6)-TAMRA (**19**) versus 2s-HA-4-N_3 (**21**)

Polarization F_{SB}

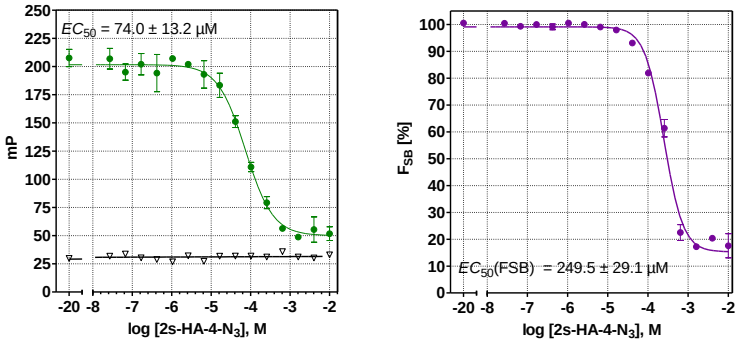

Assay conditions: sclerostin final assay concentration c = 35 nM, NC = negative control.

6.9 Competition Assays with 5s-HA-4-N_3 (22)

Competition assay: interleukin 8 + 9s-HA-4-5(6)-TAMRA (**15**) versus 5s-HA-4-N_3 (**22**)

Polarization F_{SB}

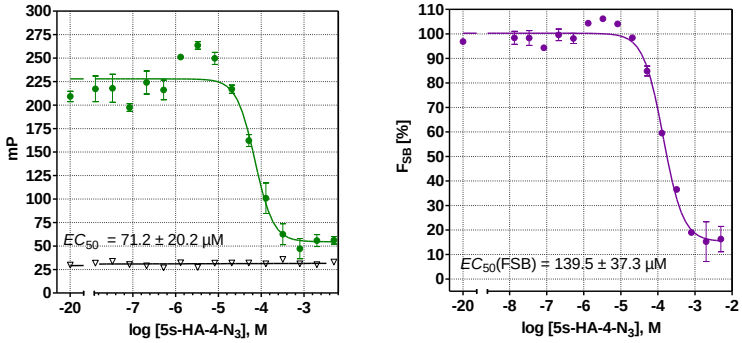

Assay conditions: interleukin-8 final assay concentration c = 800 nM (DW = 100 %), NC = negative control

Competition assay: interleukin 10 + 9s-HA-4-5(6)-TAMRA (**15**) versus 5s-HA-4-N_3 (**22**)

Polarization F_{SB}

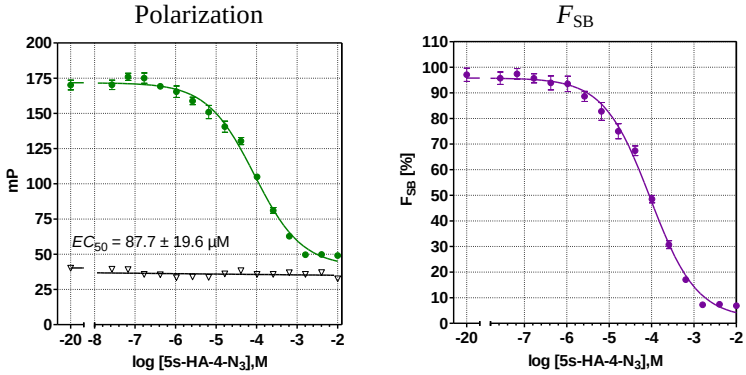

Assay conditions: interleukin-10 final assay concentration c = 3.3 µM, NC = negative control.

Competition assay: BMP-2 + 9s-HA-4-5(6)-TAMRA (**15**) versus 5s-HA-4-N_3 (**22**)

Polarization F_{SB}

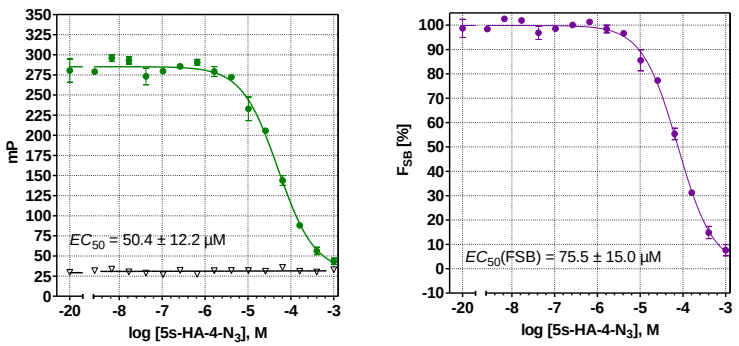

Assay conditions: BMP-2 final assay concentration c = 92 nM, NC = negative control.

Competition assay: sclerostin + 13s-HA-6-5(6)-TAMRA (**19**) versus 5s-HA-4-N_3 (**22**)

Polarization F_{SB}

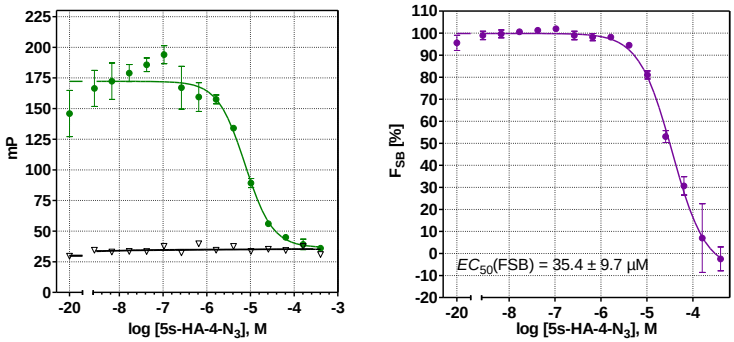

Assay conditions: sclerostin final assay concentration c = 35 nM, NC = negative control.

6.10 Competition Assays with 7s-HA-4-N_3 (23)

Competition assay: interleukin 8 + 9s-HA-4-5(6)-TAMRA (**15**) versus 7s-HA-4-N_3 (**23**)

Polarization F_{SB}

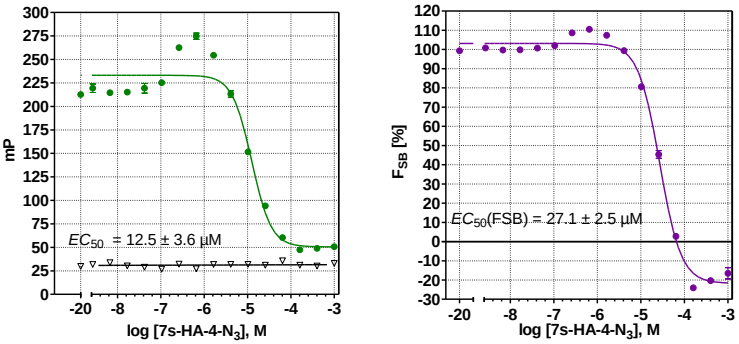

Assay conditions: interleukin-8 final assay concentration c = 800 nM (DW = 100 %), NC = negative control.

Competition assay: interleukin 10 + 9s-HA-4-5(6)-TAMRA (**15**) versus 7s-HA-4-N_3 (**23**)

Polarization F_{SB}

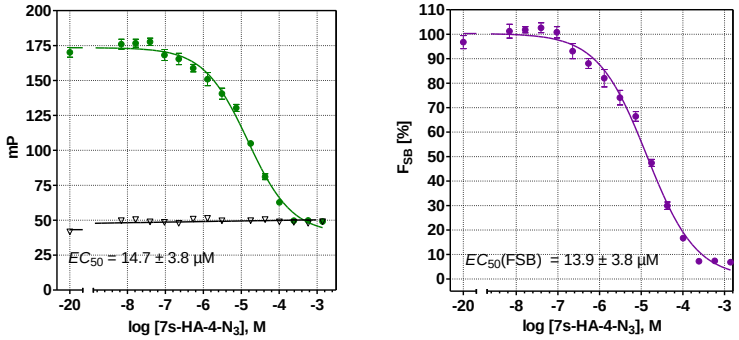

Assay conditions: interleukin-10 final assay concentration c = 3.3 µM, NC = negative control.

Competition assay: BMP-2 + 9s-HA-4-5(6)-TAMRA (**15**) versus 7s-HA-4-N_3 (**23**)

Polarization F_{SB}

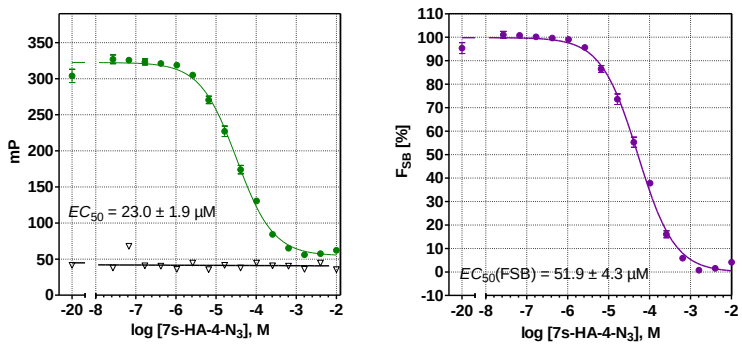

Assay conditions: BMP-2 final assay concentration c = 92 nM, NC = negative control.

Competition assay: sclerostin + 13s-HA-6-5(6)-TAMRA (**19**) versus 7s-HA-4-N_3 (**23**)

Polarization F_{SB}

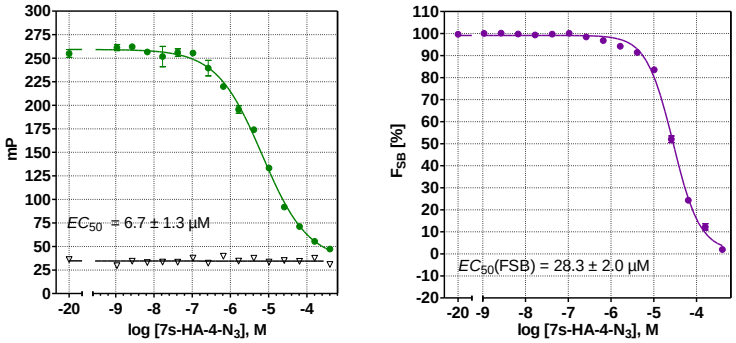

Assay conditions: sclerostin final assay concentration c = 35 nM, NC = negative control.

6.11 Competition Assays with 5s-HA-2-N_3 (24)

Competition assay: interleukin 8 + 9s-HA-4-5(6)-TAMRA (**15**) versus 5s-HA-2-N_3 (**24**)

Polarization F_{SB}

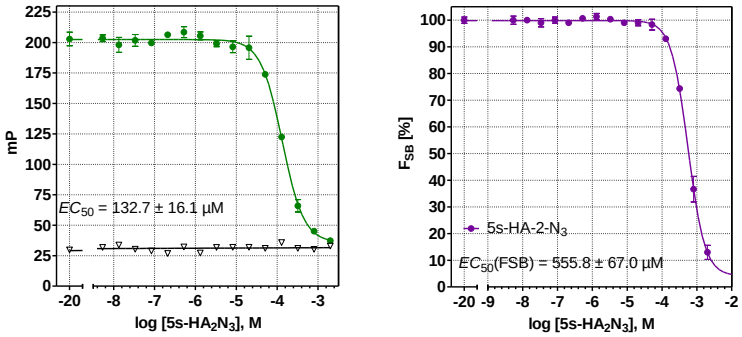

Assay conditions: interleukin-8 final assay concentration c = 800 nM (DW = 100 %), NC = negative control.

Competition assay: interleukin 10 + 9s-HA-4-5(6)-TAMRA (**15**) versus 5s-HA-2-N_3 (**24**)

Polarization F_{SB}

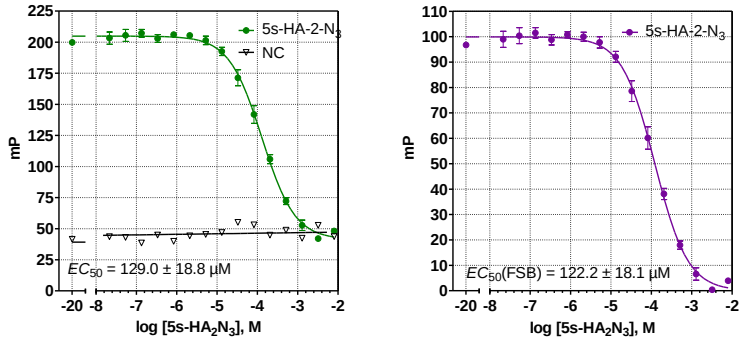

Assay conditions: interleukin-10 final assay concentration c = 3.3 µM, NC = negative control.

Competition assay: bone morphogenetic protein 2 + 9s-HA-4-5(6)-TAMRA (**15**) versus 5s-HA-2-N_3 (**24**)

Polarization F_{SB}

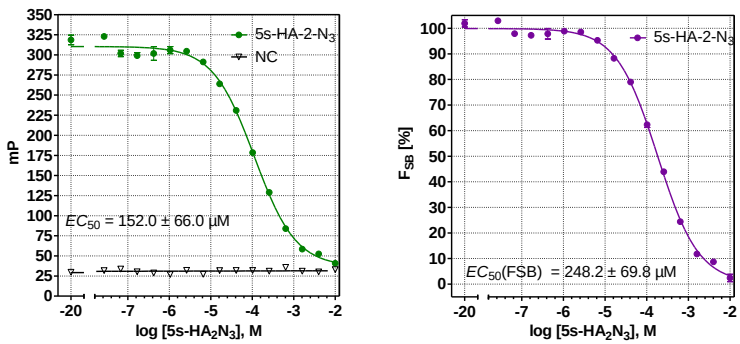

Assay conditions: BMP-2 final assay concentration c = 92 nM, NC = negative control.

Competition assay: sclerostin + 13s-HA-6-5(6)-TAMRA (**19**) versus 5s-HA-2-N_3 (**24**)

Polarization F_{SB}

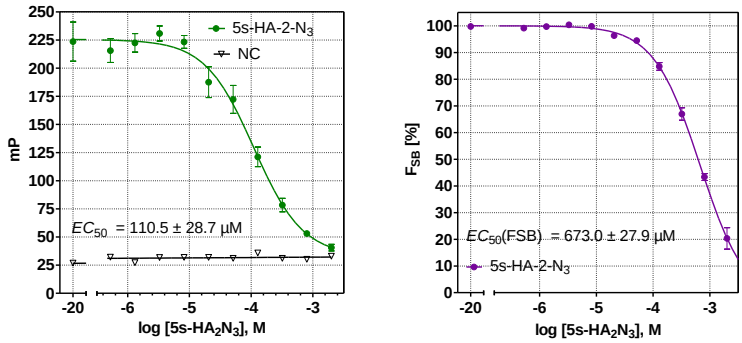

Assay conditions: sclerostin final assay concentration c = 35 nM, NC = negative control.

6.12 Competition Assays with 9s-HA-4-N_3 (25)

Competition assay: interleukin 8 + 9s-HA-4-5(6)-TAMRA (**15**) versus 9s-HA-4-N_3 (**25**)

Polarization F_{SB}

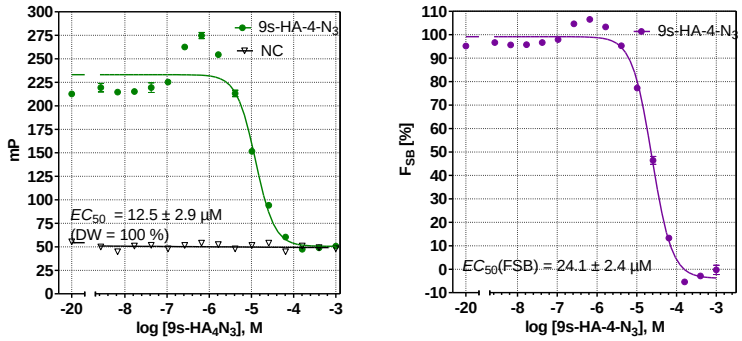

Assay conditions: interleukin-8 final assay concentration c = 800 nM (DW = 100 %), NC = negative control.

Competition assay: interleukin 10 + 9s-HA-4-5(6)-TAMRA (**15**) versus 9s-HA-4-N_3 (**25**)

Polarization F_{SB}

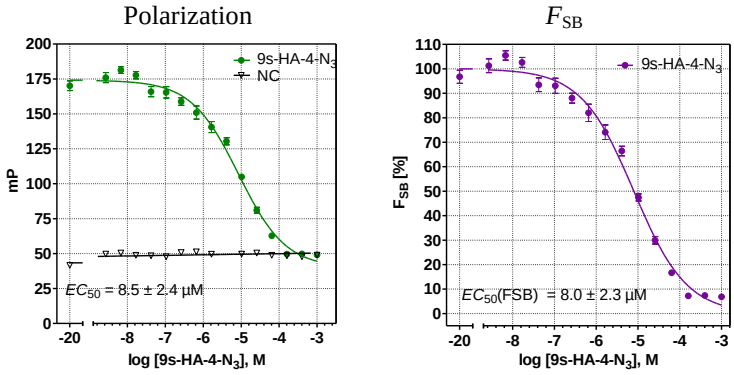

Assay conditions: interleukin-10 final assay concentration c = 3.3 µM, NC = negative control

Competition assay: bone morphogenetic protein 2 + 9s-HA-4-5(6)-TAMRA (**15**) versus 9s-HA-4-N_3 (**25**)

Polarization F_{SB}

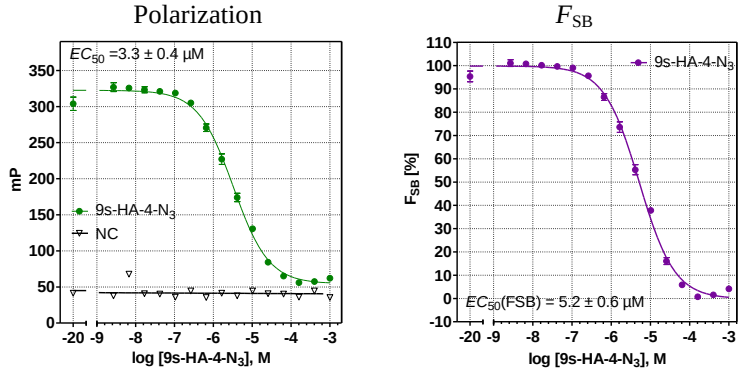

Assay conditions: BMP-2 final assay concentration c = 92 nM, NC = negative control.

Competition assay: sclerostin + 9s-HA-4-5(6)-TAMRA (**15**) versus 9s-HA-4-N_3 (**25**)

Polarization F_{SB}

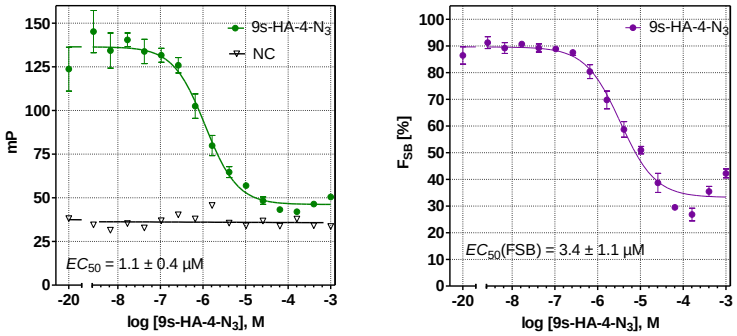

Assay conditions: sclerostin final assay concentration c = 52 nM, NC = negative control.

Competition assay: tissue inhibitor of metalloproteinase 3 + 9s-HA-4-5(6)-TAMRA (**15**) versus 9s-HA-4-N_3 (**25**)

Polarization F_{SB}

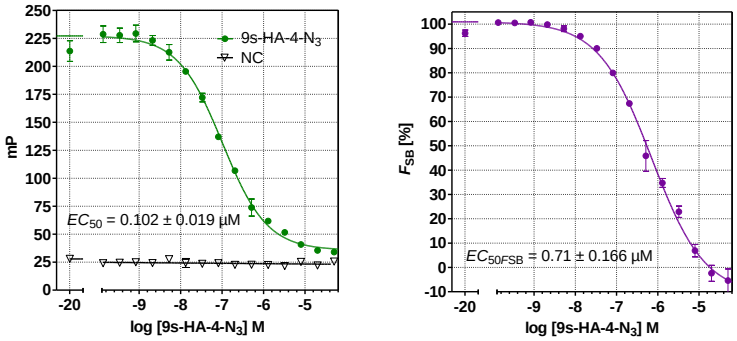

Assay conditions: TIMP-3 final assay concentration c = 41 nM, NC = negative control

Competition assay: CXCL12 (stromal derived factor) + 9s-HA-4-5(6)-TAMRA (**15**) versus 9s-HA-4-N_3 (**25**)

Polarization F_{SB}

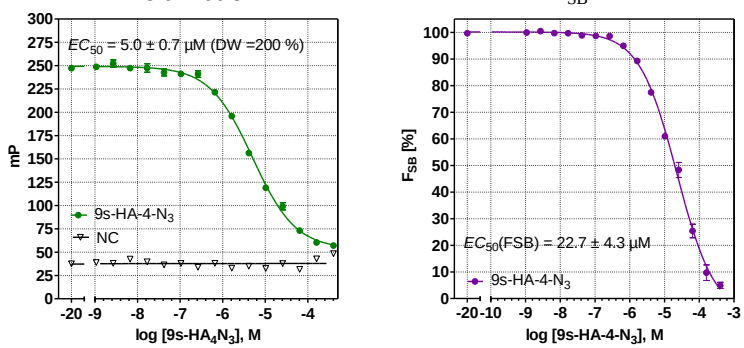

Assay conditions: CXCL12 final assay concentration c = 388 nM (DW = 200 %), NC = negative control.

Competition assay: transforming growth factor-β1+ 9s-HA-4-5(6)-TAMRA (**15**) versus 9s-HA-4-N_3 (**25**)

Polarization F_{SB}

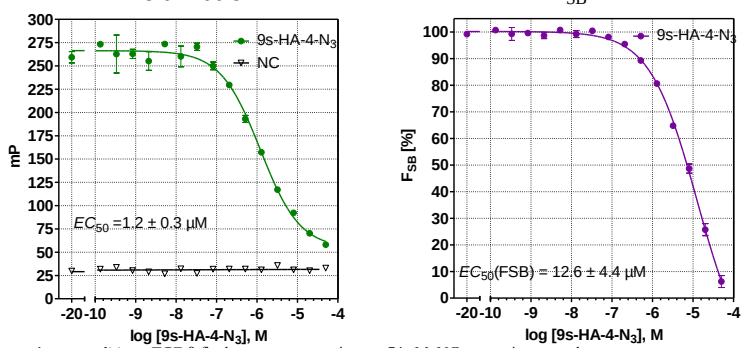

Assay conditions: TGF-β final assay concentration c = 74 nM, NC = negative control.

Competition assay: fibroblast growth factor 1 + 9s-HA-4-5(6)-TAMRA (**15**) versus 9s-HA-4-N_3 (**25**)

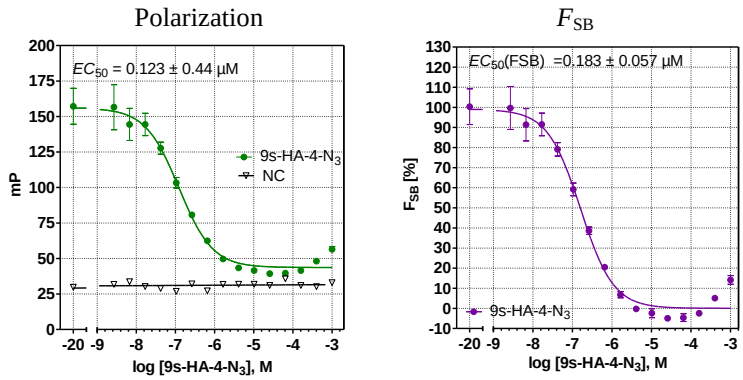

Assay conditions: FGF-1 final assay concentration c = 111 nM, NC = negative control.

Competition assay: fibroblast growth factor 2 + 9s-HA-4-5(6)-TAMRA (**15**) versus 9s-HA-4-N_3 (**25**)

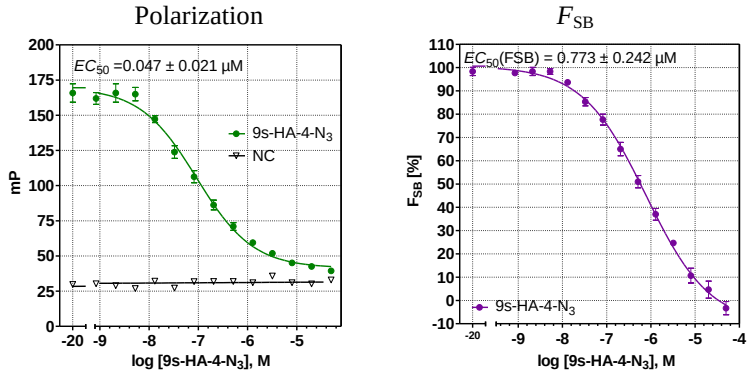

Assay conditions: FGF-2 final assay concentration c = 34 nM, NC = negative control.

Competition assay: transforming growth factor-β1+ 9s-HA-4-5(6)-TAMRA (**15**) versus 9s-HA-4-N_3 (**25**)

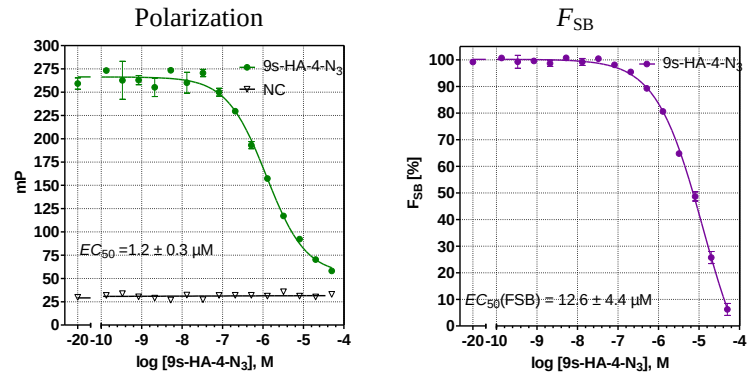

Assay conditions: TGF-β final assay concentration c = 74 nM, NC = negative control.

Competition assay: antithrombine III + 13s-HA-6-5(6)-TAMRA (**19**) versus 9s-HA-4-N_3 (**25**)

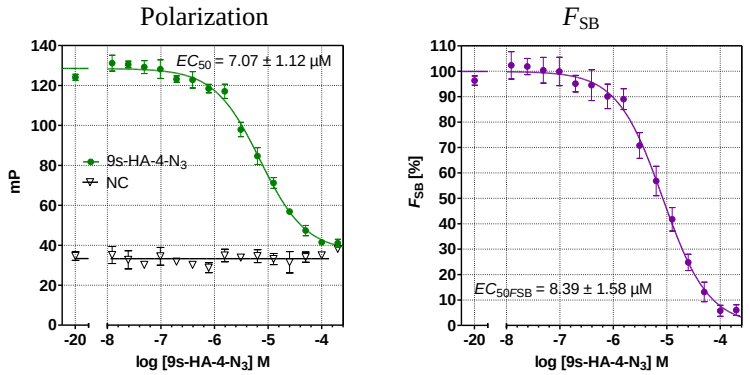

Assay conditions: AT-III final assay concentration c = 540 nM, NC = negative control

6.13 Competition Assays with 13s-HA-6-N_3 (26)

Competition assay: interleukin 8 + 13s-HA-6-5(6)-TAMRA (**19**) versus 13s-HA-6-N_3 (**26**)

Polarization

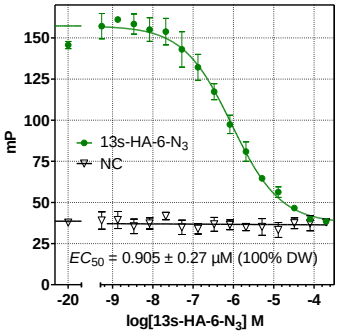

F_{SB}

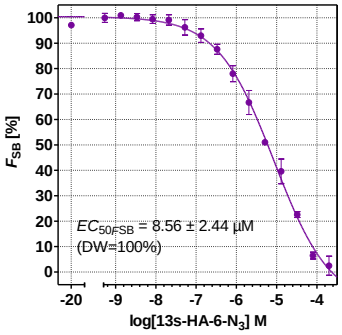

Conditions: c(IL-8) = 140 nM, DW = dynamic window, NC = negative control

Competition assay: interleukin 10 + 13s-HA-6-5(6)-TAMRA (**19**) versus 13s-HA-6-N_3 (**26**)

Polarization

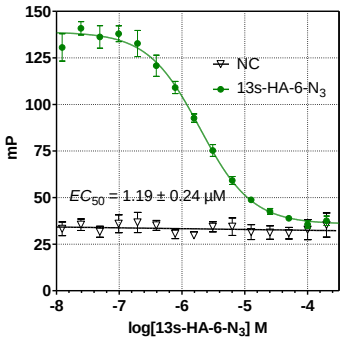

Assay conditions: IL-10 final assay concentration c = 422 nM, NC = negative control

Competition assay: CXCL12 + 13s-HA-6-5(6)-TAMRA (**19**) versus 13s-HA-6-N_3 (**26**)

Polarization

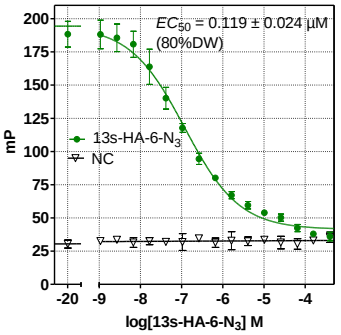

F_{SB}

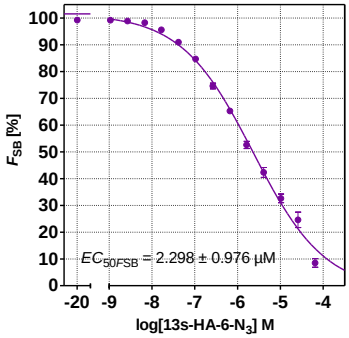

Assay conditions: CXCL12 final assay concentration c = 60 nM, DW = dynamic window, NC = negative control

Competition assay: TGF-β1 + 13s-HA-6-5(6)-TAMRA (**19**) versus 13s-HA-6-N_3 (**26**)

Polarization

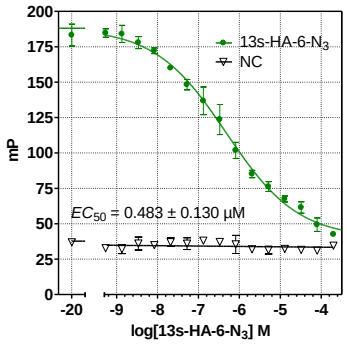

F_{SB}

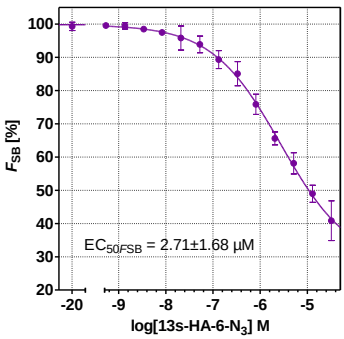

Assay conditions: TGF-ß1 final assay concentration c = 89 nM, NC = negative control

Competition assay: fibroblast growth factor 1 + 13s-HA-6-5(6)-TAMRA (**19**) versus 13s-HA-6-N_3 (**26**)

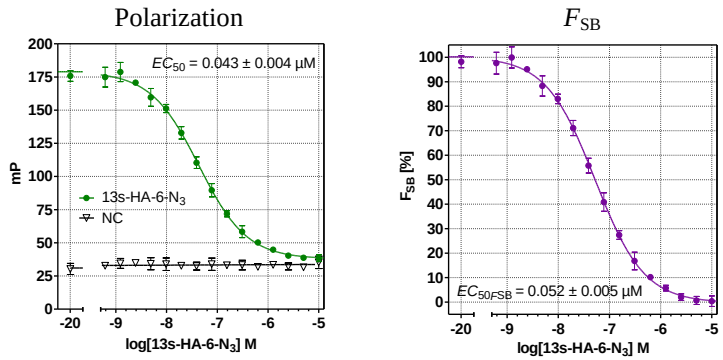

Assay conditions: FGF-1 final assay concentration c = 67 nM, NC = negative control

Competition assay: fibroblast growth factor 2 + 13s-HA-6-5(6)-TAMRA (**19**) versus 13s-HA-6-N_3 (**26**)

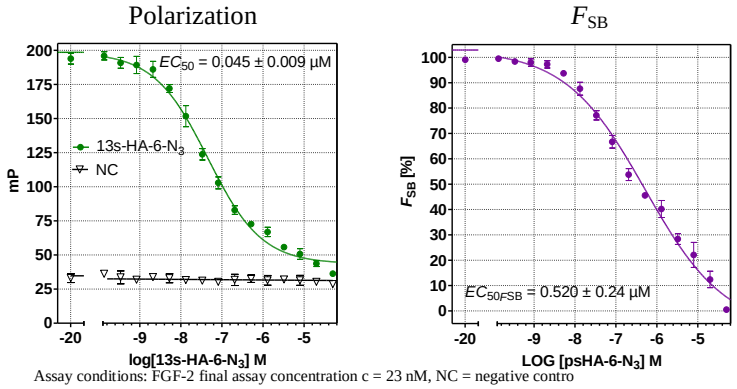

Assay conditions: FGF-2 final assay concentration c = 23 nM, NC = negative contro

Competition assay: bone morphogenetic protein 2 +13s-HA-6-5(6)-TAMRA (**19**) versus 13s-HA-6-N_3 (**26**)

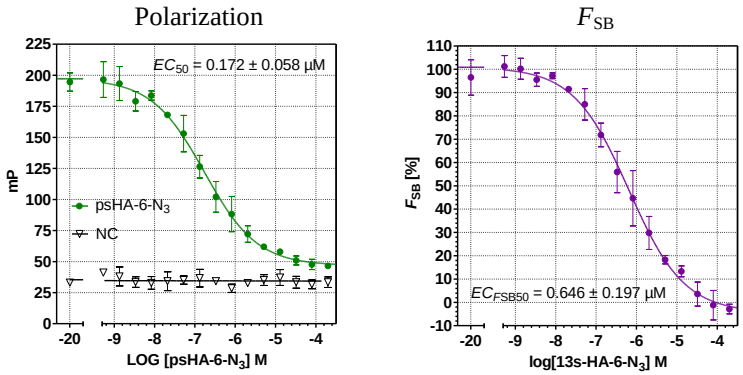

Assay conditions: BMP-2 final assay concentration c = 160 nM, NC = negative control

Competition assay: sclerostin + 13s-HA-6-5(6)-TAMRA (**19**) versus 13s-HA-6-N_3 (**26**)

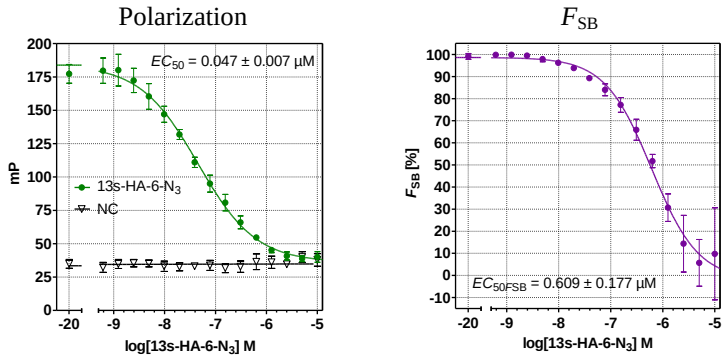

Assay conditions: sclerostin final assay concentration c = 31 nM, NC = negative control

Competition assay: TIMP-3 + 13s-HA-6-5(6)-TAMRA (**19**) versus 13s-HA-6-N_3 (**26**)

Polarization F_{SB}

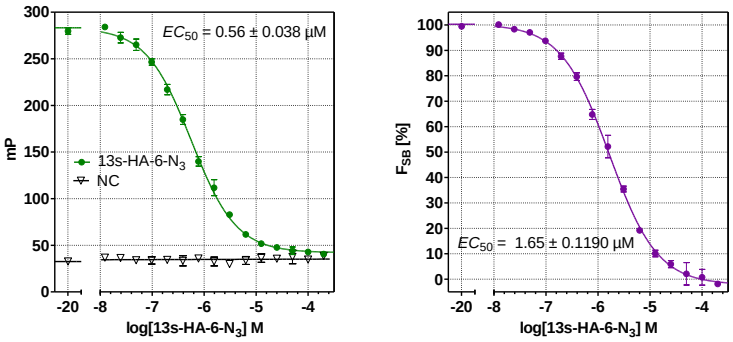

Assay conditions: TIMP-3 final assay concentration c = 67 nM, NC = negative control

Competition assay: antithrombine III + 13s-HA-6-5(6)-TAMRA (**19**) versus 13s-HA-6-N_3 (**26**)

Polarization F_{SB}

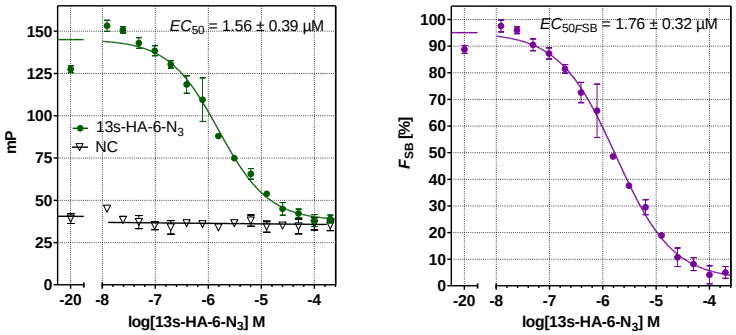

Assay conditions: AT-3 final assay concentration c = 540 nM, NC = negative control

6.14 Competition Assays with Fondaparinux (27)

Competition assay: interleukin 8 + 9s-HA-4-5(6)-TAMRA (**15**) versus Fondaparinux (**27**)

Polarization F_{SB}

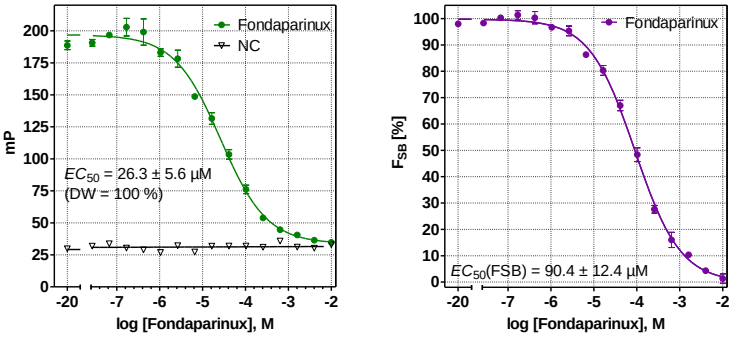

Assay conditions: interleukin-8 final assay concentration c = 800 nM (DW = 100 %), NC = negative control.

Competition assay: interleukin 10 + 9s-HA-4-5(6)-TAMRA (**15**) versus Fondaparinux (**27**)

Polarization F_{SB}

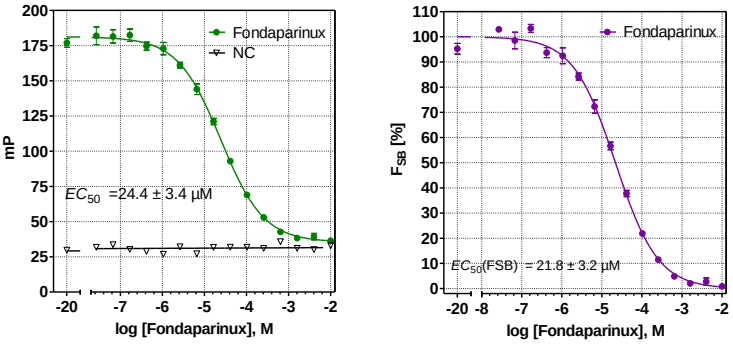

Assay conditions: interleukin-10 final assay concentration c = 3.3 µM, NC = negative control.

Competition assay: bone morphogenetic protein 2 + 9s-HA-4-5(6)-TAMRA (**15**) versus Fondaparinux (**27**)

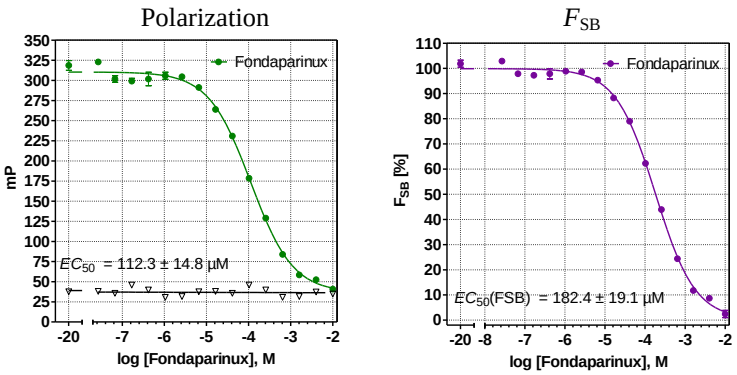

Assay conditions: BMP-2 final assay concentration c = 92 nM, NC = negative control.

Competition assay: sclerostin + 13s-HA-6-5(6)-TAMRA (**19**) versus Fondaparinux (**27**)

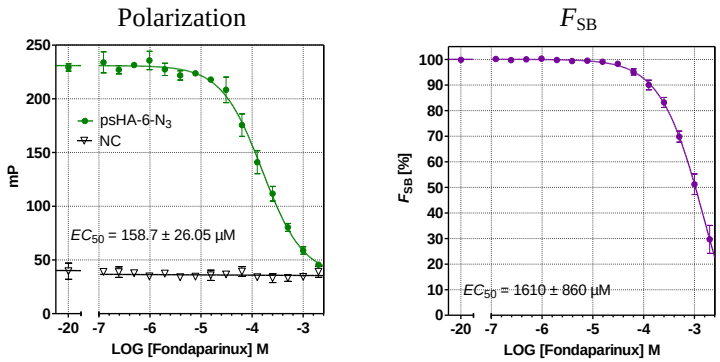

Assay conditions: sclerostin final assay concentration c = 31 nM, NC = negative control

7. Isothermal Titration Calorimetry

Titrations with 9s-HA-4-N_3 and (9s-HA-4-S-PEG-S-)$_2$ were carried out using a MicroCal iTC200 calorimeter (Microcal) at 25 °C, titrations with 9s-HA-4-TAMRA were measured on Microcal PEAQ-ITC. IL-8 was dissolved in Phosphate buffer without DTT to reduce noise before measurements. The synthesized oligosacharides were resolubilized in the same buffer to ensure a reasonable baseline. The titration of IL-8 with 9s-HA-4-TAMRA was carried out with 5 wt-% Glycerol in Phosphate buffer. The ITC titration and FP assay of IL8 vs. 9s-HA-4-N_3 in the presence of 5 wt-% glycerol showed no significant influence on binding. Concentrations for each component in each experiment are listed in the table below. For each titration 19 to 25 injections of 1.5 and 1 µl respectively of titrant were made at 180 s intervals, while stirring at 750 r.p.m. Raw data were integrated, normalized and the titration curve fitted using MicroCal PEAQ-ITC analysis software provided by Microcal.

ITC measurements with IL-8

STable 1: data of the ITC measurement for IL-8 and the sulfated oligohyaluronans **25**, **20**, **15**

Compound	$c_{protein}$ [µM]	c_{ligand} [µM]	N[a]	ΔH [kcal·M^{-1}]	-TΔS [kcal·M^{-1}]	K_D [nM]	$\bar{x}(K_D)$[b] [nM]
9s-HA-4-N_3(25)	10	50	0.388	-45.3	2.58	33.7 ± 10.4	34 ± 10
			0.314	-50.0	7.19	32.0 ± 8.88	
			0.403	-42.0	-0.42	36.8 ± 12.1	
(9s-HA-4-S-PEG-S-)$_2$(20)	10	50	0.197	-106.0	62.2	18.8 ± 15.4	16 ± 10
			0.199	-131.0	84.6	7.37 ± 5.54	
			0.202	-102.0	57.6	20.4 ± 8.88	
9s-HA-4-TAMRA (15)	10	100	0.387	-59.8	13.3	7.36 ± 4.23	9 ± 4
			0.463	-52.2	5.80	7.65 ± 4.00	
			0.420	-56.8	11.5	11.60 ± 4.59	

[a]molar binding ratio of the ligan protein interaction (observed stoichiometry)[b]mean value of the calculated K_D values.

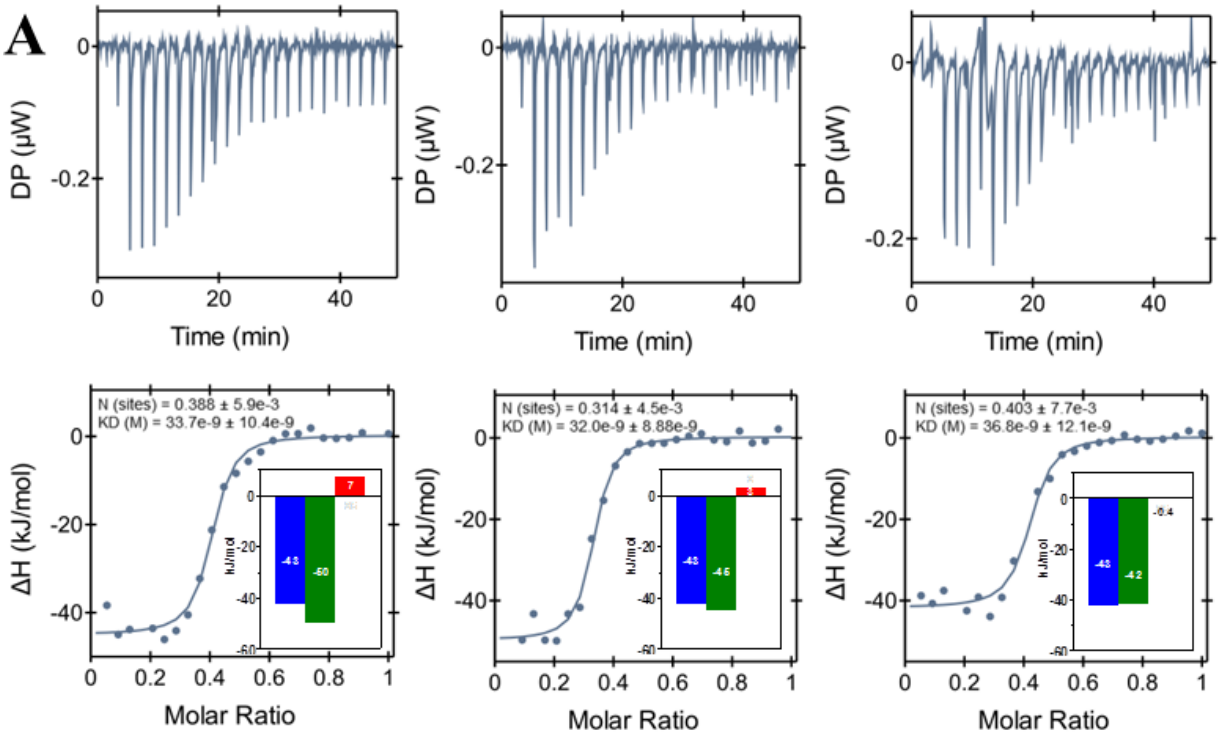

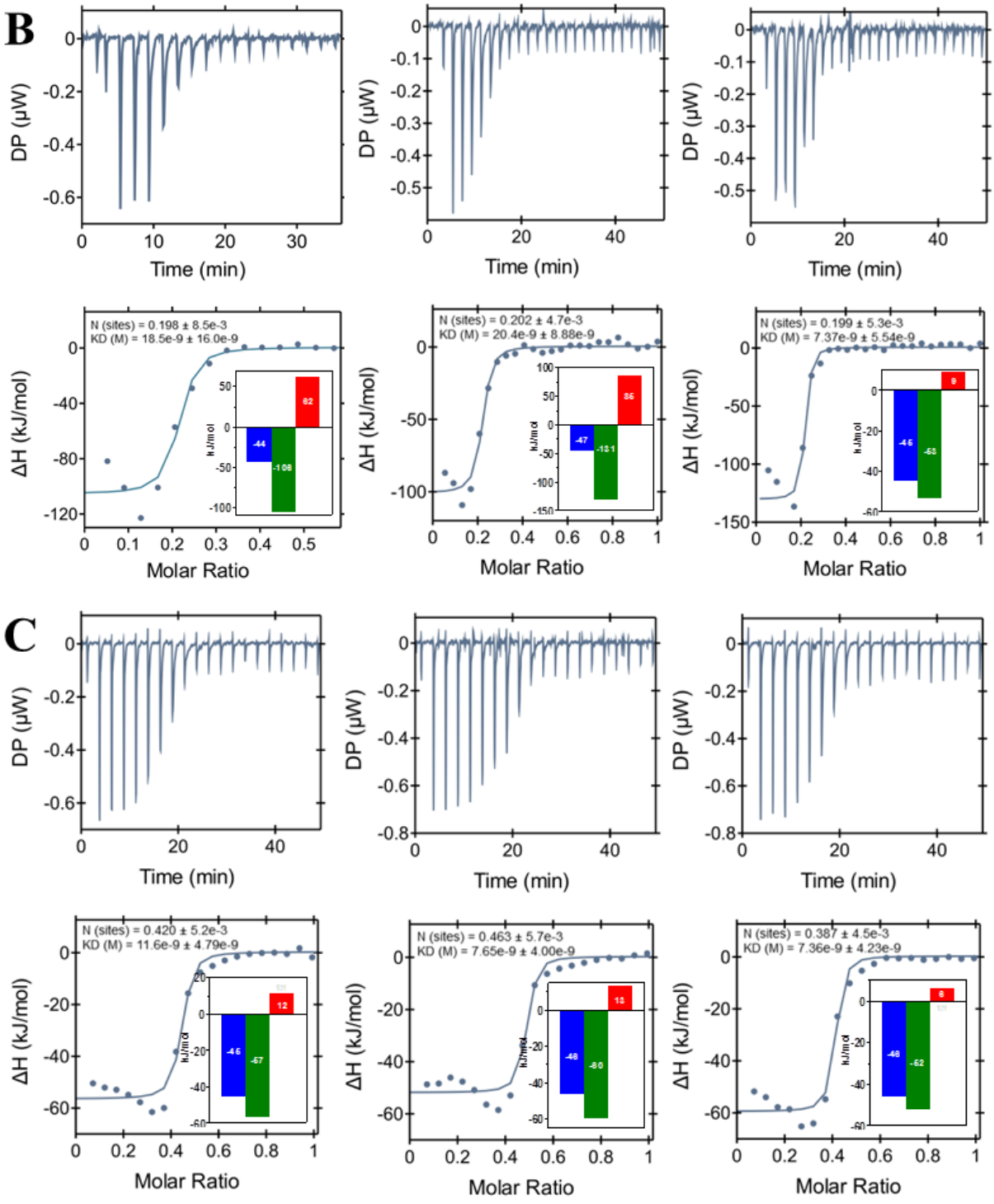

SScheme 2: Isothermal titration calorimetry data of a 50 µM solution of A) 9s-HA-4-N_3 (**25**) and B) (9s-HA-4-S-PEG-S-)$_2$ (**20**) and a 100 µM solution of C) 9s-HA-4-TAMRA (**15**) titrated to IL-8 (10 µM) yielded a dissociation constant K_D of 34 nM, 14 and 9 nM, respectively, in three independent experiments

ΔG
ΔH
-TΔS

ITC measurements with IL-10

STable 2: data of the ITC measurement for IL-10 and the sulfated oligohyaluronans **25**, **20**, **15**

Compound	$c_{protein}$ [µM]	c_{ligand} [µM]	N[a]	ΔH [kcal·M^{-1}]	-TΔS [kcal·M^{-1}]	K_D [µM]	$\bar{x}(K_D)$[b] [µM]
9s-HA-4-N$_3$ (25)	10	40	0.212	-40.9	7.77	1.58 ± 0.168	1.56 ± 0.19
			0.217	-39.7	6.56	1.55 ± 0.217	
(9s-HA-4-S-PEG-S-)$_2$ (20)	10	100	0.213	-57.4	23.5	1.16 ± 0.28	1.38 ± 0.41
			0.215	-61.3	28.1	1.57 ± 0.35	
	20		0.235	-48.9	15.5	1.41 ± 0.6	
9s-HA-4-TAMRA (15)	10	100	0.340	-52.1	15.7	0.415 ± 0.105	0.656 ± 0.450
			0.263	-68.9	33.8	0.699 ± 0.142	
			0.338	-32.7	-1.93	0853 ± 0.203	

[a]molar binding ratio of the ligand protein interaction (observed stoichiometry)[b]mean value of the calculated K_D values.

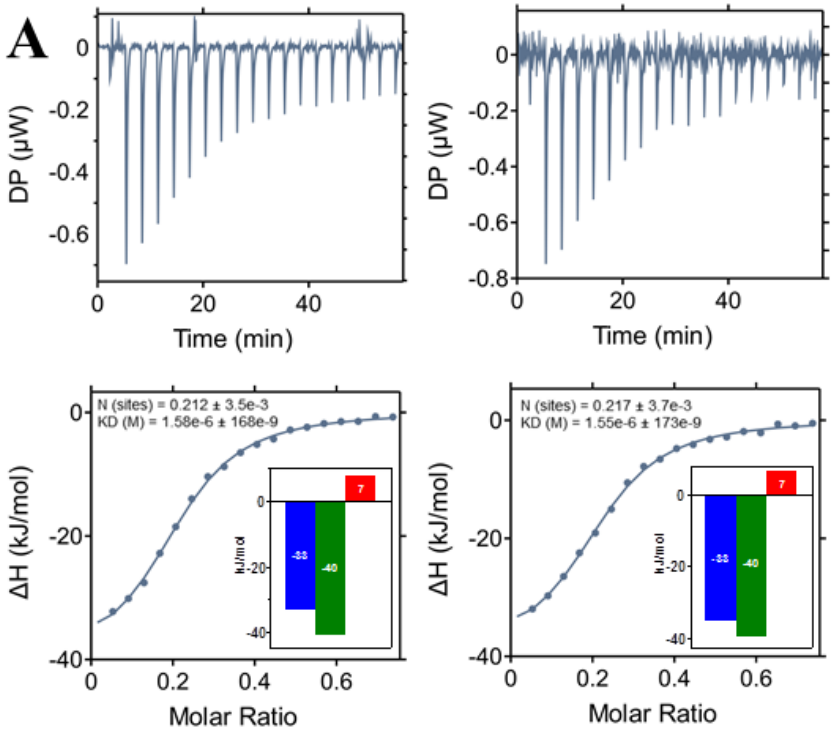

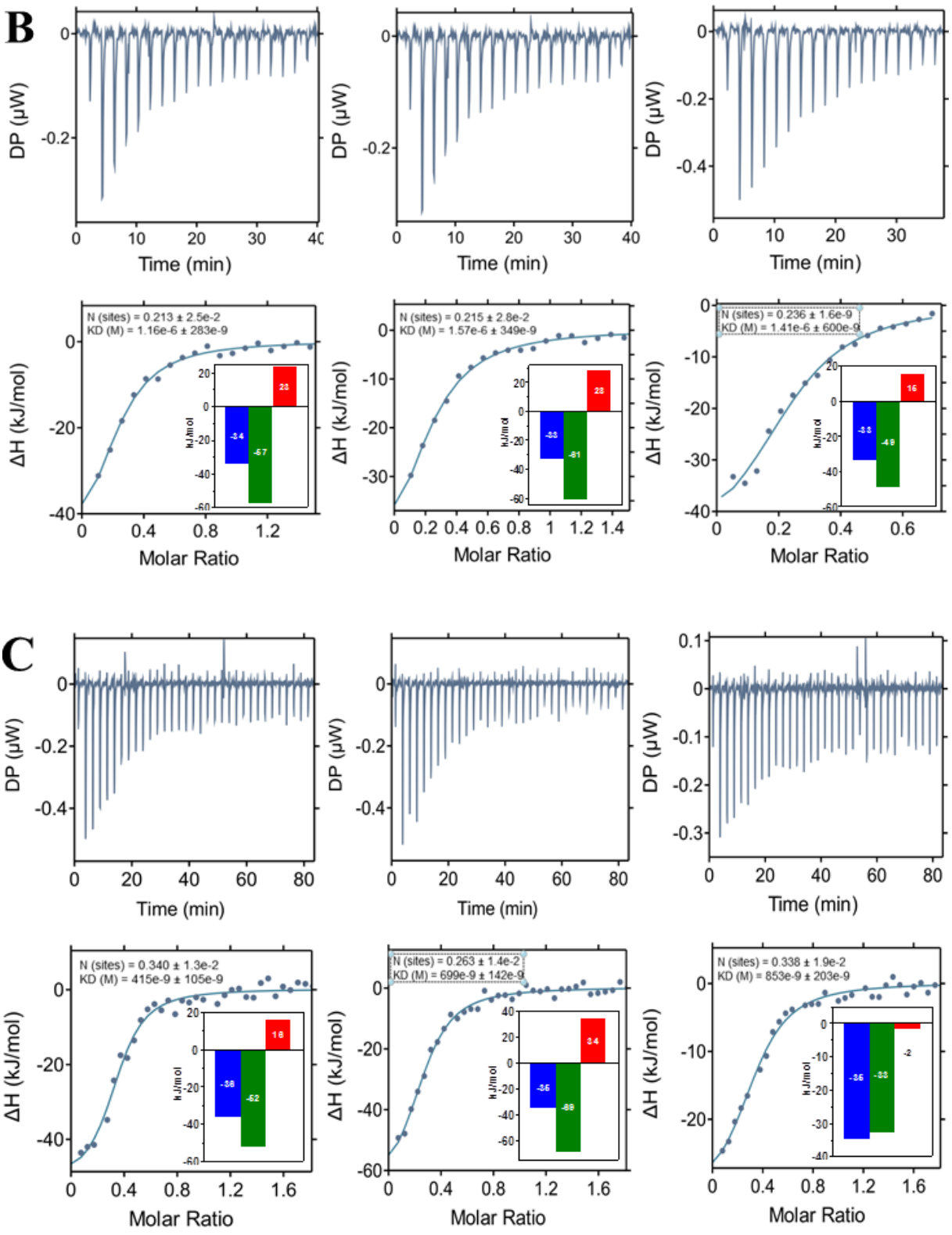

SScheme 3: Isothermal titration calorimetry data of a 100 µM solution of A) 9s-HA-4-N_3 (25) and B) (9s-HA-4-S-PEG-S-)$_2$ (20) and a 100 µM solution of C) 9s-HA-4-TAMRA (15) titrated to IL-10 (40, 10-20, and 10 µM) yielded a dissociation constant K_D of 1.56, 1.38 and 0.656 µM, respectively, in three independent experiments

ΔG
ΔH
-TΔS

8. Molecular Modeling

Molecular Docking

Sulfated hyaluronan derivatives **15-16**, **19**, **21-23**, **25-26** and truncated half moiety of **20** (psHA-4-S-PEG-SMe) were modelled using AMBER 14[10] and MOE.[11] For the bivalent compound **20**, due to the restriction on maximal number of rotatable bonds that can be taken into account in docking studies, only half a molecule (*i.e.* 9s-HA-4-S-PEG-SMe) was used at first. Charges were taken from the GLYCAM 06-j force field[12] for the different GAG units and from the literature for sulfate groups.[13] AM1-BCC charges were applied for the azide group.[14] RESP atomic charges[15] were derived at the HF/6-31G(d) calculation level for the triazole and sulfo ethylene glycol fragments and at the B3LYP/6-311G++(d,p) level for the TAMRA group using Gaussian09.[16] Crystal and NMR structures of IL-8 as monomer (PDB ID 3IL8, 2.0 Å)[17] and dimer (PDB ID 1IL8),[18] IL-10 (PDB 2ILK, 1.6 Å),[19] BMP-2 (PDB ID 2H62, 1.8 Å)[20] with the N-termini conformation as previously modeled[21] and sclerostin (PDB ID 2K8P, models 1, 10 and 16 from NMR ensemble)[22] were used.

Blind docking was used in order to predict potential GAG recognition sites on the full surface of the target protein. Docking studies of functionalized GAG with protein targets was carried out with Autodock 3.[23] Autogrid3 was used to calculate the atomic potential of each protein structure with a spacing grid of 0.375Å for IL-8 monomer, 0.475 Å for IL-8 dimer, 0.475 Å for IL-10, 0.650 Å for BMP-2 and 0.700 Å for Sclerostin. Functionalized GAGs were treated completely flexible whereas the protein targets were treated rigid. The Lamarckian genetic algorithm with an initial population size of 300 and a termination condition of 10000 generations and 9995 x 10^5 energy evaluations was used. 1000 independent runs were carried out. Spatial clustering of the top 50 docking solutions was performed with the DBSCAN algorithm.[24]

Complex refinement by Molecular Dynamics (MD) simulations

The complexes obtained from the docking studies were further refined by Molecular Dynamics (MD) simulations in AMBER14.[10] For those complexes involving IL-8 dimer and two half moieties of **20** with their SPEGS close enough in the 3-dimensional space, a disulfide bond was created to reconstruct the bivalent compound **20**. The resulting bivalent molecule was minimized in MOE using the AMBER12-EHT force field and default parameters prior to MD simulations. Charges were taken from the GLYCAM 06-j force field[12] for the different sulfated hyaluronan units and from the literature for sulfate groups[13]. AMM1-BCC charges were used for the azide group.[14] RESP atomic charges[15] were derived at the HF/6-31G(d) calculation level for the triazole and sulfo ethylene glycol fragments, and at the B3LYP/6-311G++(d,p) level for the TAMRA group using Gaussian09.[16] Parameters were taken from the GLYCAM-06j[12] for the GAG part and ff14SB force field[10] for each protein target. Missing parameters of the azide, triazole, TAMRA and sulfo ethylene glycol groups were taken from the General Amber Force Field (GAFF)[25] and literature.[26] Each GAG/protein complex was solvated in a truncated octahedral box of TIP3P water molecules and neutralized with Na^+ or Cl^- counterions. MD simulations were preceded by two energy-minimization steps: i) only the solvent and ions were relaxed with position restraints for the solute (500 kcal/mol·$Å^2$) using 1000 steps of steepest descendent minimization followed by 500 steps of conjugate gradient minimization; ii) the entire system was minimazed without restraints applying 3000 cycles of steepest descendent and 3000 steps of conjugate gradient equilibration. Then the system was heated up from 200 K to 300 K in 20 ps with weak position restraints (10 kcal/mol·$Å^2$). Langevin temperature coupling with a collision frequency γ = 1 ps^{-1} was used at this step. The system was equilibrated under constant pressure of 1 atm using periodic boundary conditions (NPT conditions) at 300 K for 500 ps. A

total of 100 ns MD production was carried out at 300 K NPT conditions. In the case of IL-8, due to lack of structure at the C-terminal α-helix previously observed in unrestrained MD simulations,[1] weak position restraints (10 kcal/mol·Å^2) were applied to the residues 68-77 during MD equilibration and production times. The SHAKE algorithm was used to constrain all bonds involving hydrogen atoms. A time step of 2 fs per step was used during SHAKE algorithm. A cutoff of 8 Å was applied to treat the nonbonded interactions, and the Particle Mesh Ewald (PME) method was used to treat long-range electrostatic interactions. MD trajectories were recorded every 10 ps. For GAGs, pyranose rings were harmonically restrained. Trajectories were visualized with VMD[27] and evaluated in terms of intermolecular H-bonds by using the CPPTRAJ module implemented in AMBER. The criterion used to consider a dynamic hydrogen bond formation was to be found at least 10% of the total simulation time. Energy decomposition per residue and pairwise as well as binding free energy post-processing analysis of 200 frames distributed along the MD productions were performed in implicit solvent using the MM-GBSA method[28] as implemented in AMBER14. Data analysis was carried out with the R-package.[29] Figures were created with PyMOL.[30]

Discussion S1

IL-10: Molecular docking and MD simulations of the sHA derivatives with IL-10 indicated that residues R104, R106, R107 and K119 play a key role for GAG recognition.[31] The calculated binding energies of the TAMRA-labeled sHA (**15**, **19**) increased compared to the azides (**25, 26**) (STables 10-11). TheTAMRA analogs were able to establish contacts with both monomer units of the cytokine. With respect to the length of GAG and in agreement with the experimental observations, a small increase in binding was observed for the hexahyaluronans (**19**, **26**) in comparison to the tetrahyaluronans (**15**, **25**), which was attributed to more favorable interactions with IL-10 residues R102, R104, R107 and K117 (SFigure 12).

BMP-2: In the BMP-2 dimer structure, the N-termini, which are crucial for GAG and receptor recognition,[32] were modeled in α-helical conformation.[21] The resulting structure was used to explore the binding of derivatives **15**, **19**, **21-23** and **25-26**. These molecules were predicted to bind at the N-termini in two different modes: in parallel and/or perpendicular orientation (STable 12 and SFigure 13A). The low sulfated azide analogs 2s-HA-4-N_3 **21** and 5s-HA-4-N_3 **22** did not show any preference for any of these two binding modes in terms of energy, while for the high sulfated derivatives 7s-HA-4-N_3 **23** and 9s-HA-4-N_3 **25** the parallel orientation was energetically favored. The same holds true for the binding poses computed for the 9s-HA-4-TAMRA **15**, which from all tetra-derivatives was the one establishing the highest number of interactions with the protein (STable 12). Furthermore, pairwise energy decomposition calculations and H-bond analysis indicated that the TAMRA moiety was implicated in additional electrostatic interactions with residue R9 of one BMP-2 monomer (STable 13, SFigure 13B). All these interactions are responsible for the 30-fold increase in binding obtained experimentally for **15** compared to **25**. Elongation of these molecules by one disaccharide unit resulted in a parallel-to-perpendicular molecular reorientation of compounds **26** and **19** (SFigure 13C). The two most energetically favorable binding poses of the 13s-HA-6-TAMRA **19** were oriented both non-reducing to the reducing end, and *vice versa*. These two orientations can be taken as equivalent considering BMP-2 dimer symmetry. The TAMRA moiety appeared either establishing interactions with the BMP-2 N-terminus or exposed to the solvent (STables 12-13). The binding free energies obtained for derivatives **15**, **19**, **21-23** and **25-26** suggested an increase in binding with the degree of sulfation, which is in accordance with our experimental results (Tables 1 and 3 in main text of the manuscript, SFigure 14). The computed values showed increase in

binding of the hexahyaluronan azide vs. its tetra-analog, while binding for both TAMRA derivatives was in the same range, which correlates very well with the differences in binding found experimentally (SFigure 14).

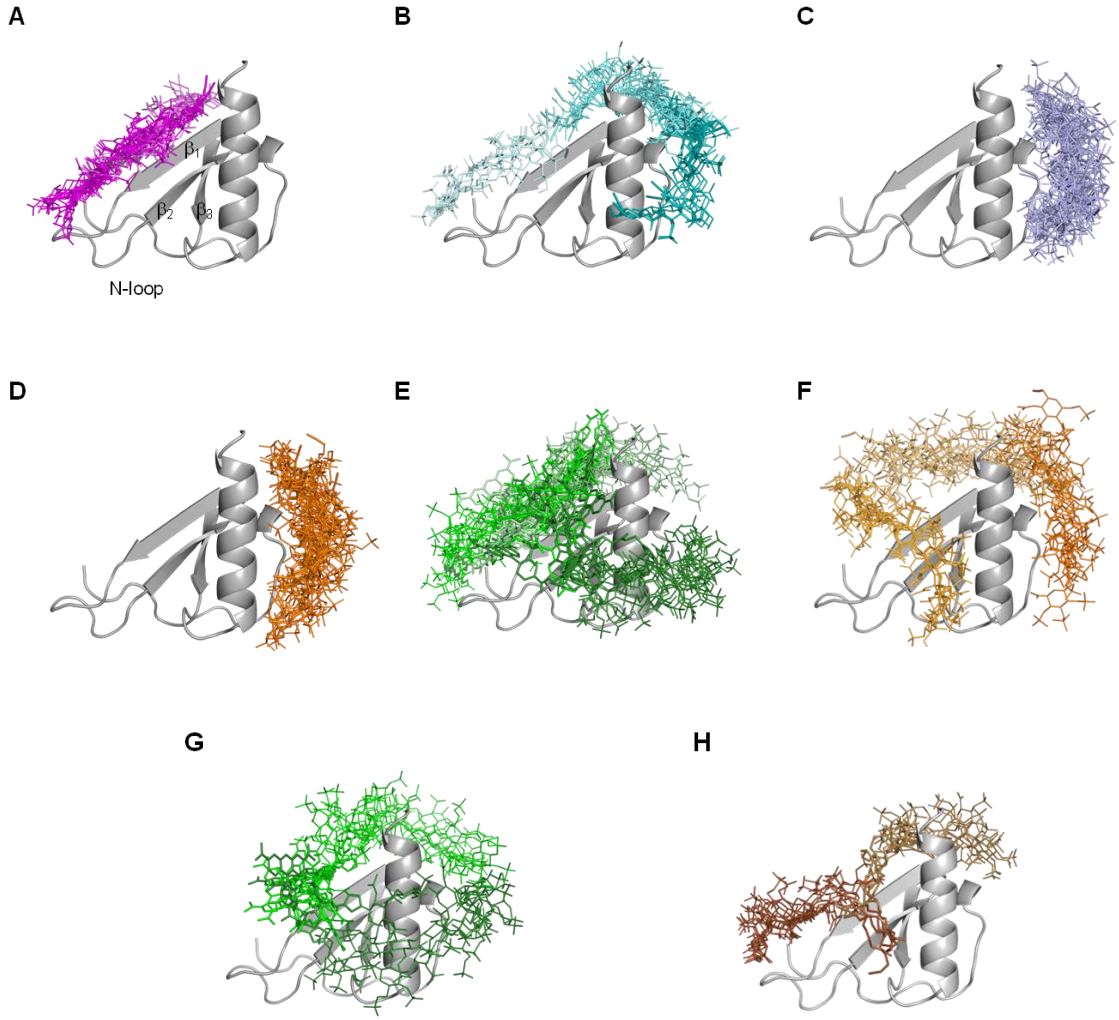

SFigure 1. Molecular modelling of IL-8 monomer interaction with sHA derivatives. Docking results using Autodock 3 and DBSCAN clustering for sHA derivatives (A) **21**, (B) **22**, (C) **23**, (D) **25**, (E) **15**, (F) **26**, (G) **19** and (H) **20** (half molecule**)**. IL-8 is shown in gray cartoon. Different clusters of sHA derivatives are shown in sticks with gradient colors: pink for **21**, cyan for **22**, violet for **23**, orange for **25**, green for **15**, orange for **26**, green for **19** and brown for **20** as 9s-HA-4-S-PEG-SMe.

STable 3. MM-GBSA binding free energies and interacting residues determined by per-residue energy decomposition and H-bond analysis for sHA **15**, **19**-**23** and **25**-**26** in complex with IL-8 monomer.

sHA derivative	IL-8 recognition region / non reducing to reducing end orientation	IL-8 interacting residues	ΔG (kcal/mol)[a]
21 (cluster1)	β_1 strand / antiparallel	L10, R11, Q13, R31	-19.9 ± 2.5
21 (cluster2)	β_1 strand / parallel	R11, R31, V32, I33, R73	-21.8 ± 5.0
22 (cluster1)	C-terminal α-helix / β_1 strand and 3_{10}-turn N-loop[b]	H23, K25, K28, R65, K69, K72, R73	-24.9 ± 6.3
22 (cluster2)	C-terminal α-helix / parallel	H23, K25, R65, K69, K72, R73	-31.6 ± 4.7
22 (cluster3)	β_1 strand / antiparallel	L10, R11, K16, R31, V32, K47, R52	-24.3 ± 7.5
23 (cluster1)	C-terminal α-helix / antiparallel	K25, R65, K69, K72, R73	-41.0 ± 4.7
23 (cluster2)	C-terminal α-helix / parallel	K25, R65, K69, K72, R73	-36.2 ± 7.8
25 (cluster1)	C-terminal α-helix / antiparallel	H23, K25, R65, K69, K72, R73	-45.6 ± 3.2
25 (cluster2)	C-terminal α-helix / parallel	H23, K25, R65, K69, K72, R73	-38.4 ± 5.2
15 (cluster1)	C-terminal α-helix / β_1 strand[b]	H23, K25, T42, K59, N61, Q64, R65, K69, K72, R73	-51.4 ± 5.5
15 (cluster2)	N-loop, β_1 strand / antiparallel	L10, R11, Q13, K28, R31, V32	-40.6 ± 14.2
15 (cluster3)	C-terminal α-helix / $\beta_{1\text{-}2}$ strands[b]	Q13, K25, K28, R31, I33, K47, S49, R73	-38.0 ± 11.7
26 (cluster 1)	β_1 strand and 3_{10}-turn N-loop[b] / β_1 strand[b]	H23, K25, K28, R31, K69, K72, R73	-31.6 ± 10.1
26 (cluster 2)	C-terminal α-helix / antiparallel	K20, H23, K25, R65, K69, K72, R73	-45.2 ± 3.1
19 (cluster1)	C-terminal α-helix / β_1 strand[b]	K25, K28, L30, R31, V32, R65, K69, R72, R73	-44.6 ± 6.5
19 (cluster2)	C-terminal α-helix / β_1 strand[b]	H23, K25, R31, K59, N61, R65, K69, K72, R73	-49.6 ± 1.9
20 (cluster1)[c]	N-loop / β_1 strand[b]	L10, R11, R31, V32	-33.7 ± 6.0
20 (cluster2)[c]	C-terminal α-helix / β_1 strand[b]	K25, K28, K69, F70, K72, R73	-37.8 ± 4.4

[a]Values represent the mean ± SD from independent 100 ns MD simulations (up to 9 per cluster depending on number of binding poses obtained in the docking studies). [b]Reducing end location. [c] 9s-HA-4-S-PEG-SMe was considered as half moiety for **20**.

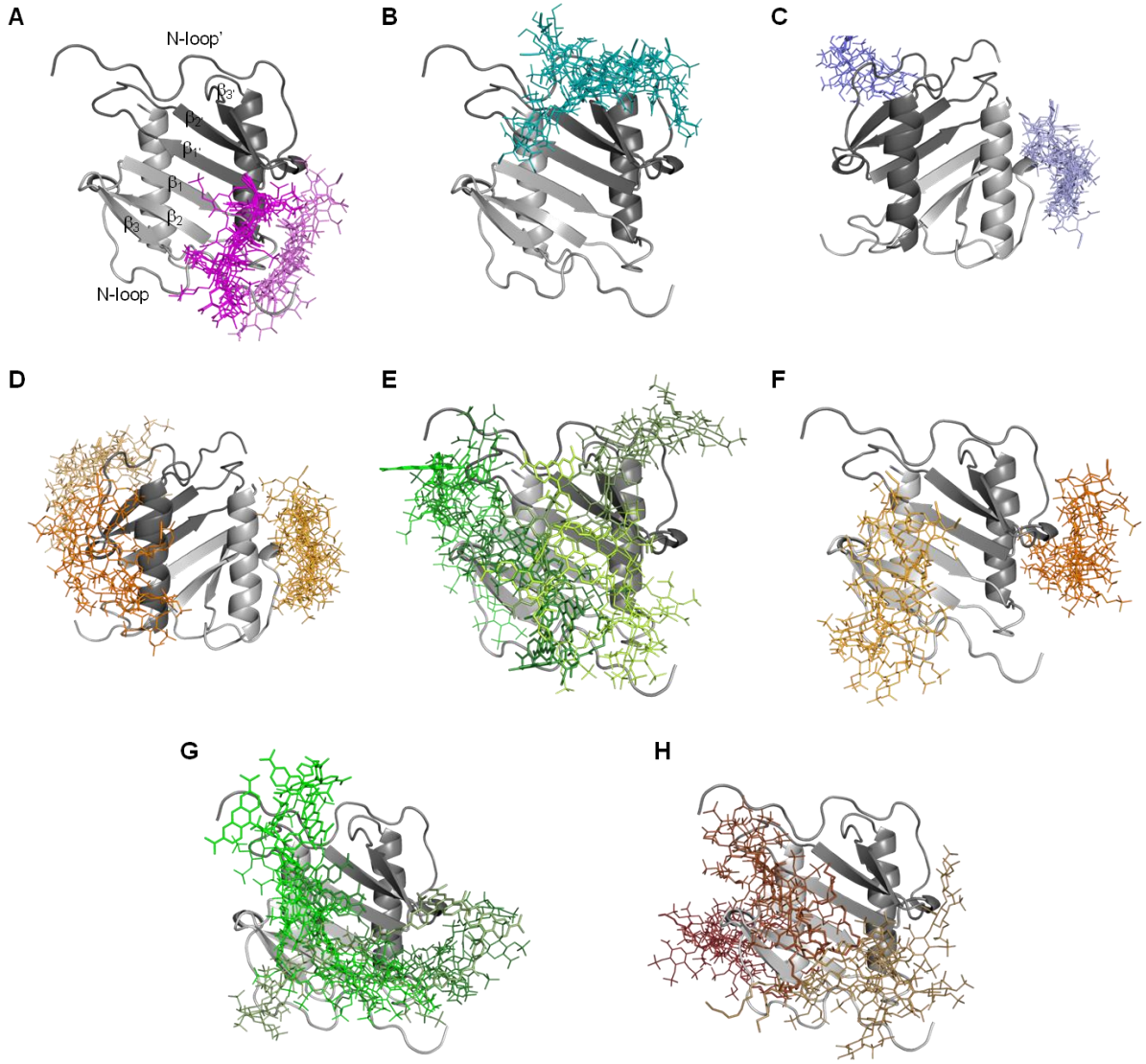

SFigure 2. Molecular modelling of IL-8 dimer interaction with sHA derivatives. Docking results using Autodock 3 and DBSCAN clustering for sHA derivatives (A) **21**, (B) **22**, (C) **23**, (D) **25**, (E) **15**, (F) **26**, (G) **19** and (H) **20 (**half molecule). IL-8 dimer is shown in gray cartoon (light and dark representing each monomer). Different clusters of sHA derivatives are shown in sticks with gradient colors: pink for **21**, cyan for **22**, violet for **23**, orange for **25** and **26**, green for **15** and **19** and, brown for **20**.

STable 4. MM-GBSA binding free energies and interacting residues determined by per-residue energy decomposition and H-bond analysis for sHA **15**, **19**-**23** and **25**-**26** in complex with IL-8 dimer.

sHA derivative	IL-8 recognition site[a]	IL-8 interacting residues[a]	$\Delta G_{IL\text{-}8dimer/sHA}$ (kcal/mol)[b]	$\Delta G_{IL8monomer\text{-}sHA/IL8monomer'}$ (kcal/mol)[b,c]
21 (cluster1)	β_1 strand[d], N-loop'	K28, A7', K8', E9', R11', Q13', K16', R31'	-33.4 ± 4.7	n.d.
21 (cluster2)	β_1-strand, N-loop'	K28, S49, K8', R11'	-26.4 ± 1.8	n.d.
22 (cluster)	N-loop[d], $\beta_{1,3'}$-strands	A7', K8', R11', Q13', K16', Y18', S19', K20', R52', A7, K8, R11, R31	-34.1 ± 6.4	n.d.
23 (cluster1)	C-terminal α-helix, 3_{10}-turn N-loop	H23, K25, R65, K69, K72, R73	-27.9 ± 4.0	n.d.
23 (cluster2)	N-loop', $\beta_{3'}$-strand	A7', K8', R11', Q13', K16', K20', R52', E53', L54'	-50.4 ± 5.7	n.d.
25 (cluster1)	C-terminal α-helix, 3_{10}-turn N-loop	K20, H23, K25, R65, K69, K72, R73	-38.0 ± 6.6	-65.9 ± 8.9
25 (cluster2)	C-terminal α-helix', 3_{10}-turn N-loop'	H23', K25', K28', R65', K69', K72', R73', N76'	-42.9 ± 5.6	-107.2 ± 5.3
25 (cluster3)	N-loop', $\beta_{3'}$-strand	A7', K8', R11', K16', Y18', K20', R52'	-38.4 ± 4.2	-101.6 ± 25.1
15 (cluster1)	N-loop[d], $\beta_{1\text{-}3}$-strands[d]	A7, K8, R11, Q13, R31, K47, A7', K8', R11', Q13', I15', R31', K47', R52'	-72.5 ± 4.8	-100.8 ± 16.8
15 (cluster2)	$\beta_{1\text{-}3}$-strands, N-loop', $\beta_{1'}$-strand	R31, K47, R52, A7', K8', R11', Q13', I15', K16', R31'	-58.1 ± 6.8	-79.3 ± 5.5
15 (cluster3)	N-loop[d], $\beta_{3'}$-strand	R11', I15', K16', Y18', S19', K20', R52', A7, K8	-51.2 ± 13.1	-108.1 ± 11.2
15 (cluster4)	C-terminal α-helix, 3_{10}-turn/N-loop	K20, H23, K25, K28, R65, K69, K72, R73	-44.5 ± 9.1	-68.7 ± 9.1
26 (cluster1)	N-loop[d], $\beta_{1\text{-}3}$-strands, $\beta_{1'}$-strand	A7, K8, E9, R11, K16, Y18, K20, R31, K47, R52, A7', K8', E9', R31'	-59.8 ± 5.5	-100.5 ± 11.7
26 (cluster2)	N-loop, C-terminal α-helix', 3_{10}-turn/N-loop'	A7, K8, H23', K25', K28', S49', R65', K69', K72', R73', N76'	-61.5 ± 7.0	-63.2 ± 1.6
19 (cluster1)	N-loop[d], $\beta_{1\text{-}3}$-strands, $\beta_{1'}$-strand	A7, K8, R11, Q13, R31, K47, R52, A7', K8', E9', R11', Q13', R31', K47'	-69.5 ± 8.2	-94.3 ± 8.1
19 (cluster2)	N-loop[d], $\beta_{1\text{-}2}$-strands[d]	A7, K8, E9, R11, R31, K47,	-70.2 ± 7.9	-96.9 ± 11.4

		K8', K25',K28', R31', K47'		
19 (cluster3)	N-loop[d], β_{1-3}-strands[d]	A7, K8, R11, K16, K20, R31, K47, R52, A7', K8', R31', K47', R52'	-85.1 ± 20.0	-118.7 ± 16.0
20 (cluster1)[e]	C-terminal α-helix	H23, K25, R65, K69, K72, R73	-42.6 ± 6.7	-102.4 ± 6.7
20 (cluster2)[e]	N-loop[d], β_{1-2}-strands[d]	A7, K8, R11, R31, K47, A7', K8', R11', R31', K47'	-68.3 ± 8.2	-94.7 ± 9.1
20 (cluster3)[e]	N-loop[d], β_{1-2}-strands[d]	A7', K8', R11', K47', R52'	-48.3 ± 8.5	-96.6 ± 15.4
20[f]	N-loop[d], β_{1-3}-strands[d]	A7, K8, E9, R11, Q13, I15, K16, K28, R31, K47, R52, A7', K8', R11', K28', R31', K47'	-87.1 ± 7.1	-119.1 ± 10.6

[a]Monomer units are distinguished by a comma. [b]Values represent the mean ± SD from independent 100 ns MD simulations (up to 10 per cluster depending on number of binding poses obtained in the docking studies). [c]Computed $\Delta G_{IL8monomer/IL8monomer'}$ = -68.4 ± 10.8 kcal/mol from 100 ns MD simulation on IL-8_{dimer} NMR structure. [d]Both IL-8 monomers. [e] 9s-HA-4-S-PEG-SMe was considered as half moiety of **20**. [f]Reconstruction of bivalent compound **20**.

STable 5. TAMRA/IL-8 and SPEGS/IL-8 pairwise interacting residues determined by MM-GBSA for the best ranked clusters.

sHA derivatives	IL-$8_{monomer}$
15 (cluster1)	T42, Q64, R65
19 (cluster2)	R31, K59
20 (cluster2)	V32

sHA derivatives	IL-8_{dimer}
15 (cluster1)	R11, K8', R11', Q13', I15'
19 (cluster3)	R52'
20 (cluster2)	K47'
20	R11, Q13

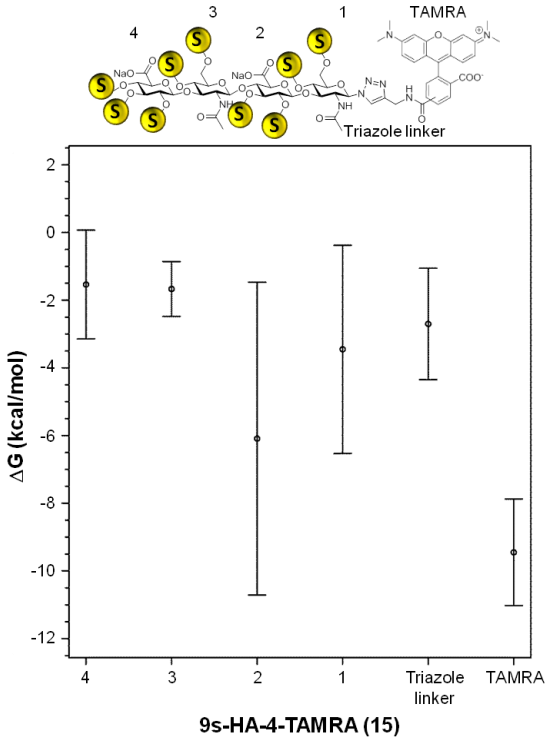

SFigure 3. Per-residue binding energy contribution calculated with MM-GBSA from independent 100 ns MD simulations of TAMRA derivative **15** in complex with IL-8 dimer (cluster 1). The errors bars represent the standard error of the mean.

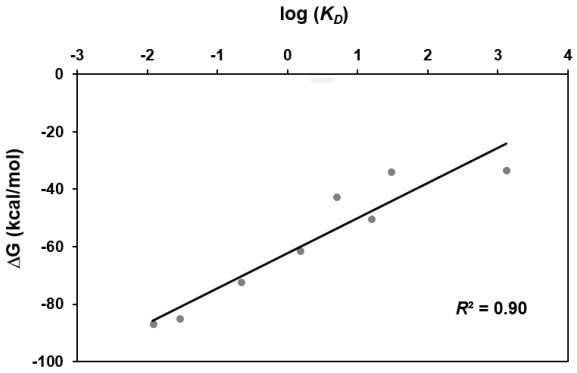

SFigure 4. Correlation between predicted binding energies (ΔG) calculated with MM-GBSA and experimental K_D binding data obtained from FP assays for IL-8. Plot of log(K_D) vs. ΔG using the most favorable calculated binding free energies (STable 4) from independent 100 ns MD simulations of IL-8 dimer in complex with defined sulfated hyaluronans **15**, **19**, **20-23** and **25-26**. The obtained coefficient of determination R^2 is shown in each plot.

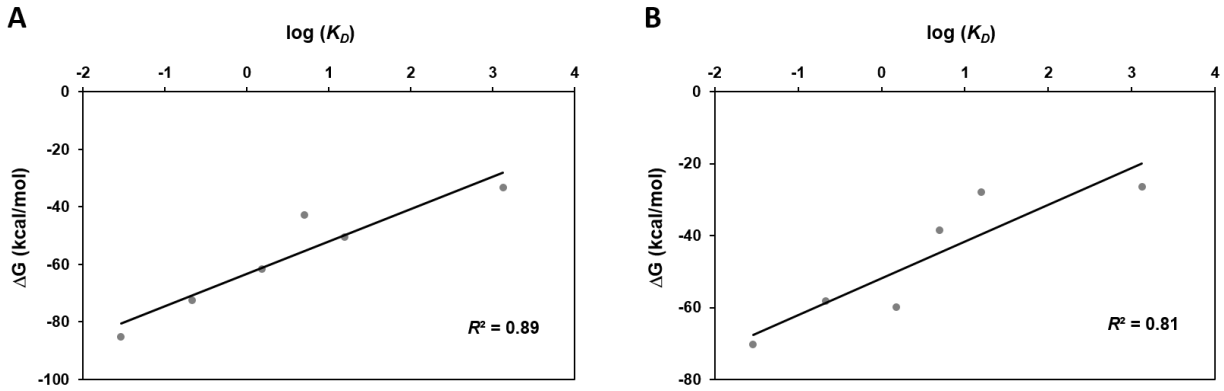

SFigure 5. Correlation between predicted binding energies (ΔG) calculated with MM-GBSA and experimental K_D binding data obtained from FP assays for IL-8. Plots of log(K_D) vs. ΔG calculated binding free energies from independent 100 ns MD simulations of IL-8 dimer in complex with defined sulfated hyaluronans **15**, **19**, **21**, **23** and **25-26** involved in (A) the first and (B) the second most favorable predicted binding sites according to STable 4. The obtained coefficient of determination R^2 is shown in each plot.

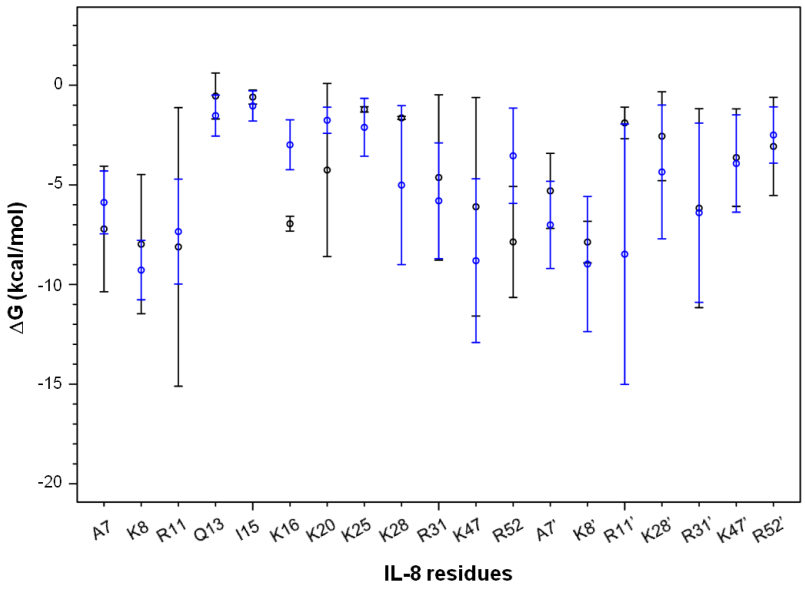

SFigure 6. Per-residue binding energy contribution calculated with MM-GBSA from independent 100 ns MD simulations of IL-8 dimer in complex with TAMRA derivative **19** (black) and the bivalent compound **20** (blue). The errors bars represent the standard error of the mean.

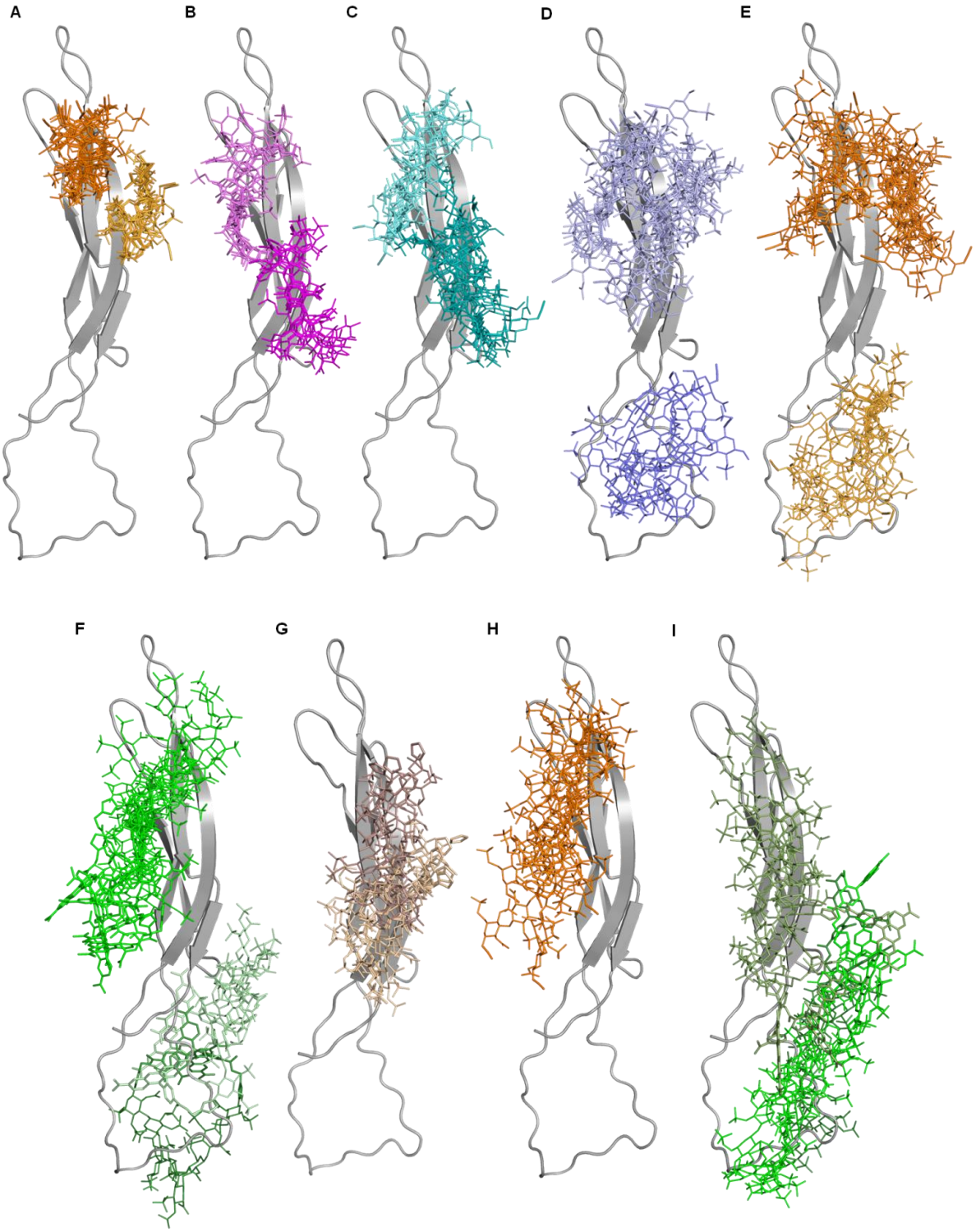

SFigure 7. Molecular modelling of sclerostin interaction with sHA derivatives. Docking results using Autodock 3 and DBSCAN clustering for sHA derivatives (A) **24**, (B) **21**, (C) **22**, (D) **23**, (E) **25**, (F) **15**, (G) **16**, (H) **26** and (I) **19**. Lowest energy structure from the NMR ensemble of sclerostin (model 1) is shown in gray cartoon. Different clusters of sHA derivatives are shown in sticks with gradient colors: pink for **21**, cyan for **22**, violet for **23**, orange for **24**, **25** and **26**, green for **15** and **19** and, brown for **16**.

STable 6. MM-GBSA binding free energies and interacting residues determined by per-residue energy decomposition and H-bond analysis for sHA **15-16** and **19**, **21-26** in complex with Sclerostin (model1).

sHA derivative	Sclerostin recognition site	ΔG (kcal/mol)[a]
24 (cluster1)	R119, R131, R133, K134, R136	-50.6 ± 5.4
24 (cluster2)	R114, A117, R119, R133, K134, R136	-48.8 ± 2.8
21 (cluster1)	R114, Y115, R136, K144	-33.5 ± 5.9
21 (cluster2)	R63, R119, R133, K134, R136	-45.3 ± 4.2
22 (cluster1)	R63, R114, R119, R133, K134, R136	-49.7 ± 5.7
22 (cluster2)	R114, K134, R136, K142, R145, R148	-55.7 ± 10.5
23 (cluster1)	R114, R116, R119, R133, K134, R136	-58.4 ± 8.4
23 (cluster2)	R89, R97, R102, K144, R145, R148	-78.1 ± 7.5
25 (cluster1)	R114, R116, R119, K134, R136	-70.0 ± 5.0
25 (cluster2)	R89, R97, K99, W100, R102, K142, K144, R145, R148	-102.3 ± 10.0
15 (cluster1)	R109, R114, R119, R131, R133, K134, R136, R148	-80.7 ± 6.1
15 (cluster2)	Y54, G86, P87, A88, L90, L91, I95, R97, K99, W100, R102, R109, R114, R136, K142, K144, R145, R148	-102.5 ± 3.7
15 (cluster3)	Y54, P87, A88, R89, R97, K99, R102	-85.0 ± 6.1
16 (cluster1)	R114, R116, R119, K134, R136, K142, K144	-70.7 ± 9.0
16 (cluster2)	R114, R116, A117, R119, R133, K134, R136	-74.1 ± 6.6
26 (cluster)	R114, R119, R131, R133, K134, R136, K142, K144	-104.6 ± 13.2
19 (cluster1)	R57, R89, L91, R97, K99, W101, R102, R114, R116, K142, K144, R145, R148	-127.0 ± 9.2
19 (cluster2)	S52, R57, C85, G86, P87, A88, R89, L90, R97, K99, R102, R114, K142, K144, R145, R148	-95.0 ± 7.3
19 (cluster3)	R89, R102, R109, R114, Y115, R116, R119, R133, K134, R136, K142, K144, R145, T147, R148	-124.3 ± 12.9

[a]Values represent the mean ± SD from independent 100 ns MD simulations (up to 10 per cluster depending on number of binding poses obtained in the docking studies).

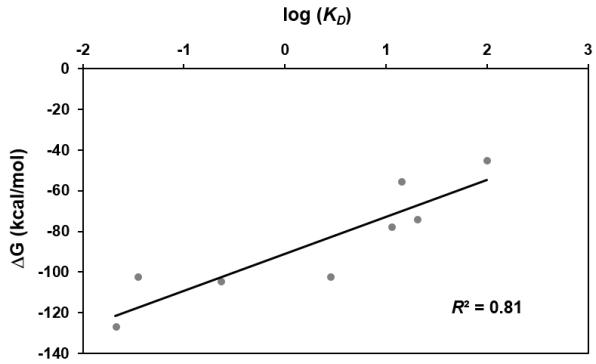

SFigure 8. Correlation between predicted binding energies (ΔG) calculated with MM-GBSA and experimental K_D binding data obtained from FP assays for sclerostin. Plot of log(K_D) vs. ΔG using the most favorable calculated binding free energies (STable 6) from independent 100 ns MD simulations of sclerostin (model 1) in complex with defined sulfated hyaluronans **15**, **16**, **19**, **21-23** and **25-26**. The obtained coefficient of determination R^2 is shown in each plot.

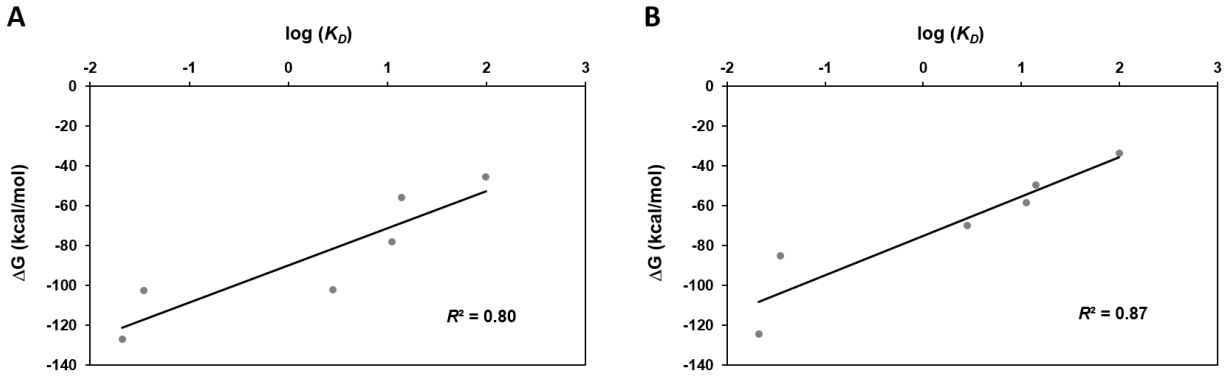

SFigure 9. Correlation between predicted binding energies (ΔG) calculated with MM-GBSA and experimental K_D binding data obtained from FP assays for sclerostin. Plots of log(K_D) vs. ΔG calculated binding free energies from independent 100 ns MD simulations of sclerostin (model 1) in complex with defined sulfated hyaluronans **15**, **19**, **21-23** and **25** involved in (A) the first and (B) the second most favorable predicted binding sites according to STable 6. The obtained coefficient of determination R^2 is shown in each plot.

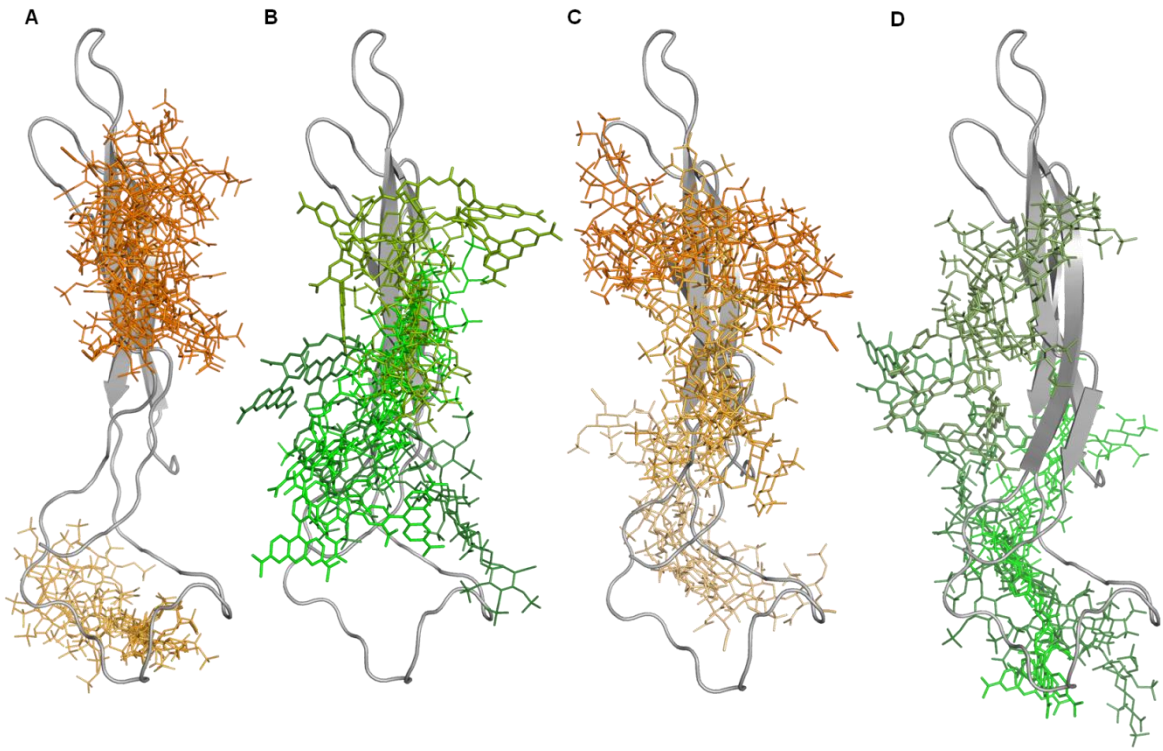

SFigure 10. Molecular modelling of sclerostin interaction with sHA derivatives. Docking results using Autodock 3 and DBSCAN clustering for sHA derivatives (A) **25**, (B) **15**, (C) **26** and (D) **19**. Sclerostin structure from the NMR ensemble (model 10) is shown in gray cartoon. Different clusters of sHA derivatives are shown in sticks with gradient colors: orange for **25** and **26** and, green for **15** and **19**.

STable 7. MM-GBSA binding free energies and interacting residues determined by per-residue energy decomposition and H-bond analysis for sHA **15**, **19**, **25** and **26** in complex with Sclerostin (model10).

sHA derivative	Sclerostin recognition site	ΔG (kcal/mol)[a]
25 (cluster1)	R114, R116, A117, R119, R133, K134, R136	-77.6 ± 3.4
25 (cluster2)	S52, R89, R97, K99, R102, R109, R145,	-99.7 ± 5.3
15 (cluster1)	R114, R116, R119, R133, K134, R136, K142, K144, R145, R148	-88.7 ± 7.9
15 (cluster2)	R63, R89, R97, F108, I111, P112, R114, R133, R136, K142, K144, R145, L146, R148	-103.3 ± 14.8
15 (cluster3)	R97, K99, R114, Y115, R116, R119, R131, R133, R136, K142, K144, R145, R148	-91.7 ± 16.6
26 (cluster1)	R63, R97, K99, R114, R116, R119, R131, R133, K134, R136	-92.4 ± 12.1
26 (cluster2)	R89, R97, K99, R114, Y115, R116, R119, R133, R136, K142, K144, R148	-126.2 ± 11.5
26 (cluster3)	S52, R57, Q84, P87, R89, R97, K99, R102, R109, K142, K144, R145	-96.2 ± 9.1
19 (cluster1)	S52, R57, Q84, P87, R89, L90, L91, R97, K99, R102, R109, R145, R148	-129.5 ± 18.9
19 (cluster2)	S52, R57, Q84, R89, R97, K99, R102, R109, K144, R145, R148	-119.8 ± 5.7
19 (cluster3)	R63, Q84, R97, K99, W100, R114, R116, R119, R131, R133, K134, R136, K142, K144, R148	-108.9 ± 4.0

[a]Values represent the mean ± SD from independent 100 ns MD simulations (up to 6 per cluster depending on number of binding poses obtained in the docking studies).

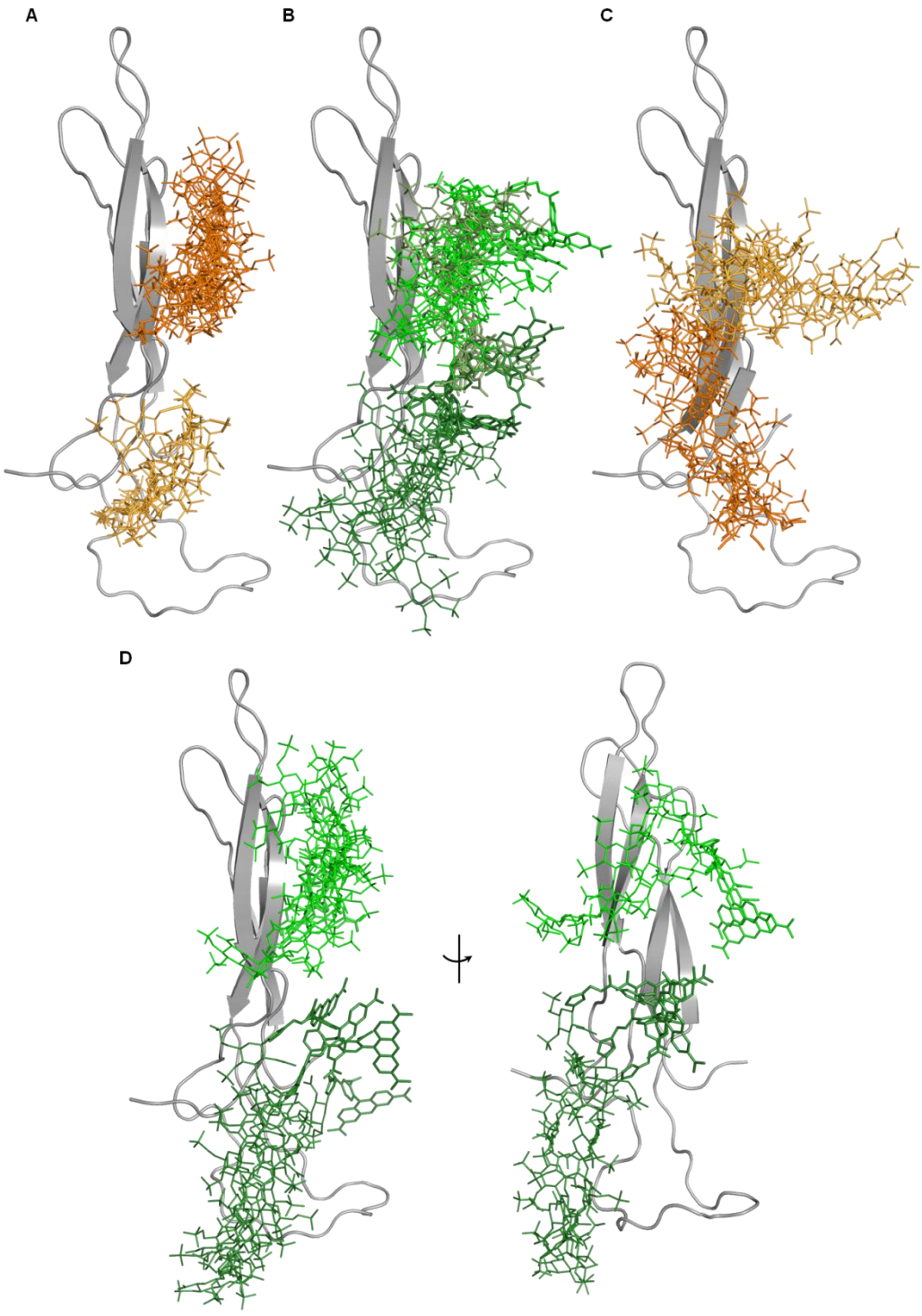

SFigure 11. Molecular modelling of sclerostin interaction with sHA derivatives. Docking results using Autodock 3 and DBSCAN clustering for sHA derivatives (A) **25**, (B) **15**, (C) **26** and (D) **19**. Sclerostin structure from the NMR ensemble (model 16) is shown in gray cartoon. Different clusters of sHA derivatives are shown in sticks with gradient colors: orange for **25** and **26** and, green for **15** and **19**.

STable 8. MM-GBSA binding free energies and interacting residues determined by per-residue energy decomposition and H-bond analysis for sHA **15**, **19**, **25** and **26** in complex with Sclerostin (model16).

sHA derivative	Sclerostin recognition site	ΔG (kcal/mol)[a]
25 (cluster1)	K74, R114, R116, A117, Q118, R119, Q121, R133, K134, R136, R145, R148	-79.6 ± 9.1
25 (cluster2)	R89, R97, K99, R102, S104, R114, R136, K142, K144, R145, R148	-94.5 ± 6.2
15 (cluster1)	K74, R114, R116, Q118, R119, Q121, K134, R136	-89.1 ± 7.7
15 (cluster2)	K74, R114, R116, Q118, R119, R133, K134, R136	-80.5 ± 12.8
15 (cluster3)	R97, K99, R102, R114, R116, R119, R136, K142, K144, R145, R148	-120.2 ± 7.4
26 (cluster1)	K74, R114, R116, Q118, R119, R133, K134, R136, K142, R145	-105.4 ± 15.2
26 (cluster2)	R97, K99, W100, R102, R114, Y115, R116, R119, R133, K134, R136, K142, K144, R145, R148	-135.3 ± 14.3
19 (cluster1)	K74, R97, R114, R116, Q118, R119, K134, R136	-95.5 ± 12.0
19 (cluster2)	R97, K99, W101, R102, R114, R116, K142, K144, R145, R148	-128.6 ± 16.6

[a]Values represent the mean ± SD from independent 100 ns MD simulations (up to 5 per cluster depending on number of binding poses obtained in the docking studies).

STable 9. TAMRA/Sclerostin pairwise interacting residues determined by MM-GBSA.

sHA derivatives	Sclerostin (model 1)	Sclerostin (model 10)	Sclerostin (model 16)
15 (cluster1)	R109, R114, R136, R148	R119, R133, K134	R116, Q118, R119, Q121
15 (cluster2)	Y54, G86, P87, A88, L90, L91, I95, R97, R102, R145, R148	R63, F108, I111, P112, R133, R136, L146	R114, R116, R148
15 (cluster3)	Y54, P87	R97, K99, R136, R148	R114, R116, R119, K142
19 (cluster1)	Y54, R57, L91, R114, R116	P87, R89, L90, L91, K99	K74
19 (cluster2)	Y54, R57, R114	S52, R57, R148	R114, R116
19 (cluster3)	R89, R102, R145, T147, R148	R63	

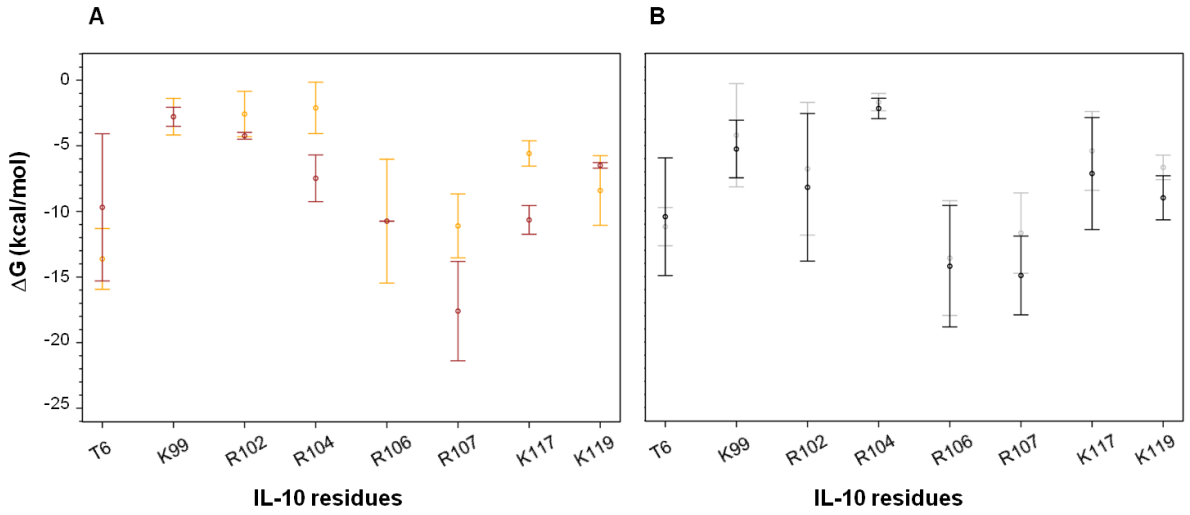

SFigure 12. Per-residue binding energy contribution calculated with MM-GBSA from independent 100 ns MD simulations of IL-10 in complex with high sulfated tetra- and hexahyaluronans (A) azide derivatives **25** (orange) and **26** (brown), (B) TAMRA derivatives **15** (gray) and **19** (black). The errors bars represent the standard error of the mean.

STable 10. MM-GBSA binding free energies and interacting residues determined by per-residue energy decomposition and H-bond analysis for sHA **15**, **19**, **25** and **26** in complex with IL-10.

sHA derivative [a]	IL-10 recognition site[b]	ΔG (kcal/mol)[c]
25 (cluster1)	T6, Q7, S8, N10, K99, R102, R104, R106, R107, N116, K117, K119	-70.2 ± 14.9
15 (cluster1)	T6, Q7, S8, N10, Q70, K99, R102, L103, R104, R106, R107, N116, K117, K119, K125, Q100', R106'	-80.3 ± 10.4
26 (cluster1)	T6, Q7, Q70, K99, R102, R104, R106, R107, R110, K117, K119	-76.1 ± 3.2
19 (cluster1)	T6, Q7, S8, Q70, K99, R102, L103, R104, R106, R107, R110, N116, K117, K119, K125, K130, K119'	-86.2 ± 6.1

[a]A main cluster was predicted. [b]Monomer units are distinguished by a comma. [c] Values represent the mean ± SD from independent 100 ns MD simulations (up to 7 per cluster depending on number of binding poses obtained in the docking studies).

STable 11. TAMRA/IL-10 pairwise interacting residues determined by MM-GBSA.

sHA derivative [a]	IL-10
15 (cluster1) [a]	Q100', R106'
19 (cluster1) [a]	Q70, K119'

[a]A main cluster was predicted.

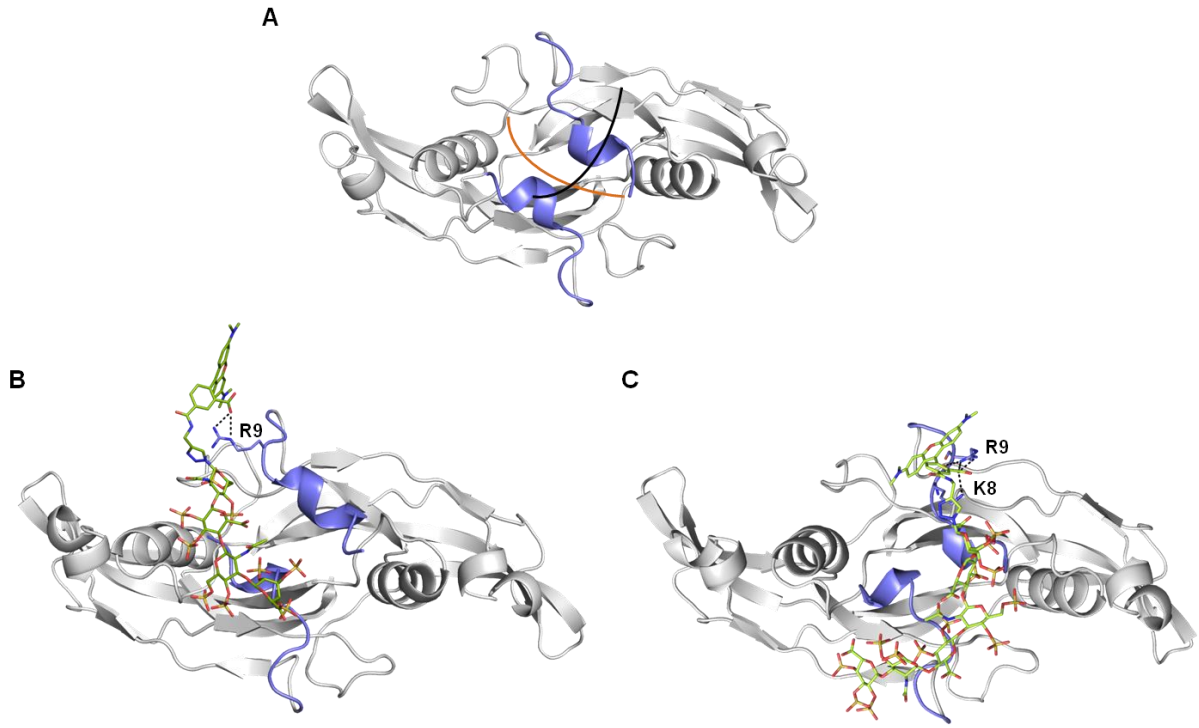

SFigure 13. Molecular modeling of BMP-2 interaction with sHA derivatives. (A) Schematic visualization of the two different binding modes predicted, parallel (orange) and perpendicular (black). Representative snapshots from 100 ns MD simulations for the most favorable binding modes of **15** (B) and **19** (C) parallel or perpendicularly oriented towards the N-termini of BMP-2, respectively, and the TAMRA moiety establishing contacts with R9 of BMP-2 are shown. BMP-2 is depicted in gray cartoon and N-termini residues relevant for recognition are highlighted in purple. sHA derivatives are shown in stick and colored by atom type.

STable 12. MM-GBSA binding free energies and interacting residues determined by per-residue energy decomposition and H-bond analysis for sHA **15**, **19**, **21**-**23** and **25**-**26** in complex with BMP-2.

sHA derivative	BMP-2 recognition site[a]	ΔG (kcal/mol)[b]
21 (cluster1)[c]	Q1, K5, Q6, R7, K8, R9, K5', Q6', R7', K8', R9'	-38.9 ± 1.7
21 (cluster2)[d]	Q1, K5, Q6, R7, K8, R9, L10, Q1', H4', K5', R7'	-38.4 ± 8.2
22 (cluster1)[c]	Q1, K5, Q6, R7, K8, R9, K76, Q1', K3', K5', R7', K8', K76'	-68.3 ± 9.3
22 (cluster2)[d]	Q1, K3, K5, Q6, R7, K8, R9, Q1', K5', K73'	-64.8 ± 4.5
23 (cluster)[c]	Q1, K5, Q6, R7, K8, R9, K76, Q1', K3', K5', K8', K76'	-94.4 ± 11.3
25 (cluster)[c]	Q1, K5, Q6, R7, K8, R9, Q1', K3', K5', Q6', R7', K8', R9'	-104.2 ± 14.3
15 (cluster1)[c]	Q1, K3, K5, Q6, R7, K8, R9, K11, R76, Q1', K3', K5', Q6', R7', K8', R9'	-120.2 ± 20.2
15 (cluster2)[c,e]	Q1, K5, Q6, R7, K8, R9, R76, Q1', K3' K5', Q6', R7'. K8', R9'	-100.1 ± 4.1
15 (cluster3)[d]	Q1, K3, K5, Q6, R7, K8, R9, K11, R76, Q1', K5', K8', R9', K73'	-106.9 ± 11.7
26 (cluster2)[c]	Q1, K3, K5, Q6, R7, K8, R9, K11, R76, Q1', K5', Q6', R7', K8', R9', K11', R76'	-109.2 ± 14.3
26 (cluster1)[d]	Q1, K3, K5, Q6, R7, K8, R9, K11, K73, K76, Q1', A2', K3', H4', K5', R7', R73'	-119.5 ± 11.1
19 (cluster1)[d]	Q1, K3, K5, Q6, R7, K8, R9, K11, K73, K76, Q1', K3', K5', Q6', R7', K8', R9', K11', K73', K76'	-123.0 ± 9.9
19 (cluster2)[d]	Q1, K3, K5, Q6, R7, K8, R9, K11, K76, Q1', K3', K5', R9', K73', K76'	-108.1 ± 16.7
19 (cluster3)[d,e]	Q1, K3, K5, Q6, R7, K8, R9, K11, K76, Q1', K3', K5', Q6'. R7', K8', R9', K11',K73', K76'	-124.6 ± 6.6

[a]Monomer units are distinguished by a comma. [b]Values represent the mean ± SD from independent 100 ns MD simulations (up to 6 per cluster depending on number of binding poses obtained in the docking studies). [c]Parallel oriented towards the BMP-2 N-termini. [d]Perpendicular oriented towards the BMP-2 N-termini. [e]TAMRA moiety does not interact with the protein.

STable 13. TAMRA/BMP-2 pairwise interacting residues determined by MM-GBSA

sHA derivatives	BMP-2[a]
15 (cluster1)	R9
15 (cluster3)	Q1, K3, R9
19 (cluster1)	K8, R9
19 (cluster2)	R9'

[a]Monomer units are distinguished by a comma.

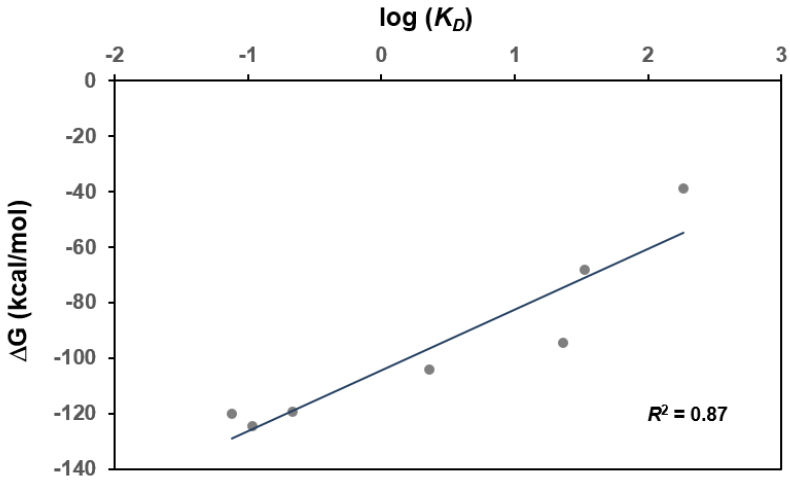

SFigure 14. Correlation between predicted binding energies (ΔG) calculated with MM-GBSA and experimental K_D binding data for BMP-2. Plot of log(K_D) vs. ΔG using the most favorable calculated binding free energies (STable 12) from independent 100 ns MD simulations of BMP-2 in complex with the sulfated hyaluronan derivatives **15**, **19**, **21-23** and **25-26**. Regression analysis was performed by linear regression. The obtained coeficient of determination R^2 is shown in the plot.

9. References

1 Pichert, A.; Samsonov, S. A.; Theisgen, S.; Thomas, L.; Baumann, L.; Schiller, J.; Beck-Sickinger, A. G.; Huster, D.; Pisabarro, M. T. *Glycobiology* **2012,** *22*, 134-45.
2 Künze, G.; Theisgen, S.; Huster, D. *Biomol. NMR Assign.* **2014,** *8*, 375-8.
3 Panitz, N.; Theisgen, S.; Samsonov, S. A.; Gehrcke, J. P.; Baumann, L.; Bellmann-Sickert, K.; Köhling, S.; Pisabarro, M. T.; Rademann, J.; Huster, D.; Beck-Sickinger, A. G. *Glycobiology* **2016,** *26*, 1209-1221.
4 Xiao, Q.; Ju, Y.; Yang, X.; Zhao, Y. F. *Rapid Commun. Mass Spectrom.* **2003,** *17*, 1405-10.
5 Köhling, S.; Exner, M. P.; Nojoumi, S.; Schiller, J.; Budisa, N.; Rademann, J. *Angew. Chem. Int. Ed. Engl.* **2016,** *55*, 15510-15514.
6 Köhling, S.; Künze, G.; Lemmnitzer, K.; Bermudez, M.; Wolber, G.; Schiller, J.; Huster, D.; Rademann, J. *Chem. Eur. J.* **2016,** *22*, 5563-74.
7 Pope, A. J.; Haupts, U. M.; Moore, K. J. *Drug Discov. Today* **1999,** *4*, 350-362.
8 https://botdb-abcc.ncifcrf.gov/BotDB/toxin/kiCalPL.jsp.
9 Nikolovska-Coleska, Z.; Wang, R.; Fang, X.; Pan, H.; Tomita, Y.; Li, P.; Roller, P. P.; Krajewski, K.; Saito, N. G.; Stuckey, J. A.; Wang, S. *Anal. Biochem.* **2004,** *332*, 261-73.
10 Case, D. A.; Berryman, J. T.; Betz, R. M.; Cerutti, D. S.; T.E. Cheatham, I.; Darden, T. A.; Duke, R. E.; Giese, T. J.; Gohlke, H.; Goetz, A. W.; Homeyer, N.; Izadi, S.; Janowski, P.; Kaus, J.; Kovalenko, A.; Lee, T. S.; LeGrand, S.; Li, P.; Luchko, T.; Luo, R.; Madej, B.; Merz, K. M.; Monard, G.; Needham, P.; Nguyen, H.; Nguyen, H. T.; Omelyan, I.; Onufriev, A.; Roe, D. R.; Roitberg, A.; Salomon-Ferrer, R.; Simmerling, C. L.; Smith, W.; Swails, J.; Walker, R. C.; Wang, J.; Wolf, R. M.; Wu, X.; York, D. M.; Kollman, P. A. *AMBER 2014*, University of California, San Francisco., 2014.
11 *Molecular Operating Environment (MOE), version 2015; Chemical Computing Group Inc.: Montreal, QC, Canada* **2015**.
12 Kirschner, K. N.; Yongye, A. B.; Tschampel, S. M.; Gonzalez-Outeirino, J.; Daniels, C. R.; Foley, B. L.; Woods, R. J. *J. Comput. Chem.* **2008,** *29*, 622-55.

13 Huige, C. J. M.; Altona, C. *J. Comput. Chem.y* **1995,** *16*, 56-79.
14 Walker, R. C.; Crowley, M. F.; Case, D. A. *J. Comput. Chem.* **2008,** *29*, 1019-31.
15 (a) Bayly, C. I.; Cieplak, P.; Cornell, W. D.; Kollman, P. A. *J. Phys. Chem.-Us* **1993,** *97*, 10269-10280; (b) Dupradeau, F. Y.; Pigache, A.; Zaffran, T.; Savineau, C.; Lelong, R.; Grivel, N.; Lelong, D.; Rosanski, W.; Cieplak, P. *Phys. Chem. Chem. Phys.* **2010,** *12*, 7821-7839.
16 Frisch, M. J.; Trucks, G. W.; Schlegel, H. B.; Scuseria, G. E.; Robb, M. A.; Cheeseman, J. R.; Scalmani, G.; Barone, V.; Mennucci, B.; Petersson, G. A.; Nakatsuji, H.; Caricato, M.; Li, X.; Hratchian, H. P.; Izmaylov, A. F.; Bloino, J.; Zheng, G.; Sonnenberg, J. L.; Hada, M.; Ehara, M.; Toyota, K.; Fukuda, R.; Hasegawa, J.; Ishida, M.; Nakajima, T.; Honda, Y.; Kitao, O.; Nakai, H.; Vreven, T.; Montgomery Jr., J. A.; Peralta, J. E.; Ogliaro, F.; Bearpark, M. J.; Heyd, J.; Brothers, E. N.; Kudin, K. N.; Staroverov, V. N.; Kobayashi, R.; Normand, J.; Raghavachari, K.; Rendell, A. P.; Burant, J. C.; Iyengar, S. S.; Tomasi, J.; Cossi, M.; Rega, N.; Millam, N. J.; Klene, M.; Knox, J. E.; Cross, J. B.; Bakken, V.; Adamo, C.; Jaramillo, J.; Gomperts, R.; Stratmann, R. E.; Yazyev, O.; Austin, A. J.; Cammi, R.; Pomelli, C.; Ochterski, J. W.; Martin, R. L.; Morokuma, K.; Zakrzewski, V. G.; Voth, G. A.; Salvador, P.; Dannenberg, J. J.; Dapprich, S.; Daniels, A. D.; Farkas, Ö.; Foresman, J. B.; Ortiz, J. V.; Cioslowski, J.; Fox, D. J. *Gaussian 09, Revision C.01*, Gaussian, Inc.: Wallingford, CT, USA, 2009.
17 Baldwin, E. T.; Weber, I. T.; St Charles, R.; Xuan, J. C.; Appella, E.; Yamada, M.; Matsushima, K.; Edwards, B. F.; Clore, G. M.; Gronenborn, A. M.; et al. *Proc. Natl. Acad. Sci. U.S.A.* **1991,** *88*, 502-6.
18 Clore, G. M.; Appella, E.; Yamada, M.; Matsushima, K.; Gronenborn, A. M. *Biochemistry* **1990,** *29*, 1689-96.
19 Zdanov, A.; SchalkHihi, C.; Wlodawer, A. *Protein Sci.* **1996,** *5*, 1955-1962.
20 Allendorph, G. P.; Vale, W. W.; Choe, S. *Proc. Natl. Acad. Sci. U.S.A.a* **2006,** *103*, 7643-8.
21 Hintze, V.; Samsonov, S. A.; Anselmi, M.; Moeller, S.; Becher, J.; Schnabelrauch, M.; Scharnweber, D.; Pisabarro, M. T. *Biomacromolecules* **2014,** *15*, 3083-92.
22 Veverka, V.; Henry, A. J.; Slocombe, P. M.; Ventom, A.; Mulloy, B.; Muskett, F. W.; Muzylak, M.; Greenslade, K.; Moore, A.; Zhang, L.; Gong, J. H.; Qian, X. M.; Paszty, C.; Taylor, R. J.; Robinson, M. K.; Carr, M. D. *J. Biol. Chem.* **2009,** *284*, 10890-10900.
23 Morris, G. M.; Goodsell, D. S.; Halliday, R. S.; Huey, R.; Hart, W. E.; Belew, R. K.; Olson, A. J. *J. Comput. Chem.* **1998,** *19*, 1639-1662.
24 Ester, M.; Kriegel, H.-P.; Sanders, J.; Xu, X. *Proc. 2nd Int. Knowl. Discov. Data Min. (KKD96)* **1996**, 226-231.
25 Wang, J.; Wolf, R. M.; Caldwell, J. W.; Kollman, P. A.; Case, D. A. *J. Comput. Chem.* **2004,** *25*, 1157-74.
26 Gouin, S. G.; Vanquelef, E.; Fernandez, J. M.; Mellet, C. O.; Dupradeau, F. Y.; Kovensky, J. *J. Org. Chem.* **2007,** *72*, 9032-45.
27 Humphrey, W.; Dalke, A.; Schulten, K. *J. Mol. Graph. Model.* **1996,** *14*, 33-38.
28 (a) Wang, J. M.; Morin, P.; Wang, W.; Kollman, P. A. *J. Am. Chem. Soc.* **2001,** *123*, 5221-5230; (b) Miller, B. R., 3rd; McGee, T. D., Jr.; Swails, J. M.; Homeyer, N.; Gohlke, H.; Roitberg, A. E. *J. Chem. Theory Comput.* **2012,** *8*, 3314-21.
29 *R-package Development Core Team. http://www.r-project.org.* **2015**.
30 *The PyMOL Molecular Graphics System*, Version 1.8 Schrödinger; LLC: 2009-2015.
31 (a) Gehrcke, J. P.; Pisabarro, M. T. *J. Mol. Graph. Model.* **2015,** *62*, 97-104; (b) Künze, G.; Köhling, S.; Vogel, A.; Rademann, J.; Huster, D. *J. Biol. Chem.* **2016,** *291*, 3100-13.
32 Ohkawara, B.; Iemura, S.; ten Dijke, P.; Ueno, N. *Curr. Biol.* **2002,** *12*, 205-209.